



THÈSE

En vue de l'obtention du

DOCTORAT DE L'UNIVERSITÉ DE TOULOUSE

Délivré par l'Université Toulouse III - Paul Sabatier
Discipline ou spécialité : *Ecologie marine*

Présentée et soutenue par *Mélanie ABECASSIS*
Le 29/05/2012

Titre :

Modélisation des interactions entre l'espadon, la tortue caouanne et les palangriers dans l'océan Pacifique Nord

JURY

Nick Hall (Président)
Didier Gascuel (Rapporteur)
Jean-Marc Fromentin (Rapporteur)
Christophe Guinet (Examineur)
Philippe Gaspar (Directeur de thèse)
Patrick Lehodey (Co-directeur de thèse)

Ecole doctorale :

Sciences de l'Univers, de l'Environnement et de l'Espace (SDU2E)

Unité de recherche :

Collecte Localisation Satellites (CLS) - Direction Océanographie Spatiale (DOS)

Directeur(s) de Thèse :

Philippe Gaspar, Coordinateur Scientifique (DOS), Toulouse
Patrick Lehodey, Chef du Département Ecosystèmes Marins (DOS), Toulouse
Jeffrey Polovina, Chef de la division Ecosystèmes et Océanographie, PIFSC/NOAA, Honolulu, USA

Résumé	6
Abstract.....	7
Avant-propos	9
Chapitre 1	17
Introduction.....	17
1. L'espadon	17
Biologie et distribution	17
Stocks	18
Reproduction	18
Régime alimentaire.....	19
Pêcheries	19
2. La tortue caouanne	21
Biologie et distribution	21
Menaces et interactions avec les pêcheries.....	23
3. SEAPODYM	27
Prédateurs-proies	28
Forçages.....	30
Habitat thermique	30
Contrainte en oxygène	30
Habitat d'alimentation (H_f).....	31
Habitat de ponte (H_s).....	31
Mouvements.....	32
Comportement d'alimentation et de ponte.....	32
Mortalité naturelle	33
Besoins nutritionnels	34
Mortalité par pêche.....	34
Optimisation et validation	35
Movemod	35
Chapitre 2	37
Analyse de marques satellites et modélisation de l'habitat vertical diurne de l'espadon dans le Pacifique Nord.....	37
Résumé.....	38
Abstract	39
Introduction.....	40
Materials and methods	41

Tagging.....	41
Tag programming and processing	41
Geolocation	42
Environmental variables.....	43
Separation of day and night	43
Mean depth	43
Generalized Additive Models (GAMs)	44
Results	44
Tagging.....	44
Horizontal movements	44
Vertical movements.....	47
Oxygen limitation	51
Light	51
Model results.....	53
Discussion and conclusions	59
Tagging.....	59
Mean depth	59
Geolocation	59
Oxygen tolerance.....	60
Constant isolume?	60
Modeling.....	61
Potential applications of the model	61
References.....	63
Supplemental Material.....	69
Summaries of the individual GAM models :	69
Diagnostic plots for the full model :	70
Plots of the smooths for ChlA, Oxygen and interaction term estimated by the full model.	71
Chapitre 3	73
Suivis de tortues caouannes et modélisation d’habitat et de mouvements	73
Résumé	73
Abstract	75
Introduction.....	75
Materials and methods	77
Processing and analysis of tagging data	77
Habitat and movement modeling	79

Results	82
Tracks processing and analysis	82
Habitat and movement modeling	86
Discussion	95
Temperature	95
Feeding habitat	96
Movements	98
References	100
Chapitre 4	106
Application de SEAPODYM à la dynamique spatiale de l'espadon du Pacifique	106
Résumé	107
Abstract	109
Introduction	110
Materials and methods	110
SEAPODYM	110
Biological parameters	111
Fishing data	112
Results	119
Estimated parameters	119
Model validation	123
Biomass and distribution of swordfish	129
Overlap between swordfish and turtles	131
Discussion and conclusions	132
Model limitations	132
Estimated parameters	133
Overlap between swordfish and turtles	136
Appendix – List of SEAPODYM notations	137
References	138
Conclusions	142
Bibliography	149

RESUME

La pêche de l'espadon à la palangre est très controversée du fait de son manque de sélectivité et de son impact sur les espèces non ciblées, notamment les tortues marines, et en particulier, la tortue caouanne. En Septembre 2011, le statut de la tortue caouanne est passé de « menacé d'extinction » à « en danger d'extinction », au sein de l'IUCN (International Union for conservation of Nature) dans l'océan Pacifique. De nombreuses mesures de mitigation ont été mises en place avec succès depuis les dix dernières années pour réduire le nombre d'interactions entre les tortues et les pêcheries, mais étant donné l'importance du déclin de la population, ces efforts pourraient s'avérer insuffisants.

Le but de ce projet de thèse est de parvenir, à partir de données de marquage électronique, à une meilleure description des habitats occupés par les espadons et les tortues caouannes dans le Pacifique Nord, puis d'utiliser ces résultats au sein de modèles numériques pour tenter de prédire leurs distributions respectives et étudier de potentielles stratégies d'évitement des tortues par les pêcheries.

L'analyse des données de marquage d'espadon a fourni une meilleure compréhension des facteurs qui contrôlent leur comportement vertical et a conduit au développement d'un modèle additif généralisé (GAM) permettant de prédire la profondeur moyenne diurne des espadons. Cette information pourrait être utilisée par les palangriers pour cibler l'espadon de jour, en profondeur, plutôt que de nuit dans la couche de surface occupée par les tortues.

De nombreuses marques satellites furent aussi déployées sur des tortues caouannes permettant d'étudier leurs mouvements de manière détaillée, en conjonction avec des variables environnementales extraites le long des trajectoires. Cette analyse a permis de caractériser la température optimale pour cette espèce (aux alentours de 17 °C), et suggère également que les tortues plus larges plongent en eau plus profonde et ciblent ensuite des eaux de surface plus chaudes pour se réchauffer. Un examen des vitesses de nage a démontré que des juvéniles mesurant à peine 25 cm sont capables de mouvements propres leur permettant de se maintenir dans une gamme de température favorable, malgré l'influence des courants océaniques. L'implémentation de ces informations dans un modèle de type eulérien a ensuite permis de modéliser un indice d'habitat des tortues caouannes en bonne adéquation avec les trajectoires observées et reflétant les mouvements Nord-Sud saisonniers avec précision. En revanche, cet exercice de modélisation semble démontrer que les courants océaniques, la température et la concentration de proies ne sont pas les seuls facteurs contrôlant la dynamique Est-Ouest des mouvements observés.

Enfin, l'adaptation du modèle SEAPODYM (Spatial Ecosystem and Populations DYnamics Model) à l'espadon dans le Pacifique, malgré des lacunes importantes dans les données de pêche disponibles pour calibrer le modèle, prédit des captures par unité d'effort en bonne adéquation avec celles observées. Les distributions prédites d'espadons juvéniles et adultes sont raisonnables et les périodes de coïncidence entre les espadons adultes et les tortues sont en accord avec les périodes d'interaction maximales entre les tortues et les pêcheries. De meilleures données de pêche et un forçage résolvant la méso-échelle permettraient rapidement d'étudier les zones de coïncidence de manière plus détaillée à des fins de gestion, ainsi que d'obtenir des estimations de biomasses plus robustes.

ABSTRACT

Longline fisheries targeting swordfish are very controversial due to their lack of selectivity and the important by-catch associated with them, most notably of marine turtles and loggerhead turtles in particular. In September 2011, loggerheads were relisted as endangered in the Pacific Ocean. Numerous mitigation measures have been taken in the past decade to reduce the number of sea turtle interactions with the fisheries, and were met with considerable success. However, they may not prove enough to offset the steep population decline that has been observed since the 1970s.

The goal of this PhD project was to yield a better description of swordfish and loggerheads habitats in the Pacific from electronic tagging data, and then to use these results to calibrate numerical models aimed at predicting the spatial distributions of both species to evaluate potential by-catch reduction strategies.

The analysis of pop-up archival satellite tags deployed on swordfish allowed for a better understanding of the factors controlling their vertical behavior and led to the development of a generalized additive model (GAM) to predict swordfish mean daytime depth. That information could help longline fishermen to target swordfish during the daytime at depth, rather than at night in the surface layer where loggerheads reside.

Close to 200 satellite tags were also deployed on loggerhead turtles, which allowed to study their movements in details in conjunction with environmental variables along their tracks. This analysis showed that loggerheads optimal temperature is around 17 °C for all the sizes in our study (25 – 81 cm) and suggested that bigger turtles may dive deeper and then target warmer surface waters to recover. The analysis of the swimming speeds along the tracks showed that turtles as small as 25 cm are capable of directed movements to maintain themselves within a range of desirable temperature against prevailing currents. These results were used to calibrate a Eulerian model. The modeled habitat index matched the observed tracks and captured the seasonal north-south movements closely. However, the model failed to replicate the observed east-west movements, suggesting temperature and foraging preferences are not the only factors explaining large-scale loggerhead movements.

Finally, the SEAPODYM (Spatial Ecosystem and Populations DYnamics Model) was adapted to swordfish in the Pacific. Despite issues with the available fishing data used to calibrate the model, the model fitted the observed catches per unit of effort closely. The predicted distributions of young and adult swordfish were reasonable and the predicted overlap periods between swordfish and loggerheads matched the timing of high occurrences of by-catch in the fisheries. A better fishing dataset and a more adequate forcing resolving the mesoscale would quickly allow to study the regions of overlap in a detailed enough manner for management purposes and would produce more robust estimates of biomass.

REMERCIEMENTS

En 2006, je devais faire un stage de 6 mois à l'étranger pour finir mon master. Comme je voulais améliorer mon anglais, j'ai envoyé des mails à un grand nombre de personnes qui travaillaient en océano dans des labos situés dans des régions anglophones et tropicales. Six mois en Angleterre sous la pluie, non merci. Après moult réponses négatives, la première, et unique, personne à répondre « Oui, et je peux te payer le billet d'avion » fut Dr. Jeffrey Polovina. A Honolulu. A Hawaïi.

Je suis arrivée à Honolulu le 7 Mars 2006. Trois jours plus tard, il s'est mis à pleuvoir. Il a plu pendant 40 jours.

Au bout de trois semaines de stage, Jeff m'a demandé ce que je comptais faire à l'automne, après avoir soutenu mon master. Avais-je envie de rester ? A Hawaïi.

Oui.

Deux ans plus tard, l'idée de ce projet de thèse a été lancée un peu par hasard, quand Jeff a rencontré Patrick Lehodey au détour d'une conférence. Jeff savait que je cherchais un projet de thèse et était intéressé par le modèle de dynamique de population que Patrick avait développé. Et Patrick cherchait à développer de nouvelles applications du modèle. Un projet collaboratif a alors été démarré, entre Toulouse et Hawaïi.

Trois ans et demi plus tard, après avoir enfin réussi à finir mon mémoire de thèse, j'ai pris une semaine de vacances. Pour dormir et faire du surf.

Il a plu toute la semaine.

Et puis il a grêlé.

Je tiens à remercier en premier lieu Jeff, pour avoir pris le risque de faire venir une étudiante dont il n'avait jamais entendu parler, depuis la France. Puis pour m'avoir embauchée. Et enfin pour m'avoir permis de faire ma thèse en travaillant à temps plein. Je lui serai éternellement reconnaissante pour ces multiples opportunités, pour sa patience, sa disponibilité constante, et tout ce qu'il m'a enseigné.

Je voudrais ensuite remercier Patrick pour avoir accepté de me prendre en thèse et Philippe Gaspar pour m'avoir accueillie à CLS au sein de l'équipe MEMMS, et pour avoir effectué les démarches nécessaires pour rendre cette thèse possible malgré le cauchemar logistique que ça a parfois pu être, que ce soit au niveau des démarches administratives auprès de la fac, ou au niveau des autorisations d'accès au réseau informatique depuis les Etats-Unis. La thèse à distance, avec douze heures de décalage horaire, ça n'a pas toujours été simple. Merci à tous les deux pour m'avoir encadrée et guidée pendant ce projet, pour avoir lu et relu et re-relu les nombreuses versions de chaque chapitre.

Merci à Jean-Marc Fromentin et Didier Gascuel qui ont accepté d'être les rapporteurs de ma thèse et aussi Christophe Guinet et Nick Hall qui ont bien voulu faire partie de mon jury. Vos commentaires ont grandement amélioré ce manuscrit.

Un grand merci à Inna Senina pour son immense aide technique, les innombrables explications sur les détails du modèle, les centaines d'emails et les nombreuses heures passées au téléphone entre Toulouse et Honolulu, à des heures impossibles, pour résoudre les problèmes de dernière minute et les bugs inexplicables (pour moi).

Merci à Beatriz Calmettes pour m'avoir fourni les nombreuses itérations des données de forçage nécessaires, et sa patience au gré des modifications nécessaires. Pour sa disponibilité et sa gentillesse. Et merci à François Royer pour son aide avec les outils de géolocalisation, sans lesquels le 1^{er} chapitre n'aurait pas donné grand-chose.

Merci à Olga, compagne d'aventures volcaniques aux premiers jours d'Hawaii et compagne de galère de thèse, hôtesse extraordinaire à Toulouse, et amie patiente ! Vivement une réunion à Hawaii ou en Espagne ! Et merci à Quentin pour sa patience infinie pendant les multiples débats techniques sur Seapodym, chez lui, le soir, après ses journées de thèse à lui.

Merci à mes collègues de bureau de CLS, Seb, Caroline, et Elise, pour leur bonne humeur et leur humour.

Et merci à mon collègue de bureau à Honolulu, Lucas, pauvre Lucas. Qui a dû subir mes incessantes conversations téléphoniques en français et qui ne s'est jamais plaint.

Merci à tous les amis d'Hawaii, François, Tom & Clara, Sunny, Dari, Adam, Anais, Cyril, Annick, Ben, Tracy, Carolina, Marc, Deb, Eric, Colette, Jan, pour le rock&roll, le surf, les barbecues sur la plage, les séances karaoke, les soirées à Tgs, les lunchs sur le campus, les lunchs à un milliard de dollars, les Noël tropicaux, les 14 juillet, les fêtes de la frite, les discussions politiques interminables, les souvenirs (et photos associées ...) innombrables.

Merci aux indéfectibles Bayonnais/Bordelais/Landais et affiliés, depuis tant d'années, qui malgré la distance me réservent toujours quelques soirées quand je rentre en France, Rodolphe, Guillaume, JB, Julie, Hélène, David, Ludivine, l'autre Guillaume, JP, Jean-Charles, Thomas, Benoît.

Un merci spécial à Guillaume D. qui a très sérieusement compilé les meilleures citations inutilisables du « Vieil homme et la mer » pour m'aider à préparer ma « soutenance sur l'espadon ».

Un merci hippie à ma prof de yoga, Shelley, sans qui mes problèmes de dos et mon stress auraient été bien pires.

Enfin, je veux remercier ma famille qui a fait le sacrifice de venir me voir à Hawaii tous les deux ans depuis que j'y suis partie, qui m'envoie à chaque anniversaire et à chaque Noël les éléments indispensables à ma survie et au succès de cette thèse (foie gras, jambon ibérico, vin, chocolats), qui accepte encore et malgré tout et presque sans râler de m'emmener dans mes restos préférés chaque fois que je rentre à la maison et les nombreux petits détails et attentions qui font que la maison reste la maison, et que la distance est rarement trop pénible.

Mahalo nui loa.

Le meilleur des meilleures citations inutilisables pour ma soutenance sur l'espadon, mais quand même très applicables à ma thèse sur l'espadon, et peut-être aussi à la plupart des thèses qui ne parlent pas de poisson :

« Garde la tête froide et endure ton mal comme un homme. Ou comme un poisson ».

« Aidez-moi, mon Dieu, je vous en prie. Je dirai cent Notre Père et cent Je vous salue Marie. Mais pas tout de suite ».

« J'aurais pas dû aller si loin, poisson [...]. Ni pour toi, ni pour moi. Pardon, poisson ».

- Ernest Hemingway.
(compilées par Guillaume Desbieys)

Sagesse locale :

« No mo' fish, no mo' fish. Eat a burger ».

(Quand y a pas de poisson, y a pas de poisson. Mange un burger)

- Chef Mark « Gooch » Noguchi.

AVANT-PROPOS

En 1992, la Conférence des Nations Unies sur l'Environnement et le Développement (CNUED), plus connue sous le nom de Sommet de Rio, a conduit à l'adoption de la Déclaration de Rio sur l'environnement et le développement qui introduisit officiellement le principe de développement durable. Le 8^e principe de la Déclaration déclare que « afin de parvenir à un développement durable et à une meilleure qualité de vie pour tous les peuples, les Etats devraient réduire et éliminer les modes de production et de consommation non viables et promouvoir des politiques démographiques appropriées ».

La même année, la Déclaration de Cancún, résultat de la Conférence internationale sur la pêche responsable, élaborée par l'Organisation des Nations Unies pour l'alimentation et l'agriculture (FAO), conduisit à l'élaboration, puis l'adoption en 1995, d'un Code mondial de conduite pour une pêche responsable. L'un des principes généraux établit que « les Etats et les utilisateurs des écosystèmes aquatiques devraient réduire au minimum le gaspillage de captures d'espèces visées et non visées de poissons et d'autres espèces ainsi que l'impact sur les espèces associées ou dépendantes ».

En 1994, une étude financée par la FAO sur l'estimation des prises accessoires et des rejets dans les pêcheries commerciales à l'échelle mondiale a estimé qu'entre 18 et 40 millions de tonnes de poissons sont rejetés chaque année (Alverson et al 1994), ce qui représenterait en moyenne 8% des captures mondiales. Cette étude a permis d'attirer l'attention sur la gravité du problème des rejets et a contribué grandement à leur réduction. Une mise à jour, publiée en 2005 et basée sur une approche différente, pêcherie par pêcherie, et des données de pêche plus récentes, a estimé les rejets moyens à 7,3 millions de tonnes par an, entre 1992 et 2001 (Kelleher 2005). Bien que ces deux estimations ne sont pas directement comparables puisqu'utilisant des méthodologies différentes, la mise à jour présente des arguments forts suggérant qu'une réduction importante des rejets a eu lieu depuis les années 1990.

A l'échelle mondiale, la réduction des impacts de la pêche commerciale sur les espèces non-ciblées est désormais au cœur des préoccupations des gestionnaires de ressources et des professionnels de la pêche. Les organisations de conservation gouvernementales et non-gouvernementales ont réussi, par la promotion de labels écologiques et au travers d'efforts d'éducation, à sensibiliser les consommateurs, et en conséquence à pousser les pêcheurs et leurs partenaires à mettre en place des pratiques de pêche plus sélectives.

A l'exception du chalutage à la crevette, la pêche à la palangre est la méthode de pêche qui présente le taux de rejets le plus élevé, de l'ordre de 28.5% des captures en moyenne (Kelleher 2005). Pour cette raison, cette méthode est l'une des plus controversées. Elle consiste à déployer de longues lignes pouvant mesurer jusqu'à plusieurs kilomètres de long sur lesquelles sont apposés de plusieurs centaines à plusieurs milliers d'hameçons équipés d'appât séparés en branches délimitées par des flotteurs. Ces lignes sont laissées à la dérive pendant plusieurs heures de jour ou de nuit selon l'espèce ciblée. De par la configuration de ces lignes, des hameçons sont ainsi présents dans une couche verticale de plusieurs dizaines à plusieurs centaines de mètres, et sont susceptibles d'attirer un grand nombre d'espèces occupant la même gamme de profondeur que l'espèce ciblée. Les espèces ciblées par ce type de pêche dans l'océan Pacifique sont diverses espèces de thons (thon obèse, thon jaune, albacore, thon rouge notamment) et l'espadon. Les thons sont généralement ciblés de jour en profondeur (aux alentours de 300 ou 400 m) alors que les espadons sont ciblés de nuit près de la surface (entre 60 et 90 m typiquement). Les palangres ciblant l'espadon posent particulièrement problème car elles sont sujettes à de nombreuses interactions avec les tortues marines et les oiseaux de mer (en particulier les albatros). Ces espèces menacées d'extinction sont l'objet de nombreuses mesures de protection et le grand nombre

d'interactions, souvent mortelles, avec les palangres ont provoqué la recherche puis la mise en place de diverses techniques d'évitement.

Pour réduire les interactions avec les oiseaux de mer, des modifications de technique de pêche furent mises en place en 2002 dans les pêcheries basées à Hawaï : utilisation d'appâts teints en bleu, obligation de lester les lignes pour les rendre moins accessibles depuis la surface, obligation de déployer les lignes une heure après le coucher de soleil quand l'espèce cible est l'espadon, obligation de limiter l'utilisation de lumières à bord de nuit, filage depuis le bord du bateau au lieu de l'arrière, utilisation de lignes d'effarouchement des oiseaux pendant le filage. Depuis la mise en place de ces mesures, le taux d'interactions entre les palangres et les oiseaux de mer a été réduit de 90% par rapport à 2000.

Les espèces de tortues marines particulièrement affectées par les palangres dans l'océan Pacifique sont la tortue caouanne et la tortue luth, qui sont toutes deux en danger critique d'extinction. Ces deux espèces ont subi des déclin de population de femelles pondeuses estimés aux alentours de 85 et 95% respectivement dans l'océan Pacifique dans les 25 dernières années (Lewison et al 2004). De nombreux facteurs jouent un rôle dans ce déclin à chaque stade biologique. Ces espèces sont affectées par les palangres durant leur phase juvénile pélagique sur laquelle nous nous sommes concentrés lors de ce projet. Les tortues juvéniles sont attirées par les appâts et peuvent se retrouver blessées par les hameçons, embrouillées par les lignes et se noyer, ou ingérer les hameçons. Lewison et al 2004 ont estimé qu'environ 30 000 tortues caouannes ont été affectées par les palangres dans le Pacifique en 2000, avec un taux d'interactions mortelles estimé entre 9 et 20%.

Outre les mesures prises dans les palangres pour protéger les oiseaux marins et qui ont généralement des effets positifs sur les interactions avec les tortues, des dispositions ont aussi été prises pour protéger les tortues spécifiquement. La pêcherie à l'espadon basée à Hawaï a été fermée de 2000 à 2004 pour étudier et mettre en place les modifications suivantes : changement d'appâts (utilisation du maquereau au lieu du calmar), utilisation d'hameçons circulaires pour permettre aux tortues de se libérer plus facilement et limiter l'ingestion des hameçons, mise en place d'observateurs scientifiques sur les palangriers (sur au moins 20% des bateaux ciblant le thon, et 100% des bateaux ciblant l'espadon), et mise en place d'un nombre maximal d'interactions (16 tortues luth et 17 tortues caouannes par an) pour l'ensemble de la pêcherie à l'espadon, au-delà duquel la pêcherie est automatiquement fermée.

Depuis leur mise en place en 2004, ces mesures ont permis depuis plusieurs années de limiter grandement les interactions avec ces espèces protégées dans la pêcherie hawaïenne. Néanmoins, malgré les modifications de technique de pêche mises en place, le nombre limite de tortues a été atteint en 2006 et 2011, entraînant la fermeture de la pêcherie et causant d'importantes pertes économiques, tant pour les pêcheurs que pour l'économie locale. L'espadon est considéré comme étant sous-exploité dans le Pacifique, à l'exception du Pacifique Est, et un équilibre doit être trouvé entre la protection des espèces menacées et l'exploitation optimale des espèces commerciales.

A ces fins, de nouveaux efforts ont été entrepris pour mieux comprendre et prédire l'évolution des distributions spatiales de chaque espèce, l'idée étant de fournir aux pêcheurs des informations sur les zones de présence des espèces menacées afin de les éviter. Dans le cas particulier de la tortue caouanne, une étude analysant statistiquement l'effort de pêche et les positions des captures de tortues a résulté en la mise en place d'un indice basé sur la température de surface, indiquant la zone de présence la plus probable des tortues (Howell et al 2008).

Ce projet de thèse propose de convertir cette approche statistique en un cadre de modélisation de l'habitat de chaque espèce, au sein duquel la dynamique spatiale est régie par des contraintes biologiques et environnementales, dans le but de fournir un cadre prédictif aux gestionnaires de ressources.

Les objectifs de ce projet sont de :

- Fournir une meilleure connaissance des préférences environnementales de l'espadon et de la tortue caouanne à partir de données de marquage satellite collectées lors d'études précédentes
- Utiliser ces résultats pour étudier la faisabilité d'adapter le modèle SEAPODYM (Spatial Ecosystem and Populations DYnamics Model, voir §3 de l'introduction pour plus de détails), initialement développé pour les thons tropicaux, à l'espadon et à la tortue caouanne, respectivement
- Si l'adaptation du modèle à chaque espèce est réalisable, étudier leurs dynamiques spatiales afin d'estimer leurs zones et/ou périodes de co-occurrence

L'adaptation de SEAPODYM aux tortues présente plusieurs défis :

- Les mécanismes du modèle, décrivant la dynamique de population de poissons tropicaux ne sont pas directement transposables à des reptiles respirant à l'air et nécessitent plusieurs modifications du modèle
- Le cycle biologique des tortues inclue des périodes terrestres (ponte, couvaison) qui ne peuvent pas être représentées dans le modèle
- Les tortues n'étant pas ciblées commercialement, très peu de données sont disponibles pour cette espèce en-dehors des données récoltées sur les plages de ponte. En particulier, leur croissance et leur mortalité naturelle sont mal connues et très difficiles à estimer

L'adaptation de SEAPODYM à l'espadon nécessite :

- L'obtention de données de pêche exhaustives à l'échelle du bassin Pacifique, pour chaque pêcherie qui capture des espadons
- Un forçage physique résolvant la méso-échelle afin de capturer les concentrations de poissons reflétées par des CPUE localisées très élevées

Tous ces défis n'ont pu être résolus lors de cette thèse, mais les résultats présentés ici constituent un premier pas vers une gestion écosystémique des ressources intégrant un cadre prédictif conjoint pour une espèce ciblée et une espèce protégée affectée par son exploitation.

Après une présentation des deux espèces étudiées et du modèle SEAPODYM en introduction, le second chapitre détaillera l'analyse de données de marques satellites déployés sur 28 espadons et la caractérisation et la modélisation de leur comportement vertical. Le troisième chapitre présentera l'analyse des données de plus d'une centaine de marques satellites déployées sur des tortues caouannes, en vue de mieux comprendre leurs préférences thermiques afin de paramétrer leurs habitats au sein d'une version simplifiée de SEAPODYM. Enfin, le dernier chapitre présentera l'adaptation de SEAPODYM à l'espadon et ses limitations et tentera de mettre en relation les habitats prédits pour les deux espèces.

CHAPITRE 1

INTRODUCTION

Ce chapitre consiste à présenter l'état des connaissances concernant les deux espèces étudiées lors de ce projet, l'espadon et la tortue caouanne, ainsi que le modèle SEAPODYM, utilisé pour modéliser leurs dynamiques de population.

1. L'ESPADON

BIOLOGIE ET DISTRIBUTION

L'espadon (*Xiphias gladius*, Linnaeus, 1758) est la seule espèce de la famille Xiphiidae. Les espadons adultes sont distribués dans tous les océans entre 50°S et 50°N, englobant toutes les zones océaniques tropicales, subtropicales et tempérées, et occupent de grands intervalles de profondeur, de la surface pendant la nuit jusqu'à plus de 1000 m pendant la journée (Palko 1981, Abecassis et al 2012). Leur distribution varie en fonction de leur taille. Dans le Pacifique, la taille moyenne des captures par palangre augmente avec la latitude, pour les deux sexes (DeMartini 1999). Les juvéniles sont plus abondants dans les zones tropicales et subtropicales.

Leurs mouvements diurnes suivent la DSL (Deep Scattering Layer), dont les changements en profondeur sont dictés par le niveau ambiant de lumière dans l'eau (Carey 1992, Abecassis et al 2012). Ils tolèrent des températures plus extrêmes que la plupart des espèces de thons et de marlins, avec des observations entre 3 et 29 °C (Abecassis et al 2012).

Au contraire des thons tropicaux dont la masse musculaire est dominée par du muscle 'rouge', les espadons possèdent principalement du muscle 'blanc', ce qui leur accorde des capacités d'accélération importantes, mais une moindre endurance (Ward & Elscot 2000). Ils sont néanmoins capables de longues migrations (plus de 4000 km, Abecassis et al 2012) sur plusieurs mois.

Les espadons sont des prédateurs visuels dotés d'une vision exceptionnelle, notamment en eau profonde et froide, grâce à un muscle unique leur permettant de réchauffer leur cerveau et leurs yeux par rapport à la température ambiante (Carey 1982).

La longévité des espadons est d'au moins 15 ans, et leur taux de croissance pendant la première année est très élevé (90 cm en un an). La croissance varie selon les régions et les conditions locales (DeMartini et al 2007). Les femelles atteignent des tailles supérieures (Fig. 1). Les mâles atteignent leur taille maximale vers 9 ans et les femelles vers 15 ans (Wilson & Dean 1983).

Dans les régions tempérées du Pacifique Nord et de l'Atlantique Nord, les espadons sont souvent observés immobiles, comme somnolant en surface pendant la journée (phénomène appelé « basking » en anglais). Les espadons sont alors complètement indifférents à l'activité alentour, ce qui les rend très vulnérables à la pêche au harpon. Les raisons de ce comportement ne sont pas bien comprises. Il est possible que cela leur permette de récupérer physiquement après des périodes prolongées passées en eaux froides ou pauvres en oxygène (Carey 1990, Dewar et al 2011, Abecassis et al 2012).

La structure des stocks d'espadon dans le Pacifique, dont la connaissance est primordiale pour une bonne gestion de la ressource, est encore mal connue. Les études génétiques les plus récentes (Reeb et al 2000, Ward et al 2001, Alvarado-Bremer et al 2006) suggèrent une structure génétique en forme de U couché, avec des différences génétiques significatives entre le nord-ouest et le sud-ouest du Pacifique, et une zone de mélange continu dans le Pacifique est. Les captures par unité d'effort (CPUE) des palangres japonaises présentent deux tendances différentes dans le Pacifique centre-ouest, et le Pacifique est, ce qui a conduit à la définition d'une « frontière » diagonale qui sépare ces deux stocks hypothétiques dans les modèles de gestion des populations récents (Courtney & Piner 2009, Ichinokawa & Brodziak 2010, Brodziak & Ishimura 2011) effectués au sein de l'ISC (International Scientific Committee for Tuna and Tuna-like Species in the North Pacific Ocean).

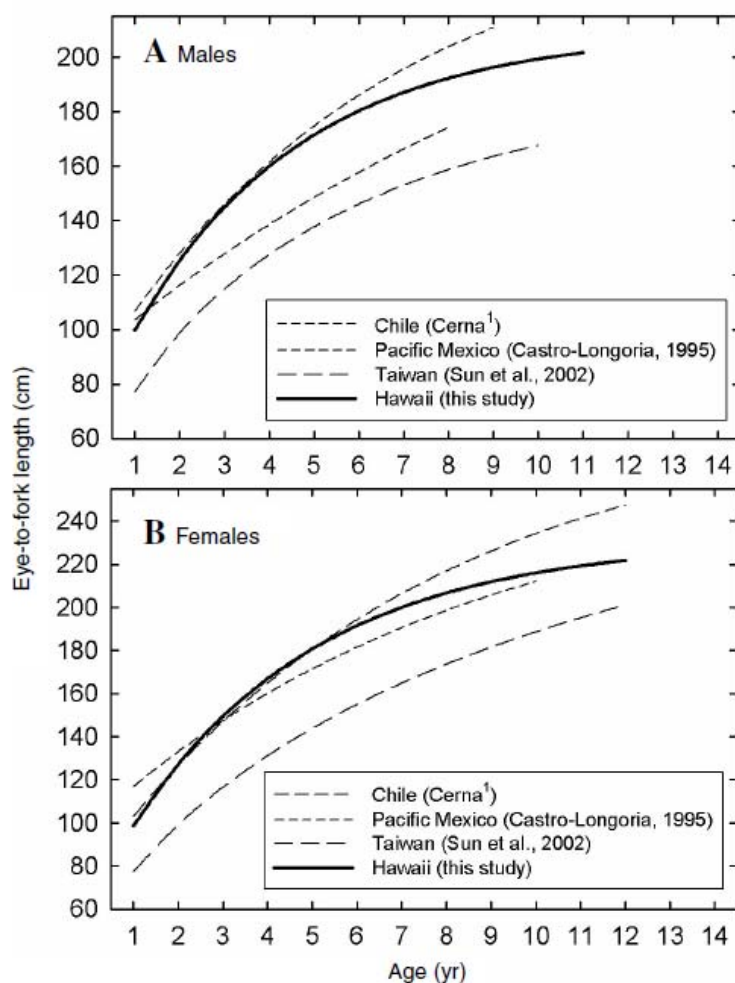


Fig. 1. Croissance des espadons dans le Pacifique (DeMartini et al 2007).

Suivant les études, l'âge de maturité des mâles est estimé entre 1 et 3 ans, et l'âge de maturité des femelles est estimé entre 3 et 5 ans.

Les espadons sont rarement en bancs. Chez l'espadon, la fertilisation est externe, et s'accomplit probablement entre des paires mâle/femelle solitaires, dans la couche de surface (Palko et al 1981). Les femelles pondent des millions d'oeufs, de 1.6 à 1-8 mm de diamètre, qui flottent dans les premiers mètres de la colonne d'eau pendant la journée, mais qui descendent vers 20-30 m pendant la nuit (Nishikawa and Ueyanagi 1974). Dans les eaux équatoriales une femelle peut pondre jusqu'à 3 fois par jour pendant 7 mois (Arocha and Lee 1996).

Les espadons ne semblent pas avoir de zones ou de saisons de reproduction bien définies. Les distributions de larves observées suggèrent que la ponte a lieu dans les eaux de surface dont la température dépasse 24°C, soit entre 35° N et 35° S. Dans les eaux équatoriales, la ponte peut donc avoir lieu toute l'année, alors qu'elle est plutôt limitée au printemps et à l'été aux latitudes plus élevées (Ward & Elscot 2000).

REGIME ALIMENTAIRE

Les espadons sont des prédateurs visuels et dépendent de leur vision exceptionnelle pour localiser leurs proies en eau profonde. Ils utilisent leur rostrum pour assommer leurs proies. Les espadons adultes sont des prédateurs opportunistes et consomment des proies très variées. La majorité de leurs proies est constituée de calmars, de poissons, et dans une moindre mesure de crustacés et de poulpes (Palko et al 1981). La ration journalière de l'espadon a été estimée à 0.9 – 1.6 % de leur poids, soit entre 3 et 6 fois leur poids total par an.

Leur comportement vertical, en profondeur pendant la journée et près de la surface la nuit, suggère qu'ils ciblent une partie de la DSL, dont les mouvements verticaux sont contrôlés par le niveau ambiant de lumière (Carey & Robison 1981, Hays 2003, Chancollon et al 2006, Abecassis et al 2012).

PECHERIES

Les espadons sont principalement pêchés à la palangre, mais de plus faibles volumes de captures sont aussi réalisés par filet dérivant, ou au harpon. D'après la FAO, 94 000 tonnes d'espadon ont été pêchées en 2008, dont 40% dans le Pacifique. Les espadons sont généralement ciblés de nuit à faible profondeur (vers 60 m) par les palangres et les filets dérivants, ou, lorsqu'ils somnolent en surface près des côtes, de jour à la surface par la pêche au harpon. Les espadons sont aussi une prise accessoire importante des palangres qui ciblent le thon, de jour, en profondeur (vers 300 – 400m de profondeur). Il est estimé qu'environ 50% des captures mondiales d'espadon sont des prises accessoires (Ward & Elscot 2001).

Les prises de palangres représentent environ 85% des captures mondiales (Ward & Elscot 2001). Dans le Pacifique, les principaux pays impliqués dans la pêche à l'espadon sont le Japon, Taiwan-RDC, la Corée, le Mexique, les Etats-Unis, et l'Australie (Fig. 2). A l'exception du Pacifique sud-est, la ressource en espadon est généralement considérée comme sous-exploitée (Le Couls & Bourjea 2010) dans le Pacifique.

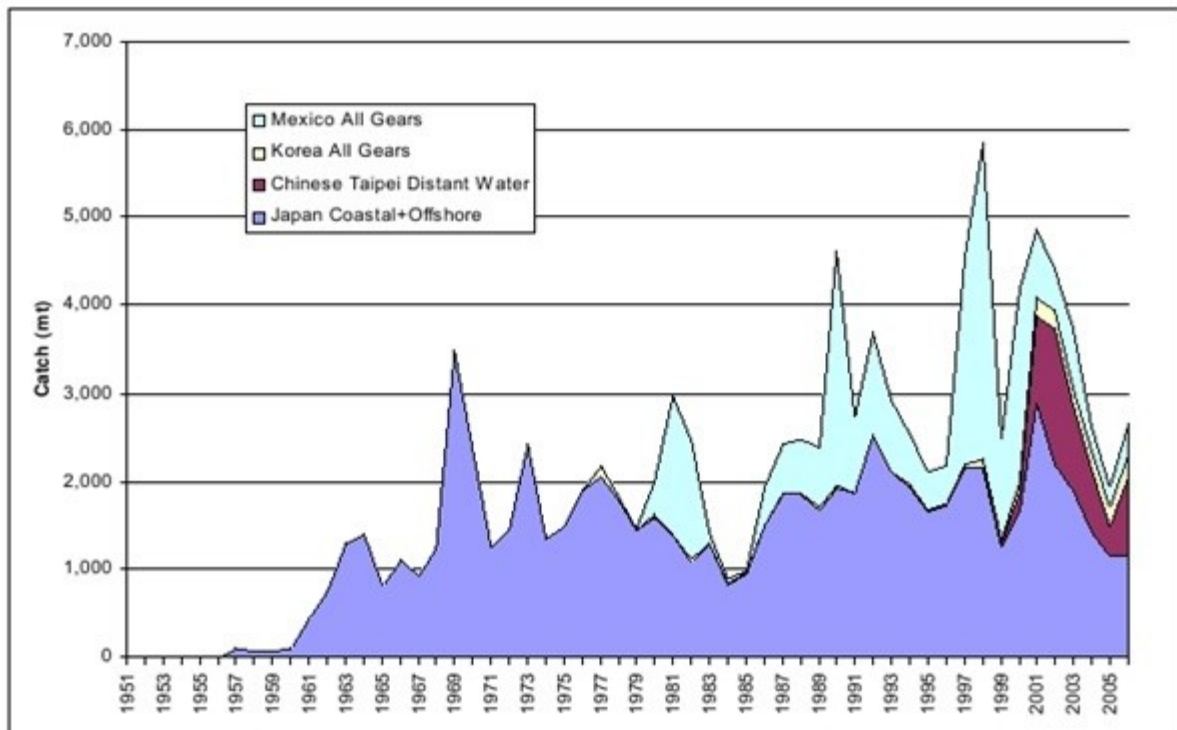
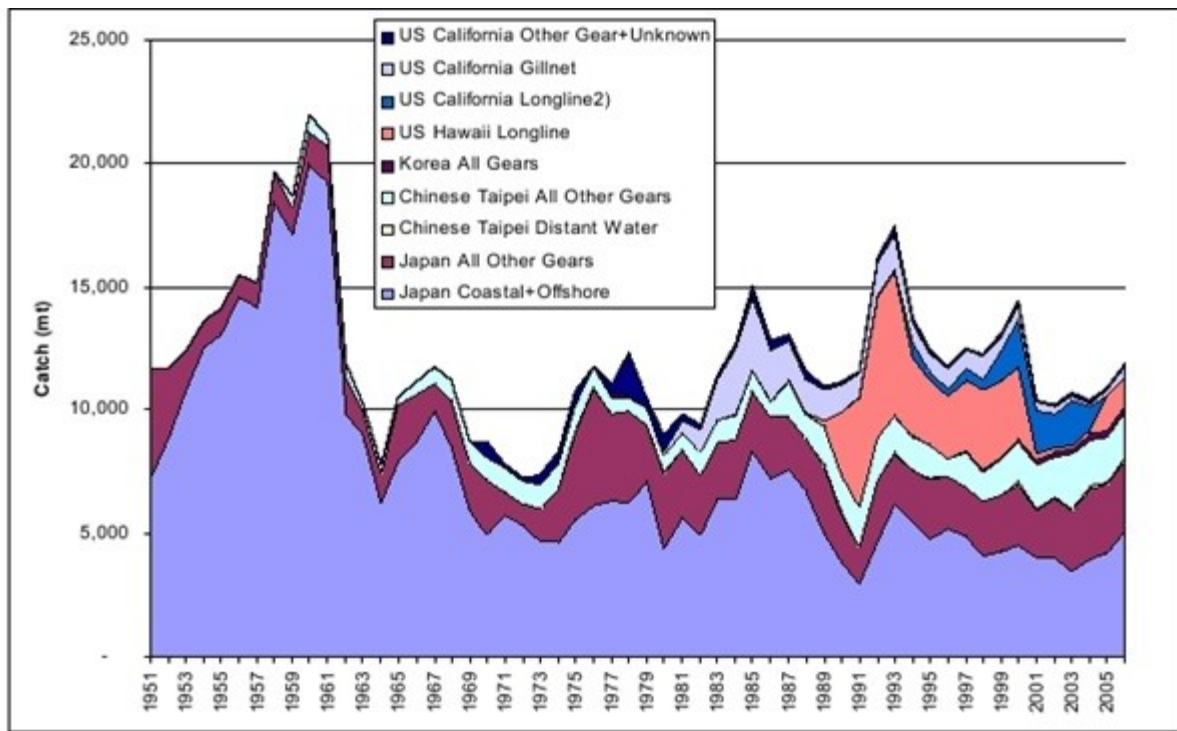


Fig. 2. Captures par pays dans le Pacifique Nord (Courtney & Piner (2009).

2. LA TORTUE CAOUANNE

BIOLOGIE ET DISTRIBUTION

La tortue caouanne (*Caretta caretta*) est l'une des six espèces de tortues marines de la famille Cheloniidae. La septième autre espèce existant de nos jours est la tortue luth (*Dermochelys coriacea*). Trois des espèces de tortues marines (la tortue luth, la tortue imbriquée (*Eretmochelys imbricata*), et la tortue de Kemp (*Lepidochelys kempii*)) sont en danger critique d'extinction d'après l'IUCN (International Union for Conservation of Nature). Trois autres (la tortue verte (*Chelonia mydas*), la tortue olivâtre (*Lepidochelys olivacea*) et la tortue caouanne (*Caretta caretta*)) sont considérées comme en danger d'extinction.

Les tortues caouanne sont distribuées dans les zones tropicales et tempérées de chaque bassin océanique et occupent des habitats pélagiques et côtiers. Elles passent la majorité de leur temps entre la surface et 30 m, mais sont capables de plonger jusqu'à plus de 100 m (Howell et al. 2010, Fig. 1). A l'âge adulte, les mâles possèdent une queue plus longue que les femelles, mais leurs proportions corporelles restent relativement égales.

Le cycle de vie des tortues caouannes (Fig. 2) est constitué d'une série de stades ontogénétiques entre habitats terrestres, côtiers et océaniques, parfois séparés par plusieurs milliers de km. Les seules plages de ponte connues dans le Pacifique se trouvent au Japon, en Australie et en Nouvelle-Calédonie (Kamezaki et al 2003, Limpus & Limpus 2003). Une fois les œufs éclos, les jeunes (mesurant environ 5 cm) quittent les plages de ponte et entrent dans une phase océanique de plusieurs dizaines d'années jusqu'à leur retour dans les habitats côtiers proches des plages de ponte. Cette phase océanique a été appelée "the lost years" (Bolten & Balazs, 1995), à cause de la difficulté rencontrée pour étudier les juvéniles en haute mer et de l'incertitude importante sur sa durée. Quand ils atteignent environ 70 cm (dans le Pacifique, Kobayashi et al 2011), les juvéniles passent alors par une phase de transition pendant laquelle ils alternent entre la haute mer et les habitats benthiques près des côtes, tout en changeant progressivement de régime alimentaire (Kamezaki & Matsui 1997). Dans le Pacifique, une des principales zones côtières d'alimentation se situe le long de la côte de la Basse Californie sud (Pitman 1990, Ramirez et al 1991) et est fréquentée par des individus originaires des plages de ponte japonaises essentiellement et australiennes plus rarement (Bowen et al 1995). Les adultes en âge de se reproduire (95 cm en moyenne dans le Pacifique, Limpus & Limpus 2003) quittent les zones d'alimentation pour retourner sur les plages de ponte. Les femelles pondent de une à sept fois par saison de ponte (Dodd, 1988) et l'intervalle moyen entre deux saisons de ponte a été estimé à 2,5 – 3 ans. Les tortues caouannes sont généralement fidèles à leurs zones de ponte et d'une saison sur l'autre, la distance entre leurs sites de ponte dépasse rarement 1 km.

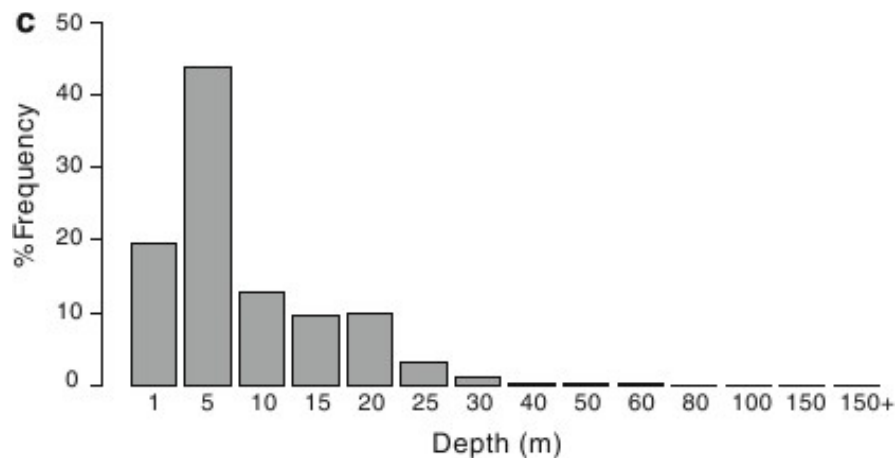


Fig. 1. Proportion de temps passé à chaque profondeur, estimé pour 14 juvéniles dans l’océan Pacifique Nord central. (Howell et al 2010)

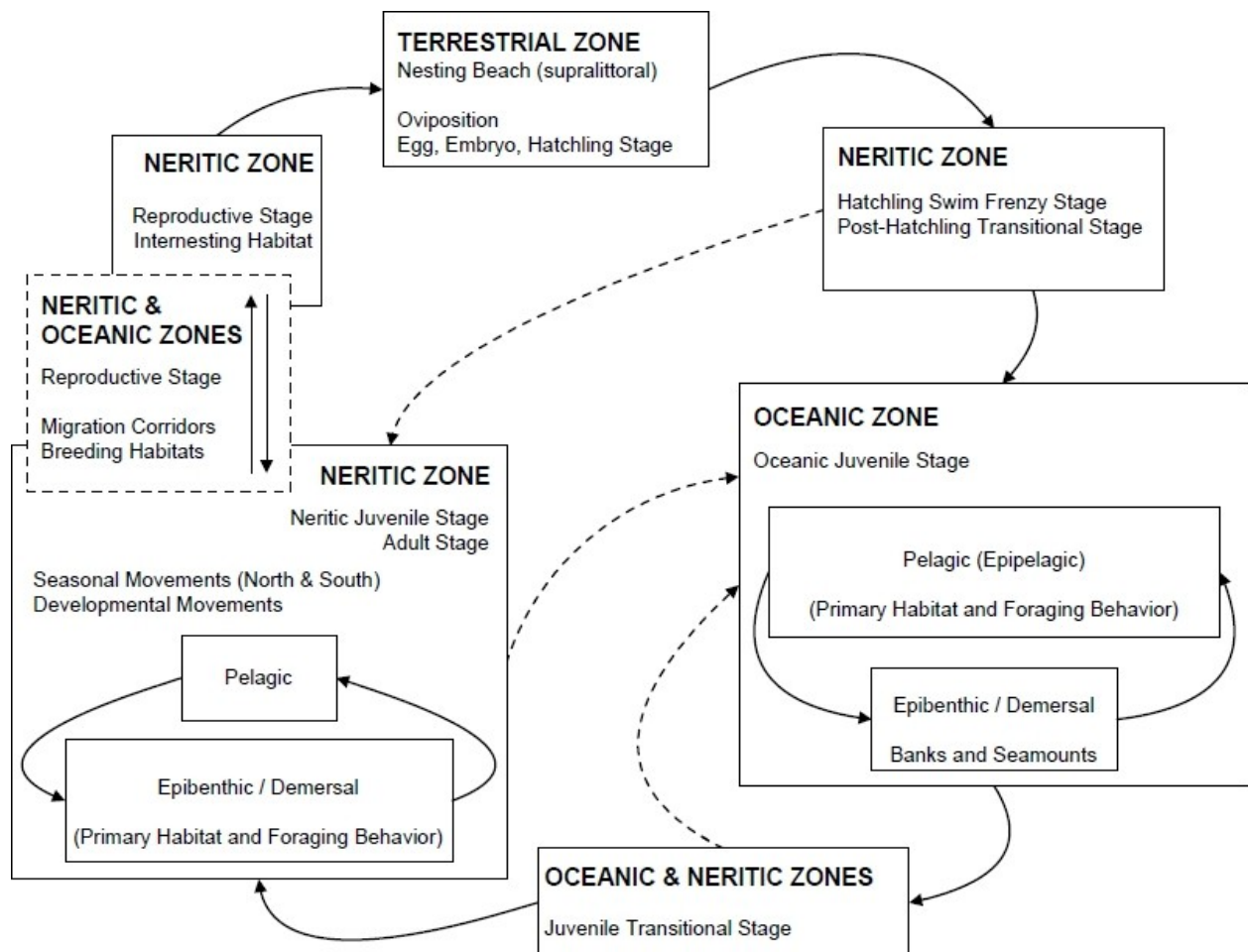


Fig.2 : Cycle de vie de la tortue caouanne dans l’Atlantique. Chaque boîte représente une phase biologique et l’écosystème correspondant. Les flèches pleines représentent les mouvements entre les différentes phases et écosystèmes, les lignes pointillées sont hypothétiques. (Bolten 2003, chap. 4)

Les adultes mesurent généralement entre 70 et 100 cm et peuvent peser jusqu'à 200 kg. Les juvéniles grandissent d'environ 10 cm par an. Le taux de croissance suit un modèle log-linéaire et une étude récente (Scott et al 2011) estime l'âge de maturité aux alentours de 45 ans (précédemment estimé entre 9 et 39 ans), ce qui positionnerait les tortues caouannes parmi les reptiles qui atteignent leur maturité le plus tard. Cette nouvelle estimation accentue encore les inquiétudes portées sur le futur de cette espèce.

Dans leurs habitats océaniques dans le Pacifique, les tortues caouannes sont généralement carnivores et se nourrissent principalement d'espèces neustoniques (flottant à la surface) : *Janthina spp.*, *Carinaria cithara*, *Velella velella*, *Lepas spp.*, *Planes spp.*, et de pyrosomes (Parker et al, 2005). Dans les habitats néritiques, elles se nourrissent essentiellement d'invertébrés. Les tortues caouannes sont généralistes, et plus de 200 taxons de leurs proies ont été répertoriés (Dodd 1988, Limpus et al. 2001).

MENACES ET INTERACTIONS AVEC LES PECHERIES

Les tortues caouannes sont exposées à de nombreuses menaces à chaque stade de leur vie (Fig. 3). Il est difficile d'en quantifier les impacts relatifs pour obtenir un modèle de dynamique de population robuste, mais un déclin d'environ 80% des femelles pondeuses a été observé dans le Pacifique entre 1970 et 2000 (Kamezaki et al. 2003, Limpus & Limpus 2003), ce qui a motivé de nombreux efforts de conservation à chaque stade biologique.

Ces menaces incluent : l'ingestion de débris marins, la contamination environnementale, des maladies (notamment le virus fibropapillomatosis), les pertes ou altérations des plages de ponte, l'éclairage artificiel des plages (ce qui désoriente les nouveau-nés), et les interactions avec les pêcheurs (prises accidentelles, étranglement dans les filets ou les lignes). Au contraire des tortues vertes et imbriquées, la chair et la carapace des tortues caouannes ne sont pas prises commercialement, mais elles partagent les mêmes habitats que nombre d'espèces commercialement importantes, ce qui rend leurs interactions avec les pêcheurs très significatives.

Les tortues caouannes sont principalement victimes de deux types de pêcheries : les palangres (ciblant le thon et l'espadon notamment) et les pêches au filet maillant et au chalut. Les palangres impactent surtout les juvéniles en haute mer, alors que les pêcheries au filet maillant et les chaluts, qui sont généralement des pêcheries plus côtières, impactent notamment les adultes et sub-adultes.

Lewison et al. (2004) estimèrent qu'environ 220 000 tortues caouannes furent victimes d'interactions avec les palangres mondiales en 2000. Dans l'océan Pacifique, la population totale était estimée à 335 000, dont 67 000 dans des classes d'âge vulnérables aux palangres. Le nombre d'interactions avec les palangres dans le Pacifique fut estimé à environ 30 000, soit 45% de la population vulnérable. Cette estimation combinée aux estimations de mortalité effectuées par la NOAA (National Oceanic & Atmospheric Administration, USA) suggère un total d'interactions mortelles avec les palangres entre 2600 et 6000 en 2000 dans le Pacifique seulement.

Par ailleurs, Lewison & Crowder (2007) estimèrent que les pêches au filet maillant pourraient avoir un impact au moins aussi important que les palangres. Ces pêcheries sont moins étendues et sont concentrées dans les zones côtières, mais le taux de mortalité reporté est de près de 50% (contre 4 à 9% pour les palangres, Argano et al. 1992, Laurent 2001).

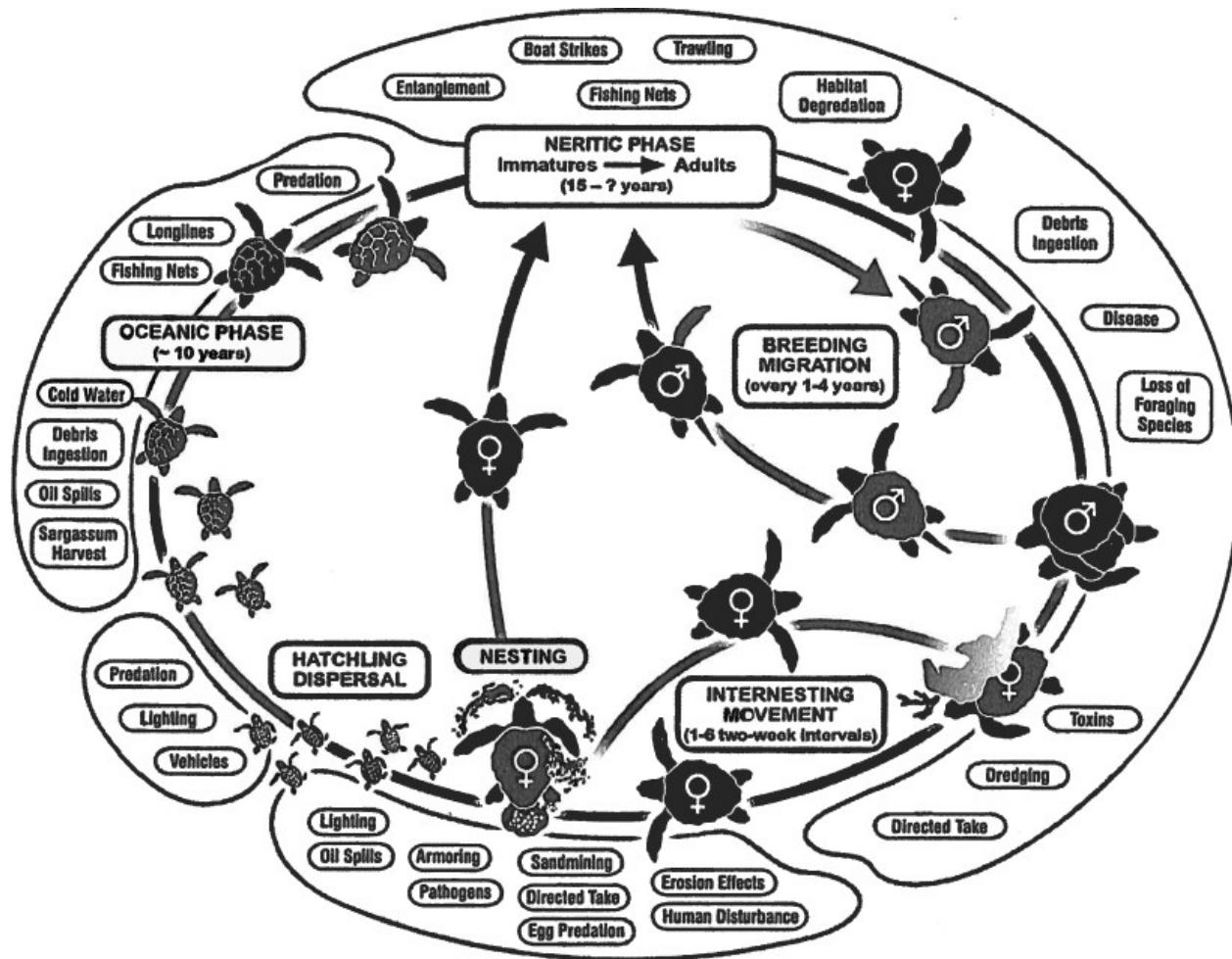


Fig. 3. Un modèle de cycle de vie des tortues caouannes cataloguant les différentes menaces potentielles à chaque stade biologique (Witherington 2003)

Au cours des 20 dernières années, de nombreux efforts de recherche et de conservation (Gilman et al 2006, 2007, Swimmer 2009) ont été menés pour tenter de réduire l'impact et le nombre des interactions avec les palangres. Des types d'hameçons différents ont été testés et progressivement adoptés pour limiter leur risque d'ingestion et faciliter la libération des tortues. (Fig. 4, Gilman et al 2007). Différents types d'appâts furent testés et dorénavant le maquereau est utilisé à la place du calmar. Diverses expérimentations ont été menées sur la configuration des lignes de pêche (profondeur, nombre et espacement des hameçons) pour réduire la zone d'interaction entre les lignes et les tortues. Les tortues sont particulièrement vulnérables aux palangres qui ciblent l'espadon près de la surface pendant la nuit. Les palangres ciblant le thon sont généralement déployées en eaux plus profondes, mais les configurations classiques comportent néanmoins un nombre non négligeable d'hameçons dans la couche de surface. Plusieurs suggestions ont été faites pour limiter ou supprimer les hameçons dans les eaux de surface (Fig. 5, Beverly et al 2004, 2009), ou pour évaluer la faisabilité de cibler l'espadon de jour en profondeur plutôt que de nuit près de la surface (Boggs 2003, Abecassis et al 2012). Enfin, plus récemment, des efforts de modélisation ont été réalisés pour tenter de prédire les zones de présence des tortues et offrir des recommandations aux pêcheurs pour les aider à éviter les zones d'interaction les plus probables (Fig. 6, Howell et al 2008, Abecassis et al, in prep, Chap. 3).



Fig. 4. Un hameçon Mustad 9/0 J (gauche) et un hameçon circulaire Lingren-Pitman avec un décalage de 10° (droite, Gilman et al 2007). Ce dernier modèle réduit grandement le taux de mortalité des tortues en leur permettant de se libérer plus facilement.

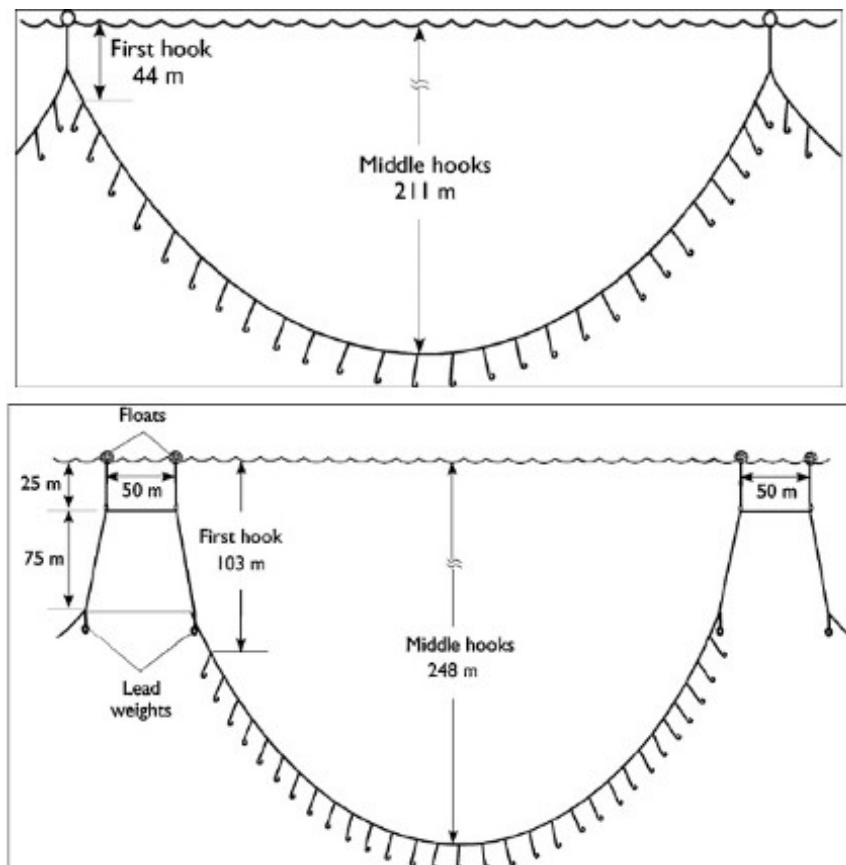
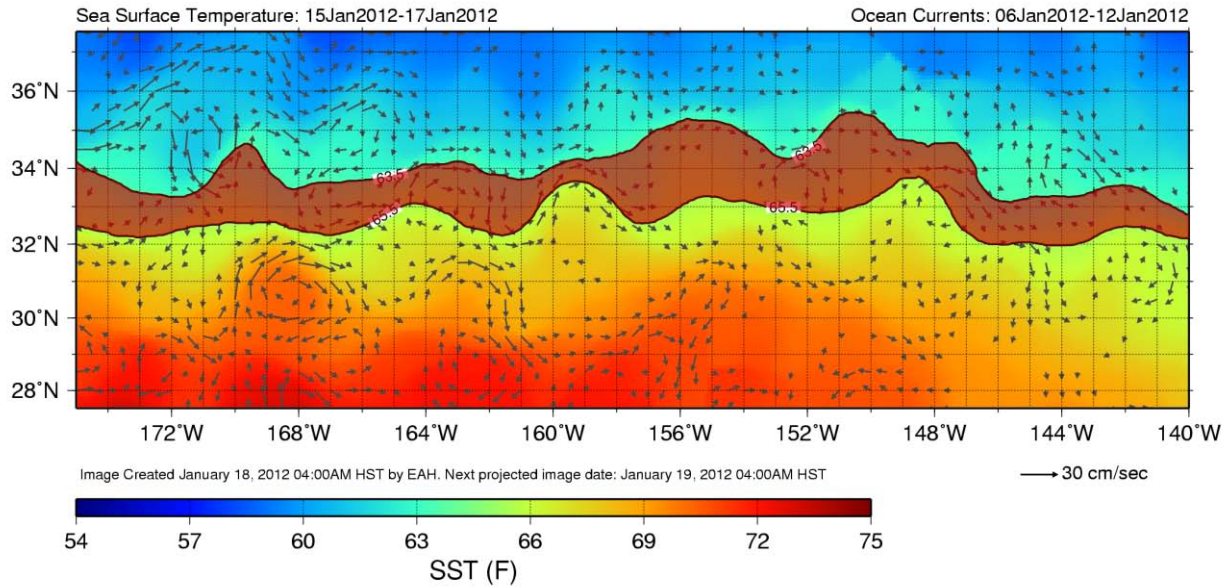


Fig.5. Exemple de changement proposé pour les palangres ciblant le thon obèse, pour éliminer les hameçons présents dans la gamme de profondeur fréquentée par les tortues près de la surface (Beverly et al 2009).

EXPERIMENTAL PRODUCT

avoid fishing between solid black 63.5°F and 65.5°F lines
to help reduce loggerhead sea turtle interactions



PACIFIC ISLANDS FISHERIES SCIENCE CENTER
ECOSYSTEMS AND OCEANOGRAPHY DIVISION
2570 Dole Street, Honolulu, HI 96822
<http://www.pifsc.noaa.gov/eod/turtlewatch.php>
contact: Evan.Howell@noaa.gov
Data provided by Central Pacific CoastWatch node

TURTLEWATCH



Fig. 6. Produit TurtleWatch élaboré par la NOAA et distribué gratuitement en ligne pour informer les pêcheurs sur les zones à éviter du fait de la forte probabilité de présence de tortues.

3. SEAPOODYM

SEAPOODYM (Spatial Ecosystem and Populations DYnamics Model, Fig. 1) est un modèle de dynamique de population de type eulérien, suivant une formulation d'advection-diffusion-réaction (ADR), initialement développé pour les thons tropicaux et progressivement adapté à d'autres espèces. Le modèle a été développé à partir d'un système d'équations ADR utilisé pour décrire les mouvements déduits d'expériences de marquages conventionnels (Sibert et al. 1999). L'approche eulérienne a été étendue à une description mécanistique des mouvements basés sur un gradient d'habitat (Bertignac et al. 1998, Lehodey 2001, Lehodey et al 2003) incluant une approche nouvelle pour la représentation des proies (Lehodey et al. 1998). Au fur et à mesure que les applications du modèle se diversifiaient, des versions de plus en plus élaborées du modèle se sont ensuite succédées pour améliorer les mécanismes, en intégrer de nouveaux, et ajouter une dimension verticale simplifiée (Lehodey 2004 a&b; Lehodey et al, 2008, 2010a). La mise au point de l'approche d'estimation des paramètres du modèle à partir de données de pêche avec des techniques de maximum de vraisemblance (Senina et al. 2008) a transformé le modèle en un véritable outil de gestion de population dans un cadre écosystémique, permettant d'estimer l'abondance d'une population exploitée et sa variabilité sous l'influence de l'environnement ou de scénarios climatiques, d'identifier l'impact de la pêche et de tester des scénarios de gestion (Lehodey & Senina 2009; Lehodey et al 2010b, c&d, 2011; Sibert et al. 2011).

Les principales caractéristiques du modèle sont résumées ci-dessous. Pour une information plus détaillée, il est nécessaire de se reporter aux références citées ci-dessus.

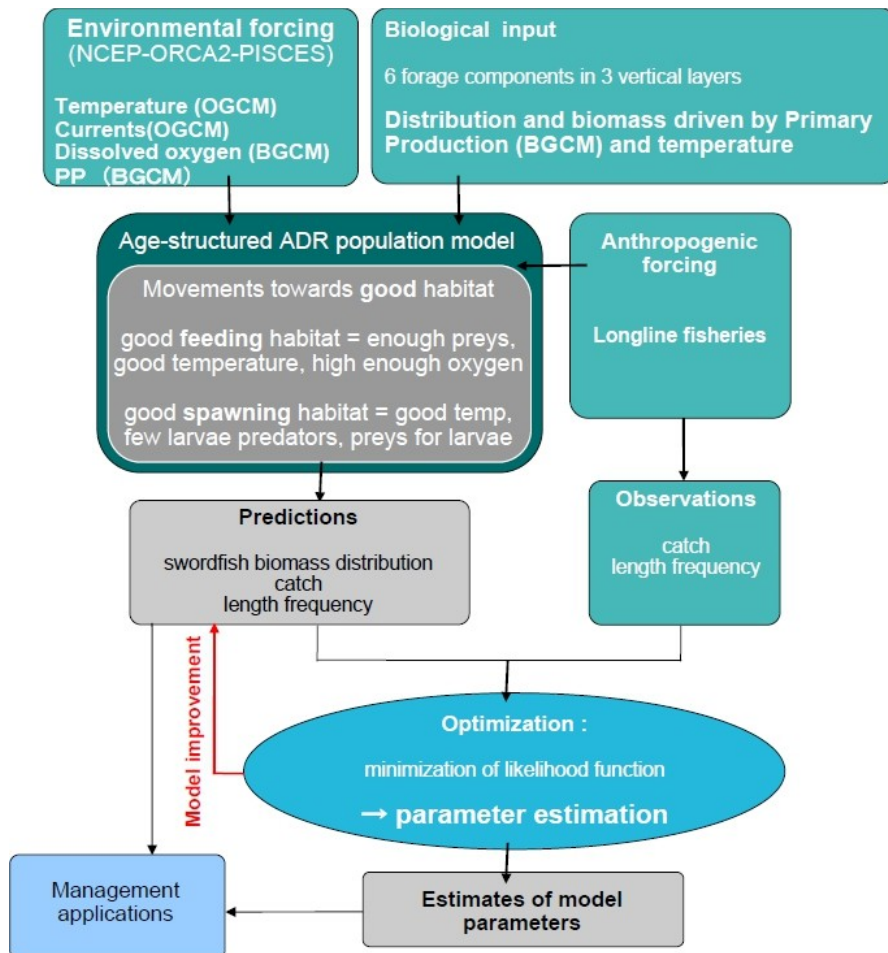


Fig. 1. Schéma général de fonctionnement de SEAPODYM. (adapté de Senina et al 2008).

PREDATEURS-PROIES

Le modèle organise l'écosystème pélagique en plusieurs composantes. Le phytoplancton, associé à la production primaire, est à la base du réseau trophique et sert à définir l'habitat de ponte et la survie larvaire (en considérant une corrélation très forte avec le zooplancton). C'est aussi la source d'énergie des groupes de micronecton qui constituent les proies des prédateurs supérieurs, dont celles étudiées en particulier : thon, espadon, ou tortue marine. Le micronecton, classiquement défini comme l'ensemble des organismes entre 2 et 20 cm, comporte six groupes fonctionnels caractérisés selon leur habitat et leur comportement vertical (Fig. 2). Les populations de prédateurs sont structurées en classes d'âge réparties sur quatre stades biologiques (Fig. 3) : les larves, soumises passivement aux courants et aux conditions d'alimentation sur le phyto- et zooplancton et de prédation par le micronecton ; les juvéniles, également soumis passivement aux courants et aux conditions d'habitat pouvant inclure la prédation par les cohortes plus âgées (cannibalisme) ; les jeunes immatures et les adultes matures capables de mouvements propres pour se diriger vers les conditions plus favorables d'alimentation, et le cas échéant, de ponte. Les courbes de croissance (en taille et en poids, documentées dans la littérature) de l'espèce, sont données en entrée du modèle.

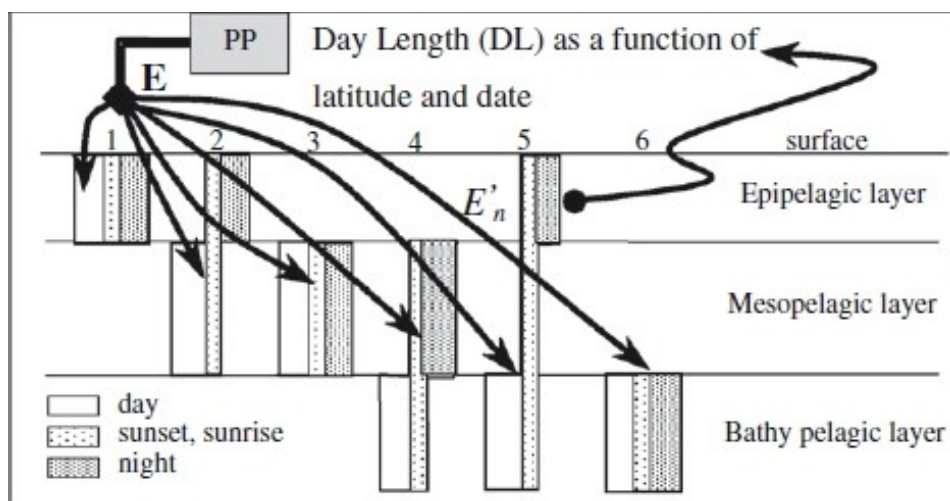


Fig. 2. Schéma conceptuel décrivant la répartition en 6 groupes du micronecton selon leur distribution verticale dans la colonne d'eau et leur comportement migrant/non-migrant (Lehodey et al 2010).

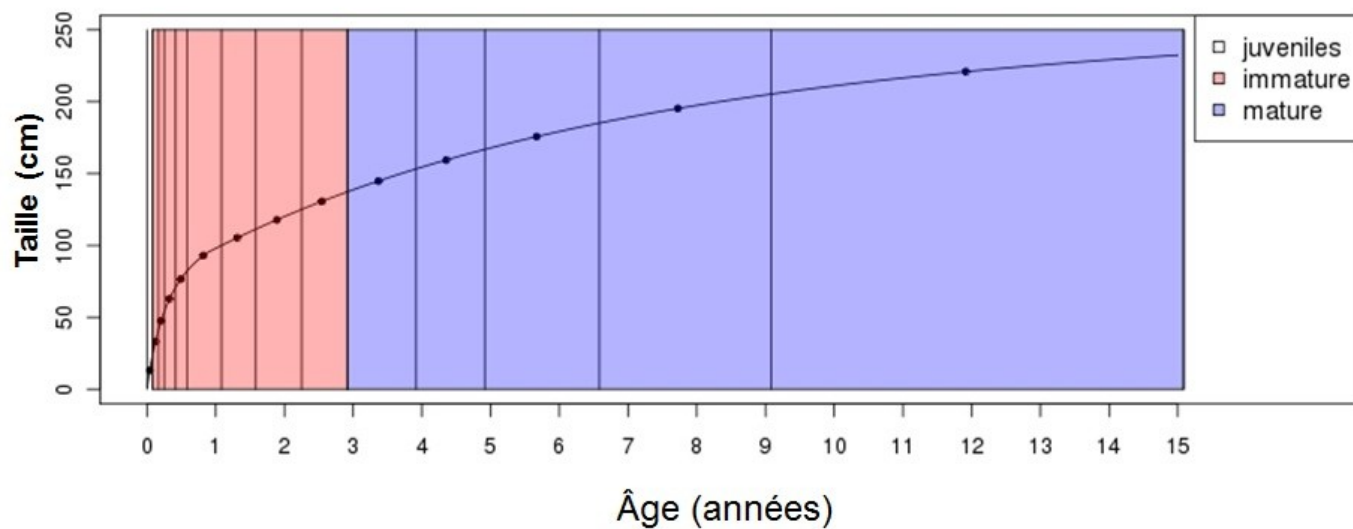


Fig. 3. Courbe de croissance moyenne de l'espadon dans le Pacifique décrivant les différents stades biologiques. Etant donné le taux de croissance très élevé de l'espadon pendant la première année et le pas de temps mensuel utilisé dans cette étude (cf. chapitre 3), le stade larvaire a été omis et une seule classe mensuelle de juvéniles a été prise en compte.

Dans SEAPODYM, l'océan est modélisé en trois couches verticales : la couche épipélagique (entre la surface et la profondeur euphotique, Z_{eu}), la couche mésopélagique (entre Z_{eu} et $3 \cdot Z_{eu}$), et la couche bathypélagique (entre $3 \cdot Z_{eu}$ et 1000 m). Le modèle utilise des champs d'entrée décrivant les conditions environnementales physiques et biogéochimiques de l'océan, issus de modèles de circulation générale couplés à des modèles de biogéochimie. Les champs utilisés en entrée de SEAPODYM sont la température, les vitesses zonales (est-ouest) et méridionales (nord-sud) des courants océaniques, et la concentration d'oxygène dissous. Ces champs sont moyennés sur chacune des trois couches, tandis que la production primaire est intégrée verticalement.

HABITAT THERMIQUE

Dans le contexte de dynamique de population de SEAPODYM, on considère qu'à l'échelle de la population, l'habitat thermique d'une classe d'âge donnée peut être représenté par une distribution gaussienne, dont la moyenne est liée à la température corporelle à l'équilibre et l'écart-type à l'inertie thermique du poisson, tous deux évoluant avec la taille du poisson (Fig. 4). L'inertie thermique augmentant avec l'âge, les poissons ciblent des températures progressivement plus basses et supportent des gammes de températures de plus en plus larges.

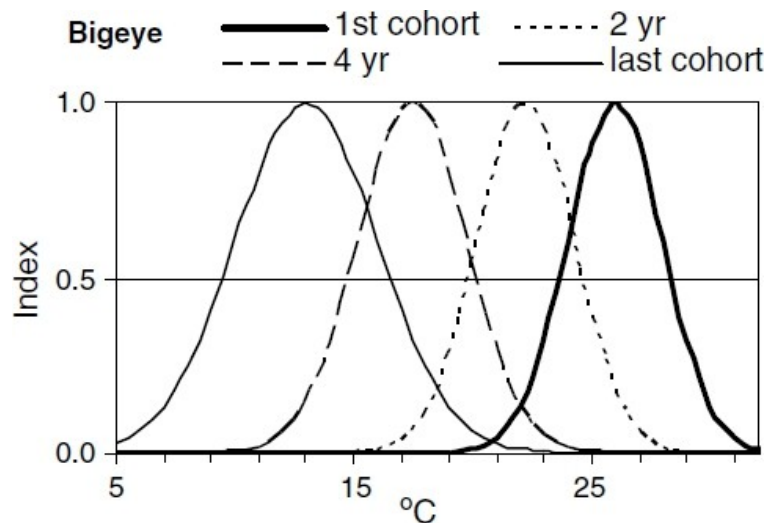


Fig. 4. Exemple de définition de l'habitat en température pour le thon obèse, pour 4 classes d'âge différentes, avec une température moyenne décroissante et un écart type croissant avec l'âge. (Lehodey et al 2008).

CONTRAINTE EN OXYGENE

Chaque espèce a développé un seuil de tolérance différent face aux faibles concentrations en oxygène dissous dans l'océan. Dans une gamme de température favorable, un poisson est généralement limité verticalement par la concentration en oxygène minimale qu'il peut tolérer. Cette contrainte est modélisée dans SEAPODYM par une fonction sigmoïde donnant un indice entre 0 et 1, caractérisé par la valeur seuil correspondant à l'indice 0.5 (Fig. 5).

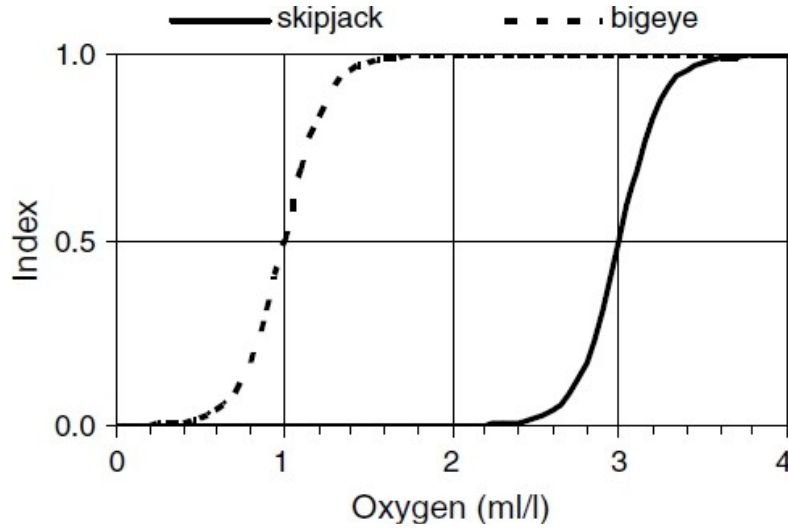


Fig. 5. Exemples d'indices de tolérance en oxygène pour le thon obèse (valeur seuil : 1 ml/ l) et la bonite (valeur seuil : 3 ml/l). (Lehodey et al. 2008)

HABITAT D'ALIMENTATION (H_F)

L'habitat d'alimentation est défini par un indice normalisé entre 0 et 1, représentant l'adéquation entre la présence et la concentration de proies d'une part et leur accessibilité (Θ_z) par chaque classe d'âge d'autre part. Cette accessibilité dépend des conditions physiques (température et concentration en oxygène pour les thons et espèces associées) dans la couche verticale (z) occupée par chaque groupe de micronecton, de jour et de nuit. Elle est égale au produit des fonctions définissant l'habitat thermique et la contrainte en oxygène.

H_F est donc la somme des biomasses des groupes fonctionnels de micronecton (F_n) pondérées par l'accessibilité aux couches habitées par ces groupes. Lorsqu'un groupe de micronecton migre d'une couche à l'autre entre le jour et la nuit, la température et la concentration en oxygène utilisées sont calculées par une moyenne pondérée par la durée du jour et de la nuit.

L'habitation d'alimentation pour n groupes de micronecton est donc :

$$H_F = \sum_z \Theta_z \left(F_{zz} + \tau \sum_{k \neq z} F_{zk} + (1 - \tau) \sum_{k \neq z} F_{kz} \right)$$

Avec τ la durée (fraction) de jour sur 24h à la date donnée, z et k les indices identifiant les couches occupées de jour et de nuit respectivement suivant la matrice ci-dessous, dont les éléments diagonaux constituent les groupes résidents et les éléments non-diagonaux les groupes migrants.

$$F = \begin{pmatrix} F_{11} & 0 & 0 \\ F_{21} & F_{22} & 0 \\ F_{31} & F_{32} & F_{33} \end{pmatrix}$$

HABITAT DE PONTE (H_S)

L'habitat de ponte est utilisé pour contraindre le succès de la ponte aux zones de conditions environnementales favorables. Le gradient de cet habitat sert également à diriger la biomasse des adultes en âge de se reproduire vers les zones de ponte favorables. Il est défini par l'adéquation entre une température optimale pour les larves, la présence de nourriture pour les larves (production primaire) selon le principe de match/mismatch de Cushing (1975), et la densité de prédateurs des larves (micronecton dans la couche de surface de jour et de nuit). La quantité d'œufs recrutés au final dans une cellule du modèle à un temps donné est le produit de cet indice d'habitat et d'un coefficient de type stock-recrutement de Beverton-Holt, définissant le succès de ponte en fonction de la biomasse de ponte.

MOUVEMENTS

Les mouvements sont dirigés selon un système d'équations d'advection-diffusion. L'advection est la somme de l'advection par les courants océaniques et du mouvement dirigé des poissons selon le gradient d'habitat. La diffusion représente la dispersion des animaux. Elle dépend également de l'indice d'habitat. L'advection et la diffusion sont toutes deux liées à la taille de l'animal utilisée pour exprimer une vitesse maximum soutenable (MSS), ainsi qu'à l'indice et au gradient d'habitat en un point donné, de sorte que les individus auront tendance à rester dans les zones où l'habitat est favorable et à quitter les zones défavorables dans la direction où le gradient d'habitat est maximal, d'autant plus rapidement que l'habitat est défavorable.

COMPORTEMENT D'ALIMENTATION ET DE PONTE

Dans SEAPODYM, le basculement d'un comportement d'alimentation vers celui de ponte s'effectue par une transition entre l'utilisation des indices correspondant pour contrôler le déplacement. La transition (uniquement pour les individus en âge de se reproduire) est contrôlée par le gradient de la durée du jour (qui varie avec la latitude). Ainsi, lorsque le taux d'allongement des journées dépasse un certain seuil, les adultes matures commencent à se diriger vers les zones correspondant à un fort index d'habitat H_s (généralement situées dans les régions tropicales pour les thons et les espadons). Logiquement, la transition interviendra plus tôt dans l'année pour les animaux situés aux latitudes les plus élevées (donc les plus éloignés des tropiques, Fig. 6). Aux basses latitudes, le gradient est trop faible, et l'habitat des adultes est uniquement contrôlé par l'indice d'habitat d'alimentation, rendant la reproduction opportuniste, c'est-à-dire dépendant des conditions de ponte rencontrées sur les zones prospectées pour s'alimenter.

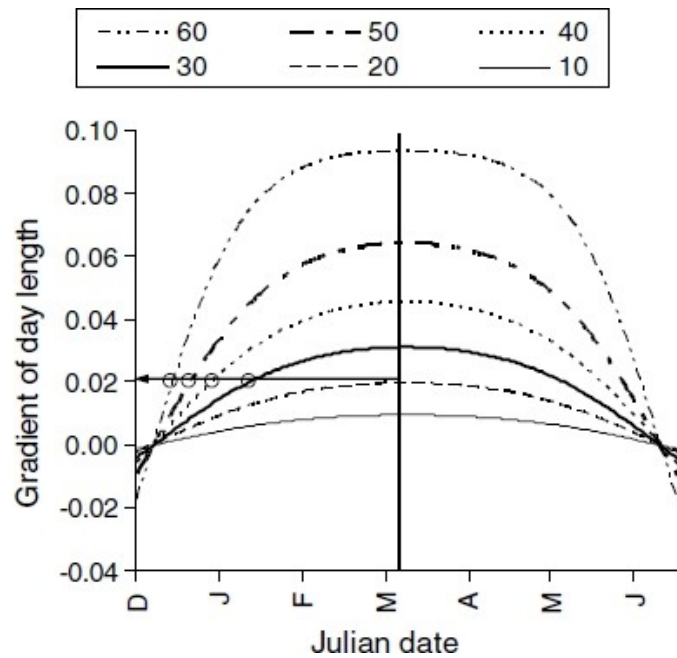


Fig. 6. Exemples de cycles saisonniers de la durée du jour à différentes latitudes dans l'hémisphère Nord (Lehodey et al 2008).

MORTALITE NATURELLE

Le taux moyen de mortalité naturelle par cohorte (Fig. 7) est la somme de deux fonctions :

- une fonction exponentielle décroissante avec l'âge représentant la mortalité des premières cohortes (principalement par prédation et par manque de nourriture)
- une fonction exponentielle croissante pour les cohortes adultes, représentant la mortalité due à la sénescence et aux maladies.

Ce taux moyen est autorisé à varier dans une certaine gamme de valeurs dans le temps et l'espace en fonction des conditions locales, notamment les besoins nutritionnels.

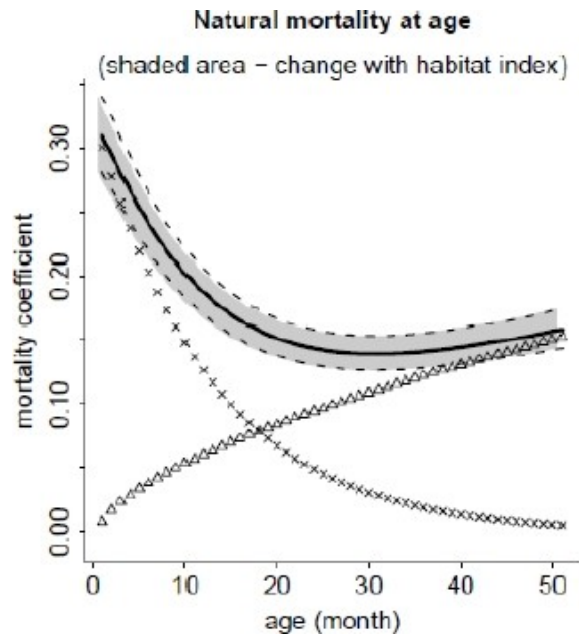


Fig. 7. Exemple de courbe de mortalité naturelle (Lehodey et al 2011)

BESOINS NUTRITIONNELS

L'indice de besoin nutritionnel a été élaboré pour ajuster le taux de mortalité naturelle localement, en fonction de la compétition intra et inter spécifique. Cet indice est la somme, normalisée, des besoins nutritionnels de chaque cohorte relativement aux besoins de l'ensemble des autres cohortes et à la biomasse de proies disponible. Il est conçu pour varier entre 0 et 1, valant 0 quand le besoin nutritionnel total en un point est très supérieur à la nourriture disponible, et 1 dans le cas inverse. Il dépend de la concentration de micronecton dans chaque couche, de la ration quotidienne nécessaire à chaque cohorte, du poids moyen d'un individu dans chaque cohorte, et de l'accessibilité relative à chaque groupe de micronecton durant le jour ou la nuit.

MORTALITE PAR PECHE

Chaque pêcherie est représentée dans le modèle par une fonction de sélectivité (variant avec l'âge, Fig. 8) et un coefficient de capturabilité. L'effort de pêche observé fourni par les organismes de pêche régionaux est utilisé en entrée du modèle pour simuler les captures.

Comme chaque pêcherie est représentée par une seule sélectivité et une seule capturabilité (éventuellement pouvant croître ou décroître linéairement), un grand soin est nécessaire pour s'assurer que chaque pêcherie implémentée au sein du modèle correspond à une pêcherie homogène en termes de technique de pêche utilisée, et d'espèce ciblée.

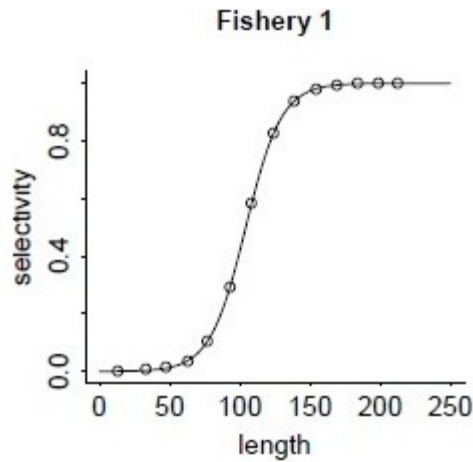


Fig. 8. Exemple de fonction de sélectivité pour une pêcherie de palangre.

OPTIMISATION ET VALIDATION

A partir de l'effort observé pour chaque pêcherie et de la définition de la capturabilité et sélectivité, le modèle prédit des captures qui peuvent être comparées aux captures observées au sein d'une fonction coût (Fig. 1), et les paramètres sont ainsi automatiquement estimés par maximum de vraisemblance. Cette approche d'assimilation de données permet d'accorder une plus grande confiance aux paramètres d'habitat et aux prédictions faites par le modèle.

Au terme de la procédure d'optimisation, l'ajustement des captures prédites par le modèle (spatialement et temporellement) aux captures observées est mesurée à l'aide de plusieurs métriques: R^2 , goodness of fit, puis le modèle est testé sur une période qui n'a pas été utilisée dans la phase d'optimisation, et l'adéquation entre captures observées et prédites est à nouveau évaluée pour s'assurer que le modèle n'est pas « sur-ajusté » et représente bien des mécanismes plutôt que des tendances dans les données.

MOVEMOD

Dans une approche exploratoire ou lorsque la structure en âge de l'espèce étudiée, la mortalité ou la reproduction ne sont pas suffisamment documentés, une version simplifiée de SEAPODYM peut être utilisée pour étudier les habitats et la dynamique spatiale d'une classe d'âge donnée. C'est le cas notamment, dans cette thèse, pour la tortue caouanne (chap. 2). Cette version du modèle s'appelle Movemod.

Il est également possible, au sein de Movemod, d'étudier l'évolution des distributions de densité d'individus (ex. : tortues) lâchées dans une ou plusieurs cellules de la grille du modèle afin d'étudier les mouvements des animaux une fois leur habitat calibré.

CHAPITRE 2

ANALYSE DE MARQUES SATELLITES ET MODELISATION DE L'HABITAT VERTICAL DIURNE DE L'ESPADON DANS LE PACIFIQUE NORD

(ACCEPTÉ POUR PUBLICATION DANS *MARINE ECOLOGY PROGRESS SERIES*, 04/01/2012)

RESUME

28 marques satellites de la marque Wildlife Computers furent déployées sur des espadons entre 2002 et 2009 dans le Pacifique Nord. 4 furent déployées depuis des palangriers dans le Pacifique central, et 24 par des bateaux pratiquant la pêche au harpon au large de San Diego en Californie.

Ces marques enregistrent la profondeur du poisson, la température de l'eau et le niveau de lumière ambiant. Ces données furent analysées pour étudier le comportement diurne de l'espadon. Les marques transmettent des données abrégées entre 1°S et 44°N en latitude et entre 206°E et 249°E en longitude. Cinq des marques furent récupérées physiquement, ce qui permit d'analyser la totalité des données haute résolution enregistrées.

Ces données montrent que lorsque les espadons n'ont pas un comportement de somnolence à la surface pendant la journée (« basking »), ils se maintiennent dans un intervalle de lumière ambiante très restreint pendant la journée et la nuit, ce qui suggérerait que les espadons ciblent des organismes de la couche dispersante profonde dont ils se nourrissent de jour comme de nuit.

En l'absence de « basking », la profondeur diurne moyenne des individus marqués varie entre 32 et 760m. La moyenne sur tous les individus est de 375m. 77% de la variabilité de la profondeur diurne moyenne peut s'expliquer par 3 variables environnementales au sein d'un modèle additif généralisé (GAM) : la concentration en chlorophylle de surface, dérivée des données du satellite MODIS-Aqua, la concentration en oxygène dissous à 400m (profondeur choisie pour refléter la moyenne générale de la profondeur diurne des animaux de cette étude), obtenues à partir des données du World Ocean Atlas, et la température de l'eau à 400m, enregistrée par les marques.

Ce modèle, utilisé en mode prédictif, permet de générer des cartes de la profondeur diurne moyenne de l'espadon à l'échelle du bassin. La profondeur prédite au nord d'Hawaii (où opèrent les palangriers) se situe aux alentours de 600m, contre environ 300m au large de la côte Californienne (où opèrent les harponniers).

Actuellement, les palangriers ciblent l'espadon de nuit, près de la surface. Ces pêcheries sont très controversées car les tortues caouannes et les tortues luth, toutes deux menacées d'extinction, en sont des prises accessoires très importantes. Ces espèces de tortues résident principalement dans la couche de surface, et sont extrêmement susceptibles aux lignes déployées par les palangriers, qui restent généralement dans l'eau toute la nuit. Plusieurs essais de palangres de jour ont été conduits ces dernières années sans grand succès, probablement parce que les profondeurs ciblées étaient trop peu profondes, d'après notre modèle, pour capturer des espadons en grand nombre. Les résultats de cette étude pourraient permettre aux palangriers de pêcher l'espadon de jour plutôt que de nuit en leur fournissant une profondeur cible plus adéquate, ce qui améliorerait les captures diurnes, et devraient réduire significativement les prises accessoires d'espèces protégées en éliminant les hameçons proches de la surface, rendus inutiles.

Modeling swordfish daytime vertical habitat in the North Pacific Ocean from pop-up archival tags

Melanie Abecassis¹, Heidi Dewar², Donald Hawn¹, Jeffrey Polovina³

¹Joint Institute for Marine and Atmospheric Research, University of Hawaii, 1000 Pope Rd., Honolulu, HI, 96822, USA

Email : melanie.abecassis@noaa.gov

²Southwest Fisheries Science Center, NOAA Fisheries, 8604 La Jolla Shore Dr., La Jolla, CA 92037 USA

³Pacific Islands Fisheries Science Center, NOAA Fisheries, 2570 Dole St., Honolulu, HI, 96822, USA

ABSTRACT

The daytime foraging depth of swordfish in the North Pacific was investigated with data from an 8-year tagging program, using 28 Wildlife Computer pop-up archival tags deployed on swordfish in the North Pacific. The tags transmitted data, from 1° S to 44° N latitude and from 206° E to 249° E longitude. Five tags were recovered, providing a full archival record that showed that when swordfish did not engage in daytime basking behavior they remained within a narrow range of light level during both day and night, suggesting swordfish stay within a sound scattering layer (SSL) to feed during both day and night. Daytime mean depth of non-basking swordfish ranged from 32 to 760 m. Seventy-seven percent of the daytime mean depth could be explained with a generalized additive model (GAM) that used 3 environmental indices: satellite-derived surface chlorophyll as a proxy for light at depth, oxygen at 400 m obtained from the World Ocean Atlas, and temperature at 400 m inferred from the tag data. This model used in a predictive mode generated a basin-wide map of swordfish daytime mean depth that showed depths exceeding 600 m to the north of Hawaii shoaling to 300 m off the coast of California. This information could improve daytime swordfish catch by longliners and potentially allow them to switch from shallow night sets that result in interactions with sea turtles. This approach in effect defines the habitat of swordfish prey, giving us insight into the vertical behavior of those mid-trophic level organisms inhabiting the SSL. Our model could be easily applied to other deep-foraging species.

keywords : *Xiphias gladius*, swordfish, satellite tracking, Generalized additive model, habitat modeling

INTRODUCTION

The swordfish (*Xiphias gladius*) is a globally distributed highly migratory species of billfish whose habitat in the Pacific Ocean ranges from 50°S to 50°N and from the surface to depths greater than 1000 m. Swordfish support important commercial fisheries in all ocean basins as well as the Mediterranean Sea, most of which use shallow-set longlines. In 2008, more than 94,000 mt of swordfish were harvested worldwide, with 40% of the catch from the Pacific Ocean (<http://www.fao.org/fishery/statistics/global-capture-production/en>, accessed 01/10/2011). The two main gear types used to target swordfish in the North Pacific are shallow-set longlines and drift gillnets. Using either gear type, swordfish are typically targeted at night in the upper part of the water column. Unfortunately, the near-surface waters are where the overlap between swordfish and non-target species is the greatest. As a result, swordfish fisheries have been the focus of dramatic management actions to reduce bycatch, most notably because of their interactions with loggerhead (*Caretta caretta*) and leatherback (*Dermochelys coriacea*) sea turtles. Both of these species are considered to be endangered in most oceans (Lewison et al. 2004, Garcia-Cortes & Mejuto 2005, Watson et al. 2005, Baez et al. 2007, Gilman et al. 2007, Petersen et al. 2009, Piovano et al. 2009). Loggerhead turtles were relisted as endangered in the North and South Pacific by the National Marine Fisheries Service and the U.S. Fish and Wildlife Service in September 2011. Developing a quantitative understanding of factors influencing the vertical movement of swordfish will help determine the potential for targeting swordfish while avoiding sea turtles.

Despite the commercial importance of swordfish, limited tagging studies have been conducted in the North Pacific (Carey & Robison 1981, Takahashi et al. 2003, Sepulveda et al. 2010, Dewar et al. 2011). Carey & Robison (1981) used acoustic telemetry to follow 5 swordfish during 1 to 6 days in Baja California, Mexico. Holts et al (1994) acoustically tracked one swordfish in the Southern California Bight for 24 h. Takahashi et al. (2003) recovered an archival tag deployed on a swordfish off the coast of Japan and examined vertical movement patterns and inferred possible tracks for the 11-month deployment. Sepulveda et al. (2010) present observations from 9 pop-up satellite archival tags (PSAT) that were deployed and recovered in the Southern California Bight, with deployments ranging between 1 and 89 days. Dewar et al. (2011) compiled observations from 9 and 15 swordfish tagged in the central and eastern North Pacific, respectively (8 of which, dataset CA1, are also part of this study), with fish being at liberty for 5 to 287 days. Common results across all studies are diel vertical movement patterns with occasional basking events, more frequently observed near shore. The influence of light, temperature, and oxygen on daytime and night-time depths were also investigated (Dewar et al. 2011). Despite providing valuable insights into the vertical movement patterns and general behavior of swordfish, none of the deployments using archival and satellite tags in these studies were analyzed with recent geolocation procedures that allow for the estimation of movements between tag and release (Neilson et al. 2009, Lam et al. 2010). Calculation of the tracks allows for more detailed studies of the physical and biological characteristics along the track rather than just at the beginning and end points. This approach increases the ability to quantify the relationship between environment and vertical movement patterns.

This study includes a reanalysis of prior tag data (Dewar et al 2011) and new data spanning 8 years (2002-2009), all deployed in the central and eastern North Pacific Ocean. Specific objectives were to analyze the horizontal and vertical movements of the tagged individuals to improve our understanding of swordfish behavior and help inform fisheries management practices. Recent analytical methods (Neilson et al 2009) were used to calculate daily positions of the fish and to model the impact of environmental factors on vertical movements. This approach provides a broader and more robust assessment of swordfish depth distributions and should advance efforts to target swordfish during the daytime at depth in the longline fisheries.

MATERIALS AND METHODS

TAGGING

Forty-three Wildlife Computer (Redmond, WA, USA) PSATs, versions 2, 3, 4 and MK10, were deployed between 2002 and 2008 on commercial-sized swordfish caught in the Hawaii-based longline and California harpoon fisheries. Estimated weights of tagged fish ranged between 45 and 140 kg.

Central Pacific tags

Fish in the central North Pacific were caught by Hawaii-based commercial longline fishery vessels. The tagging method was identical to that described in Polovina et al. (2008) except that tag placement differed: the hardware tethered to each tag consisted of a single strand of 1.8-mm diameter fluorocarbon line, two stainless-steel sleeves, a single mechanical guillotine (to prevent tag implosion if the tag traveled deeper than 1500 m), and a 3.5×1.7 cm modified titanium dart head. The fish selected for tagging were usually caught during the first 2 hours of the gear-hauling phase, to maximize the condition of tagged fish. If fish were in good condition, their branch line was released from the longline and immediately transferred to a 40-m braided tarred line. The fish was then brought to the side of the vessel and tagged using a modified harpoon with a stainless steel applicator. The tag was anchored at a depth of 10–12 cm mid-to-posterior to the base of the dorsal fin. The fish was subsequently released by severing the leader closer to the hook.

California tags

The tags were rigged similarly as described above, although two different anchor types were used : a black umbrella dart (see photo in Domeier 2005) and a white nylon dart with two additional hinged flanges, similar to a spear fishing head (Dewar et al. 2011). The tags were deployed off Southern California by the local harpoon fleet. When a swordfish was sighted, a harpoon modified to hold the dart applicator tip was used to tag the fish at the base of the dorsal fin.

TAG PROGRAMMING AND PROCESSING

Programmed tag durations varied from 180 to 305 days.

Temperature bins for Time-at-Temperature data recording were manually set to 14 bins for the MK10 tags: $< 0^\circ$, $0-5^\circ$, $5-7.5^\circ$, $7.5-10^\circ$, $10-12^\circ$, $12-14^\circ$, $14-16^\circ$, $16-18^\circ$, $18-20^\circ$, $20-22^\circ$, $22-25^\circ$, $25-27.5^\circ$, $27.5-30^\circ$, $> 30^\circ$. Similarly, the depth bins were set to : < -1.5 m, $1.5-5$ m, $5-20$ m, $20-50$ m, $50-75$ m, $75-100$ m, $100-150$ m, $150-200$ m, $200-300$ m, $300-400$ m, $400-500$ m, $500-750$ m, $750-1000$ m, > 1000 m. The PAT2, PAT3, PAT4 tags had 2 fewer bins. To allow for comparisons, the additional bins on the MK10 tags were pooled, and distributions were computed on the same 12 bins across tags (Howell et al. 2010). The binning schemes of 2 central Pacific tags (#52498 and #64219) precluded their inclusion in the analysis of depth and temperature distributions.

The binned data, as well as the Profile-Depth-Temperature (PDT — eight discrete temperature and depth values collected during each time bin) data, were collected over time intervals of 2, 4, 6 or 8 hours, depending on the tag. All tags were programmed to GMT time.

Light levels recorded by the tags are used to estimate positions of the fish (light-based geolocation). Light levels are not measurements of absolute values of irradiance, but rather relative values ranging from about 50 (no unit) for a covered sensor to about 180 in a bright room (Wildlife Computers, PAT4 Manual, <http://www.wildlifecomputers.com/Downloads/Documentation/PAT4%20Manual.pdf>). Light sensors are not calibrated between tags by the manufacturer.

All raw data transmitted via Argos satellites were re-processed in 2009 with the latest available version of the manufacturer software, WC-AMP (which translates the raw Argos messages into binned data), and WC-GPE (which produces preliminary geolocation estimates from the tag's light level data). This allowed us to obtain the binned and preliminary geolocation data in a consistent manner across all tags (Howell et al. 2010).

GEOLOCATION

All tracks were processed using the “Track&Lock” geolocation filter (Table 1), developed at Collecte Localisation Satellites (CLS), France, in the MATLAB (<http://www.mathworks.com/products/matlab/>) environment (Royer et al. 2005, Royer & Lutcavage 2008, 2009, Neilson et al. 2009). The algorithm relies on a state-space model to represent process (movement) and observation uncertainty. Track&Lock uses sea surface temperature and bottom topography data to better constrain the tracks. An Ensemble Kalman Filter is applied to solve for the trajectory, thus estimating the state vector and its covariance from a set of samples rather than the usual deterministic equations. This allows one to account for non-linear features such as sharp and convoluted thermal gradients, and include the effect of boundaries such as coastal and bathymetric features. Sea surface temperature fields were provided at a 9-km resolution by a blended microwave and infrared SST product from REMSS, while bottom topography data (to estimate movement constraints) were retrieved from ETOPO2 (Smith and Sandwell 1997). For some of the fish that stayed close to the coast, the diffusion parameter of the state-space model had to be adjusted manually to lower values to ensure the fish's track did not cross Baja California into the Sea of Cortez (the bathymetry data constrains the fish to sea areas, but if the diffusion parameter is too high, plausible presence areas emerged in the Sea of Cortez).

For N=4 tags, we were unable to obtain convergence with the above method, and the “trackit” package, developed by Anders Nielsen for the R environment (The R Project for Statistical Computing, <http://www.r-project.org/>) at SOEST, Hawaii, U.S.A., was used as an alternative (Nielsen & Sibert 2007, Lam et al. 2008, 2010, <http://www.soest.hawaii.edu/tag-data/trackit/>).

Both tools rely on light data, a state-space model to estimate the position of the fish, and an extension of the Kalman filter to solve the optimization problem. Trackit possesses the capability to use sea surface temperature as well, but our attempts to include that information were unsuccessful, so only light information was used for those 4 tracks and the resulting tracks were then linearly interpolated to obtain one position per day, matching the output of both methods.

ENVIRONMENTAL VARIABLES

Environmental variables that were extracted along the tracks include the following: dissolved oxygen (World Ocean Atlas—WOA) , chlorophyll *a* concentration (chl—MODIS-Aqua), Photosynthetically Active Radiation—PAR (MODIS-Aqua), sea surface temperature—SST (AVHRR Pathfinder v4 and GAC), mixed layer depth—MLD (Naval Research Laboratory), thermocline depth, moon illumination, and time of sunset and sunrise (U.S. Naval Observatory). The World Ocean Atlas (Boyer et al. 2006) provides objectively analyzed climatological fields of *in situ* data at standard depth levels for annual, seasonal, and monthly compositing periods for the world's oceans and is available online at <http://www.nodc.noaa.gov/OC5/WOA05/woa05data.html>. We used monthly 1° data for all analyses. We used 4-km weekly data for MODIS, available from NASA's Goddard Space Flight Center website (<http://oceancolor.gsfc.nasa.gov/>). The 9-km weekly Pathfinder data is available on the National Oceanographic Data Center website (<http://www.nodc.noaa.gov/>). The 1° monthly climatologies of MLD were constructed by the Naval Research Laboratory and are available at <http://www7320.nrlssc.navy.mil/nmld/nmld.html>. Astronomical data from the U.S. Naval Observatory are available at: <http://www.usno.navy.mil/USNO/astronomical-applications>. Thermocline depth was computed from the PDT data and from the WOA following the method described in Polovina et al 1995 as the depth at which the temperature gradient is maximal. When the fish was staying at depth or at the surface, the thermocline depth information was just considered as missing for the particular time period.

SEPARATION OF DAY AND NIGHT

To characterize daytime behavior, great care was taken to separate daytime from nighttime and to exclude crepuscular periods (transition behavior). To achieve this, the U.S. Naval Observatory's sunrise and sunset data were used to identify the latest time of sunrise and earliest time of sunset in GMT time along each track, to define a “pure daytime” period common to every day of the track.

Time-bin programming varied from tag to tag (2, 4, 6, 8 hours), and some time bins overlapped sunrise or sunset and had to be discarded : for some tags, the remaining daytime period used in the analyses was much shorter than the actual duration of daytime. As a result of this approach, it was not possible to identify a daytime period of equal duration for all tags (10:00 to 14:00 local time for example). Durations of the estimated “pure daytime” periods varied between tags, but the priority was to use as many tags as possible in the analysis. The term “daytime” hereinafter refers to the estimated “pure daytime.” The same approach was used to obtain “pure nighttime” periods.

MEAN DEPTH

Mean daily depths were estimated from the time-at-depth (TaD) data for each daytime and nighttime period and calculated as the sum of the product of the bin frequency multiplied by the bin interval midpoint. Daytime mean depth was used as a proxy for daytime foraging depth. As this approach can introduce biases in the mean depth values obtained, depending on the width of the programmed depth bins, daytime mean depth was also computed directly from the archived data for the recovered tags and compared to daytime mean depth computed from the TaD data those tags transmitted so that potential biases could be estimated.

GENERALIZED ADDITIVE MODELS (GAMS)

We used GAMS (Hastie & Tibshirani 1990) to model the relationships between daytime mean depth and various environmental parameters: depth of various oxyclines (0.5, 1, 2 mL L⁻¹) and isotherms (5, 8, 20°C), depth of the thermocline (from the PDT data and from the WOA), mixed layer depth, as well as oxygen concentration and temperature (interpolated from the PDT data) at various depths, chlorophyll *a* concentration and PAR.

As the variable of interest was daytime foraging at depth, we removed all basking events (daytime bins for which the time spent in the 2 shallowest depth bins was not zero, or all daytime depths < 50 m for the archival data) from the time series before computing the GAMS.

GAMS were constructed in R (version 2.11.1) using the *gam* function of the *mgcv* package (Wood 2006). The Gaussian family with an identity-link function was used. Model selection was performed manually, and we retained candidate predictors that were statistically significant at the 0.05 level, minimized the GCV (General Cross Validation, Wood 2006) score, and improved the predictions. All candidate variables were modeled as continuous variables. We set *gamma* = 1.4 to avoid overfitting (Wood 2006), and penalized regression smoothers were used. Basis dimensions for these were chosen according to the *choose.k* method described at <http://stat.ethz.ch/R-manual/R-devel/library/mgcv/html/choose.k.html> but subsequently manually adjusted to “straighten” the smoothers and further avoid overfitting.

Potential confounding between statistically significant covariates was investigated with variance inflation factors (Graham 2003, Kutner et al 2005) using the *vif* function of the *HH* package.

Model predictions were made via the *predict* function of the *mgcv* package. We computed predicted daytime mean depth for individual tracks, as well as monthly prediction maps. To make the prediction maps more legible, the kriging function *krige.conv* from the R package *geoR* was used. For individual track predictions, the model was computed for all tags except the tag of interest, and the predictions were then run for the tag data (“leave-one-out method”).

RESULTS

TAGGING

Of the 43 tags deployed, only 28 tags yielded usable data (Table 1, Figs. 1 & 2); 9 never reported; 3 popped-off and reported, but transmitted no data; and 2 transmitted data, but based on the depth data the animals apparently died right after deployment (Domeier et al. 2003). One earlier tag (PAT 2) transmitted data, but the reprocessing with a newer version of the software yielded no usable data.

Tag deployments ranged from 10 to 180 days. Five tags were recovered from which the entire archived record was obtained (see Table 1).

HORIZONTAL MOVEMENTS

Of the 28 tags from which data were obtained, tracks were estimated for 23 tags (Figs. 1 & 2, Table 1). For the 2 recovered tags that did not transmit data, it was not possible to estimate geolocations using the

raw light data and no tracks were obtained. Geolocation was also not possible for 3 of the earlier tags (PAT2/3, Table 1) either, possibly because of poor light records.

The northernmost and southernmost positions reached by a fish during our deployment period were 43.7°N (tag #52498), and 1.3°S (tag #67458), respectively.

We compiled the percentages of days without preliminary geolocation estimates (obtained with the manufacturer's software from the light data) or SST information for each tag. These gaps amounted on average to 58 and 25% respectively, and 15% for days with neither information. Fig. 3 shows the time-series of state-space model estimated and tag-derived longitude, latitude and SST for all the tracks processed with the Track&Loc method. Average errors ranged from 0.5 to 25.6 °, 4.1 to 28.9 °, 0.3 to 3.9 °C, for longitude, latitude and SST respectively. Median errors, ranged from 0.2 to 21.6 °, 1.2 to 13.2 °, and 0.2 to 3.6 °C.

Of the 24 fish tagged off San Diego (for the tags for which a track could not be obtained, the analysis is based on movements between deployment and pop-off locations), 15 radiated away from California (hereafter referred to as EP tags), following a primarily south-southeast course before diverging into the central North Pacific or along the coast of Baja California, while 9 remained in the vicinity of San Diego (SD tags), 1 of them for the full 180 days of the track (Figs. 1 & 2). One of the central Pacific tags (#64219) followed a north-eastward course approaching the California coast (about 234°E) before turning towards the north-west. The remaining 3 first followed a southward course. The longer track (tag #52498) then switched to a northward course in May (Fig. 2).

Argos ID	Serial ID	tag type	weight (kg)	deploy date	deploy lat (N)	deploy lon (E)	popup date	popup lat (N)	popup lon (E)	days of data	geolocation
8832 ²	02P345	PAT2	73	10/31/04	33.23	241.97	11/24/04	32.9	242.48	24	no
19203	02P043	PAT2	68	09/11/02	33.2	241.9	10/23/02	22.3	228	42	no
19910	02P046	PAT2	45	11/16/02	35.48	229.7	01/20/03	7.19	216.18	64	no
30319	02P063	PAT2	45	02/09/03	30.88	205.65	02/28/03	24.66	205.37	18	trackit
30406	02P060	PAT3	79	12/16/03	32.69	242.19	02/14/04	25.73	218.63	59	no
30410	02P060	PAT3	113	11/04/03	33.2	241.95	12/15/03	32.11	241.87	40	trackit
40560	02P060	PAT3		11/20/03	33.21	241.9	12/24/03	20.9	236.32	34	track&lock
41732	03P017	PAT3	68	10/30/04	33.32	241.87	02/15/05	17.92	247.53	105	track&lock
41737	03P189	PAT3	82	10/23/04	33.27	242.05	04/11/05	25.57	217.84	170	track&lock
49070 ¹	03P059	PAT4	90	03/26/05	24.27	213.45	04/07/05	21.69	212.21	10	track&lock
52498	04P017	PAT4	60	03/28/05	24.45	213.92	08/26/05	41.76	207.63	147	trackit
59270	05P001	PAT4	73	11/05/05	33.48	241.88	01/18/06	5.26	239.96	71	track&lock
59275	05P002	PAT4	91	09/04/05	33.88	241.79	12/16/05	17.5	237.73	101	track&lock
59276	05P002	PAT4	91	09/04/05	33.33	242.25	02/22/06	22.47	249	167	track&lock
64219	06A010	MK10	120	07/03/06	27.82	212.04	12/14/06	39.62	228.09	163	track&lock
67457	06A022	MK10	91	11/24/07	33.37	241.91	05/22/08	31.92	229.08	180	track&lock
67458	06A022	MK10	91	08/30/07	33.04	242.45	02/26/08	-1.34	217.19	180	track&lock
67461	06A022	MK10		08/25/08	33.02	242.15	10/06/08	32.9	241.89	39	trackit
67462	06A022	MK10	118	11/19/07	33.35	241.88	01/06/08	31.44	241.32	47	track&lock
67463	06A022	MK10		07/23/08	33.15	242.4	11/27/08	32.72	242.78	125	track&lock
67464 ²	06A023	MK10	91	11/15/08	33.39	241.79	12/04/08	32.93	242.52	19	no
67465	06A023	MK10		08/25/08	33.04	242.16	02/22/09	30.86	241.9	179	track&lock
67466 ¹	06A023	MK10	91	11/20/07	33.52	241.82	02/2/08	31.29	206.68	98	track&lock
75939 ¹	07A017	MK10		10/29/08	33.25	242.35	11/28/08	32.73	242.79	28	track&lock
88148	08A060	MK10		12/06/08	32.73	242.52	06/04/09	18.97	220.03	171	track&lock
88149	08A060	MK10		10/20/08	33.21	242.39	01/13/09	26.88	245.67	82	track&lock
88150	08A060	MK10		10/16/08	33.32	241.97	02/08/09	33.89	226.46	112	track&lock
88151	08A060	MK10		10/17/08	33.32	242.28	04/15/09	27.08	225.66	178	track&lock

Table 1: Summary of deployments. ¹recovered tag. ²recovered tag that did not transmit.

Mean and median daily speeds across all tracks were calculated at 22.7 and 13.1 km d⁻¹, respectively. When daily speeds were computed as 5-day moving averages to obtain more robust estimates, mean and median daily speeds were calculated at 22.6 and 13.1 km d⁻¹, respectively.

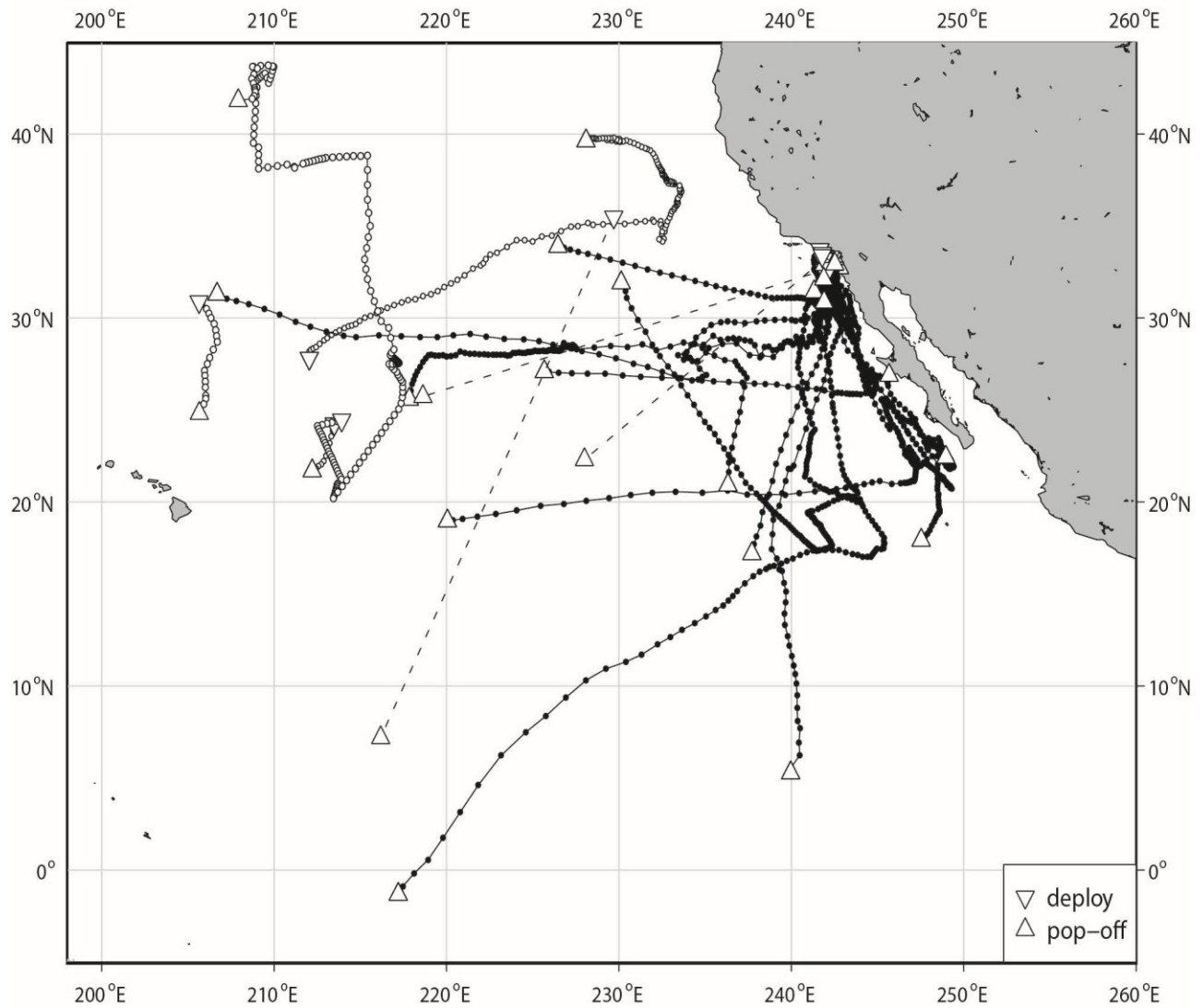


Fig. 1 : Map of tag deployments ($n = 28$) for the period 2002-2008. Dots indicate daily positions along tracks. Dashed lines indicate tags for which tracks could not be obtained. White and black dots were used for fish tagged in the central and eastern Pacific, respectively.

VERTICAL MOVEMENTS

Swordfish encountered a broad range of depth and temperature. Temperature and depth ranges for all fish combined were 3.2 to 28.8°C and 0 to 1227 m, respectively. Five fish dove as deep as 1200 m. Mean SST from MODIS estimated along the tracks across tags was 19.9°C (ranging between 13.4 and 27.9°C). The minimum temperature measured by the tags during the daytime (in absence of basking) ranged from 3.8 to 17°C with a mean of 7.0°C.

Data from 26 tags with similar binning strategies were pooled together (Fig. 4a). The depth data showed a bimodal distribution with swordfish spending 60% and 22% of their time between 0 and 100 m and

between 200 and 400 m, respectively. They only spent 7% of their time below 500 m. Similarly, the temperature distribution exhibited 2 modes, one between 7.5 and 10°C and another between 16 and 18°C, where fish spent 22% and 20% of their time, respectively.

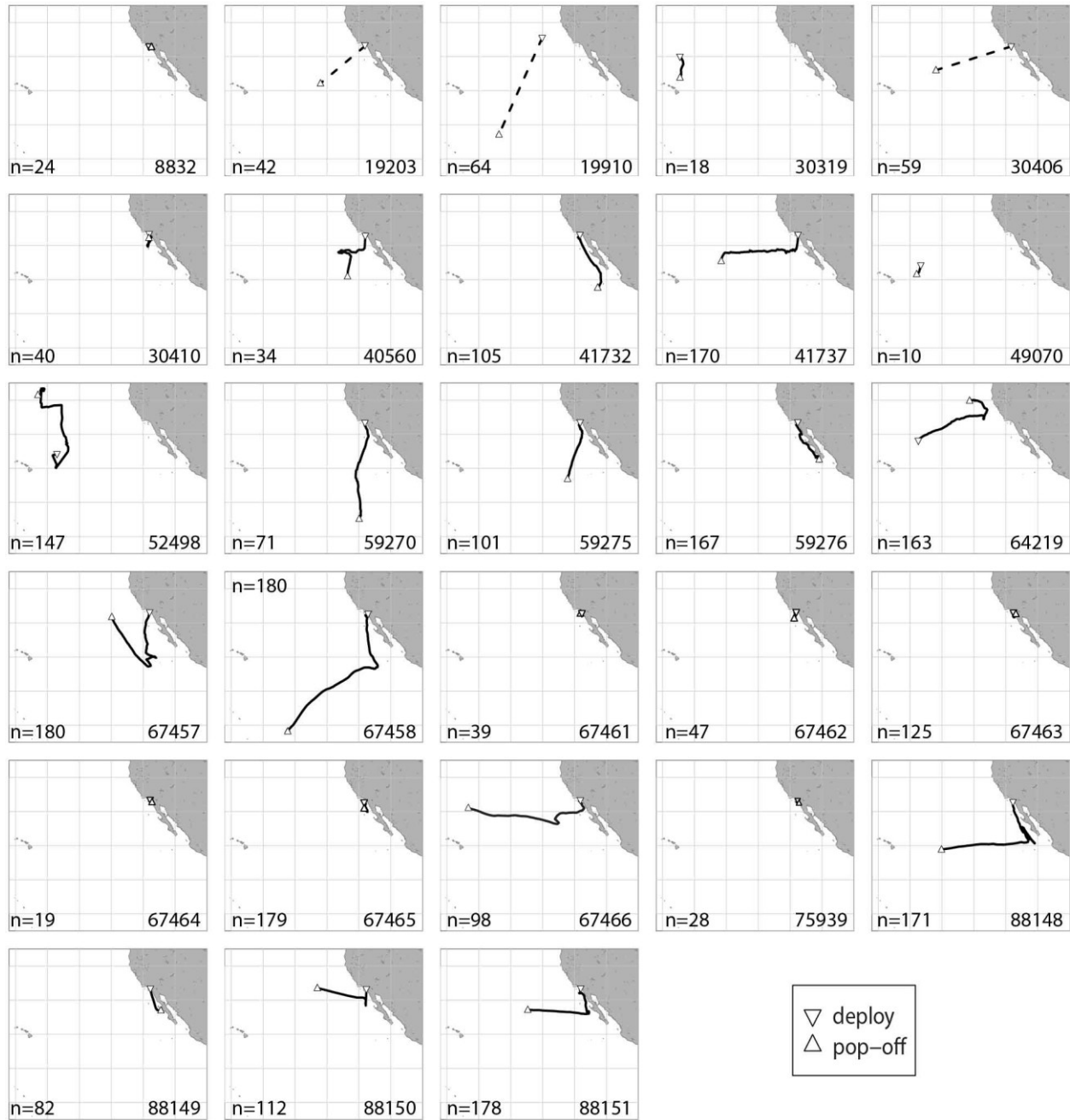


Fig. 2 : Individual tracks. Dashed lines indicate tags for which tracks could not be obtained. Those include tags #8832, 19203, 19910, 30406, and 67464. *n* is the number of days at liberty for each tag.

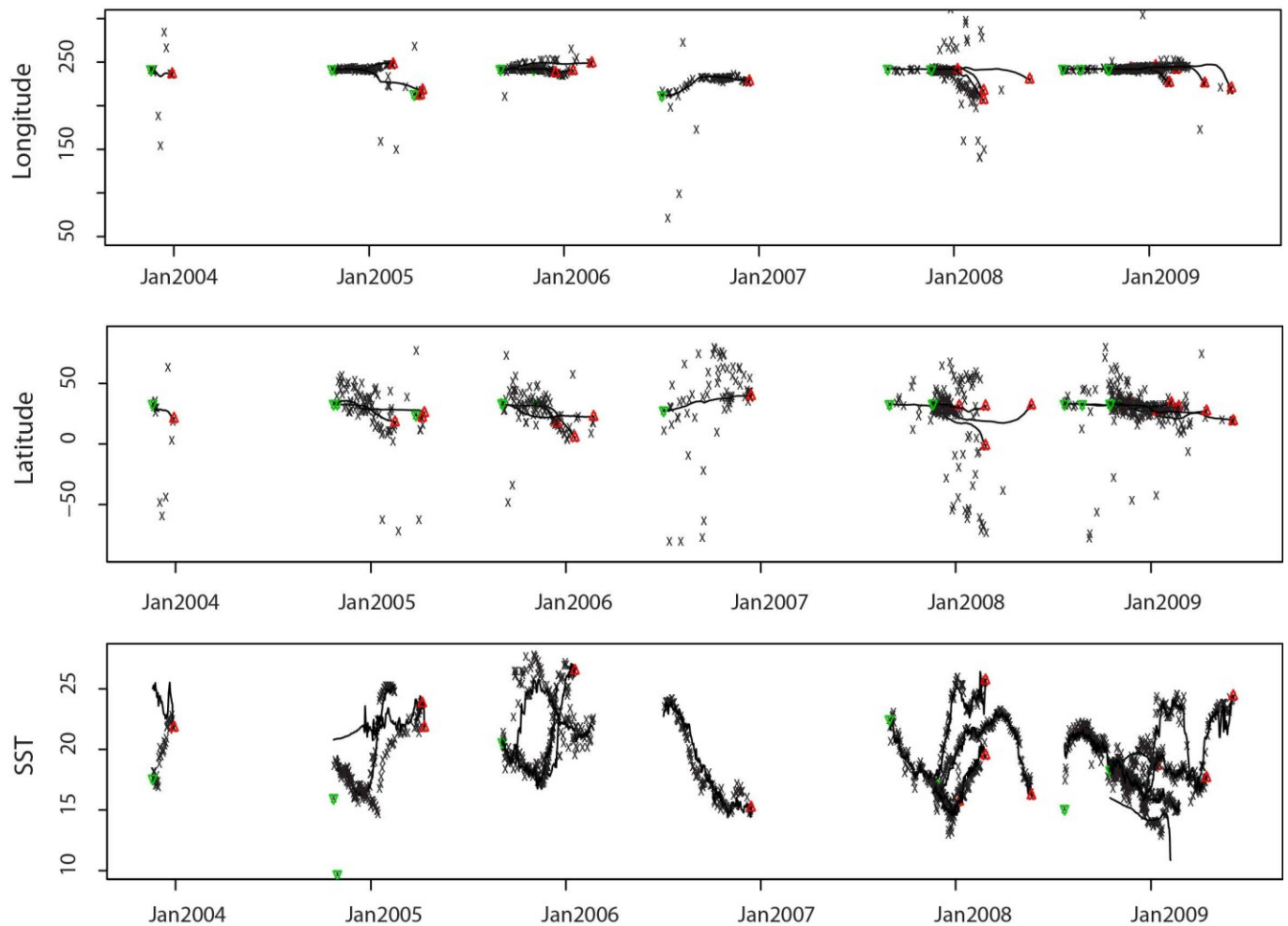


Fig. 3 : Time-series of state-space model estimated (black line) vs. tag-derived (x) longitude (top), latitude (middle) and SST (bottom) for all the tracks processed with the Track&Loc method. The green and red dots represent the points of release and pop-up of each tag respectively.

Daytime and nighttime distributions are shown in Figs. 4 b and c. Because of the different bin intervals used across tags, only 20 tags had time bins that could be characterized as daytime bins and 22 as nighttime bins. Classic diel movement (shallow at night, between 0 and 100 m, vs. deeper than 200 m during the day) was observed, with the exception of occasional daytime basking occurring in the general area of the California current in the fall and winter (Figs. 4 & 5). During the day (Fig. 4 b), 66% of the fish's time was spent at depth, between 200 and 750 m, corresponding to 65% of the time spent between 5 and 10°C, while 24% of the time was spent above 50 m (basking). During the night (Fig. 4 c), 97% of the animals' time was spent above 100 m, 37% of which was spent near the surface (< 5 m), which corresponds to 91% of swordfish time above 16°C, with a peak between 16 and 18°C (31%).

Archival records from the recovered tags were used to check the agreement between estimated daytime/nighttime and observed dive patterns (Fig. 5). Fig. 5 shows the depth records for tags #75939 and #49070. Both records confirm that the estimated daytime and nighttime periods did not include any crepuscular period. For tag #49070 (Fig. 5 b, tagged close to Hawaii), the limits of the estimated daytime periods matched closely the diel movement of the fish. The fish seemed to start diving shortly before sunrise, stay at depth during the whole day, and ascend to shallow waters around sunset. During estimated nighttimes, the fish made frequent shallow dives (up to 200 m).

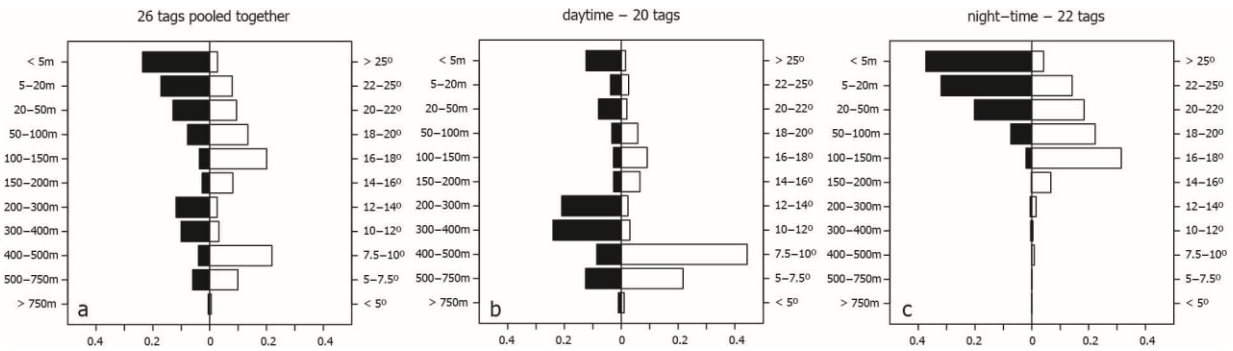


Fig. 4 : Distribution of % time spent at each depth or temperature bin for all tag data pooled together. a : over whole tracks, b : during the daytime, c : during the nighttime.

However, for tag #75939 (Fig. 5 a), which stayed close to San Diego for 28 days, the pattern was not as obvious. The general bell-shaped dive pattern was the same as for tag #49070 on most days, but often featured excursions to the surface during the day (basking). On occasion, a majority of the daytime was spent at the surface. At night, the fish stayed almost exclusively at the surface. Fig. 5 b (bottom) also shows moon illumination along tag #49070's track. It was full moon at the very beginning of the track and close to new moon by the end of it. This variation in illumination at night coincided with a transition of the fish from around 107 m to about 15 m.

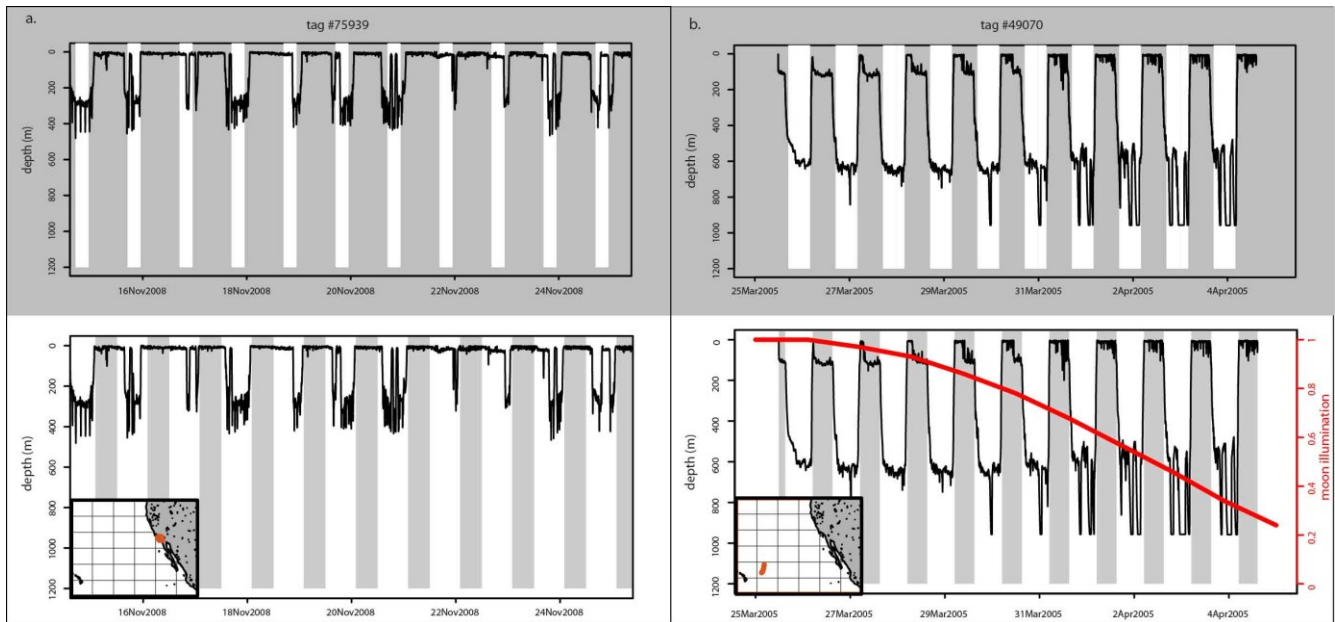


Fig. 5 : Depth records from two recovered tags, (a) #75939 (11 days selected from the whole track for better legibility) and (b) #49070. White areas (top graphs) are estimated daytime periods and gray areas (bottom graphs) are estimated night-time periods. Insets show the respective estimated tracks. The thick red line on the bottom right plot is moon illumination (1 corresponding to full moon, 0 to new moon).

Once basking events were removed from the data, the overall average daytime mean depth calculated using the histogram data across tags was 375 m in comparison to 376 m for the recovered tags only (304 m for tag #8832, 588 m for tag #49070, 276 m for tag #67464 and 387 m for tag #67466); daytime mean depth calculated directly from the archived data was 294 m for tag #8832, 557 m for tag #49070, 281 m for tag #67464 and 337 m for tag #67466 ; data for tag #75939 had to be excluded from this analysis, since the fish basked almost every day along the track. The difference between the two methods in calculating the average daytime depth ranged from 5 to 50 m.

OXYGEN LIMITATION

Fig. 6 presents daytime dive ranges (top and bottom of the PDT data) overlaid onto contours of dissolved oxygen concentration along the track for tag #59276 (top), where the fish followed the coast of Baja California and tag #67466 (bottom), for which the fish spent about 6 weeks around the coast before swimming westward and northward of Hawaii. While the depths don't appear to follow a specific oxygen concentration, depths track the oxycline over the course of the track.

We also interpolated WOA oxygen data along the tracks to estimate the oxygen concentration at the maximum daily depths (Table 2). The minimum oxygen concentration reached by the fish we tagged was 0.16 mL L^{-1} (tag #67457), at a depth of 504 m, in March 2008 (longitude = 242.3°E , latitude = 17.7°N).

	Min.	1st Qu.	Median	Mean	3rd Qu.	Max.
Ox conc. (mL/L)	0.16	0.61	0.99	1.47	1.71	5.73

Table 2: Summary of the values of oxygen concentration at maximum depth (mL L^{-1}) : minimum, first quartile, median, mean, third quartile and maximum values.

LIGHT

Carey & Robison (1981) initially hypothesized that swordfish stay around a constant light level, most likely following the diel migrations of cephalopods and other epi-mesopelagic organisms that are foraging in association with the SSL (Nelson et al. 1997, Dagorn et al. 2000, Brill et al. 2005). Since then it has been shown that swordfish do not strictly follow isolumens, especially when basking occurs (Carey 1990, Sepulveda et al. 2010). The selected 15-day depth record for tag #67466 (Fig. 7 left) exhibited the typical diel behavior, with the corresponding light level staying relatively constant at a very low level (around 30 readings) over a 600 m depth range. In contrast, data for the selected 15-day period for tag #75939 (Fig. 7 right) showed basking events almost daily with light reaching levels of over 200 lumens.

To examine light levels experienced by fish at daytime foraging depths, average light levels in the absence of basking were examined for the recovered tags (except #75939, see above). For the 4 tags, mean hourly light level across days without basking was computed (Fig. 8). Except for tag #49070, the mean hourly light level stayed remarkably constant over a 24-hour period. Nighttime light level for tag #49070 was slightly higher than daytime light level, most likely due to the full moon at the beginning of the track (Fig. 5 b) and some very deep dives during the daytime.

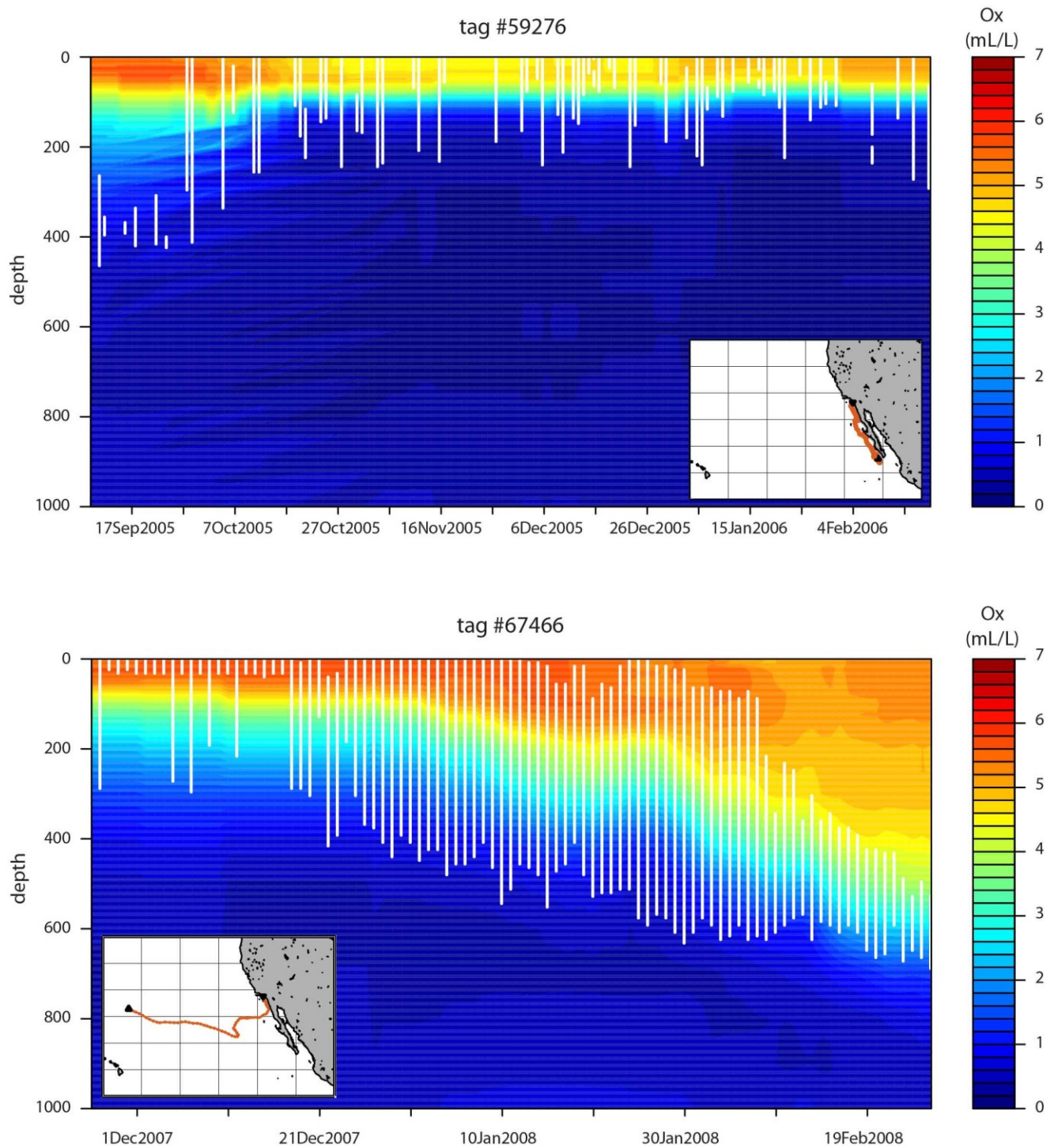


Fig. 6 : Swordfish daytime minimum and maximum depth (white lines) overlaid on oxygen concentration contours (in mL L^{-1}), for tags #59276 (top) and #67466 over the (bottom). Insets show the respective estimated tracks

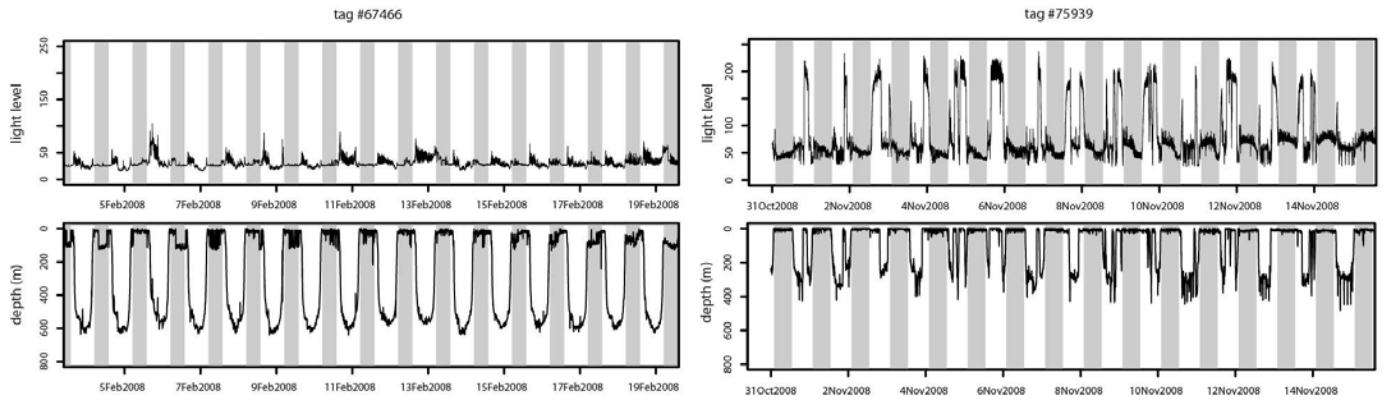


Fig. 7 : Fifteen-day long light level (top) and depth (m - bottom) selected records for tags #67466 (left) and #75939 (right). Shaded areas represent night-time periods

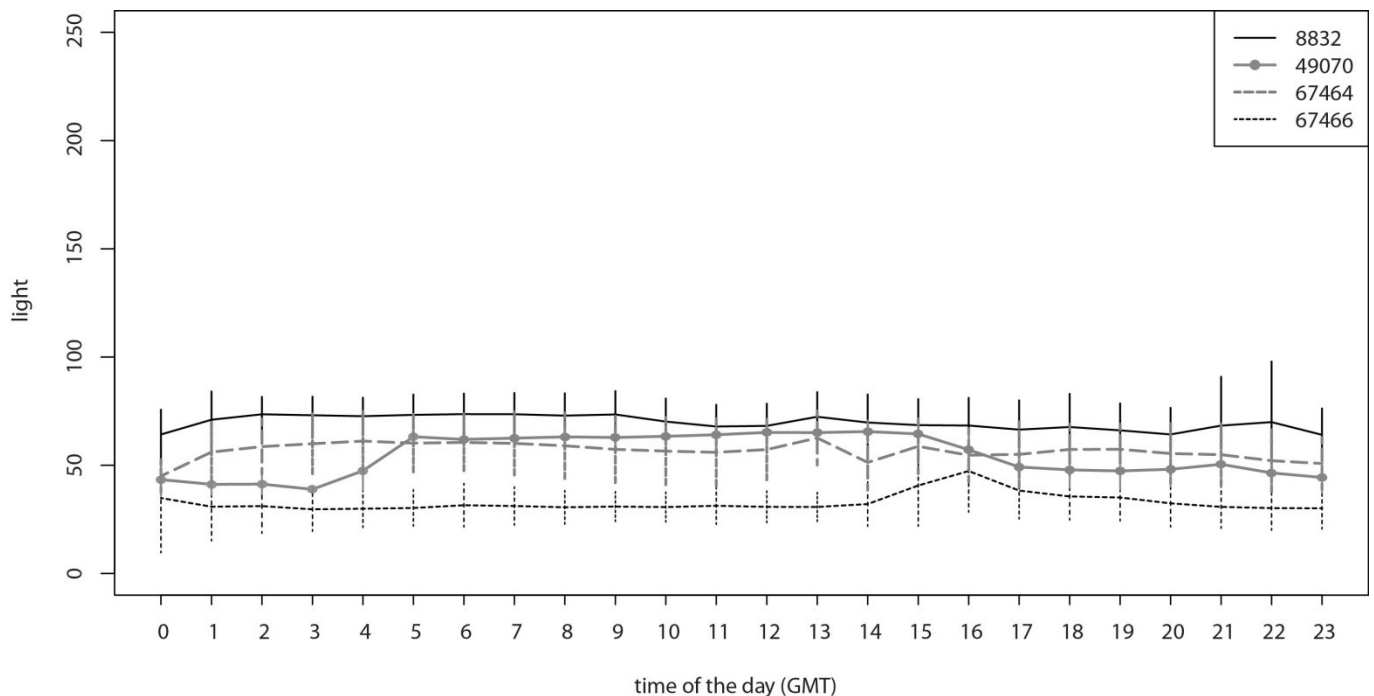


Fig. 8 : Typical light level over a day in the absence of basking for four recovered tags, with 1-standard deviation error bars

MODEL RESULTS

After careful examination of the significance of the different environmental factors considered, three covariates were retained - temperature, dissolved oxygen and light. Several GAMs were designed to assess their separate and combined effects. Given that the World Ocean Atlas (WOA) only has information for dissolved oxygen at certain depths, we used oxygen at 400 m (which was the depth level available closest to the overall mean depth of 375m). Similarly, only temperature at 400 m was retained in

the models. Chlorophyll *a* concentration and PAR were used as proxies for light (Tont 1975, Matciak 1997), but only the former appeared to be a significant factor.

The respective variance inflation factors (Table 3) were all less than 2 suggesting low collinearity (Graham 2003, Kutner et al 2005).

ox400	T400	chl
1.106	1.275	1.321

Table 3. Variance inflation factors for dissolved oxygen at 400 m, temperature at 400 m, and chlorophyll *a* concentration

Three models looked at the separate effects of chl *a* concentration, dissolved oxygen at 400 m (ox400), and temperature of the water column at 400 m (T400). Chl *a* concentration by itself explained 55% of the variation in daytime mean depth, while dissolved oxygen concentration at 400 m and temperature at 400 m explained 49%, and 47% of the variation, respectively. Fig. 9 shows the estimated plots of the smoothers for those three separate models. Daytime mean depth decreased as chl *a* increased but increased as oxygen concentration and temperature at 400 m increased.

The best model combining all three factors was:

daily daytime mean depth $\sim s(\log(\text{chl})) + s(\text{ox400}) + s(\text{ox400}, \text{T400})$

It explained about 77% of the observed deviance (Table 4). When an oxygen-temperature interaction term was included, the temperature term alone was not significant in the full model (daily daytime mean depth $\sim s(\log(\text{chl})) + s(\text{ox400}) + s(\text{T400}) + s(\text{ox400}, \text{T400})$)).

Parametric coefficients:				
	Estimate	Std. Error	t value	Pr(> t)
(Intercept)	380.197	2.836	134.1	<2e-16
Approximate significance of smooth terms:				
	edf	Ref.df	F	p-value
s(log(chl))	11.83	12.33	13.57	< 2e-16
s(ox400)	10.52	11.02	4.59	9.7e-7
s(ox400,T400)	17.37	17.87	14.62	< 2e-16
R-sq.(adj) = 0.754	Deviance explained = 76.8%			
GCV score = 5973.1	Scale est. =	n = 661		

Table 4: Model summary

The summaries of the individual models, the diagnostics plots, and the smooths of the combined model are available as supplemental material online to allow the reader to evaluate the validity of the model. This model performed well in predicting daytime depth (77% of the deviance) for individual tagged fish (Fig. 10) and allowed for the development of monthly maps that predict the mean daytime depths of swordfish (Fig. 11).

A similar approach to build a model for nighttime depth was attempted without success. We were unable to identify clear mechanisms or primary factors that would account for a significant portion of the variability in nighttime mean depth, which showed more variability than daytime mean depth, although within a much narrower range.

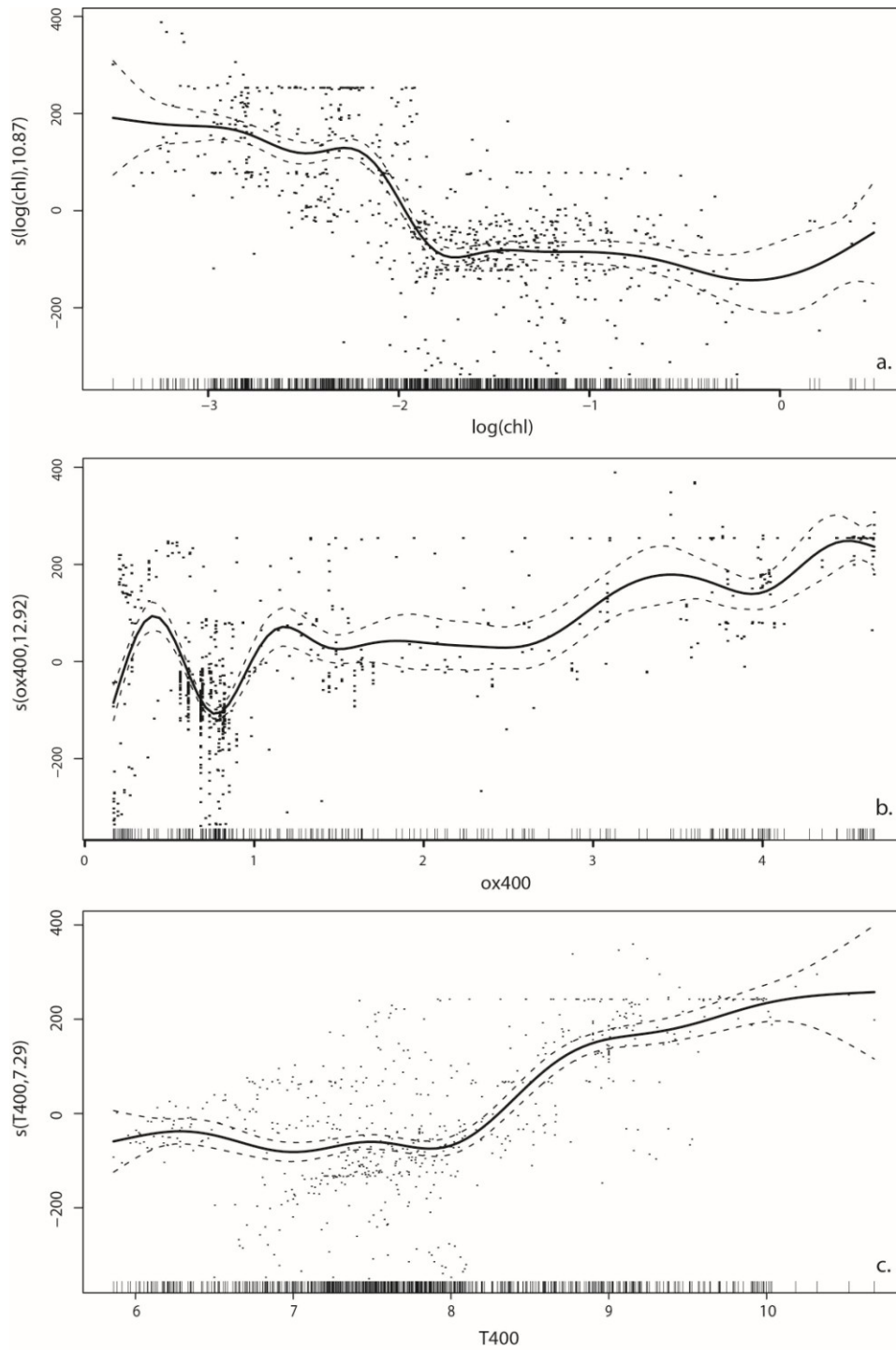


Fig. 9 : Plots of the estimated individual effects (solid line) of (a) chlorophyll concentration, (b) dissolved oxygen concentration at 400 m, and (c) temperature at 400 m. Dashed lines represent the 95% confidence limits and residuals are plotted as dots. Ticks on the bottom axis represent values for which there is data. Positive values on the y-axis indicate deeper depths

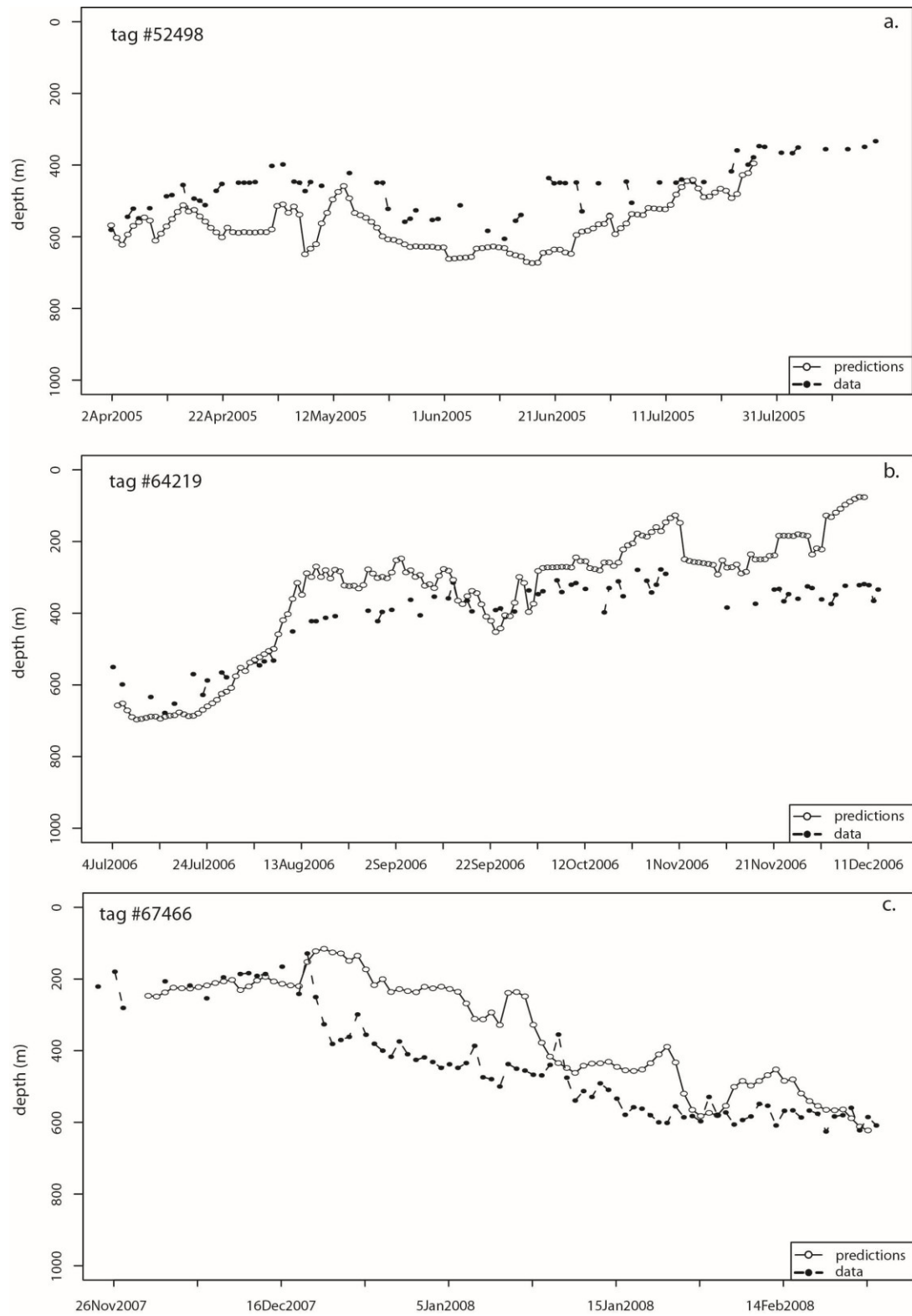


Fig. 10 : Model predictions (white dots) and actual data (black dots) for daytime mean depth (m) in the absence of basking for three individual tags (a) #52498, (b) #64219, (c) #67466.

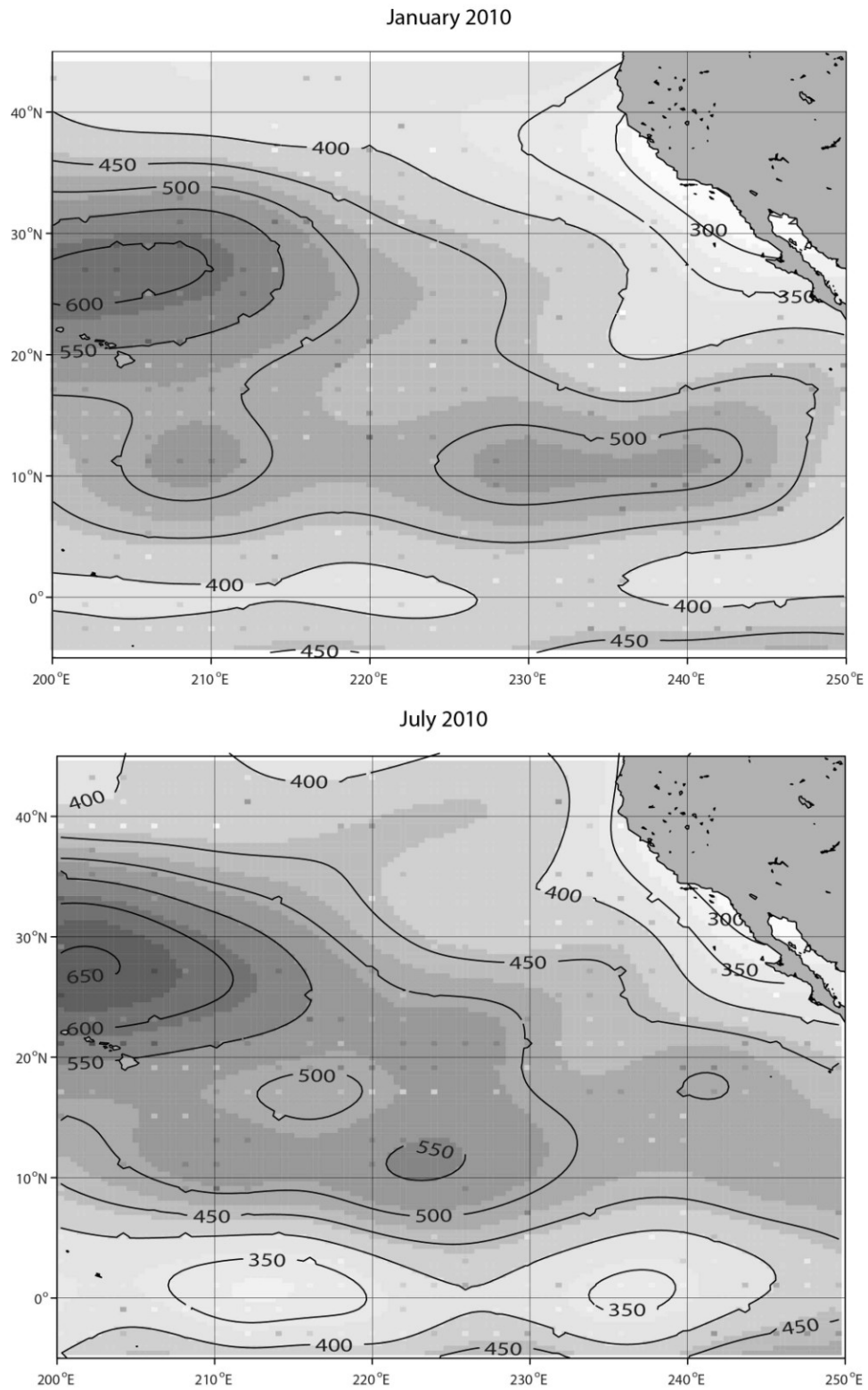


Fig. 11: Prediction maps for North Pacific swordfish daytime mean depth, for January 2010 (top) and July 2010 (bottom). Numbered lines represent depth contours (m).

DISCUSSION AND CONCLUSIONS

Our results, expanding on the analysis of Dewar et al. (2011), represent the most comprehensive tagging data set and complex analysis for swordfish in the North Pacific. Our findings emphasize the wide range of habitats swordfish occupy, from the surface to over 1200 m (Fritsches et al 2005), with the capability of tolerating extremely low oxygen concentrations.

TAGGING

Our deployments were fairly short compared to those reported by Neilson et al. (2009) in the Atlantic Ocean (up to 400 days), probably a result of different tag attachment methods and programmed deployment durations. Only 65% of the tags deployed provided usable data, and only 3 tags (7%) stayed on for the full duration of their programmed deployment period. Tag shedding is a recurrent problem with PSATs deployed on a variety of species (Gunn & Block 2001, Wilson et al. 2005, Hays et al. 2007, Holdsworth et al. 2009).

MEAN DEPTH

While the summarized data transmitted by PSAT tags masks detailed movement patterns, the mean depth obtained from the histograms provided an estimate similar to that obtained from the archival tags providing confidence in this method. The comparison of mean depths computed from the archival and binned data differed by only 10 to 50 m.

GEOLOCATION

Our results indicate the potential for using light based geolocation to track swordfish over relatively long time periods. Our geolocation errors and confidence intervals are similar to those reported by Neilson et al (2009) for the same species, geolocation software and obtained using similar technology. Our study used environmental data at, or closest to, the location given by the most probable track. A better insight into the distribution of error in latitude and longitude around each daily position could allow for computing a weighted average of environmental variables, as used by Sippel (2010). This would be a more robust approach, although more precise matching of locations to environmental variable is limited by the temporal and spatial resolution of the World Ocean Atlas.

Geolocation proved particularly challenging for swordfish because of their crepuscular diving behavior (Holdsworth et al. 2007) and their deep and rapid dives (Carey & Robison 1981, Neilson et al. 2009), making it difficult to identify sunrise and sunset events. The use of sea surface temperature and bathymetry constraints in the Kalman filter did improve the geolocation estimates (Fig. 3, Teo et al. 2004, Neilson et al. 2009, Lam et al. 2010). Fig. 3 illustrates the weight given to the SST information in the fitting process for some of the tracks where gaps in light data were important. On the other hand, it can be noted that when light information is available and relatively clean, the fit to SST can become poor.

Fish trajectories varied greatly. Among the 24 fish tagged off San Diego, 9 stayed close to the tagging location for the whole duration of the track, while courses followed by the remaining individuals diverged into the central North Pacific or along the coast of Baja California. The four fish tagged in the central Pacific mostly stayed in that area. No obvious seasonal pattern seemed to explain such different patterns

in horizontal movements between individual fish. Tracks obtained over longer time periods will be needed to resolve stock structure in the Central and East Pacific.

OXYGEN TOLERANCE

Results confirm that swordfish have a high tolerance for low oxygen levels. The minimum oxygen values encountered by our fish, lower than 0.2 mL L^{-1} , are much lower than values reported in the literature for bigeye tuna, less than 1.5 mL L^{-1} (Brill 1994, Musyl et al. 2003, Brill et al. 2005), and slightly lower than figures recently reported for swordfish, around 0.5 mL L^{-1} minima at maximum depths (Abascal et al. 2010, Dewar et al. 2011). However, absolute values presented here are to be taken with caution given the use of 1° monthly climatologies from the WOA and the large uncertainties associated with the geolocation process (Neilson et al. 2009). Recent findings by Wegner et al. (2010) point out that “the branching of the gill filaments in swordfish appears to increase their gill surface area above that of other billfishes and may allow them to penetrate oxygen-poor waters at depth”. Carey & Robison (1981) also suggest that swordfish’s large mass of white muscle might allow them to tolerate more hypoxic conditions than tunas by accumulating an oxygen debt that they likely compensate by basking. Daytime basking was only observed in the eastern Pacific, in the general area of the California current, where the Oxygen Minimum Layer (OML) is much shallower than in the rest of the central North Pacific, although basking has also been observed in the Central Pacific and Atlantic Ocean where there is a much deeper or nonexistent OML (Dewar et al. 2011).

Despite such remarkable oxygen tolerance, swordfish vertical habitat is greatly reduced in areas where the OML is shallow, as has been observed in other studies and for a range of other species (Carey & Robison 1981, Prince & Goodyear 2006, Nasby-Lucas et al. 2009, Abascal et al. 2010, Prince et al. 2010). The dive pattern for tag #59276 (Fig. 6 top) shows strong evidence of hypoxia-based vertical habitat compression (Prince & Goodyear 2006, Nasby-Lucas et al. 2009, Prince et al. 2010) in the eastern Pacific, with swordfish apparently restricted to much shallower depths than in the rest of the North Pacific.

CONSTANT ISOLUME?

Many SSL organisms follow an isolume in their daily vertical migrations and the actual light levels have been shown to vary across species (Boden & Kampa 1967, Longhurst 1975). Based on early acoustic telemetry observations, Carey & Robison (1981) concluded that the swordfish's daily diving patterns, at least under some conditions, also tend to follow an isolume, although a later experiment with a photometer following the dusk and dawn excursions of 1 swordfish suggested that the animal was diving more rapidly than if its movement was directly controlled by light (Carey 1990).

Our results are the first empirical confirmation that in the absence of daytime basking, swordfish stay within a very narrow range of light level. Light level sensors are not calibrated between tags by the manufacturer, and the different light levels observed among the 4 archival tags are within the sensors’ operational variability (Wildlife Computers, pers. comm.). These results suggest that swordfish may be following a specific component of the SSL on which they prey during both day and night (Hays 2003, Chancollon et al. 2006).

MODELING

Using tag and environmental data along the tracks, a model was built that allows for the prediction of swordfish daytime foraging depth. Only environmental factors were considered (rather than spatial or temporal, such as longitude, latitude or month), so that the resultant model would describe physiological or behavioral mechanisms, which, in turn, can be translated in terms of spatial and temporal variation. Only three factors were necessary to describe most (77%, Table 4) of the observed variability: chlorophyll *a* concentration, as a proxy for light (in less productive waters, light reaches deeper depths), which affects the depth of the SSL; and dissolved oxygen and temperature at depth, as indicators of potential physiological constraints.

The model performed well in predicting individual daytime mean depth over a wide variation in depth (Fig. 10). The resulting patterns in prediction maps produced for two different seasons (Fig. 11) are in good agreement with general patterns observed for the depth of the SSL in the North Pacific—from 200 m near the coast to 400 m farther offshore in the California Current, and around 500 to 600 m near Hawaii (Tont 1975, Kalish et al. 1986, Johnston et al. 2008).

Nighttime mean depth was more variable than daytime mean depth and our attempts to use a similar modeling approach were unsuccessful.

POTENTIAL APPLICATIONS OF THE MODEL

The ability to predict the daytime depth of swordfish has implications for longline fisheries management in the North Pacific. Hawaii-based longline vessels targeting swordfish typically deploy shallow sets (around 60 m deep, Bigelow et al. 2006) at night, and use mackerel-type bait (federal regulation to reduce turtle bycatch) and light-sticks (Ito et al. 1998). Our results could potentially be used to aid fishermen trying to target swordfish at depth during the daytime, when habitat separation between swordfish and sea turtles is the greatest (Polovina et al. 2003, Gilman et al. 2006, Gilman et al. 2007, Dewar et al. 2011). Experiments conducted in Australia, with new, deep longline settings were aimed at eliminating shallow hooks to reduce bycatch while increasing the catch of target species, showing promise for bigeye tuna but slightly reducing swordfish catch (Beverly et al. 2004). However, the deepest hooks were typically set around 300 m, which would be too shallow for swordfish in most of the North Pacific, and possibly in Australian waters. A longline trial using Hawaii-based vessels was conducted in 2002 (Boggs 2003) to test the effect of switching to deep daytime tuna-style sets, while maintaining the standard swordfish-style number of branchlines per set, on the catch of marine turtles and swordfish. Although limited to a small number of sets (33 for control and 33 for deep setting), the trial resulted in no catch of turtles and an 85% reduction in swordfish catch. However, time-depth-recorder data showed that the mean depth of the gear was 244 m, typical of bigeye tuna sets (Boggs 2003) which is shallower than the daytime depth of swordfish in this region according to our results (Fig. 11). Another study conducted using Hawaii-based vessels eliminated all hooks shallower than 100 m and dramatically reduced the bycatch of incidental species, with no impact on the catch of bigeye tuna (Beverly et al. 2009).

Further field trials could be carried out in the area where Hawaii-based longline vessels targeting swordfish typically operate to examine the viability of deeper (500–600 m) daytime sets.

Deep day sets should be easier in the eastern Pacific in the California Current where daytime depths of ~300 m are closer to the surface but still below the typical daytime depths of sea turtles in the region, although basking might complicate efforts.

Our approach, in essence, defines the vertical habitat of the part of the SSL on which swordfish prey and gives insight into how the behavior of these poorly studied organisms is influenced by their environment. The oxygen, temperature and light relationships determined by our model may reflect the physiological constraints of swordfish prey rather than swordfish themselves. Our model could be easily adapted and applied to other deep-foraging species to improve knowledge about their prey and foraging habitats and provide information about resource partitioning (Potier et al. 2007). However, as the diet of smaller swordfish differs significantly from that of larger swordfish (Young et al 2006), our results are likely only valid for the size ranges presented here: 45 to 120 kg, or 147 to 211 cm (Uchiyama et al 1999).

Finally, our tagging data set, in conjunction with the GAM we designed, will help parameterize a configuration of the SEAPODYM model (Lehodey et al. 2008, Senina et al. 2008, Lehodey & Senina 2009, Lehodey et al. 2010) that is being built for swordfish in the Pacific. SEAPODYM is an age-structured spatially explicit population dynamics model. Initial parameterization includes definition of temperature preferences, oxygen tolerance, foraging habitat, and speed of the animals. Once fully parameterized, such a model should be able to resolve the stock structure of swordfish in the Pacific Ocean and will allow us the exploration of the impacts of different climate change scenarios on swordfish habitat. In particular, OMLs are forecast to expand (Stramma et al. 2010), which could result in further habitat compression.

Acknowledgements

The authors would like to thank greatly François Royer and Beatriz Calmettes from CLS, France, for processing most of the tracks with the “Track&Lock” software, and Anders Nielsen and Chi Lam, who developed the geolocation package “trackit”. Lucas Moxey of the NOAA - CoastWatch program provided access to satellite data and Evan Howell provided a script for data extraction. Colette Wabnitz, Evan Howell, Dean Courtney, Jon Brodziak, Pierre Kleiber, Phoebe Woodworth, Jeff Drazen and Patrick Lehodey provided discussions and revisions that significantly improved this manuscript. Some of the tag deployments off California were supported by the Tagging of Pacific Predators program. The authors also wish to thank the anonymous reviewers who helped strengthen this manuscript.

Authors' Contributions

Conceived and designed the experiments: JJP, HD. Performed the experiments: HD, DH.

Analyzed the data: MA, with important intellectual input from JJP and HD. Wrote the paper: MA, with important revisions from JJP and HD.

This project was partly funded by Cooperative Agreement NA17RJ1230 between the Joint Institute for Marine and Atmospheric Research (JIMAR) and the National Oceanic and Atmospheric Administration (NOAA). The views expressed herein are those of the authors and do not necessarily reflect the views of NOAA or any of its subdivisions.

REFERENCES

- Abascal FJ, Mejuto J, Quintans M, Ramos-Cartelle A (2010) Horizontal and vertical movements of swordfish in the southeast Pacific. *ICES J Mar Sci* 67:466–474
- Alvarado-Bremer JR, Hinton MG, Greig TW (2006) Evidence of spatial genetic heterogeneity in Pacific swordfish (*Xiphias gladius*) revealed by the analysis of *ldh-A* sequences. *Bull Mar Sci* 79:493–503
- Baez JC, Real R, Caminas JA (2007) Differential Distribution Within Longline Transects of Loggerhead Turtles and Swordfish Captured By the Spanish Mediterranean Surface Longline Fishery. *J Mar Biol Ass U K* 87:801–803
- Benson S, Dewar H, Dutton P, Fahy C, Heberer C, Squires D, Stohs S (2009) Swordfish and leatherback use of temperate habitat (SLUTH). Tech. Rep. LJ-09-06, Southwest Fisheries Science Center, NMFS/NOAA
- Beverly S, Robinson E, Itano D (2004) Trial setting of deep longline techniques to reduce bycatch and increase targeting of deep-swimming tunas. Tech. Rep. FTWG - WP-7a, Standing Committee on Tuna and Billfish
- Beverly S, Curran D, Musyl M, Molony B (2009) Effects of eliminating shallow hooks from tuna longline sets on target and non-target species in the Hawaii-based pelagic tuna fishery. *Fish Res* 96:281–288
- Bigelow K, Musyl MK, Poisson F, Kleiber P (2006) Pelagic longline gear depth and shoaling. *Fish Res* 77:173–183
- Boden B, Kampa E (1967) The influence of natural light on the vertical migrations of an animal community in the sea. In: Marshall, N.B. (ed.) *Aspects of Marine Zoology*. Proc. Symp. zool. Soc. London. Vol. 19, 15–26
- Boggs, C.H. (2004) Pacific research on longline sea turtle bycatch. In: K.J. Long and B.A. Schroeder (eds). *Proceedings of the International Technical Expert Workshop on Marine Turtle Bycatch in Longline Fisheries*. US Department of Commerce, NOAA Technical Memorandum NMFS-F/OPR-26, Silver Spring, MD, USA, p. 189.
- Boyer T, Antonov J, Garcia H, Johnson D, Locarnini R, Mishonov A, Pitcher M, Baranova O, Smolyar I (2006) *World Ocean Database 2005*. NOAA Atlas NESDIS 60, U.S. Government Printing Office, Washington, D.C
- Brill R (1994) A review of temperature and oxygen tolerance studies of tunas pertinent to fisheries oceanography, movement models and stock assessments. *Fish Oceanogr* 3:204–216
- Brill RW, Bigelow KA, Musyl MK, Fritches KA, Warrant EJ (2005) Bigeye tuna (*Thunnus obesus*) behaviour and physiology and their relevance to stock assessments and fishery biology. In: J Porter, ed., *Collective Volume of Scientific Papers. Second World Meeting on Bigeye Tuna*, ICCAT, Madrid, Spain, vol. 57, 142–161

- Brodziak J, Ishimura G (2011) Development of bayesian production models for assessing the north pacific swordfish population. *Fish Sci* 77:23–24
- Carey F, Robison B (1981) Daily patterns in the activities of swordfish, *Xiphias gladius*, observed by acoustic telemetry. *Fish Bull* 79:277–292
- Carey FG (1990) Further acoustic telemetry observations of swordfish. In: Planning the future of billfishes. Research and management in 90s and beyond. (Proc. Second Int. Billfish Symp.)
- Chancollon O, Pusineri C, Ridoux V (2006) Food and feeding ecology of Northeast Atlantic swordfish (*Xiphias gladius*) off the Bay of Biscay. *ICES J Mar Sci* 63:1075–1085
- Courtney D, Piner K (2009) Preliminary age structured stock assessment of North Pacific swordfish (*Xiphias gladius*) with stock synthesis under a two stock scenario. Tech. Rep. ISC/09/BILLWG-3/07
- Dagorn L, Bach P, Josse E (2000) Movement patterns of large bigeye tuna (*Thunnus obesus*) in the open ocean, determined using ultrasonic telemetry. *Mar Biol* 136:361–371
- Dewar H, Prince E, Musyl RMK, Brill RW, Sepulveda C, Luo J, Foley D, Orbesen ES, Domeier ML, Nasby-Lucas N, Snodgrass D, Laurs RM, Hoolihan JP, Block BA, McNaughton LM (2011) Movements and behaviors of swordfish in the Atlantic and Pacific oceans examined using pop-up satellite archival tags. *Fish Oceanogr* 20:219–241
- Domeier ML, Dewar H and Nasby-Lucas N (2003) Mortality rate of striped marlin (*Tetrapturus audax*) caught with recreational tackle. *Mar Freshwater Res* 54:435–445
- Domeier ML, Kiefer D, Nasby-Lucas N, Wagschal A, O'Brien F (2005) Tracking Pacific bluefin tuna (*Thunnus thynnus orientalis*) in the northeastern Pacific with an automated algorithm that estimates latitude by matching sea-surface-temperature data from satellites with temperature data from tags on fish. *Fish Bull* 103:292–306
- Fritsches KA, Brill RW, Warrant EJ (2005) Warm Eyes Provide Superior Vision in Swordfishes. *Curr Biol* 15:55–58
- Garcia-Cortes B, Mejuto J (2005) Scientific estimations of bycatch landed by the Spanish surface longline fleet targeting swordfish (*Xiphias gladius*) in the Indian ocean: 2001 - 2003 period. Tech. Rep. IOTC-2005-WPBy-14
- Gilman E, Zollett E, Beverly S, Nakano H, Davis K, Shiode D, Dalzell P, Kinan I (2006) Reducing sea turtle by-catch in pelagic longline fisheries. *Fish and Fisheries* 7:2–23
- Gilman E, Kobayashi D, Swenarton T, Brothers N, Dalzell P, Kinan-Kelly I (2007) Reducing sea turtle interactions in the Hawaii-based longline swordfish fishery. *Biol Conserv* 139:19–28
- Graham, MH (2003) Confronting multicollinearity in ecological multiple regression. *Ecology* 84:2809–2815
- Gunn J, Block B (2001) Advances in acoustic, archival, and satellite tagging of tunas. *Fish Physiol* 19:167–224

- Hastie T, Tibshirani R (1990) Generalized Additive Models. Chapman and Hall, London, U. K.
- Hays GC (2003) A review of the adaptive significance and ecosystem consequences of zooplankton diel vertical migrations. *Hydrobiologia* 503:163–170
- Hays GC, Bradshaw C, James M, Lovell P, Sims D (2007) Why do Argos satellite tags deployed on marine animals stop transmitting? *J Exp Mar Biol Ecol* 349:52–60
- Holdsworth JC, Sippel TJ, Saul PJ (2007) An investigation into swordfish stock structure using satellite tag and release methods. Tech. Rep. WCPFC-SC3-BI SWG/WP- 3
- Holdsworth JC, Sippel TJ, Block BA (2009) Near real time satellite tracking of striped marlin (*Kajikia audax*) movements in the pacific ocean. *Mar Biol* 156:505–514
- Holts DB, Bartoo NW, Bedford DW (1994) Swordfish tracking in the southern California Bight. Admin. Rep. NOAA-SWFSC-LJ-94-15
- Howell EA, Hawn DR, Polovina JJ (2010) Spatiotemporal variability in bigeye tuna (*Thunnus obesus*) dive behavior in the central north Pacific Ocean. *Prog Oceanogr* 86:81–93
- Ichinokawa M, Brodziak J (2010) Using adaptive area stratification to standardize catch rates with application to North Pacific swordfish (*Xiphias gladius*). *Fish Res* 106:249–260
- Ito RY, Dollar RA, Kawamoto KE (1998) The Hawaii-based longline fishery for swordfish, *Xiphias gladius*. Tech. Rep. NOAA-NMFS-142
- Johnston D, McDonald M, Polovina J, Domokos R, Wiggins S, Hildebrand J (2008) Temporal patterns in the acoustic signals of beaked whales at Cross Seamount. *Biol Lett* 4:208–211
- Kalish JM, Greenlaw CF, Pearcy WG, Van Holliday D (1986) The biological and acoustical structure of sound scattering layers off Oregon. *Deep-Sea Res Part A* 33:631–653
- Kutner MH, Nachtsheim CJ, Neter J, Li W (2005) Applied linear statistical models. McGraw-Hill/Irwin, 5th ed., NY
- Lam CH, Nielsen A, Sibert JR (2008) Improving light and temperature based geolocation by unscented Kalman filtering. *Fish Res* 91:15–25
- Lam CH, Nielsen A, Sibert JR (2010) Incorporating sea-surface temperature to the light-based geolocation model trackit. *Mar Ecol Prog Ser* 419:71–84
- Lehodey P, Senina I, Murtugudde R (2008) A spatial ecosystem and populations dynamics model (SEAPODYM) - modeling of tuna and tuna-like populations. *Prog Oceanogr* 78:304–318
- Lehodey P, Senina I (2009) An update of recent developments and applications of the SEAPODYM model. Tech. Rep. WCPFC-SC5-2009/EB-WP-10

- Lehodey P, Senina I, Sibert J, Bopp L, Calmettes B, Hampton J, Murtugudde R (2010) Preliminary forecasts of population trends for Pacific bigeye tuna under the A2 IPCC scenario. *Prog Oceanogr* 86: 302–315
- Lewison RL, Freeman SA, Crowder LB (2004) Quantifying the effects of fisheries on threatened species: the impact of pelagic longlines on loggerhead and leatherback sea turtles. *Ecol Lett* 7:221–231
- Longhurst A (1975) Ecology of the season, W.B.Saunders Co., Philadelphia, chap. Vertical migration. 116–137
- Matciak, M. (1997) Estimation of the attenuation of the visible light in waters of the Gulf of Gdansk with the use of Secchi transparency. *Oceanol Stud* 26:35–40.
- Musyl M, Brill R, Boggs C, Curran D, Kazama T, Seki M (2003) Vertical movements of bigeye tuna (*Thunnus obesus*) associated with islands, buoys, and seamounts near the main Hawaiian islands from archival tagging data. *Fish Oceanogr* 12:152–169
- Nasby-Lucas N, Dewar H, Lam CH, Goldman KJ, Domeier ML (2009) White shark offshore habitat: A behavioral and environmental characterization of the eastern Pacific shared offshore foraging area. *PLOSone* 4:e1863
- Neilson JD, Smith S, Royer F, Paul SD, Porter JM, Lutcavage M (2009) Tagging and Tracking of Marine Animals with Electronic Devices, Springer Netherlands, chap. Investigations of Horizontal Movements of Atlantic Swordfish Using Pop- up Satellite Archival Tags. 145–159
- Nelson DR, McKibben JN, Strong WR Jr, Lowe CG, Sisneros JA, Schroeder DM, Lavenberg RJ (1997) An acoustic tracking of a megamouth shark, *Megachasma pelagios*: a crepuscular vertical migrator. *Environ Biol Fish* 49:389–399
- Nielsen A, Sibert J (2007) State-space model for light-based tracking of marine animals. *Can J Fish Aquat Sci* 64:1055–1068
- Petersen SL, Honig MB, Ryan PG, Nel R, Underhill LG (2009) Turtle bycatch in the pelagic longline fishery off southern Africa. *Afr J Mar Sci* 31:87-96.
- Piovano S, Swimmer Y, Giacomini C (2009) Are circle hooks effective in reducing incidental captures of loggerhead sea turtles in a Mediterranean longline fishery? *Aquat Conserv* 19:779–785
- Polovina JJ, Howell E, Parker DM, Balazs GH (2003) Dive-depth distribution of loggerhead and olive ridley sea turtles in the central North Pacific: might deep longline sets catch fewer turtles? *Fish Bull* 101:189–193
- Polovina JJ, Hawn D, Abecassis M (2008) Vertical movement and habitat of opah (*Lampris guttatus*) in the central North Pacific recorded with pop-up archival tags. *Mar Biol* 153:257–267
- Potier M, Marsac F, Cherel Y, Lucas V, Sabatie R, Maury O, Menard F (2007) Forage fauna in the diet of three large pelagic fishes (lancetfish, swordfish and yellowfin tuna) in the western equatorial Indian Ocean. *Fish Res* 83:60–72

- Prince ED, Goodyear CP (2006) Hypoxia-based habitat compression of tropical pelagic fishes. *Fish Oceanogr* 15:451 – 464
- Prince ED, Luo J, Goodyear CP, Hoolihan JP, Snodgrass D, Orbesen ES, Serafy JE, Ortiz M, Schirripa MJ (2010) Ocean scale hypoxia-based habitat compression of Atlantic istiophorid billfishes. *Fish Oceanogr* 19:448–462
- Reeb C, Arcangeli L, Block B (2000) Structure and migration corridors in Pacific populations of the swordfish *Xiphias gladius*, as inferred through analyses of mitochondrial DNA. *Mar Biol* 136:1123–1131
- Royer F, Lutcavage M (2008) Filtering and interpreting location errors in satellite telemetry of marine animals. *J Exp Mar Biol Ecol* 359:1–10
- Royer F, Lutcavage M (2009) Tagging and Tracking of Marine Animals with Electronic Devices, Springer Netherlands, chap. Positioning pelagic fish from sunrise and sunset times: error assessment and improvement through constrained, robust modeling. 323–341
- Royer F, Fromentin JM, Gaspar P (2005) A state-space model to derive bluefin tuna movement and habitat from archival tags. *Oikos* 109:473–484
- Sepulveda CA, Knight A, Nasby-Lucas N, Domeier ML (2010) Fine-scale movements of the swordfish *Xiphias gladius* in the Southern California Bight. *Fish Oceanogr* 19:279–289
- Senina I, Sibert J, Lehodey P (2008) Parameter estimation for basin-scale ecosystem-linked population models of large pelagic predators: Application to skipjack tuna. *Prog Oceanogr* 78:319–335
- Sippel T (2010) Tracking of striped marlin (*Kajikia audax*) in the southwest Pacific Ocean: environmental influences on movement and behaviour. Ph.D. thesis, University of Auckland, New Zealand
- Smith HF, Sandwell DT (1997) Global Sea Floor Topography from Satellite Altimetry and Ship Depth Soundings, *Science* 277:1956-1962.
- Stramma L, Schmidtko S, Levin LA, Johnson GC (2010) Ocean oxygen minima expansions and their biological impacts. *Deep-Sea Res Part I* 57:587–595
- Takahashi M, Okamura H, Yokawa K, Okazaki M (2003) Swimming behaviour and migration of a swordfish recorded by an archival tag. *Mar Freshw Res* 54:527–534
- Teo SLH, Boustany A, Blackwell S, Walli A, Weng KC, Block BA (2004) Validation of geolocation estimates based on light level and sea surface temperature from electronic tags. *Mar Ecol Prog Ser* 283:81–98
- Tont S (1975) Deep scattering layers: patterns in the Pacific. Tech. Rep. 18, SCRIPPS – CalCOFI
- Uchiyama JH, Demartini EE, Williams HA (1999) Length-Weight Interrelationships For Swordfish, *Xiphias Gladis* L., Caught In The Central North Pacific. Tech. Rep. NOAA-TM-NMFS-SWFSC-284

- Ward R, Reeb C, Block B (2001) Population structure of Australian swordfish, *Xiphias gladius*. Final Report to the Australian Fisheries Management Authority, Canberra, CSIRO
- Watson J, Epperly S, Shah A, Foster D (2005) Fishing methods to reduce sea turtle mortality associated with pelagic longlines. *Can J Fish Aquat Sci* 62:965–981
- Wegner NC, Sepulveda CA, Bull KB, Graham JB (2010) Gill morphometrics in relation to gas transfer and ram ventilation in high-energy demand teleosts: Scombrids and billfishes. *J Morphol* 271:36.49
- Wilson SG, Lutcavage ME, Brill RW, Genovese MP, Cooper AB, Everly AW (2005) Movements of bluefin tuna (*Thunnus thynnus*) in the northwestern Atlantic Ocean recorded by pop-up satellite archival tags. *Mar Biol* 146(2):409–423
- Wood S (2006) Generalized Additive Models: An Introduction with R. CRC Press, Boca Raton, FL.
- Young J, Lansdell M, Riddoch S, Revill A (2006) Feeding ecology of broadbill swordfish, *Xiphias gladius*, off eastern Australia in relation to physical and environmental variables. *Bull Mar Sci* 79:793-80

SUPPLEMENTAL MATERIAL

SUMMARIES OF THE INDIVIDUAL GAM MODELS :

mean depth ~ s(log(chl))

	Estimate	Std. Error	t value	Pr(> t)
(Intercept)	371.98	3.71	100.3	< 2e-16
	edf	Ref.df	F	p-value
s(log(chl))	10.87	12.55	68.1	<2e-16
R-sq.(adj) = 0.545	Deviance explained = 55.2%			
GCV score = 10103	Scale est. = 9800.8		n = 713	

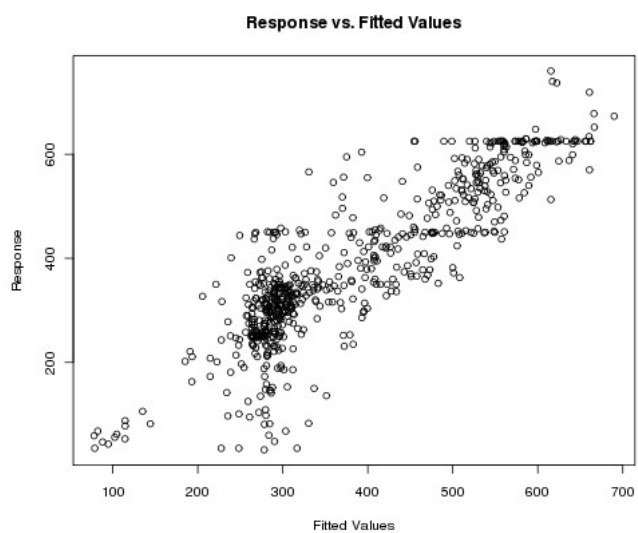
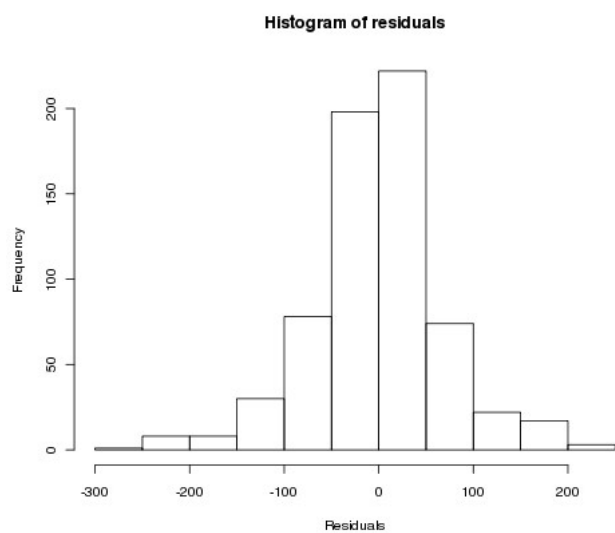
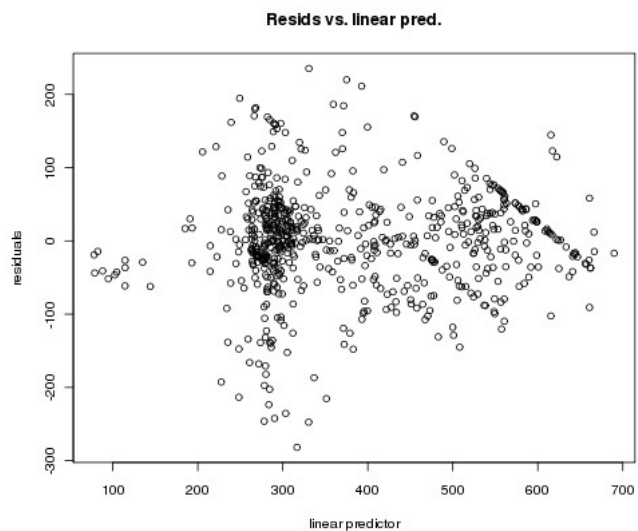
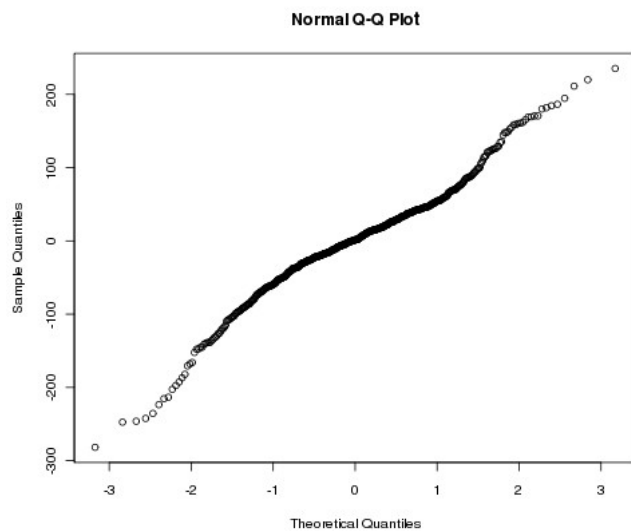
Mean depth ~ s(ox400)

	Estimate	Std. Error	t value	Pr(> t)
(Intercept)	370.68	3.91	94.83	<2e-16
	edf	Ref.df	F	p-value
s(ox400)	12.92	13.79	48.58	<2e-16
R-sq.(adj) = 0.475	Deviance explained = 48.5%			
GCV score = 11672	Scale est. = 11277		n = 738	

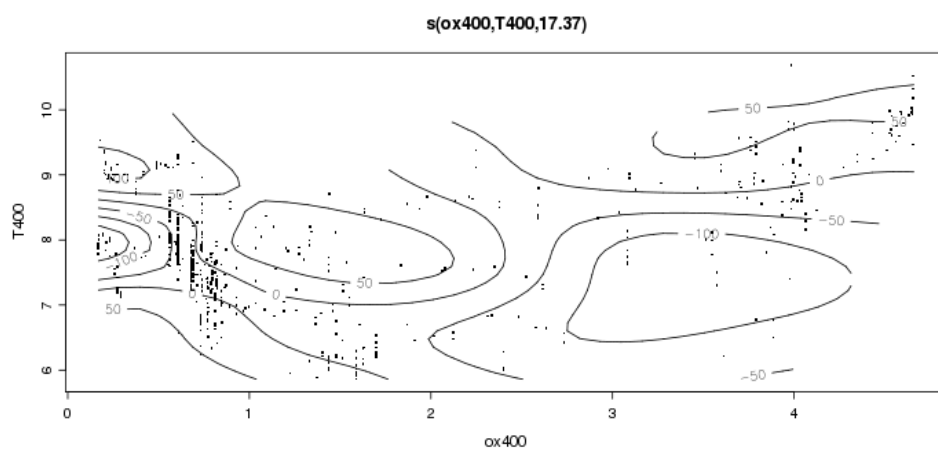
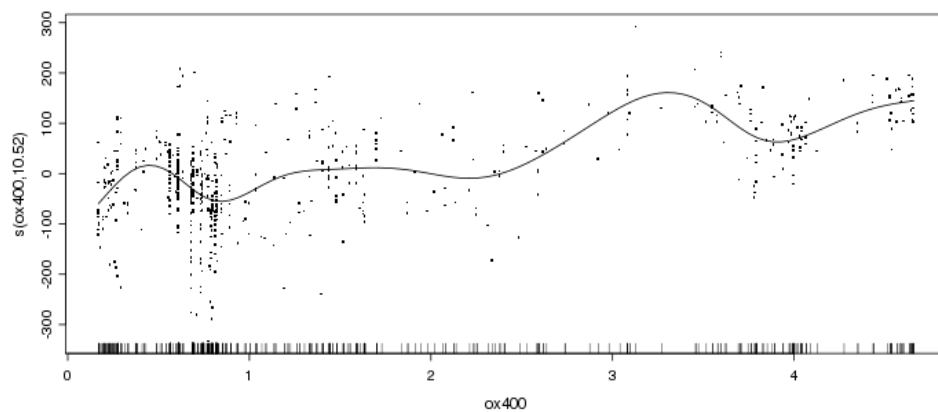
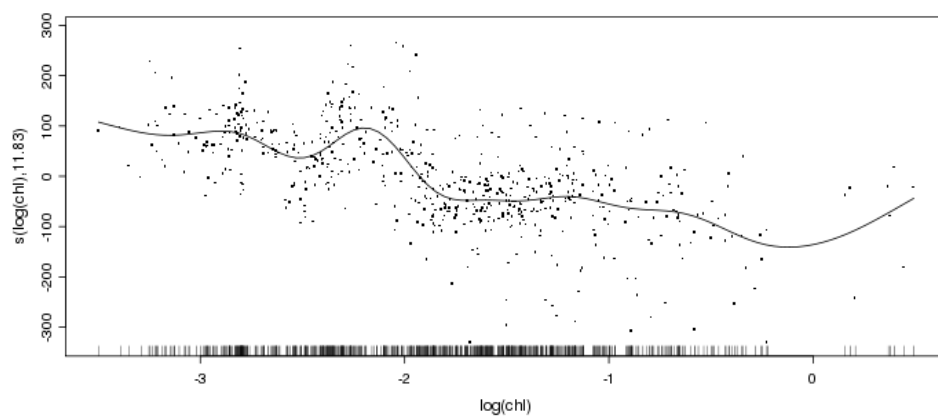
Mean depth ~ s(T400)

	Estimate	Std. Error	t value	Pr(> t)
(Intercept)	379.67	4.12	92.26	<2e-16
	edf	Ref.df	F	p-value
s(T400)	7.25	7.83	74.94	<2e-16
R-sq.(adj) = 0.462	Deviance explained = 46.8%			
GCV score = 11789	Scale est. = 11532		n = 681	

DIAGNOSTIC PLOTS FOR THE FULL MODEL :



PLOTS OF THE SMOOTHS FOR CHLA, OXYGEN AND INTERACTION TERM ESTIMATED BY THE FULL MODEL.



CHAPITRE 3

SUIVIS DE TORTUES CAOUANNES ET MODELISATION D'HABITAT ET DE MOUVEMENTS

En préparation. Non soumis pour publication.

RESUME

40 tortues caouannes (*Caretta caretta*), capturées accidentellement par des palangriers dans le Pacifique Nord ont été équipées de balises satellites par des observateurs scientifiques à bord de bateaux de pêche entre 1997 et 2000, et 184 tortues élevées en captivité à l'aquarium du Port de Nagoya, au Japon, ont été similairement équipées et relâchées en haute mer au cours de 8 campagnes scientifiques entre 2003 et 2007. Les individus relâchés mesuraient entre 23 et 81 cm.

Leurs préférences environnementales ont été analysées dans cette étude. Plusieurs variables environnementales (température et courants de surface) ont été extraites le long des trajectoires pour étudier les variations de la température préférée et de la vitesse des animaux en fonction de leur taille. La température de surface moyenne le long des traces observées varie entre 18 et 23°C.

Généralement, les tortues de taille plus importante se trouvaient dans des eaux de surface plus chaudes mais étaient soumises à des variations de température plus importantes que les petites tortues. Des variations saisonnières entre les petits et grands individus suggèrent que les plus grands plongent parfois sous la couche de mélange en été lorsque la colonne d'eau est très stratifiée et ciblent ensuite des eaux de surface plus chaudes pour se réchauffer.

Les vitesses de nage moyennes le long des traces sont inférieures à 1 km/h et augmentent avec la taille de l'animal pour les individus de taille supérieure à 30 cm. Néanmoins, lorsque la vitesse est exprimée en longueurs corporelles par seconde (bl s^{-1}), les petites tortues ont des vitesses de nage plus élevées ($> 1 \text{ bl s}^{-1}$) que les plus grandes (0.5 bl s^{-1}).

Les valeurs de température et de vitesse de nage spécifiques à chaque taille ont ensuite été utilisées comme paramètres d'un modèle eulérien basé sur les préférences en habitat, pour prédire les zones de probabilité de présence maximales des tortues caouannes dans le Pacifique nord. Le modèle utilisé dans cette étude est une version simplifiée (appelée MOVEMOD) du modèle de dynamique spatiale SEAPODYM, développé à l'origine pour les thons tropicaux. L'indice d'habitat prédit par MOVEMOD est en très bon accord avec les traces observées, et capture les mouvements saisonniers nord-sud des animaux, mais le modèle ne reproduit pas les mouvements est-ouest des tortues marquées, ce qui suggère que la dynamique est-ouest à grande échelle des tortues caouannes est contrôlée par des mécanismes additionnels en plus de leur préférence en température et de la concentration de proies.

Analysis of loggerhead turtles tracks in the North Pacific to parameterize a feeding habitat and movement model

Melanie Abecassis¹, Patrick Lehodey², Jeffrey Polovina³, Inna Senina², Philippe Gaspar²,
Beatriz Calmettes², George Balazs³, Denise Parker¹

¹Joint Institute for Marine and Atmospheric Research, University of Hawaii, 1000 Pope Rd., Honolulu, HI, 96822, USA

Email : melanie.abecassis@noaa.gov

²Collecte Localisation Satellite, 8 rue Hermes, 31520 Ramonville-Saint-Agne, France

³Pacific Islands Fisheries Science Center, NOAA Fisheries, 2570 Dole St., Honolulu, HI, 96822, USA

ABSTRACT

Habitat preferences for loggerhead turtles in the North Pacific were investigated with data from two several-year long tagging programs, using 224 satellite transmitters deployed on wild and captivity-reared turtles. Animals ranged between 23 and 81 cm in size. Tracks were used to investigate changes in temperature preferences and speed of the animals with size. Average sea surface temperatures along the tracks ranged from 18 to 23 °C. Bigger turtles generally experienced larger temperature ranges and were encountered in warmer surface waters. Seasonal differences between small and big turtles suggest that the larger ones dive deeper than the mixed layer and subsequently target warmer surface waters to rewarm. Average swimming speeds were under 1 km/h and increased with size for turtles bigger than 30 cm. However, when expressed in body lengths per second (bl s^{-1}), smaller turtles had much higher swimming speeds ($> 1 \text{ bl s}^{-1}$) than bigger ones (0.5 bl s^{-1}). Temperature and speed values at size estimated from the tracks were used to parameterize a habitat-based Eulerian model to predict areas of highest probability of presence in the North Pacific. The model-generated habitat index generally matched the tracks closely, capturing the north-south movements of tracked animals, but the model failed to replicate observed east-west movements, suggesting temperature and foraging preferences are not the only factors explaining large-scale loggerhead movements.

INTRODUCTION

Loggerhead sea turtles (*Caretta caretta*) are distributed in tropical and temperate areas of each ocean basin and occupy pelagic, coastal and terrestrial habitats during their life cycle. Their only known nesting areas in the Pacific are located in Japan, Australia and New Caledonia (Kamezaki et al. 2003, Limpus & Limpus 2003). During their juvenile phase, loggerheads spend years, and probably decades in the open ocean. Some juvenile populations are also found in coastal regions. One such area is located in Baja California where turtles from both nesting regions (but predominantly turtles originating from Japan) occur (Bowen et al. 1995). Most likely, loggerheads possess two different foraging strategies, yielding some to spend their entire juvenile phase in the open ocean, and some others in coastal areas (Polovina et al 2006, Peckham et al 2011). When they reach sexual maturity, the adults then undertake long migrations towards the nesting beaches, every 2.5 – 3 years. There is a lot of uncertainty on the age at maturity of loggerheads, but the most recent study estimates it is around 45

years, which makes them one of the reptile species that reach maturity the latest and heightens concerns for their conservation (Scott et al 2011).

Loggerheads were relisted as endangered in the North and South Pacific by the U.S. National Marine Fisheries Service and the U.S. Fish and Wildlife Service in September 2011. One particular threat they face is incidental takes in pelagic longlines, especially shallow longlines targeting swordfish. These fisheries are highly controversial and considerable efforts to reduce bycatch of turtles have been expanded in recent years, in particular in the US, following temporary closures of the Hawaii-based fishery and stronger regulations. Substantial reductions in interactions with protected species have been observed since then (Lewison et al. 2004; Swimmer & Brill 2006; Gilman et al. 2007; Howell et al. 2008). In the Hawaii-based longline fishery, there is now 100% observer coverage and the fishery closes if more than 17 loggerhead sea turtles are caught in any calendar year. However, bycatch mortality remains and some studies suggest that there may have been a transfer of the bycatch mortality to foreign fleets due to the higher regulations in the US fisheries (Benson et al. 2009).

Further reductions of loggerhead takes in the longline fishery may be achieved if longline fisheries target swordfish in places and during times when loggerhead turtles are not occupying the same habitat as swordfish (Polovina et al. 2003; Gilman et al. 2006, 2007; Beverly et al. 2004, 2009; Abecassis et al. in prep). To achieve this will require an understanding of the pelagic habitats of swordfish and loggerhead turtles. The pelagic habitat of loggerhead turtles in the North Pacific has been fairly well described as a result of considerable electronic tagging (Kobayashi et al. 2008; Polovina et al. 2000, 2003, 2004, 2006; Howell et al. 2010). An analysis of fishing and electronic tagging data was used to design a first index of high probability of presence of turtles which was developed by the Pacific Islands Fisheries Science Center (PIFSC, NOAA). The index, called TurtleWatch, is displayed on maps and distributed weekly to fishermen (Howell et al 2008).

The main focus of this paper is to use tracking data to evaluate the feasibility of adapting a spatial population dynamics model, initially developed for tropical tunas, to predict more precisely the feeding habitat and movements of loggerhead turtles in the North Pacific.

MATERIALS AND METHODS

PROCESSING AND ANALYSIS OF TAGGING DATA

Tagging and tracks processing

Forty electronic tags were placed by scientific observers on loggerhead turtles caught in the Hawaii-based longline fishery from 1997 to 2000 (hereafter called Hawaiian releases); 184 loggerhead turtles were reared in captivity at the Port of Nagoya Aquarium, and released in the ocean in several different locations during 8 deployments between 2003 and 2007 (hereafter referred to as Japanese releases. See Tables 1 and 2).

Turtles were outfitted with satellite transmitters attached to the carapace using the procedures described in Balazs et al. (1996). They were equipped with Telonics (Mesa, AZ, USA) model ST-18, ST-19, ST-24, and Wildlife Computers (Redmond, WA, USA) model SDR-T10, SDR-T16, or SPOT 3/4/5 Argos-linked satellite transmitters. Tracking data were collected through the ARGOS system by the Pacific Island Fisheries Science Center (NOAA), Marine Turtle Research Program, Honolulu, Hawaii.

To filter out Argos location errors, all tracks were processed the same way as in Gaspar et al. (2006). First, all locations yielding velocities greater than 10 km/h were removed. Then, to remove artificial “spikes” from the data, an Epanechnikov filter (Seifert & Gasser 1998) was applied with a two-day window, centered on each individual location, using the *lpepa* function of the *lpridge* package in the R environment (The R Project for Statistical Computing, <http://www.r-project.org/>). The points providing the 5% largest differences between filtered and observed locations were removed. The original track without those extreme locations was then resampled at a 3-hour interval. Finally, a second Epanechnikov filter was applied every 3-hour with a 2-day window to smooth the track.

id	date deployed	longitude	latitude	SCL	# days out
24181	01/23/1997	190.21 E	28.708N	44.5	55
19580	02/02/1997	196.7 E	29.480N	52.0	115
19585	02/15/1997	199.01 E	29.782N	41.0	90
19582	03/17/1997	205.57 E	30.863N	62.0	136
24184	03/30/1997	199.42 E	26.160N	73.0	42
19587	04/10/1997	191.01 E	26.743N	73.6	13
19581	04/20/1997	205.32 E	29.232N	53.7	12
19586	04/22/1997	203.42 E	28.758N	81.0	178
24182	09/11/1997	228.93 E	37.722N	45.0	67
19599	01/06/1998	216.97 E	33.567N	45.5	206
19598	01/07/1998	217.46 E	34.383N	48.0	191
19594	02/07/1998	205.35 E	30.567N	58.0	103
24185	02/07/1998	204.95 E	30.533N	61.0	71
7298	03/10/1998	190.35 E	28.967N	74.0	0
7299	03/15/1998	190.63 E	28.533N	73.5	0
19591	04/06/1998	201.76 E	27.911N	76.0	1
19590	08/26/1998	196.7 E	36.438N	57.7	106
19608	08/26/1998	197.36 E	36.288N	58.0	167
19601	10/18/1998	195.22 E	37.717N	52.5	41
19606	10/20/1998	220.4 E	38.477N	59.1	161
19604	11/02/1998	198.1 E	36.667N	62.5	51
25360	12/05/1998	197.53 E	34.250N	67.0	1
24189	12/05/1998	197.53 E	34.250N	59.0	1
24190	12/10/1998	223.9 E	34.230N	56.5	6
25359	12/23/1998	210.02 E	33.642N	57.5	211
19605	01/04/1999	207.72 E	32.183N	46.0	0
25358	01/04/1999	207.72 E	32.183N	54.0	1
25361	01/30/1999	206.35 E	32.038N	53.5	0
19602	01/31/1999	203.68 E	24.767N	83.0	51
19597	02/03/1999	215.32 E	31.917N	60.0	1
24179	02/03/1999	206.18 E	32.028N	52.5	131
22174	12/14/1999	209.08 E	32.921N	51.5	271
22173	01/17/2000	216.71 E	32.772N	62.0	72
24188	01/31/2000	215.52 E	31.833N	54.0	0
22152	02/03/2000	190.72 E	32.686N	67.0	157
22172	02/12/2000	221.45 E	32.256N	55.0	49
22150	03/05/2000	213.45 E	31.133N	60.0	597
22153	03/07/2000	213.29 E	31.065N	56.0	246
24747	05/30/2000	205.23 E	24.955N	83.0	138
22534	08/19/2000	226.4 E	35.794N	61.0	177

Table 1. Releases from Hawaii-based longline vessels

date deployed	longitude	latitude	# deployed	SCL (cm)	# days out
04/24/2003	140.166E	34.643N	7	38.9 - 59.4	67 - 565
11/28/2003	140.233E	34.867N	18	26.2 - 56.0	48 - 1270
04/23/2004	141.122E	35.431N	13	25.6 - 64.8	27 - 626
11/19/2004	140.590E	34.867N	26	28.4 - 35.3	85 - 462
05/04/2005	176.617E	32.667N	44	29.6 - 38.4	229 - 1368
07/30/2005	136.900E	33.950N	16	39.2 - 47.0	0 - 438
10/27/2006	176.832E	32.852N	35	23.3 - 30.2	47 - 493
09/24/2007	140.590E	34.867N	25	23.6 - 28.2	62 - 465

Table 2. Releases of turtles reared at the Port of Nagoya aquarium

Size, temperature preference and swimming speed

The temperature preference and swimming speed were estimated from the loggerhead turtle satellite tracks using 0.1° - weekly Pathfinder-GAC satellite SST data, provided by the NOAA-Coastwatch program, and filtered 1°x1°x5d ocean surface currents data, downloaded from the NOAA-OSCAR website. Both data sets covered the entire tracking period (1997 to 2008). Values were extracted along each processed track using the Generic Mapping Tools (<http://gmt.soest.hawaii.edu/>).

The change in curved carapace length (CCL) along the tracks was estimated using recently published results on loggerhead turtles growth rates (Scott et al. 2011) to account for the change in size, especially during long tracks: growth rate (cm/yr CCL) = $-10.6 * \log_{10}(\text{CCL}) + 21.5$. CCL was converted to Straight Carapace Length (SCL) using the relationship in Peckham et al. (2011): $\text{SCL} = 0.369 + 0.932 * \text{CCL}$.

To evaluate the change in temperature habitat with size, a generalized additive model (GAM, Hastie & Tibshirani 1990) was built using the *mgcv* library in R to study the relationship between SST along the tracks and size, while accounting for other potential sources of variability in SST, such as the inter-annual (year) and seasonal (month) variations, as well as latitude and longitude.

The observed velocity of a swimming animal (V_g) is the sum of the animal's own velocity (V) and the velocity of the current (V_c). To study the turtles active movements, and separate swimming from drifting, ocean currents were removed from the tracks ($V = V_g - V_c$, Gaspar et al. 2006). Loggerhead turtles spend 90 % of their time within the first 5 m of the water column (Howell et al. 2010) which justifies the use of OSCAR surface currents for this analysis.

An estimate of maximum sustainable speed (MSS) was then computed as the monthly 90th percentile of the animals' active movement speed and was converted in body lengths (bl) per second (bl s⁻¹) by dividing it by the animal's monthly estimated SCL. The 90th percentile was chosen arbitrarily as a proxy for MSS.

HABITAT AND MOVEMENT MODELING

To model loggerhead turtle habitats and movements, we used MOVEMOD which is a simplified non age-structured version of the SEAPODYM (Spatial Ecosystem And Populations Dynamics Model) model, forced by the most realistic 3D physical available ocean reanalysis and by satellite-derived primary production.

Environmental forcing fields for simulations

The Mercator-Ocean GLORYS-1 (GLobal Ocean ReanALYsis and Simulations) reanalysis was used to provide temperature and ocean currents forcing fields, in conjunction with net primary production data derived from ocean colour satellite data (<http://www.science.oregonstate.edu/ocean.productivity/>). GLORYS-1 is an eddy-permitting global ocean reanalysis produced for the period 2002-2007 with the ocean general circulation model configuration ORCA025 NEMO (Barnier et al. 2006) at a spatial resolution of $\frac{1}{4}^\circ$. Its results are available at a daily time step. The assimilation method is based on a reduced order Kalman filter (SEEK formulation, Pham et al. 1998) adapted to this configuration (Tranchant et al. 2008). Because satellite (SST and altimetry) and in situ data are assimilated in this ocean reanalysis, predicted fields of temperature and currents are coherent with those of primary production derived from ocean color data, using the VGPM model of Behrenfeld and Falkowsky (Behrenfeld & Falkowski 1997). To be used as forcings for the SEAPODYM model, both GLORYS-1 outputs and primary production data were interpolated on a regular grid of 0.25° with a time step of 6 days.

SEAPODYM

SEAPODYM was developed initially to simulate the age-structured spatial dynamics of tropical tuna populations in pelagic ecosystems, in interaction with their environment (Lehodey 2001; Lehodey et al. 2003, 2008; Senina et al. 2008; Lehodey et al. 2010). It uses physical-biogeochemical environmental fields to simulate the upper trophic levels of marine ecosystems organized in two groups: the predator species (e.g. tuna, billfish, or turtles) and their prey species of the mid-trophic levels (i.e. micronekton). SEAPODYM is built with a three-layer structure: epipelagic between the surface and one euphotic depth (Z_{eu}), mesopelagic between 1 and 3 Z_{eu} , and bathypelagic between 3 Z_{eu} and 7 Z_{eu} . The micronekton functional groups are described with several components characterized by their habitat and vertical behaviour (Lehodey et al. 2010). Predator movements are described by advection-diffusion equations. Diffusion is used to represent random movements (kinesis), and advection to reproduce both the transport due to currents and directed movements in response to external stimuli (taxis). Directed movements follow the gradient of a habitat index depending on temperature preference, oxygen constraints (for fish) and prey availability.

MOVEMOD

As information is scarce on loggerhead natural mortality and reproductive dynamics, a simplified single age/size class version of the SEAPODYM model, called MOVEMOD, was used, where temperature and feeding habitats only are modeled for a given cohort. This model was adapted to air-breathing turtles by removing any oxygen constraint from the habitat definitions. As loggerhead turtles usually stay in close proximity to the surface and spend most of their time in the first 30m (Howell et al. 2010), we used GLORYS.1 temperature and horizontal currents averaged over the first 30 m of the water column instead of the euphotic depth to prevent the ocean currents and temperature signals to be diluted when averaged across the whole epipelagic layer, as defined in SEAPODYM. For the prey field however, we used the whole epipelagic component (comprising prey items that reside in the epipelagic layer during both day and night, as well as migrants from deeper layers during the night (Lehodey et al.

2010). For a cohort of a given age and size, the feeding habitat defined by the accessibility to the forage species is controlled, in the case of turtles, simply by a temperature preference that needs to be parameterized and by the concentration of prey. Then the gradient of this habitat is used to influence the directed (advection) and random (diffusion) movements of the animals. Temperature preference is modeled by a Gaussian-shape index (between 0 and 1), the mean and standard deviation of which represent the animal's optimal temperature and temperature tolerance, respectively (Lehodey et al. 2008). Advection and diffusion both depend on the feeding habitat, the animal's size and maximum sustainable speed (MSS) expressed in body lengths per second.

Simulations and validation

Using values of temperature preference and speed assessed from the tagging data analysis, the predicted habitat was simulated for two different batches of releases (Nov. 2004 and May 2005, Table 2), using the average of the turtle sizes for each batch. Those two releases were chosen because their ranges of sizes were small enough to reasonably treat all the turtles released on each day as one single cohort in Movemod. The habitat index predicted by the model was compared to the corresponding tracks and to the TurtleWatch index defined by a statistical analysis between locations of turtle by-catch and SST (Howell et al. 2008; <http://www.pifsc.noaa.gov/eod/turtlewatch.php>).

To study the spatial dynamics of the animals once the habitat preferences were determined, we simulated the release of a batch of 2000 “virtual” turtles, or seeds, in MOVEMOD, in the same locations and times the tagging deployments occurred, and ran the model to estimate the distribution of population density over a one-year period. We compared the simulated density distributions with the locations of the tagged turtles every quarter to assess the validity of the modeled habitats. The simulation for the May 2005 release was then repeated after switching the mechanisms of active swimming off, to compare the agreement between the modeled turtle density distribution and the observed positions at the end of the year in each case (passive drifting in ocean currents vs movement including advection by currents and active swimming).

Because forcing data for the earlier years during which the Hawaiian turtles were released (1997-2001) were not available, we assumed that the main patterns of ocean circulation would not change drastically from one year to another and tried to simulate three Hawaiian releases in 2005.

And to test the impact of longer times at liberty and departures during different years (characterized by different El Niño/La Niña events for example) on movements, we ran several simulations starting at the same location and time of the year as the May 2005 release, using the entirety of the forcing available to us: from May 2002, 2003, 2004, 2005 and 2006 (respectively) to Dec. 2007.

RESULTS

TRACKS PROCESSING AND ANALYSIS

Track durations varied between 0 and 1270 days. Twelve and 8 of the Hawaiian and Japanese releases, respectively, transmitted data for less than ten days and were thus discarded from the study. Another set of 16 Japanese tracks had to be excluded because they exhibited data gaps too large (typically over 3° in longitude or latitude) for the interpolation to behave properly. Remaining processed tracks are shown in Fig. 1.

The turtles tagged in the course of the various deployments ranged between 23 and 81 cm in size (Fig.2 left). The turtle sizes estimated by taking into account turtle growth during the tracks are shown in Fig. 2 (right). Most of the Japanese releases were smaller than 40 cm upon release, whereas all Hawaiian releases were bigger than 40cm.

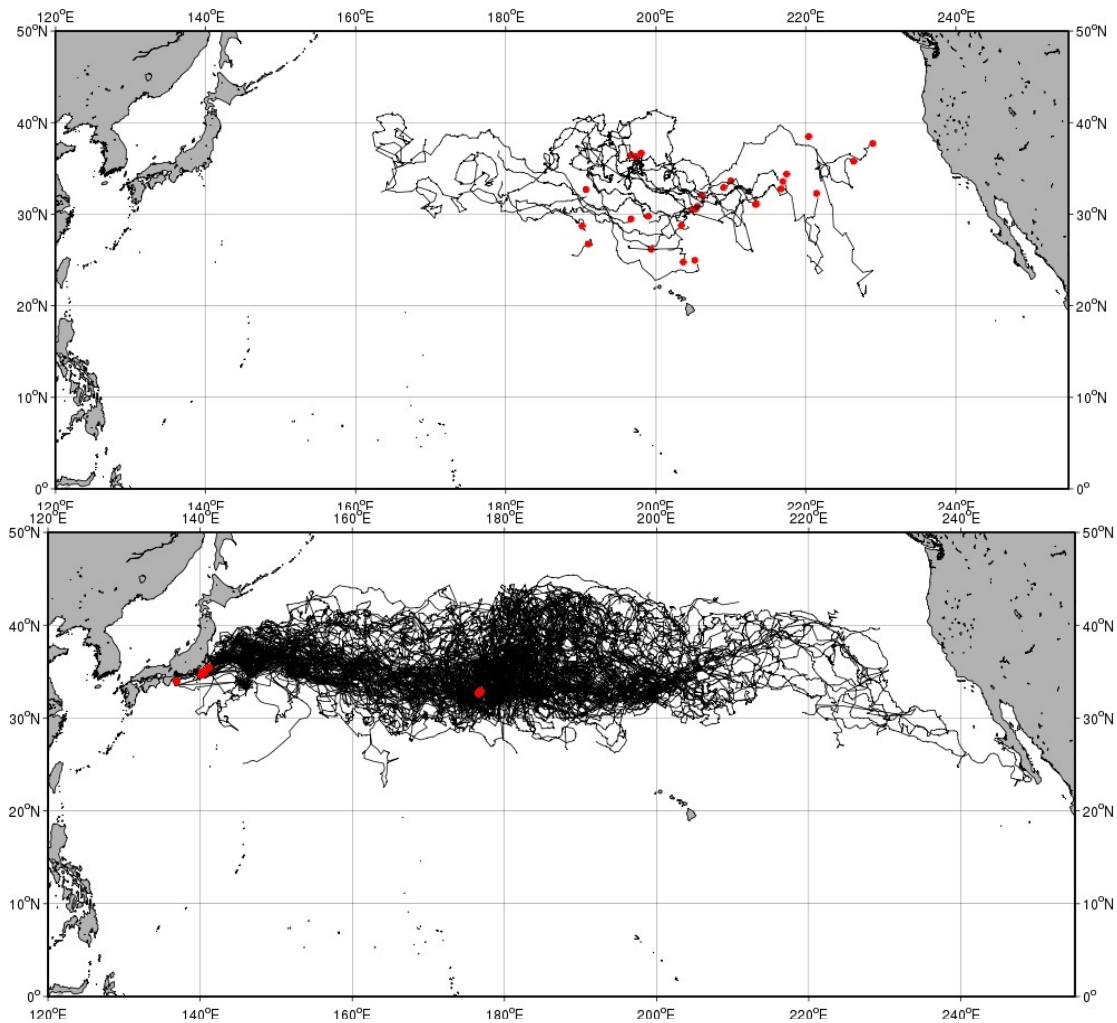


Figure 1: Maps of the tracks from the Hawaiian (top) and Japanese (bottom) releases. Red dots indicate release locations.

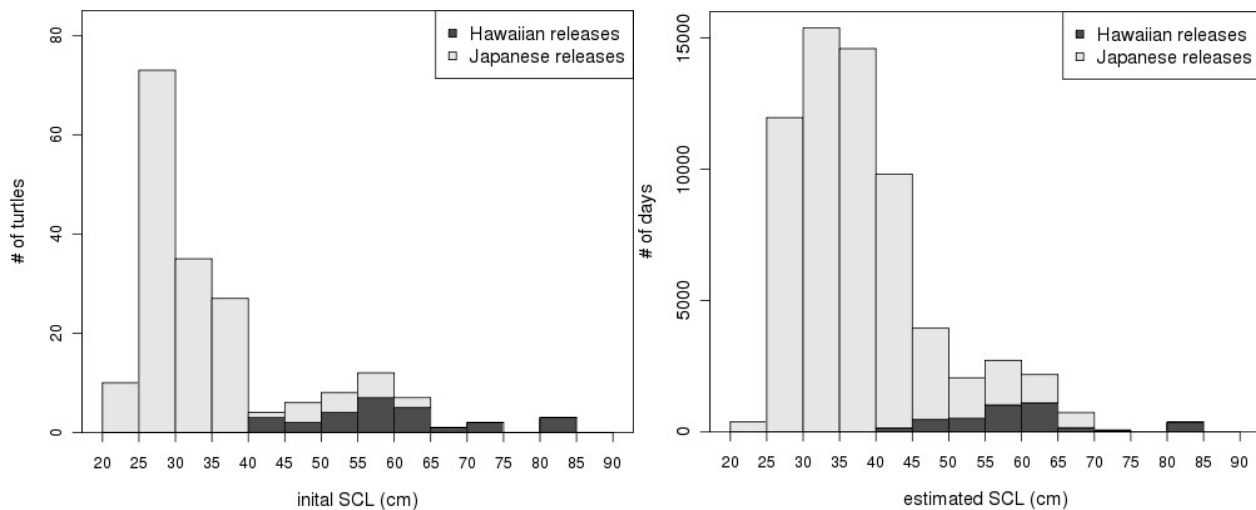


Figure 2: Size frequency at time of release (left) and estimated size frequency accounting for growth along the tracks (in # of days of data in each size bin, right)

Size vs surface temperature “preference”

To investigate the relationship between SST experienced along the track and the size of individuals, we grouped the data in 4 groups depending on the estimated size along the tracks (Figs. 2 & 3) and compared the mean and standard deviation of the corresponding SST values in each group. Those were plotted as Gaussian curves (Fig. 3) describing a “preference” index, between 0 and 1. The standard deviations of SST increased with size between the 4 groups, as well as the means. To avoid areas in the central Pacific gyre from being compared with locations in the Kuroshio Current (where water temperatures are generally lower than in the gyre, but where no big turtle was released), this part of the analysis was restricted to locations east of 180°E only. The group of largest turtles was experiencing a wider range of SST and tended to be in warmer surface waters (mean SST of 19.0 °C) than the small individuals (mean SST of 17.6 °C for the first group).

Then, the potential impact of seasonal variability was explored with two different GAMs, considering winter (December to March, when the surface layer is not stratified) and summer (June to September, when stratification is strong) separately and including SCL, the inter-annual (year) variation, as well as latitude and longitude, to account for other sources of variability in SST. An interesting difference appears in the relationship between SST and loggerhead turtle size (Fig. 4). While there is not much difference in the SST encountered by big or small turtles in the winter (SST range: 16.7-17.5 °C), the contrast is stronger in the summer (SST range: 19.5-21 °C). To test whether this difference might be due to the fact that smaller turtles were less capable of actively swimming to keep up with oceanic changes to maintain themselves at their preferred temperature, the mean latitude of the turtles released in May 2005 (mean size: 35 cm) was compared with the mean latitude of the 17°C SST isotherm at 190°E longitude (Fig. 4). The close match of data suggests that juvenile turtles very likely have the capability to stay within a desirable range of temperature.

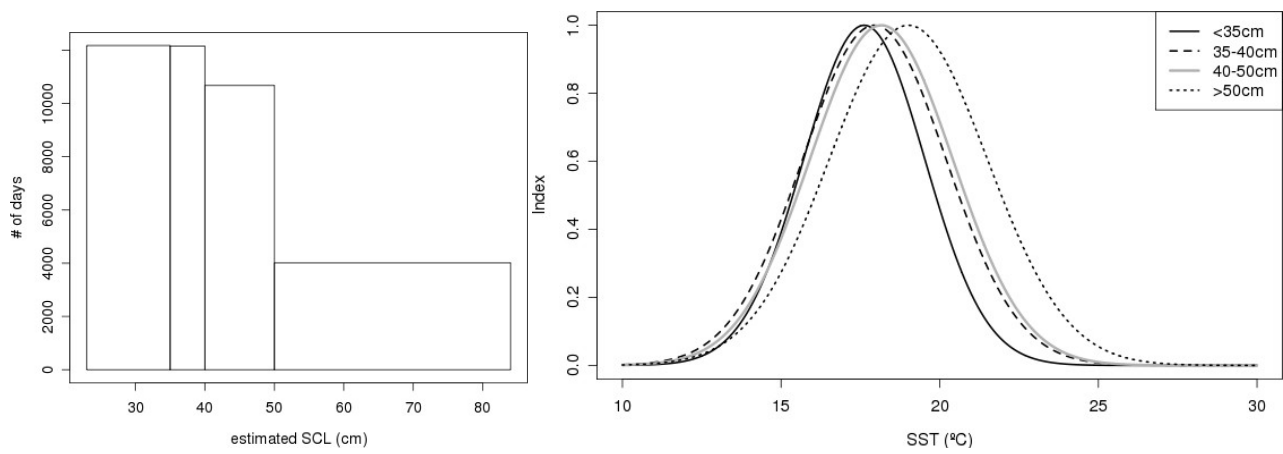


Figure 3: Size histogram for 4 size classes (left) and respective temperature “preference” index

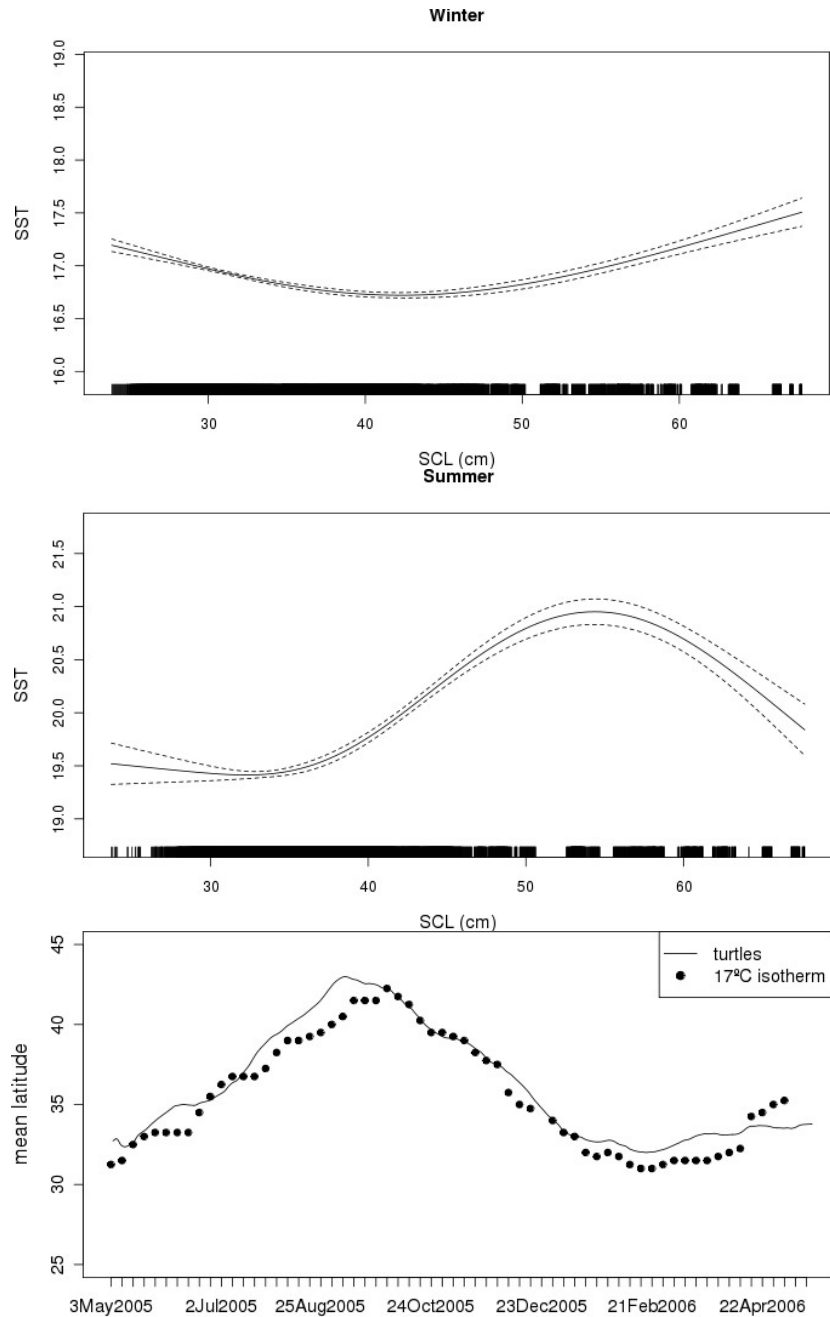


Figure 4. Relationship between SST and size of loggerhead turtles. a) Smooth of SST vs SCL during the winter (Dec. to Mar., top) and b) the summer (Jun. to Sept., middle); c) Mean latitude of observed turtles (solid line) and of the 17°C SST isotherm at 190E longitude (29 – 38 cm, bottom)

Maximum sustainable speed

Once the ocean currents speed was removed from the animals' velocity, we were able to study the animals' swimming speed ($V = \sqrt{V_x^2 + V_y^2}$, with V_x and V_y the meridional and zonal components of the velocity vectors, respectively). However, as relative errors on the estimation of the

current speeds are about constant (Rio et al. 2011), the artificial distribution of the turtles - with the smaller ones released in the highly dynamic Kuroshio current region and the bigger ones in the central gyre - could be problematic. To remain conservative, only locations east of the dateline, where currents and their estimation errors are relatively weak, were considered (62% of the data).

Characteristic values of V for different size groups (Fig. 3 left) are presented in Table 3. It is interesting to note that even the smallest turtles exhibit non-zero speeds indicating that they do not always drift passively at those sizes. Mean swimming speeds for all size groups were under 1 km/h and increased with size, from 0.58 to 0.69 km/h, for turtles larger than 30 cm. Mean swimming speed for turtles smaller than 30 cm (0.61 km/h) was slightly higher than for medium-size turtles (Table 3).

MSS expressed in bl s^{-1} exhibited a decreasing relationship with SCL (Fig. 5 left). Using the same approach as above, we ran a GAM to quantify the variation of MSS with SCL and other factors (longitude, latitude, month and year): 35% of the variability in MSS could be explained by SCL, and the smooth from the full model (Fig. 5 right) allowed us to identify the value of MSS at a given size. The relationship suggests clearly that MSS rapidly decreases from about 1.6 to 0.5 bl s^{-1} for individuals under 60 cm SCL and then stabilizes around 0.5 bl s^{-1} for larger individuals.

size	range of V	mean V	median V
< 30 cm	0.02 - 7.54	0.61	0.56
30 - 40 cm	0.002 - 5.04	0.58	0.54
40 - 60 cm	0.008 - 8.56	0.59	0.53
≥ 60 cm	0.008 - 5.47	0.69	0.64

Table 3: Values of swimming speeds (km/h) for different size groups

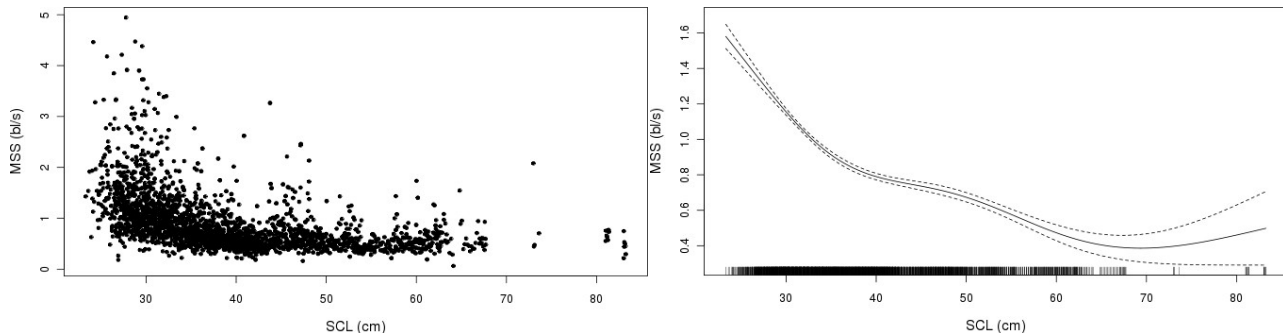


Figure 5. Observed (left) and predicted (right) maximum sustainable speed (MSS, bl/s) against SCL (cm)

HABITAT AND MOVEMENT MODELING

Feeding habitat H_a

Based on the previous analyses of temperature preference and speed for a given size, we simulated the predicted habitat for the November 2004 and the May 2005 releases (Table 2) in MOVEMOD, using the average of the turtle sizes for each batch. We used a mean temperature of 17°C for both releases,

estimated from Fig. 4 (top). We postulated that in absence of stratification, the animals would stay within a temperature range close to their optimal preference, which would then be around 17°C. The standard deviations of SST were estimated from the tracks (Table 4). Figures 6 & 7 show snapshots, at quarterly intervals, of the predicted habitat index (H_a) overlaid with the portions of tracks corresponding to the same 6-day (time step of the physical forcing) period. H_a is indicated by a color scale between 0 and 1, with 1 being optimal habitat (optimal temperature and abundance of foraging preys), and 0 being least optimal. The areas with higher values of H_a thus define areas of higher probability of presence. Figures 6 & 7 indicate that the simulated H_a tracks the real turtles trajectories and their seasonal changes closely. In some of the snapshots, H_a also presents eddy-like features that match the tracks, which gives us confidence in the forcing used for this study.

release	Average size	MSS	Mean SST	Std SST
November 2004	30.0	1.1	17.0	1.5
May 2005	34.7	0.9	17.0	1.5

Table 4. Parameters used for the simulations

It is interesting to compare our habitat index with the NOAA TurtleWatch product (Howell et al. 2008). This latter is the result of a statistical analysis between SST, loggerhead turtles tracks in the shallow Hawaii-based longline fishing grounds and the locations of high occurrence of bycatch within that fishery. It has been defined as the area between the 17.5 and 18.5°C SST isotherms. Figure 8 gives an illustration of how both indices match together from May 2005 to 2006, corresponding to the period when the turtles released in May 2005 were tracked. Both indices define roughly the same general area with a narrower latitudinal extension for the TurtleWatch index, usually centered on the maximum values of the habitat index H_a . By setting a threshold to increasing values of H_a , the index can be restricted to more and more favorable habitat, to identify hotspots of highest probability of turtle presence (Fig. 9), and corresponding to a closer match with TurtleWatch, but not always. In September, a maximum discrepancy between the two indices occurs, especially in the central Pacific, with H_a being more to the south of TurtleWatch, while still in good agreement with the observed tracks (Figs. 6 & 7).

The maximum extension of favorable habitat for loggerheads in the North Pacific is predicted to occur around September, with a broad area of high H_a across the full basin length, and especially in the Eastern Pacific. Then, the overall extension of predicted hotspot areas for juvenile loggerhead turtles is contracting during winter, reaching a minimum in March, with only a few remaining favorable hotspots off the coast of Baja California. During spring and summer, the extension of favorable areas expands again, reaching its maximum in September. Another important hotspot can be identified in the summer in the East China Sea (Fig. 9).

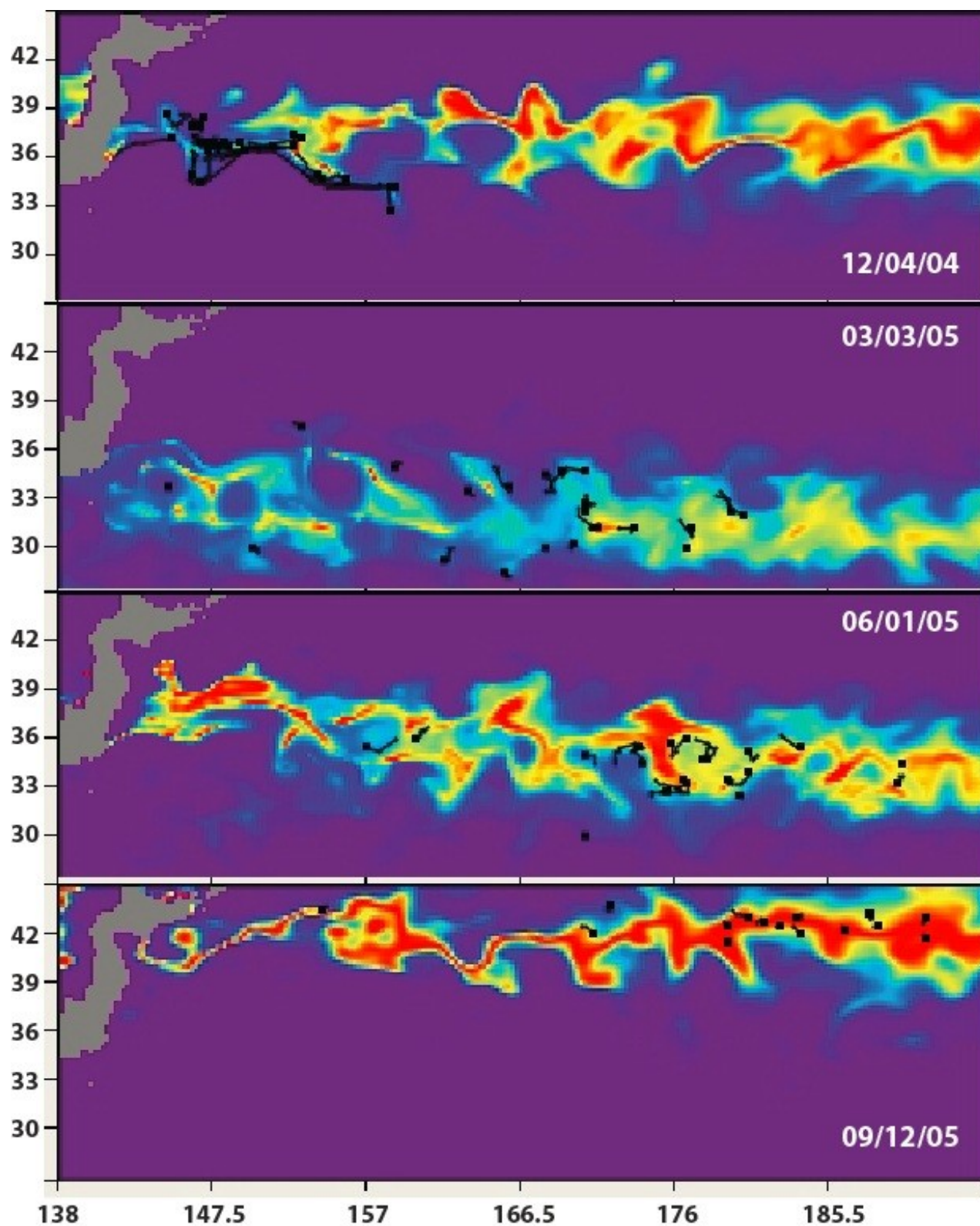


Figure 6: Modeled habitat index (color scale) overlaid with tracks (black segments) for the November 2004 release. From top to bottom: Dec. 4, 2004; Mar. 3, 2005; Jun. 1, 2005; Sep. 12, 2005

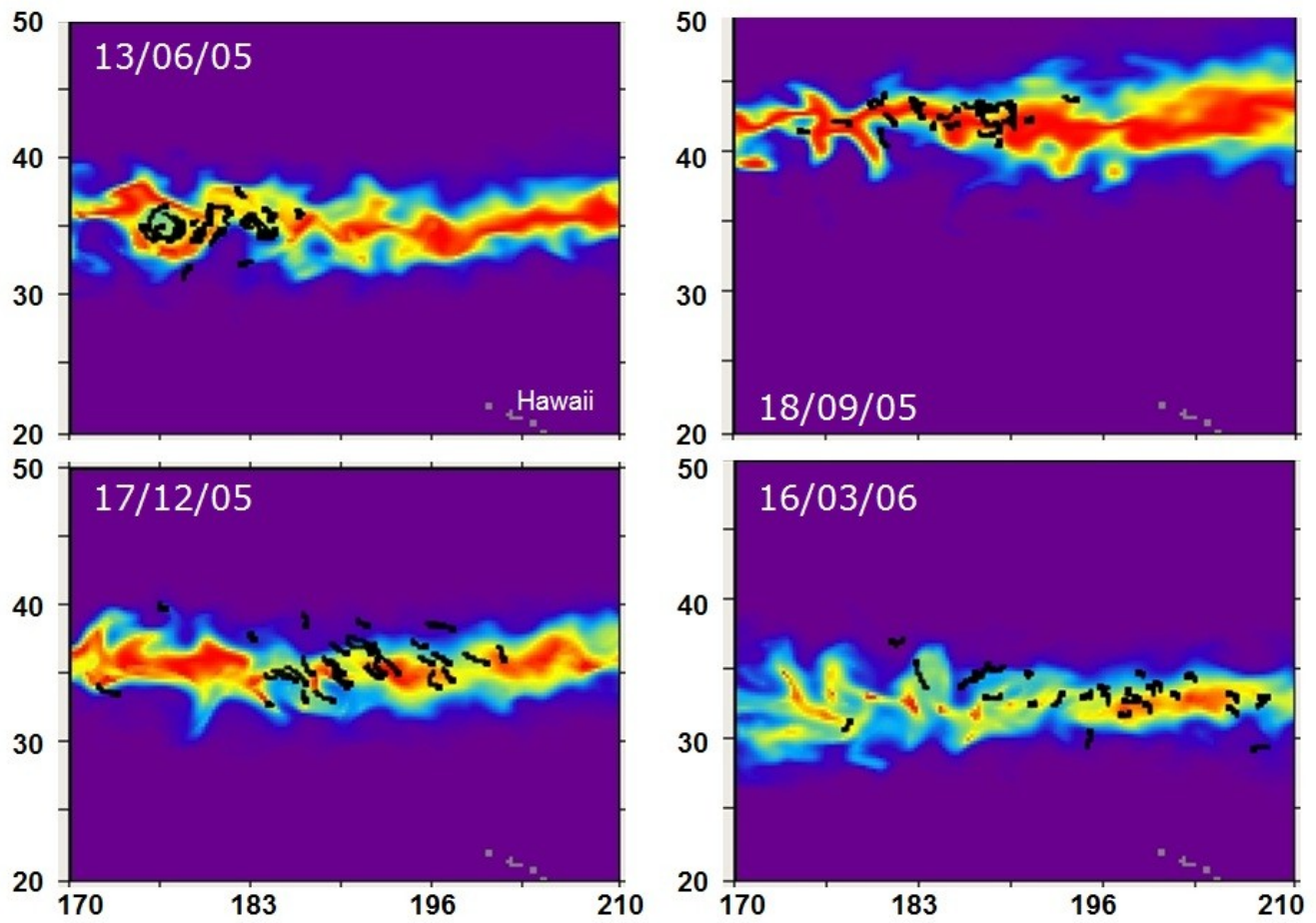


Figure 7: Modeled habitat index (color scale) overlaid with tracks (black segments) for the May 2005 release. From top to bottom: Jun. 13, 2005; Sep. 18, 2005; Dec. 17, 2005; Mar. 16, 2006

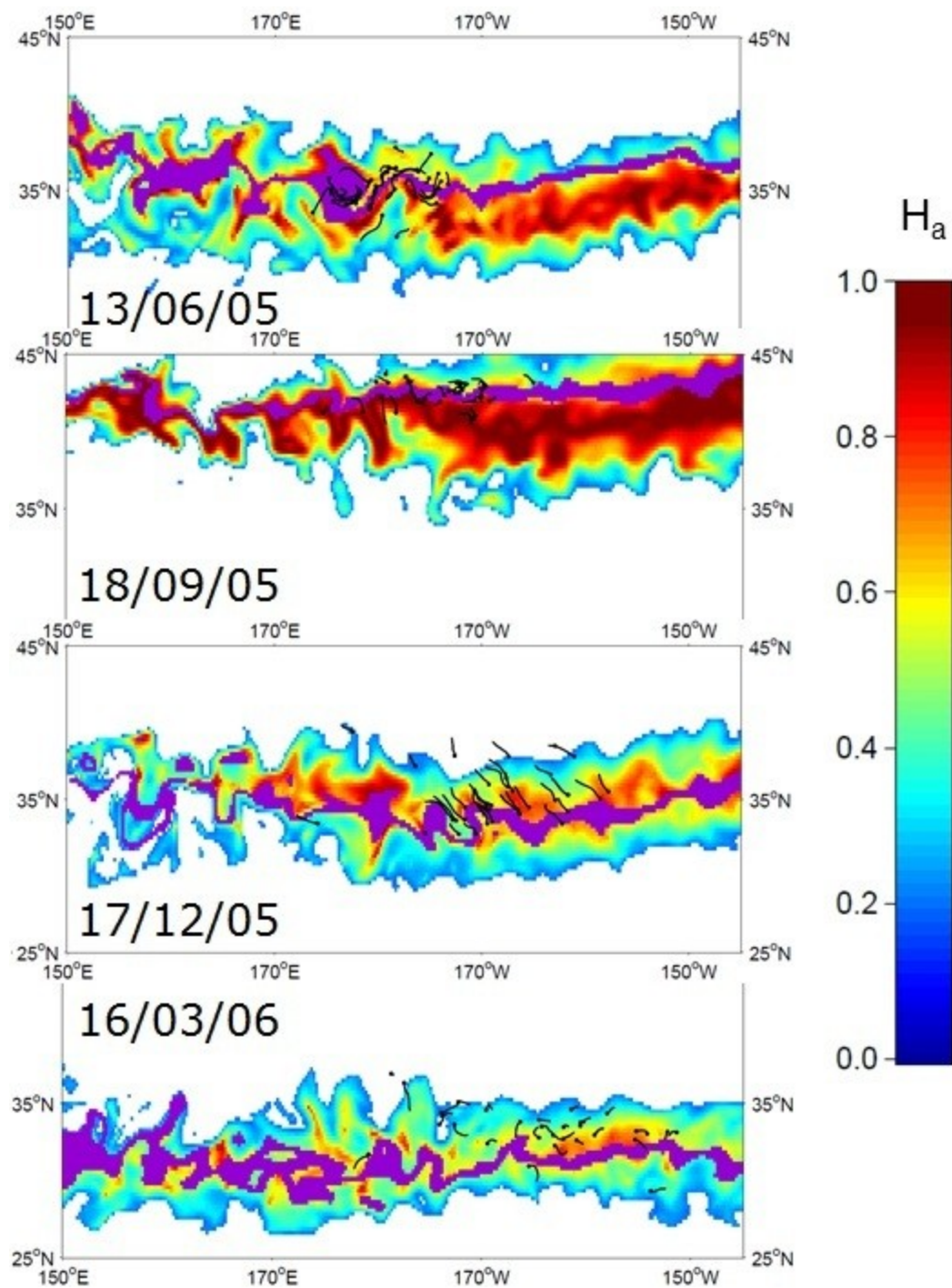


Figure 8: Modeled habitat index (color scale) overlaid with TurtleWatch region (purple area). For the May 2005 release (mean size: 35 cm). From top to bottom: Jun. 13, 2005; Sep. 18, 2005; Dec. 17, 2005; Mar. 16, 2006

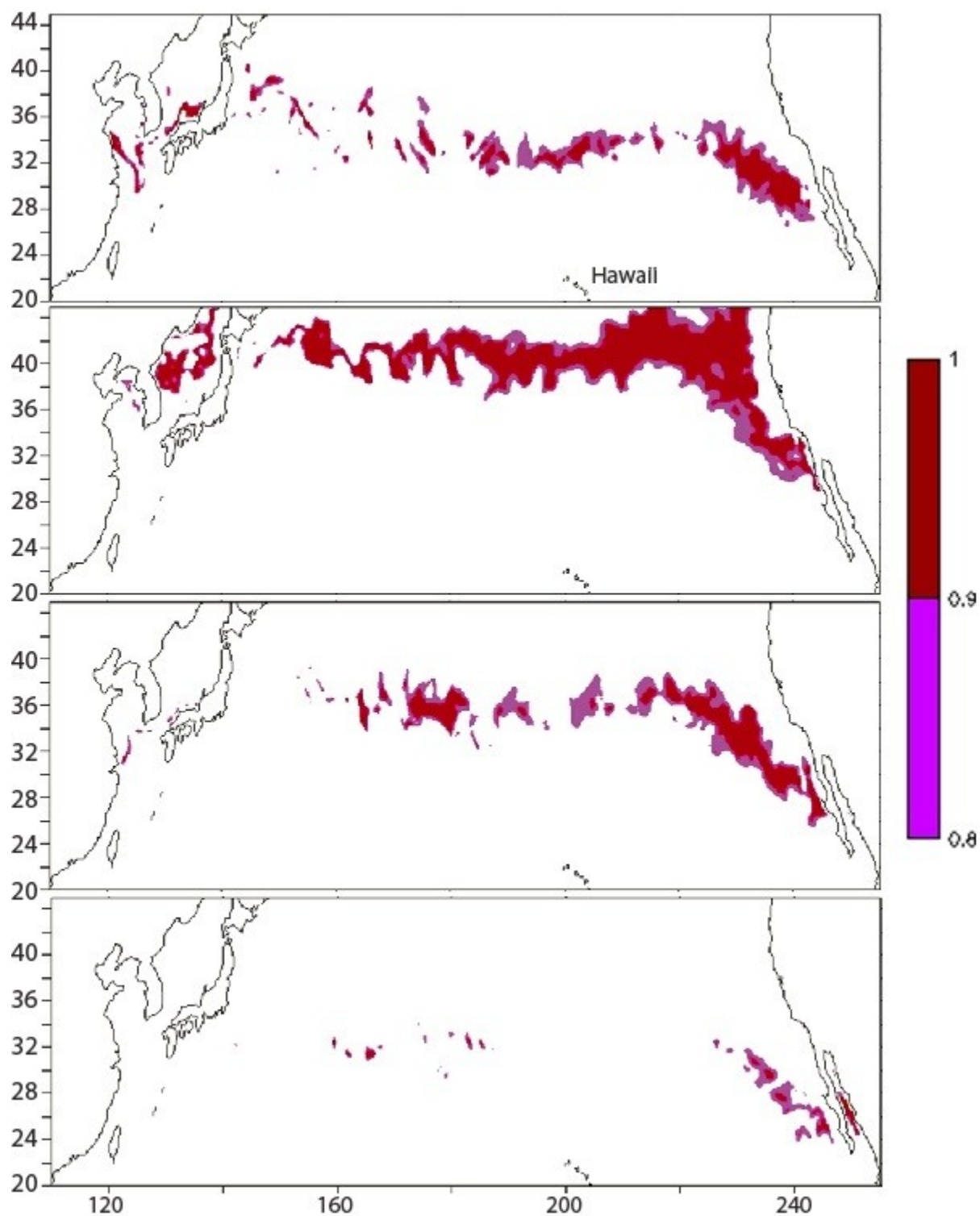


Figure 9: Predicted hotspots of habitat ($H_a > 0.8$). For the May 2005 release (mean size: 35 cm). From top to bottom: Jun. 1, 2005; Sep. 12, 2005; Dec. 5, 2005; Mar. 4, 2006

Movements

Once the habitat was parameterized (Table 4), turtle movements were simulated with MOVEMOD. Simulated turtles were released in the model in the same location and date as the observed ones and predicted distributions compared with tracks and final positions after one year of displacements. Following the movement mechanisms defined in the model (Lehodey et al. 2008), simulated turtles are pushed to move along positive gradients of habitat to leave poor habitat areas and move towards high habitat values. However, these rules of movement are also affected by the ocean currents. Fig. 10 shows four similar snapshots of the simulated turtles density overlaid with the observed tracks for the May 2005 release and Fig. 11 shows the simulated density at the end of one year, when the full movement equation is used, and when only passive drifting is considered, overlaid with the final positions of the released turtles. Density is expressed in number of individuals per $0.25^\circ \times 0.25^\circ$ cell. There is generally a good match between the simulated density and the tracks, except in September when the observed turtle tracks went further north, even though H_a in September was in good agreement with the tracks (Fig. 7). Some turtles also went further east than the simulated ones. As suggested by Fig. 5, even the smallest turtles in our dataset exhibited some active movement. Fig. 11 illustrates to what extent this affects the animals' movements. When combining advection by ocean currents with the animals' directed movements (Fig. 11 bottom), the predicted turtles' density after a year matched the observed turtles positions significantly better than when pure drift only is considered (Fig. 11 top) and the concentrations of turtles were generally better represented.

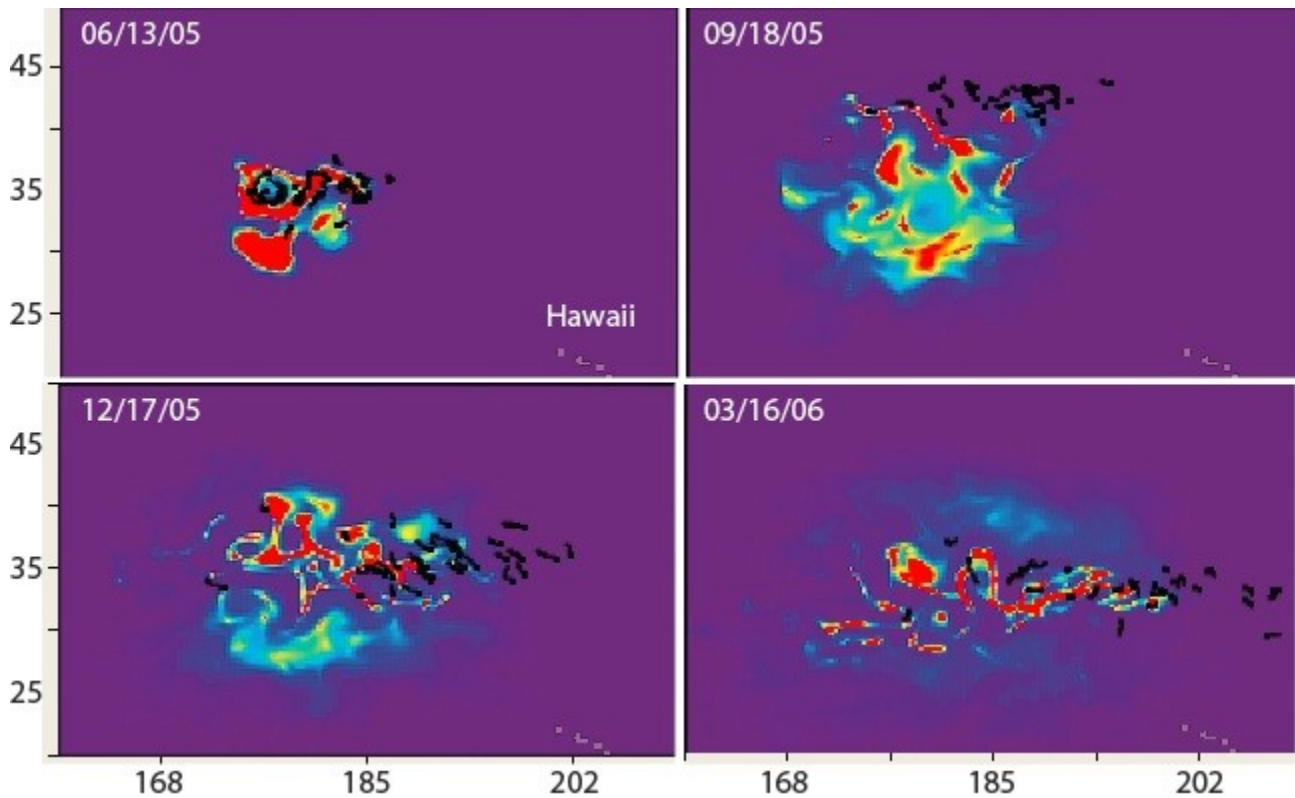


Figure 10: Density of turtles (# ind./cell, color scale) simulated with the habitat and movement model overlaid with tracks (black segments). The May 2005 release of juvenile loggerheads is simulated

during one year and predicted density distributions are shown at quarterly intervals (a, b, c, d) with corresponding positions of observed tracked turtles.

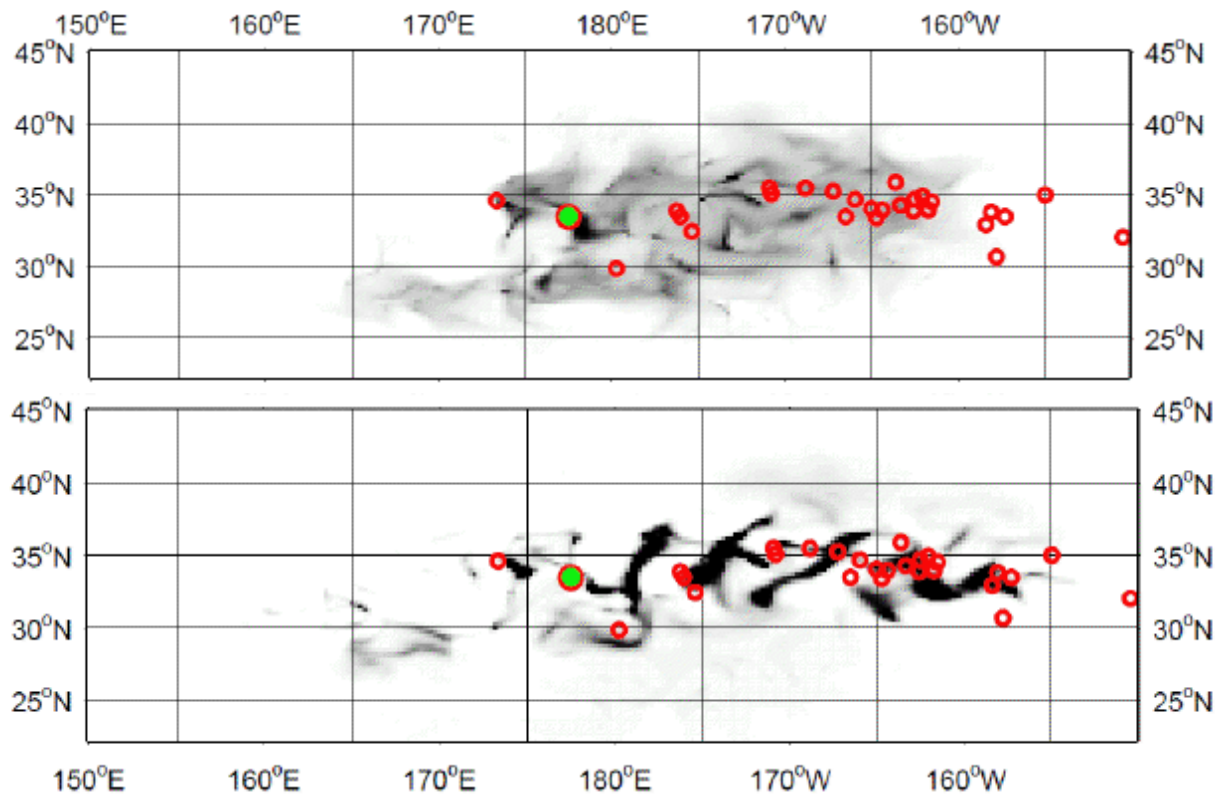


Figure 11: Final predicted density distributions and observed individual positions (white circles) are compared between simulations combining directed movement and currents (bottom) and currents only (top).

Most Hawaiian releases went westward (Fig. 1). We used the release day of the year and the release location for tags #19585, 19586 and 19594 (Table 1) in 2005, and using the same method as above, we were able to simulate a habitat index that matched each track closely (Fig. 12). However the density of simulated turtles diverged drastically from the real tracks (Fig. 11). Increasing speed or diffusion did not improve the results notably.

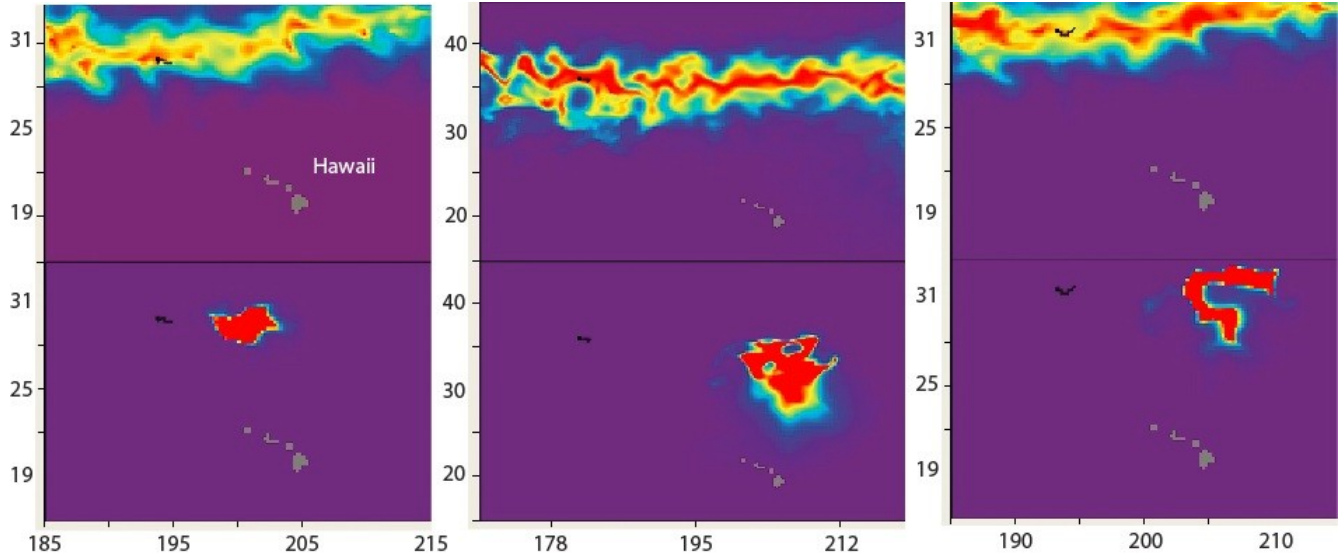


Figure 12: Snapshots of simulated habitat index (top graphs) and density (bottom graphs) for Hawaiian releases: #19585, #19586, #19594, from left to right. Overlaid with tracks (black segments)

To test whether longer times at liberty and departures during different years (characterized by different El Niño/La Niña events for example) would explain the observed westward movements, we ran several simulations starting at the same location and time of the year as the May 2005 release, using the entirety of the forcing available to us: from May 2002, 2003, 2004, 2005 and 2006 (respectively) to Dec. 2007. Although a small subset of the seeds exhibited some brief (up to a month long) westward excursions, no broad westward directed movement or “return leg” was observed at any point of the different simulations, including the 5.5-yr long one.

DISCUSSION

The knowledge on biology and ecology of juvenile loggerhead turtles is very limited due to the challenge of sampling those populations in the open ocean. In this context, the various deployments and tracking of such a significant number of juveniles that was achieved through a collaboration between the PIFSC Marine Turtle Research Program and the Port of Nagoya Aquarium provided the most comprehensive dataset in the Pacific Ocean, allowing to investigate this poorly described life stage. However, some caution has to be taken since the turtles from the Japanese releases were reared in captivity, but hopefully they constitute a good proxy to infer wild behaviours, assuming that reared turtles possess some innate sense from birth. No study to date has observed obvious oddities in migration or swimming behaviours of captivity-reared turtles (Polovina et al. (2000, 2003, 2004, 2006); Howell et al. (2008, 2010); Kobayashi et al. (2008, 2011)). Nevertheless, further simulations comparing habitat and behavior of wild and reared turtles with the same physical forcing would be valuable to confirm the results described in the present study.

The exceptional duration of the tracks in this study, with 59 individual tracks longer than one year and 14 longer than two years, rose the concern of accounting for growth during the time at liberty. Since there is no information on the growth of Pacific loggerhead turtles of medium to large sizes (> 42 cm SCL, Zug et al. 1995), the growth rate used in this study was taken from recent North Atlantic estimates (Scott et al. 2011). However it is similar to growth rates in the North Pacific for small turtles (< 42 cm SCL) turtles (Scott et al. 2011, Zug et al. 1995). Questions remain as growth rates could vary between both areas, especially for bigger turtles, but given the scarcity of available information and the long durations of our tracks, using the North Atlantic relationship seemed more appropriate than using only the size at release for our analyses.

TEMPERATURE

In ectotherm species, colder optimal temperatures and wider temperature ranges should be expected for larger individuals, since their larger sizes should increase their internal body temperature by reducing heat diffusivity (as is the case for tunas, e.g. Holland et al 1992, Brill 1987).

The range of surface temperatures experienced by the bigger turtles in our dataset was larger than that experienced by smaller turtles (Fig. 3), as would be expected, but the smaller turtles tended to be in colder surface waters than the bigger ones (Fig. 3), which is surprising. However, when considering winter and summer separately, coinciding respectively with weak (mixed-layer deeper than 40m) and strong (mixed layer between 10-40 m deep) stratification of the water column, small and large turtles remained in the same narrow range of temperature (16.7-17.5 °C) in the winter, but were in two slightly different ranges in the summer (roughly 19-20 and 20-21°C, respectively, Fig. 4). We could assume when stratification is strong, turtles can quickly reach cold subsurface waters below the mixed-layer and thus could benefit from higher surface temperatures for rewarming. The observed higher SST values associated with larger individuals also concord with the idea that bigger turtles likely dive deeper than small ones and thus may target warmer surface waters. In winter however, when the mixed layer is too deep, all turtles would stay in a temperature range close to their optimal preference, which would be consequently close to 17°C.

Unfortunately, the relationship between diving depth and size has not yet been investigated in details from electronic tagging data. The study by Howell et al (2010), based on a small subset (n=17) of the animals used in this present study that were equipped with depth sensors, did not allow such an analysis since all those individuals were in a relatively narrow range of sizes (43.5–66.5 cm). No significant relationship between the size of the turtles and the number or duration of the dives was found (E. Howell, pers. comm.). That group of juvenile loggerheads spent more than 80% of their time at depths above 5 m, were able to dive at depths between 30-70 m, but remained in water temperatures warmer than 15°C. Another study (Hochscheid et al. 2010) showed that, in the Mediterranean, loggerhead dives over a large temperature range were sometimes linked to extended surface time, suggesting a rewarming function. Thus, the apparent preference of bigger turtles for warmer SSTs might be explained by differences in the diving depths with size, but further studies need to confirm this idea.

FEEDING HABITAT

Loggerhead turtles at the oceanic stage in the central North Pacific feed mostly on neustonic (associated to the surface) prey items, such as *Carinaria cithara*, *Janthina spp.*, *Lepas spp.*, and *Velella velella* (Parker et al. 2005), but only forage comprised in the whole epipelagic layer is available to date in SEAPODYM, which we used as a first approximation to describe loggerhead turtles foraging preference. However, it may be interesting for further analyses to develop a new functional group in SEAPODYM representing neustonic organisms. Based on the mechanisms of the model (Lehodey et al. 2010), we can expect a higher amplitude in the temperature cycle of the neustonic layer (i.e., the first 5 m) as well as stronger averaged currents with slightly different directions, thus leading to differences both in the time of development of organisms and their distribution. Interestingly, the largest discrepancy between habitat distribution and observed tracks occurs from August to early September in the most northern range of the habitat (40°-45°N), which is the period during which the upper ocean is most stratified and hence the period during which the SST differs most from the average temperature of the euphotic layer, used for the simulation of the epipelagic component of the micronekton (Fig. 12). Despite this limitation, our approach resulted in the definition of a habitat that matches the tracks very closely, suggesting that temperature is the predominant factor to define accessibility to forage species, the interaction of both parameters driving the large scale movements of the species.

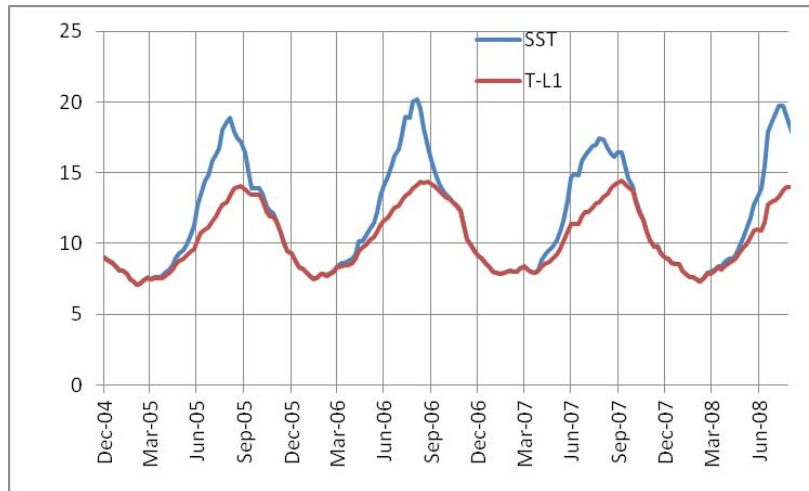


Figure 13: SST (blue line) and average temperature of the euphotic layer (red line) from Dec. 2004 to Sept. 2008.

Habitat hotspots resulting from these interactions emerged from the simulations (Fig 8). One permanent hotspot is located off the coast of Baja California. This area has been identified for long has a major feeding ground of juvenile loggerhead turtles (Bowen et al 1995, Resendiz et al 1998, Nichols et al 2000, Etnoyer et al 2006, Peckham et al 2007, 2008, 2011, Howell et al 2010). A genetics study (Bowen et al 1995) showed that 95% of sampled turtles along the coast of Baja California originated from Japanese nesting areas. The modeled habitat (Figs. 6 & 7) predicts a clear transpacific route of migration between these two regions that is consistent with these observations. In addition, the maximum extension and favorability of this migration corridor occurs in Sep-Oct (Fig. 8) which coincides with the period of the year when hatchlings would leave nesting beaches after 2 - 3 months of incubation following the peak of the nesting season between the end of June and the beginning of July, in Japan (Sato et al 1997, Matsuzawa 2002).

Polovina et al. (2006) identified the Kuroshio Extension Bifurcation Region (KEBR), between 155 and 180°E (ie. between Japan nesting grounds and Baja California foraging grounds), as a forage hotspot for loggerhead turtles because of the high primary production (PP) in that highly dynamic region during the fall, winter and spring. That region was predicted to be a semi-permanent hotspot by our model, but was not predicted to be an area as highly favorable as the Baja California hot spot. It is probably, however, a key area to support high survival rates of juveniles. This hotspot might also be underestimated by the model because of the definition of the epipelagic forage component in SEAPODYM, as discussed above. Although that area exhibits high PP, the development time defined for the epipelagic micronekton organisms considered as prey in this version of the model might be too long and cause the biomass of forage to be advected eastward too rapidly by the strong Kuroshio current. For the same reason probably, the hotspot in the East China Sea identified by Kobayashi et al. (2011) was identified as a hotspot by our model, but only during the summer (Fig. 8).

The feeding habitat index proposed here does not take into account any information from the longline fishery as was done to define the TurtleWatch index, but is purely based on temperature preferences and subsequent forage accessibility. Though they are not directly comparable, both indices predict the

same general areas of highest probability of encountering loggerhead turtles, and thus, areas with highest risk of bycatch, in the North Pacific. An exception occurs around September, when the feeding habitat seems to peak at its maximum extension all over the North Pacific. At that time the TurtleWatch index seems to characterize the most northern limit of the habitat and could miss the main areas of concentration south of this limit. However, since the Hawaiian longline fishery mainly operates during the first and second quarters of the year, the TurtleWatch index does not really apply to this period of the year.

The feeding habitat index allows to characterize the whole areas of highest probability of presence of loggerhead turtles year-round, and is independent of fisheries data. An analysis combining this feeding habitat and Pacific swordfish longline catches will provide a first evaluation of the interest for using this new index to reduce bycatch of loggerhead turtles not only in Hawaiian waters but in the entire Pacific (Abecassis et al, in prep).

MOVEMENTS

A more quantitative way to measure the accuracy of the match between observed and predicted movements needs to be developed. For example, a tool calculating the values of predicted habitat index or density at each location along the observed tracks would help evaluating the performance of each simulation.

Nonetheless, the present study suggests that even the smallest turtles in our dataset (25 cm SCL) exhibit some level of active swimming, with mean swimming speeds around 0.6 km/h. This is valuable information as turtles of this size are rarely observed in the wild, and very little is known about their behaviour and abilities. In fact, the oceanic stage between the departure from hatching to the return to neritic areas (around 70 cm in size) many years later has been called “the lost years” (Bolten & Witherington 2003) to refer to this lack of observability. Most tagging studies on wild turtles have been conducted on animals bigger in size, either around nesting areas or caught in the various fisheries (Avens et al. 2003; Avens & Lohmann 2004; Eckert et al. 2008; Polovina et al. 2006; Revelles et al. 2007b,a).

We chose the November 2004 and the May 2005 releases to illustrate our modeling approach because their ranges of sizes were small enough to reasonably treat all the turtles released on each day as one single cohort. The May 2005 release is also of particular interest because it was conducted in the area of operation of the Hawaii-based shallow longline fishery. The observed tracks seem to be more concentrated in areas of high predicted habitat index (H_a) when H_a reaches its peak in September. Conversely, when H_a reaches minimum values basin-wide in March, tracks appear much more dispersed (Fig. 6). This pattern would tend to validate the approach used to describe the movement mechanisms proposed in the Eulerian framework of SEAPODYM, with increasing diffusion when habitat index values decrease and stronger advection (i.e., directed movements) linked to increasing gradients of habitat, both being proportional to the size of the animals (Lehodey et al. 2008). Additionally, observed and predicted turtles positions after one year at liberty are clearly in better agreement when using these rules of movement (including also the impact of currents) than when considering pure drifting only, providing confidence in the modeling of both the habitat and the movement.

Nevertheless, the model still needs to be tested for other release experiments, especially with larger individuals. In that case, one issue will be to differentiate between feeding behavior and spawning migrations. A version of SEAPODYM that allows tracking data assimilation is being developed (Senina et al in prep), which could help estimate more precisely the feeding habitat parameters. For spawning migrations however, temperature and availability of prey would not be the only factors affecting the large-scale movements of loggerhead turtles. This modeling framework could be easily used to introduce and test various migration hypotheses, e.g. based on magnetic fields (Lohman et al 2004, 2008).

When sub-adult turtles get closer to their age at maturity, it's possible that they would start to follow some homing instinct towards their Japanese nesting grounds (the only known nesting beaches in the North Pacific are all located in Japan, Bolten & Witherington 2003). Those westward movements would be used as “practice runs” before the transition to the neritic stage (Bolten & Witherington 2003). Twenty-six turtles of our dataset, with sizes ranging between 35 and 83 cm, exhibited a net displacement of at least 1 degree westward between the first and last locations of their tracks, while all others had a net eastward displacement. However, our model does not reproduce those westward movements. This suggests that temperature and availability of prey are not the only factors affecting the large-scale movements of loggerhead turtles.

The oceanic stage of loggerhead turtles has been estimated to last between 7 and 11.5 years (Bjorndal et al. 2000), while our longest track was about 3.5 years. Until tracking capabilities allow for datasets encompassing the entire oceanic stage, understanding the timing of the east-west dynamics of juvenile loggerheads will remain challenging. Nevertheless, confronting these individual tracks to dynamic habitat and movement models reveals already a promising development with direct potential applications that could be rapidly used for assisting in the conservation of these endangered species.

REFERENCES

- Abecassis M, Dewar H, Hawn D, Polovina J (in press) Modeling swordfish daytime vertical habitat in the north pacific ocean from pop-up archival tags
- Avens L, Lohmann K (2004) Navigation and seasonal migratory orientation in juvenile sea turtles. *Journal of Experimental Biology* 207(11):1771–1778
- Avens L, Braun-McNeill J, Epperly S, Lohmann K (2003) Site fidelity and homing behavior in juvenile loggerhead sea turtles (*Caretta caretta*). *Marine biology* 143(2):211–220
- Balazs G, Miya R, Beavers S (1996) Procedures to attach a satellite transmitter to the carapace of an adult green turtle, *Chelonia mydas*. In: *Proceedings of the Fifteenth Annual Symposium on Sea Turtle Biology and Conservation*.
- Barnier B, Madec G, Penduff T, Molines JM, Treguier AM, Le Sommer J, Beckmann A, Biastoch A, Banić C, Dengg J, Derval C, Durand E, Gulev S, Remy E, Talandier C, Theetten S, Maltrud M, Mcclean J, De Cuevas B (2006) Impact of partial steps and momentum advection schemes in a global ocean circulation model at eddy permitting resolution. *Ocean dynamics* 56:543–567
- Behrenfeld MJ, Falkowski PG (1997) Photosynthetic rates derived from satellite-based chlorophyll concentration. *Limnology and Oceanography* 42:1–20
- Benson S, Dewar H, Dutton P, Fahy C, Heberer C, Squires D, Stohs S (2009) Swordfish and leatherback use of temperate habitat. Tech. Rep. LJ-09-06, Southwest Fisheries Science Center, NMFS/NOAA
- Beverly S, Robinson E, Itano D (2004) Trial setting of deep longline techniques to reduce bycatch and increase targeting of deep-swimming tunas. Tech. Rep. FTWG - WP-7a, Standing Committee on Tuna and Billfish
- Beverly S, Curran D, Musyl M, Molony B (2009) Effects of eliminating shallow hooks from tuna longline sets on target and non-target species in the hawaii-based pelagic tuna fishery. *Fish Res* 96:281–288
- Bjorndal KA, Bolten AB, Martins HR (2000) Somatic growth model of juvenile loggerhead sea turtles *Caretta caretta* : duration of pelagic stage. *Marine Ecology Progress Series* 202:265–272
- Bolten AB, Witherington BE (2003) *Loggerhead sea turtles*. Smithsonian Books, Washington
- Bowen BW, Abreu-Grobois FA, Balazs GH, Kamezaki N, Limpus CJ, Ferl RJ (1995) Trans-Pacific migrations of the loggerhead turtle (*Caretta caretta*) demonstrated with mitochondrial DNA markers. *Proceedings of the National Academy of Sciences* 92(9):3731–3734
- Brill RW (1987) On the standard metabolic rates of tropical tunas including the effect of body size and acute temperature change. *Fish Bull US* 85: 25-35

- Eckert S, Moore J, Dunn D, van Buiten R, Eckert K, Halpin P (2008) Modeling loggerhead turtle movement in the mediterranean: Importance of body size and oceanography. *Ecological Applications* 18(2):290–308
- Etnoyer P, Canny D, Mate BR, Morgan LE, Ortega-Ortiz JG, Nichols WJ (2006) Sea-surface temperature gradients across blue whale and sea turtle foraging trajectories off the Baja California Peninsula, Mexico. *Deep-Sea Research II* 53(3-4):340–358
- Gaspar P, Georges JY, Fossette S, Lenoble A, Ferraroli S, Le Maho Y (2006) Marine animal behaviour: neglecting ocean currents can lead us up the wrong track. *Proceedings - Royal Society of London Biological sciences* 273(1602):2697–2702
- Gilman E, Zollett E, Beverly S, Nakano H, Davis K, Shiode D, Dalzell P, Kinan I (2006) Reducing sea turtle by-catch in pelagic longline fisheries. *Fish and Fisheries* 7:2–23
- Gilman E, Kobayashi D, Swenarton T, Brothers N, Dalzell P, Kinan-Kelly I (2007) Reducing sea turtle interactions in the hawaii-based longline swordfish fishery. *Biological Conservation* 139(1-2):19 – 28
- Hastie T, Tibshirani R (1990) *Generalized Additive Models*. Chapman and Hall, London, U. K.
- Hochscheid S, Bentivegna F, Hamza A, Hays GC (2010) When surfacers do not dive: multiple significance of extended surface times in marine turtles. *Journal of Experimental Biology* 213:1328–1337
- Holland KN, Brill RW, Chang RKC, Sibert JR, Fournier DA (1992) Physiological and behavioral thermoregulation in bigeye tuna (*Thunnus obesus*). *Nature, Lond* 358: 410-412
- Howell E, Kobayashi D, Parker D, Balazs G, Polovina J (2008) Turtlewatch: a tool to aid in the bycatch reduction of logger-head turtles *Caretta caretta* in the hawaii-based pelagic longline fishery. *Endangered Species Research* 5(2-3):267–278
- Howell EA, Dutton PH, Polovina JJ, Bailey H, Parker DM, Balazs GH (2010) Oceanographic influences on the dive behavior of juvenile loggerhead turtles (*Caretta caretta*) in the north pacific ocean. *Marine Biology* 157:1011–1026
- Kobayashi D, Polovina J, Parker D, Kamezaki N, Cheng I, Uchida I, Dutton P, Balazs G (2008) Pelagic habitat characterization of loggerhead sea turtles, *Caretta caretta*, in the north pacific ocean (1997-2006): Insights from satellite tag tracking and remotely sensed data. *Journal of Experimental Marine Biology and Ecology* 356(1-2):96–114
- Kobayashi DR, Cheng IJ, Parker DM, Polovina JJ, Kamezaki N, Balazs GH (2011) Loggerhead turtle (*Caretta caretta*) movement off the coast of Taiwan: characterization of a hotspot in the east china sea and investigation of mesoscale eddies. *ICES J Mar Sci* advanced access
- Lehodey P (2001) The pelagic ecosystem of the tropical pacific ocean: dynamic spatial modelling and biological consequences of ENSO. *Progress in Oceanography* 49(1-4):439–468

- Lehodey P, Chai F, Hampton J (2003) Modelling climate-related variability of tuna populations from a coupled ocean-biogeochemical-populations dynamics model. *Fisheries Oceanography* 12(4-5):483–494
- Lehodey P, Senina I, Murtugudde R (2008) A spatial ecosystem and populations dynamics model (SEAPODYM) - modeling of tuna and tuna-like populations. *Progress In Oceanography* 78:304–318
- Lehodey P, Murtugudde R, Senina I (2010) Bridging the gap from ocean models to population dynamics of large marine predators: a model of mid-trophic functional groups. *Progress in Oceanography* 84:69–84.
- Lewison RL, Freeman SA, Crowder LB (2004) Quantifying the effects of fisheries on threatened species: the impact of pelagic longlines on loggerhead and leatherback sea turtles. *Ecology Letters* 7:221–231
- Lohmann K, Lohmann C, Ehrhart L, Bagley D, Swing T (2004) Animal behaviour – geomagnetic map used in sea-turtle navigation. *Nature* 428(6986):909–910
- Lohmann K, Luschi P, Hays G (2008) Goal navigation and island-finding in sea turtles. *Journal of Experimental Marine Biology and Ecology* 356(1-2):83–95
- Matsuzawa, Y., K. Sato, W. Sakamoto, and K. A. Bjorndal (2002) Seasonal fluctuations in sand temperature: effects on the incubation period and mortality of Loggerhead Sea Turtle (*Caretta caretta*) pre-emergent hatchlings in Minabe, Japan. *Marine Biology* 140:639–646
- Nichols WJ, Resendiz A, Seminoff JA, Resendiz B (2000) Transpacific migration of a loggerhead turtle monitored by satellite telemetry. *Bulletin of marine science* 67(3):937–947
- Parker DM, Cooke WJ, Balazs GH (2005) Diet of oceanic loggerhead sea turtles (*Caretta caretta*) in the central north pacific. *Fishery Bulletin* 103:142–152
- Peckham SH, Maldonado Diaz D, Walli A, Ruiz G, Crowder LB, Nichols WJ (2007) Small-scale fisheries bycatch jeopardizes endangered Pacific loggerhead turtles. *PLoS ONE* 2(10):e1041
- Peckham SH, Maldonado-Diaz D, Koch V, Mancini A, Gaos A, Tinker MT, Nichols WJ (2008) High mortality of loggerhead turtles due to bycatch, human consumption and strandings at Baja California Sur, Mexico, 2003 to 2007. *Endangered Species Research* 5(2-3):171–183
- Peckham SH, Maldonado-Diaz D, Tremblay Y, Ochoa R, Polovina J, Balazs G, Dutton PH, Nichols WJ (2011) Demographic implications of alternative foraging strategies in juvenile loggerhead turtles *Caretta caretta* of the North Pacific ocean. *Mar Ecol Prog Ser* 425:269–280
- Pham DT, Verron J, Roubaud MC (1998) A singular evolutive extended kalman filter for data assimilation in oceanography. *Journal of Marine Systems* 16:323–340

- Polovina J, Kobayashi R, Parker M, Seki P, Balazs H (2000) Turtles on the edge: movement of loggerhead turtles (*Caretta caretta*) along oceanic fronts, spanning longline fishing grounds in the central north pacific, 1997-1998. *Fisheries Oceanography* 9(1):71–82
- Polovina JJ, Howell E, Parker DM, Balazs GH (2003) Dive-depth distribution of loggerhead and olive ridley sea turtles in the central north pacific: might deep longline sets catch fewer turtles? *Fishery Bulletin* 101(1):189–193
- Polovina J, Balazs G, Howell E, Parker D, Seki M, Dutton P (2004) Forage and migration habitat of loggerhead (*Caretta caretta*) and olive ridley (*Lepidochelys olivacea*) sea turtles in the central north pacific ocean. *Fisheries Oceanography* 13(1):36–51
- Polovina J, Uchida I, Balazs G, Howell EA, Parker D, Dutton P (2006) The Kuroshio extension bifurcation region: A pelagic hotspot for juvenile loggerhead sea turtles. *Deep Sea Research (Part II, Topical Studies in Oceanography)* 53(3-4):326–339
- Resendiz A, Resendiz B, Nichols W, Seminoff J, Kamezaki N (1998) First confirmed east-west transpacific movement of a loggerhead sea turtle, *Caretta caretta*, released in Baja California, Mexico. *Pacific Science* 52(2):151–153.
- Revelles M, Cardona L, Aguilar A, San Felix M, Fernandez G (2007a) Habitat use by immature loggerhead sea turtles in the Algerian basin (western Mediterranean): swimming behaviour, seasonality and dispersal pattern. *Marine Biology* 151(4):1501–1515
- Revelles M, Isern-Fontanet J, Cardona L, San Felix M, Carreras C, Aguilar A (2007b) Mesoscale eddies, surface circulation and the scale of habitat selection by immature loggerhead sea turtles. *Journal of Experimental Marine Biology and Ecology* 347(1-2):41–57
- Rio M, Guinehut S, Larnicol G (2011) New cnes-cla09 global mean dynamic topography computed from the combination of grace data, altimetry, and in situ measurements. *J Geophys Res* 116:1–25
- Sato K, Bando T, Matsuzawa Y, Tanaka H, Sakamoto W, Minamikawa S, Goto K (1997) Decline of the loggerhead turtle, *Caretta caretta*, nesting on Senri Beach in Minabe, Wakayama, Japan. *Chelonian Conserv Biol* 2:600–603
- Scott R, Marsh R, Hays GC (2011) Life in the really slow lane: loggerhead sea turtles mature late relative to other reptiles. *Functional Ecology* xx:1–9
- Seifert B, Gasser T (1998) *Encyclopedia of Statistical Sciences, Update Vol.2*, Wiley, chap. Local polynomial smoothing. 367–372
- Senina I, Sibert J, Lehodey P (2008) Parameter estimation for basin-scale ecosystem-linked population models of large pelagic predators: Application to skipjack tuna. *Progress In Oceanography* 78:319–335
- Swimmer Y, Brill R (2006) Sea turtle and pelagic fish sensory biology: Developing techniques to reduce sea turtle bycatch in longline fisheries. Technical Memorandum NMFS-PIFSC-7, NOAA

Tranchant B, Testut CE, Renault L, Ferry N, Birol F, Brasseur P (2008) Expected impact of the future smos and aquarius ocean surface salinity missions in the mercator ocean operational systems: New perspectives to monitor ocean circulation. *Remote Sensing of Environment* 112:1476–1487

Zug GR, Balazs GH, Wetherall JA (1995) Growth in juvenile loggerhead sea turtles (*Caretta caretta*) in the north pacific pelagic habitat. *Copeia* 1995(2):484–487

CHAPITRE 4

APPLICATION DE SEAPODYM A LA DYNAMIQUE SPATIALE DE L'ESPADON DU PACIFIQUE

RESUME

Ce chapitre décrit le développement d'une application du modèle SEAPODYM à l'espadon dans l'océan Pacifique.

Après avoir défini la structure de la population à partir d'informations sur la biologie de l'espèce trouvées dans la littérature, et une calibration initiale, des tests d'optimisation furent effectués en utilisant les données de pêche disponibles (captures, effort, fréquences de taille). Ces données sont assimilées dans le modèle afin d'affiner les paramètres d'habitat de manière objective. Malgré des lacunes importantes dans le jeu de données (l'Inter-American Tropical Tuna Commission ayant refusé de fournir des données pour le Pacifique Est, et les données disponibles ne comportant pas d'information sur l'espèce ciblée), les tests d'optimisation fournirent des valeurs de paramètres d'habitat de ponte et d'alimentation raisonnables, et des captures et fréquences de taille prédites en bonne adéquation avec les observations. Néanmoins, certains paramètres ne purent être estimés par le modèle et durent être fixés.

La biomasse d'adultes estimée par le modèle est d'environ 400 000 t entre 1995 et 2000 dans le Pacifique. Différentes études de gestion des stocks récentes, combinées entre elles, estimèrent une biomasse d'adultes d'environ 180 000 t sur la même période. Une telle différence n'est pas étonnante car l'utilisation d'un forçage à basse résolution ($2^\circ \times 2^\circ$ dans cette étude) conduit couramment à une surestimation de la biomasse au sein de SEAPODYM. La tendance à la hausse prédite pour la biomasse est en accord avec celles estimées par les études des stocks dans le Pacifique Est menées récemment (Courtney & Piner 2009, Hinton & Maunder 2011), mais pas avec celles concernant les régions occidentales du bassin (Courtney & Piner 2009, Kolody et al 2009) qui estiment au contraire une stagnation voire une diminution de la biomasse. Notre modèle prédit une augmentation dans chacune des régions.

Les distributions spatiales d'adultes et de jeunes espadons sont en accord avec la distribution des captures des pêcheries qui les ciblent, néanmoins, la variabilité saisonnière ne semble pas être reproduite de manière satisfaisante pour la distribution des adultes dans le Pacifique Nord.

Les périodes de coïncidence entre la biomasse d'espadons adultes et les hotspots de tortues caouannes (modélisés dans le chapitre précédent) correspondent aux périodes pendant lesquelles les prises accessoires de tortues par les palangriers sont maximales dans la pêcherie basée à Hawaïi. Toutefois, la résolution spatiale du forçage utilisée pour l'application espadon ne permet pas d'analyser les zones de coïncidence de manière suffisamment détaillée à des fins de gestion des ressources.

Le passage à un forçage à plus haute résolution, et l'obtention de données de pêche plus exhaustives et de meilleure qualité contribueraient grandement à améliorer cette étude.

Swordfish habitats and population dynamics in the North Pacific, investigated with the SEAPODYM model

Melanie Abecassis¹, Inna Senina, Patrick Lehodey², Jeffrey Polovina³, Beatriz Calmettes²,
George Balazs³, Denise Parker¹, Peter Williams⁴

¹Joint Institute for Marine and Atmospheric Research, University of Hawaii, 1000 Pope Rd., Honolulu, HI, 96822, USA

Email : melanie.abecassis@noaa.gov

²Collecte Localisation Satellite, 8 rue Hermes, 31520 Ramonville-Saint-Agne, France

³Pacific Islands Fisheries Science Center, NOAA Fisheries, 2570 Dole St., Honolulu, HI, 96822, USA

⁴Oceanic Fisheries Programme, Secretariat of the Pacific Community, B.P. D5 - 98848, Noumea Cedex, New Caledonia

ABSTRACT

A SEAPODYM application to Pacific swordfish is developed. After definition of the population structure and initial parameterization, optimization experiments are conducted based on accessible fishing data (catch, effort and size frequency). Despite a lack of comprehensive fishing data, the model optimization experiments yielded reasonable estimated values of parameters defining the spawning and feeding habitat of the population at the Pacific basin scale, and provided a good fit between observed and predicted catch, and catch size. However, a few parameters still remain unestimated and had to be set to the most plausible fixed values.

The model estimates adult biomass around 400 000 mt (metric tons), which is higher than recent stock assessment estimates (around 180 000). However this is somewhat to be expected with the coarse resolution of the forcing used in this study (2°x2°). The increasing trend in biomass predicted by the model is in agreement with trends assessed by other studies in the eastern Pacific, but not in the western parts of the basin. The spatial distributions of adult and young fish are in reasonable agreement with catch data.

Timing in overlap between predicted spatial distributions of adult swordfish and predicted hotspots of loggerhead turtles is consistent with periods of high bycatch incidence in the longline fisheries. However, the coarse resolution used makes it challenging to study detailed areas/periods of overlap for management purposes. It would be valuable to pursue this study using a more realistic environmental forcing at higher resolution.

INTRODUCTION

Loggerhead turtles are endangered in the Pacific Ocean and an important bycatch of the longline fisheries targeting swordfish. Tremendous efforts have been expanded in recent years to reduce the interactions between marine turtles and the fisheries, from changes in the gear (circle hooks instead of J hooks) and bait (mackerel instead of squid), to the presence of scientific observers onboard fishing vessels, trained to handle and release entangled or hooked turtles. Those efforts have been met with great success but interactions still occur. Given the steep decline in the nesting populations since the 1970s, even smaller numbers of interactions are cause for concern, and new efforts are aimed at reducing the overlap between the fisheries and the turtles. Trials have attempted to target swordfish during the daytime at depth, therefore eliminating shallow hooks from the surface waters inhabited by the turtles (Boggs 2003, Beverly et al 2004). While reducing the bycatch occurrences, these trials have failed to yield high catches per unit of effort (CPUEs) of swordfish. A recent modeling study (Abecassis et al 2012) aimed at better defining the daytime mean depth of swordfish to improve on those early trials.

A different approach consists in informing the fishermen about the areas of highest probability of turtle presence. One such tool is TurtleWatch (Howell et al 2008), developed by the Pacific Islands Fisheries Science Center (PIFSC/NOAA). It advises fishermen to avoid fishing between the 17.5 and 18.5°C isotherms and provides online weekly maps displaying the recommended avoidance zone based on Sea Surface Temperature (SST) preferences.

Abecassis et al (in prep, see Chap. 2) studied the feasibility of adapting a habitat-based population dynamics model (SEAPODYM, Lehodey et al 2008) to obtain a more refined index of turtle presence. This paper constitutes the second part of the study by developing an application of the SEAPODYM model to study the habitats and spatial dynamics of swordfish in the North Pacific and predict the zones of interaction. This paper details the modeling work and the limits encountered. An attempt at comparing the preliminary results of swordfish distributions with those of loggerhead turtles (Abecassis et al, in prep, & Chap.2) to characterize the areas and periods of maximum overlap between the two species is then briefly presented.

MATERIALS AND METHODS

SEAPODYM

The SEAPODYM (Spatial Ecosystem And Populations Dynamics Model) model was developed initially to simulate the age-structured spatial dynamics of tropical tuna populations in pelagic ecosystems, in interaction with their environment (Lehodey 2001; Lehodey et al. 2003, 2008; Senina et al. 2008; Lehodey et al. 2010, Lehodey et al. 2011). It uses physical-biogeochemical environmental fields (temperature, currents, primary production, euphotic depth and dissolved oxygen concentration) to predict the biomass of upper trophic levels of marine ecosystems organized in two groups: the predator species (e.g. tuna, billfish, or turtles) and their prey species (i.e. micronekton). Although SEAPODYM is a 2D model, it has a pseudo-3D representation with a three-layer structure: epipelagic between the surface and one euphotic depth (Zeu), mesopelagic between 1 and 3 Zeu, and bathypelagic between 3 Zeu and 7 Zeu. The micronekton species are combined into six functional groups

characterized by their habitat and vertical behaviour (Lehodey et al. 2010). Predator spatio-temporal dynamics are described by advection-diffusion-reaction equations. Diffusion is used to represent random movements (kinesis), and advection to reproduce both the transport due to currents and directed movements in response to external stimuli (taxis) characterized by habitat indices. Directed movements follow the gradient of habitat indices depending on temperature preference, oxygen constraints and prey availability.

The environmental forcing is provided by the ORCA2 ocean circulation model coupled to the PISCES biogeochemical model and forced by the NCEP-NCAR atmospheric reanalysis (http://www.cgd.ucar.edu/cas/guide/Data/ncep-ncar_reanalysis.html). ORCA2 is the standard configuration of the ocean general circulation model OPA (Version 9.0) for the global ocean (<http://www.nemo-ocean.eu/>), and PISCES describes the marine biogeochemical cycles of carbon and the main nutrients (N, P, Si and Fe) which limit phytoplankton growth (Aumont et al 2003, Bopp et al 2005, Gorgues et al 2005, Aumont 2006). This long hindcast ocean simulation (1948 - 2003) was chosen to cover the historical period of swordfish fisheries, to use sufficiently long time series to cover several lifespans of the species and to reduce the impact of initial conditions in the optimization approach.

The model domain covered the Pacific Basin at a spatial resolution of $2^\circ \times 2^\circ$ and a monthly time resolution. A land mask was used to limit the domain to the Pacific Ocean and save computational time, but it was open at the Indian Ocean boundary to prevent the biomass from artificially accumulating in the Indonesian region and subsequently in the equatorial western Pacific. Biomasses were then extracted only for the Pacific region.

Catch per unit of effort (CPUE), effort, and length-frequency data from the fisheries operating in the study area were assimilated into the model (see below) to estimate the model parameters within a maximum likelihood scheme (Senina et al 2008). Fishing data are also used as a forcing to compute the fishing mortality of each age class.

BIOLOGICAL PARAMETERS

The model simulates age-structured swordfish populations with one length and one weight coefficient per age cohort (males and females combined) obtained from independent studies. We used the average between three different growth curves from the central Pacific (DeMartini et al 2007), Australia (Young & Drake 2004) and the eastern Pacific (Cerna 2009). The growth curve available from Taiwan (Sun et al 2002) was too different from the other ones and may reflect very local conditions, so we decided to leave it out of the mean growth curve we used for this study. The weight curve was derived from the length-weight relationship in Uchiyama et al. (1999). Different life stages are typically considered in the model: larvae, juveniles and (immature and mature) adults; the age window for each cohort is set so that the change in growth between cohorts would be as nearly constant across the lifespan.

Due to the very rapid growth of swordfish during the first months of life and the monthly resolution of our forcing, the age structure was defined as follows: no larvae class; one monthly age class for juveniles; and 13 adult cohorts of varying durations - 8 for immature adults up to age 3 yr, when 50% of the fish are sexually mature (we used the mean age at maturity for females as they are considered to

represent the spawning biomass, Ward & Elscot 2000), and 5 cohorts for mature adults up to age 9 yr with older fish accumulating in the last cohort (Fig. 1). After the juvenile phase, swordfish become autonomous, i.e., they have their own movement (linked to their size and feeding habitat) in addition to being transported by oceanic currents.

Due to the relatively long lifespan of swordfish (around 15 years; 9+ years in the model structure), the parameter estimation is very sensitive to initial conditions. To mitigate this, the parameter estimation was conducted using historical fishing data over the period 1978 - 2003, with the predictions from the first two years excluded from the likelihood computation.

FISHING DATA

The fishing data sets available for this study were high-resolution catch data provided by NOAA/NMFS for the Hawaii-based longline fisheries and low-resolution public domain spatially-disaggregated monthly catch data provided by the Oceanic Fisheries Program of the Secretariat for the Pacific Community (SPC), in charge of data collection for the Western and Central Pacific Fisheries Commission (WCPFC). Quarterly length frequency data associated with each fishery over the historical fishing period were also available. Table 1 summarizes the fishing data included in this analysis. Swordfish catch data for fleets fishing in the eastern Pacific and reporting catches to the Inter-American Tropical Tuna Commission (IATTC) were not available for the study.

Fishing data provided by NMFS included high-resolution catch data ($0.1^\circ \times 0.1^\circ \times 1$ day degraded to $1^\circ \times 1^\circ \times 1$ month) for 3 Hawaii-based longline fisheries (deep, mixed and shallow sets, defined as L1 to L3 respectively, Table 1). The spatial resolution for Hawaii fisheries was further degraded to $2^\circ \times 2^\circ$ to be used at the resolution of the model.

The SPC catch and effort data are $5^\circ \times 5^\circ \times 1$ month aggregated by flag. Figure 2 shows the composition of catch by flag for the WCPFC member countries. The Japanese, Korean, Taiwanese and Australian fisheries (L4 to L7 respectively, Table 1), along with the Hawaiian fisheries represent nearly 100% of the catch (Fig. 2). No information on target species or hooks per float was available for L4 to L7, which would have been helpful to stratify the catch data by set depth. In addition, these data only partially cover the swordfish catch in the Pacific Ocean (Courtney & Piner 2009; Hinton & Maunder 2011 - draft, Figs. 3 - 5). In particular, data for Mexico, Spain, Chile, and Peru were not available.

Australian data prior to 1996 were not used, as they represent a period during which the swordfish longline fishery was developing in Australia, with a switch to bigger boats and better targeting of swordfish (Ward & Elscot 2000). Such abrupt changes in fishing techniques make the data unsuitable for the optimization as the model defines a unique constant catchability parameter per fishery, with an optional constant linear trend.

High-resolution length-frequency (LF) data were available from the Hawaii longline observer program for the three Hawaiian fisheries. The LF data provided by the SPC, on the other hand, only covered a small portion of the areas fished by the main fisheries (Japan, Korea, Taiwan-RDC) and only some years between 1987 and 2007. The Australian fishery was not included in that LF dataset. Due to the limited amount of LF data available for L3, L4, and L6, the weight of the LF component for those fisheries was increased in the likelihood to obtain a better fit. Spatial distributions of available size

frequency data are shown in Figure 6. The SPC LF data was converted from lower-jaw fork length (LJFL) to eye fork length (EFL) to be consistent with the growth curve and the Hawaii LF data.

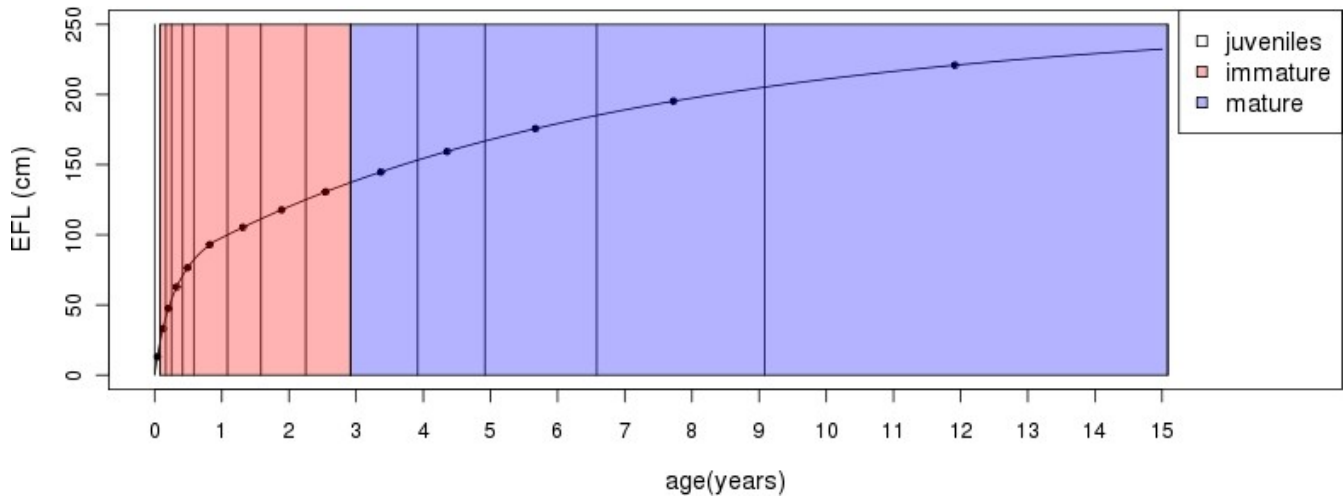


Figure 1: Age cohorts used in the swordfish configuration

N	Gear	Region	Description	Nationality	available catch/effort	resolution	available LF	Resolution
L1	LL	171 - 234 E 2 - 46 N	night-time shallow sets targeting swordfish	US (Hawaii)	1995 - 2010	0.1°x0.1°	171 - 234 E 2 - 46 N	0.1°x0.1°
L2	LL	174 - 238 E 0 - 46 N	mixed sets targeting swordfish	US (Hawaii)	1995 - 2006	0.1°x0.1°	174 - 238 E 0 - 46 N	0.1°x0.1°
L3	LL	182 - 232 E -17 - 42 N	daytime deep sets targeting bigeye tuna	US (Hawaii)	1995 - 2010	0.1°x0.1°	182 - 232 E -17 - 42 N	0.1°x0.1°
L4	LL	102.5 - 287.5 E -57.5 - 57.5 N	pooled LL	Japan	1950 - 2008	5°x5°	102.5 - 122.5 E -47.5 - 12.5 N	5°x5°
L5	LL	102.5 - 287.5 E -62.5 - 62.5 N	pooled LL	Korea	1962 - 2008	5°x5°	142.5 - 237.5 E -12.5 - 12.5 N	5°x5°
L6	LL	102.5 - 282.5 E -42.5 - 47.5 N	pooled LL	Taiwan	1958 - 2008	5°x5°	102.5 - 222.5 E -17.5 - 17.5 N	5°x5°
L7	LL	142.5 - 172.5 E 47.5 - 12.5 S	pooled LL	Australia	1996 - 2008	5°x5°	-	-

Table 1: Longline fisheries included

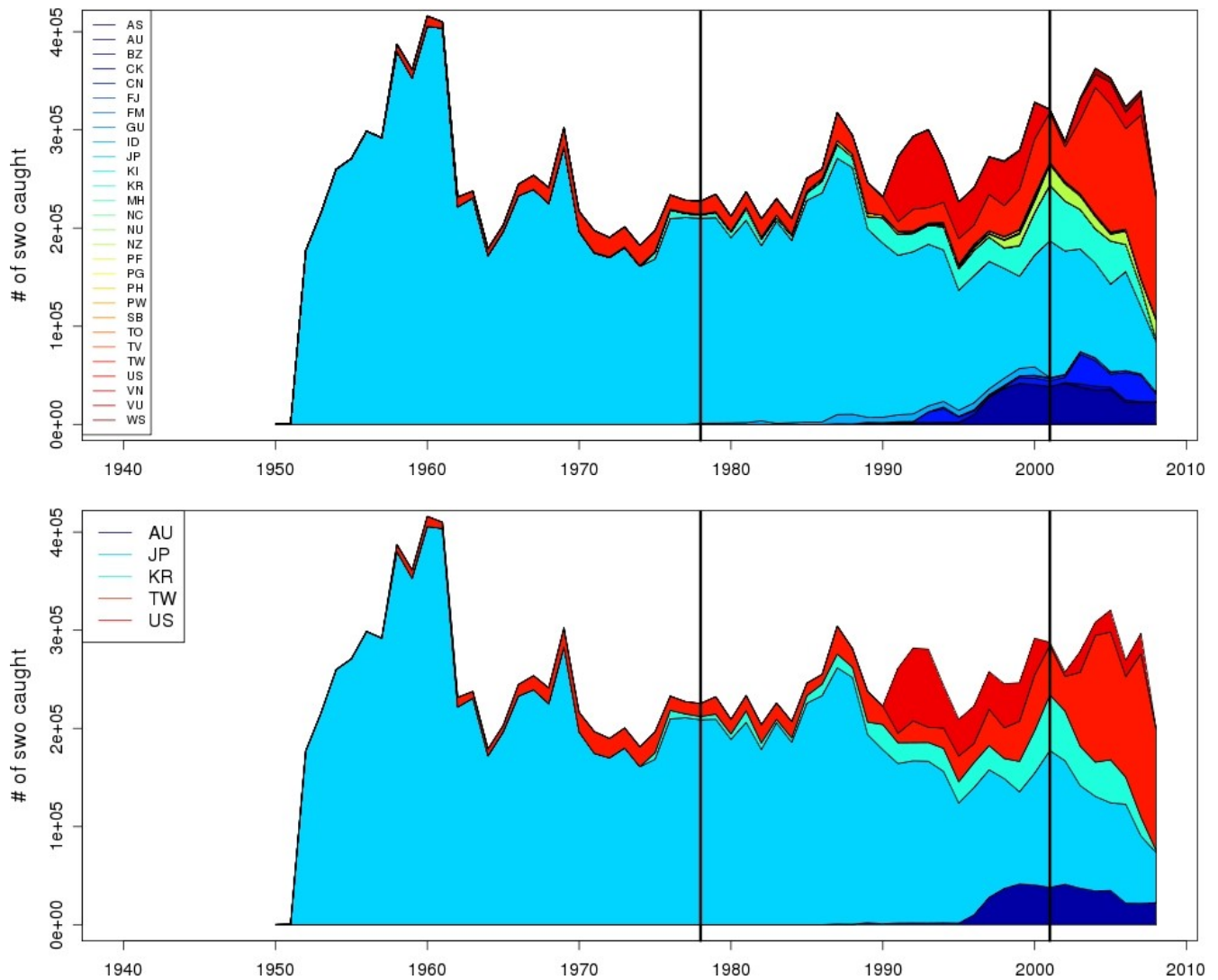


Figure 2: Top : Data provided by the SPC for the whole Pacific Ocean for the WCPFC member countries, composition of catch (# of fish caught) by flag. Vertical lines highlight the period used for parameter optimization (1978 – 2001). Bottom : Same, for the main contributors during the optimization period: 1995-2000. Australia (10%), Japan (50%), Korea (10%), Taiwan (13%), USA (17%)

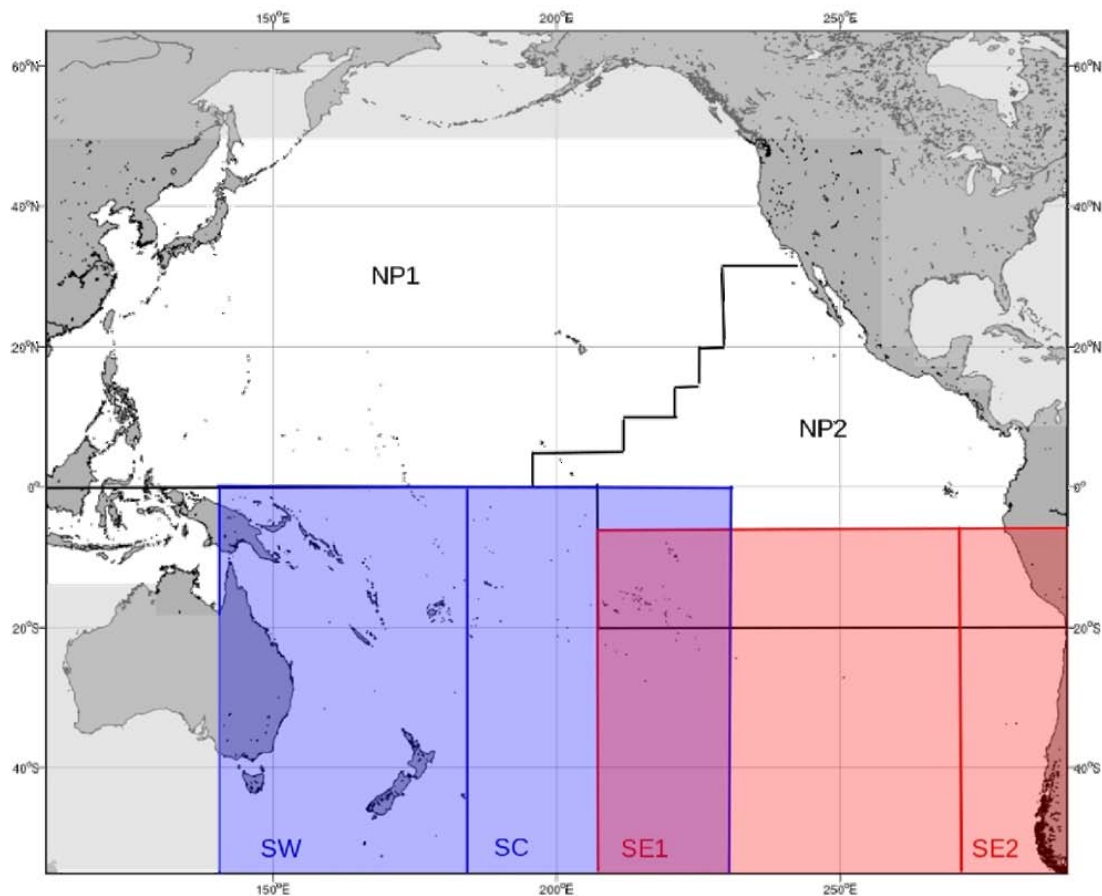


Figure 3: Areas used in the various stock assessments for swordfish in the Pacific Ocean. blue: WCPFC (Kolody et al. (2009)), red : IATTC (Hinton & Maunder (2011 - draft)), white delineated by black lines : ISC (Courtney & Piner 2009).

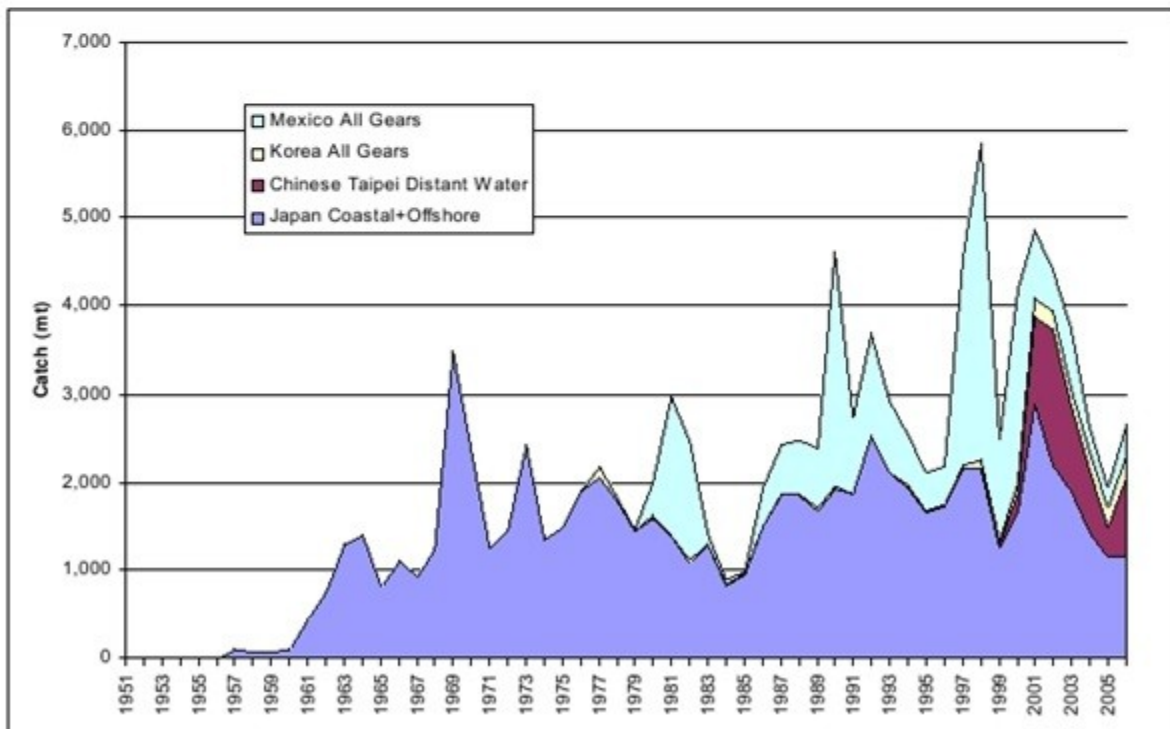
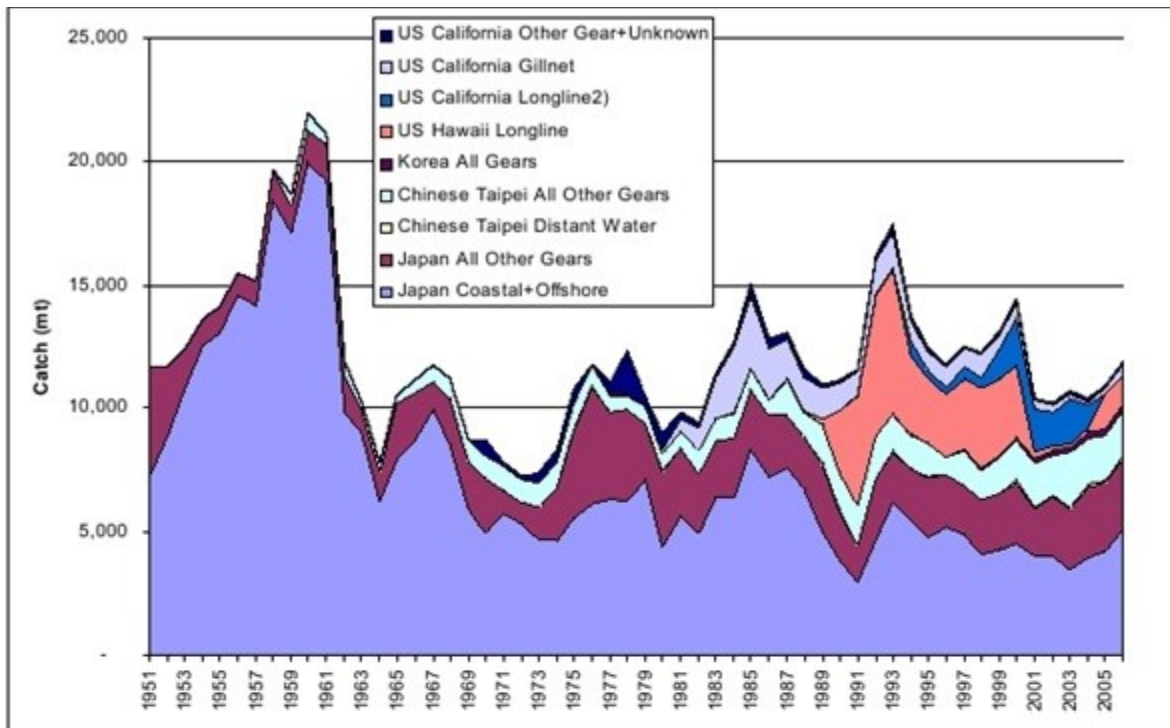


Figure 4: North Pacific catches, corresponding to areas NP1 (top) and NP2 (bottom) on Fig. 3 (from Courtney & Piner (2009))

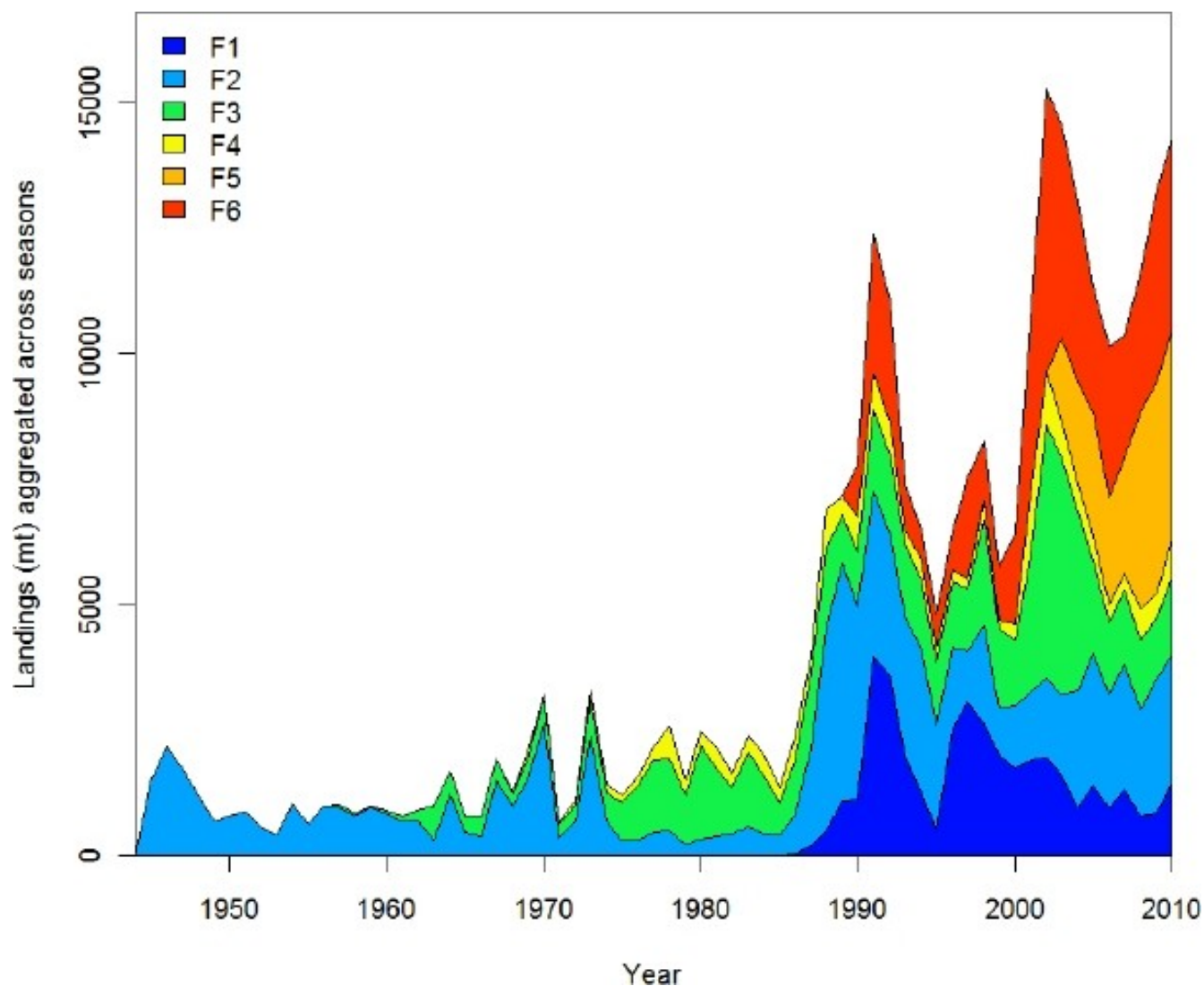


Figure 5: South-east Pacific catches. F1: Chile industrial longline, offshore, F2: Chile artisanal and Peru, coastal, F3: Japan and Japan-like longline, offshore, F4: Japan and Japan-like tuna longline, coastal, F5: Spain longline, offshore, F6: Spain longline, coastal. (from Hinton & Maunder (2011 - draft)). The offshore and coastal areas are denominated SE1 and SE2 respectively in Fig. 3.

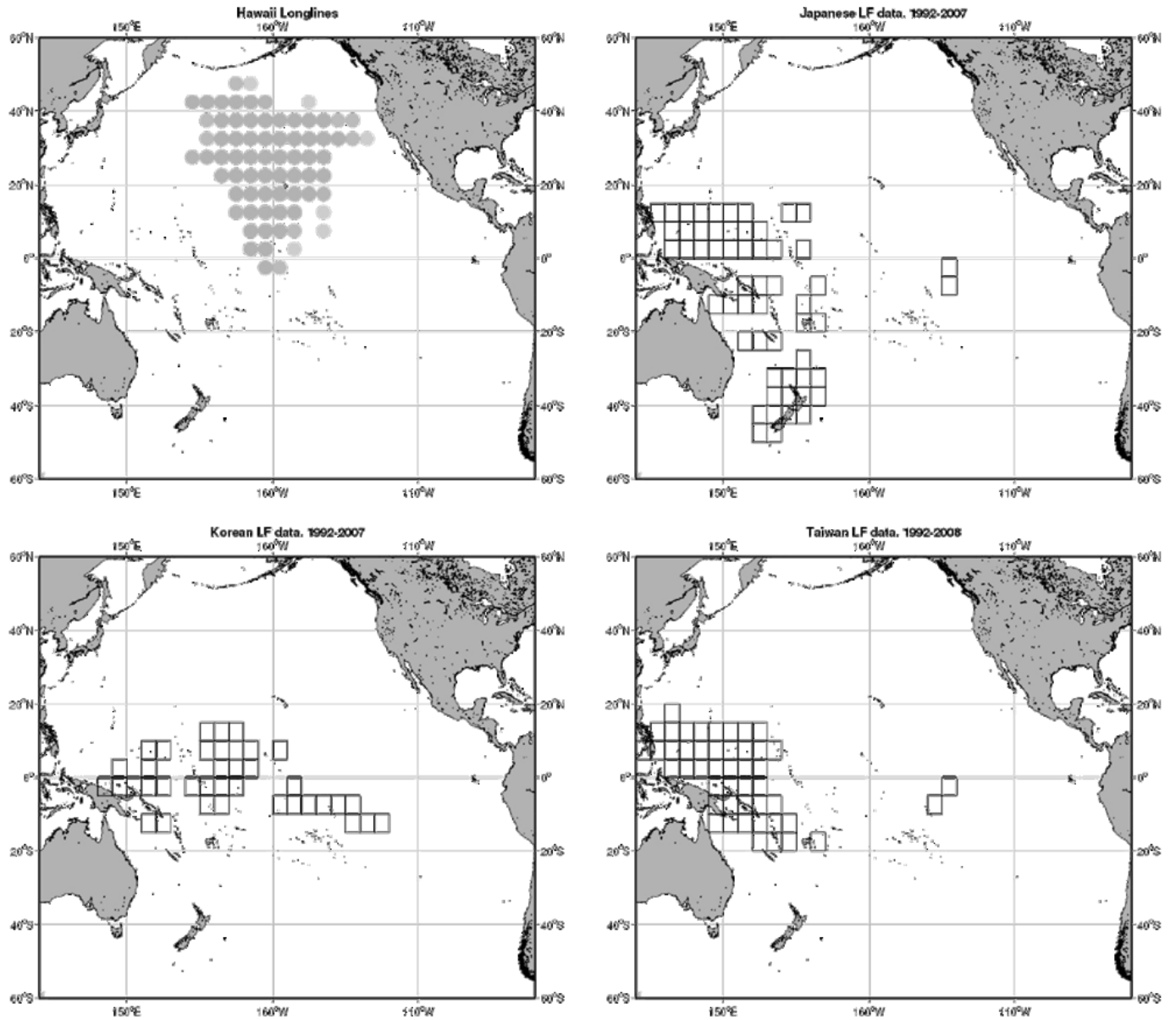


Figure 6: Regions included in the length-frequency data provided for Hawaii, Japan, Korea, and Taiwan (from top left, clockwise)

RESULTS

ESTIMATED PARAMETERS

Current estimates of the parameters are presented in Table 2 (see Appendix for a list of the model notations). As a result of the lack of detailed information on fishing gear (e.g., shallow or deep longline), fishing strategy (target species), and partial catch and LF data, a number of parameters had to be fixed (Table 3) while some other estimated parameters are close to the bounds. In particular, diffusion, natural mortality of juveniles, and the standard deviations of the temperature preferences could not be estimated all at the same time, and thus were eventually fixed to the most plausible values.

N	Name	min	max	Start, $n = 0$	Finish, $n = 108$
1	N_{FE}			0	140
2	L (types 3 3 3 3 3 3 3)			880523	817795
3	G_{max}			41812200	161888
4	Mp mean exp(0)	0	1	0.112978	0.151382
5	Ms mean max(0)	0	0.01	0.000140861	8.78684e-05
6	Ms mean slope(0)	0	1.35	1.16646	1.24357
7	b sst spawning(0)	24	30	26.9199	26.8739
8	alpha spawning(0)	0	2	1.04364e-08	1.25022e-05
9	b sst habitat(0)	5	20	8	5.01337
10	b oxy habitat(0)	0.01	4	3.16583	3.19833
11	MSS species(0)	0.001	3	0.853525	0.641021
12	nb recruitment(0)	0	1	0.000925157	0.000565591
13	a adults spawning(0)	0.1	2	0.100003	0.12131
14	spawning season peak(0)	0	366	263.634	267.094
15	spawning season start(0)	0.9	1.5	1.20287	1.24388
16	q(0,0)	0	0.1	0.00180648	0.00127991
17	q(0,1)	0	0.01	0.0099	0.00999999
18	q(0,2)	0	0.01	0.000349967	0.000699095
19	q(0,3)	0	0.01	0.00702994	0.00619386
20	q(0,4)	0	0.01	0.000411432	0.000545695
21	q(0,5)	0	0.01	0.000402451	0.000703336
22	q(0,6)	0	0.01	0.00714345	0.00763258
23	s sp fishery(0,0)	0.4	30	29.9999	30
24	length threshold(0,0)	33.084	231.663	122.923	123.49
25	right asymptote(0,0)	0	1	0.144837	0.228252
26	s sp fishery(0,1)	0.4	40	28.9378	27.7442
27	length threshold(0,1)	33.084	231.663	119.687	121.255
28	right asymptote(0,1)	0	1	0.117175	0.190581
29	s sp fishery(0,2)	0.01	2	0.921129	1.19802
30	length threshold(0,2)	33.084	231.663	48.8143	47.2334
31	s sp fishery(0,3)	0.03	1	0.0884181	0.0812054
32	length threshold(0,3)	33.084	231.663	142.707	137.691
33	s sp fishery(0,5)	0.01	1	0.10907	0.124849
34	length threshold(0,5)	33.084	231.663	60.847	51.9437
35	s sp fishery(0,6)	0.03	2	1.81825	1.98491
36	length threshold(0,6)	33.084	231.663	142.71	134.824

Table 2. Estimated parameters (#, name, lower bound allowed during optimization, upper bound, starting value before optimization, estimated value after optimization)

N	Name	Parameter
1	Mp mean max(0)	0.275
2	Ms mean half(0)	100
3	M mean range(0)	0
4	a sst spawning(0)	1.5
5	a sst habitat(0)	1
6	a oxy habitat(0)	1e-06
7	hp cannibalism(0)	0.001
8	sigma species(0)	0.07
9	c diff fish(0)	9.99996
10	s sp fishery(0,4)	0.28
11	length threshold(0,4)	84

Table 3. Fixed parameters

Natural mortality

Natural mortality rates and recruitment are the most difficult parameters to estimate in population dynamics models. For swordfish, recent stock assessment studies used a rate between 0.4/yr for younger fish and 0.35/yr for fish older than 7 years (Courtney & Piner 2009). Hinton & Maunder (2011 - draft) mention that natural mortality for swordfish could be as low as 0.2/yr but used a constant annual instantaneous natural mortality rate of 0.4/yr. In SEAPODYM, natural mortality is defined as the sum of a predation and a senescence functions allowing the mortality rates to vary with age (size), but also spatially and temporally within a range of values related to a food availability index (which varies between 0 and 1). However the parameter controlling that variation (M mean range, Table 3) could not be estimated from the data, and was fixed at 0. The estimated natural mortality curve is shown in Fig. 7. The lowest mortality rate corresponds to fish about 3 years old.

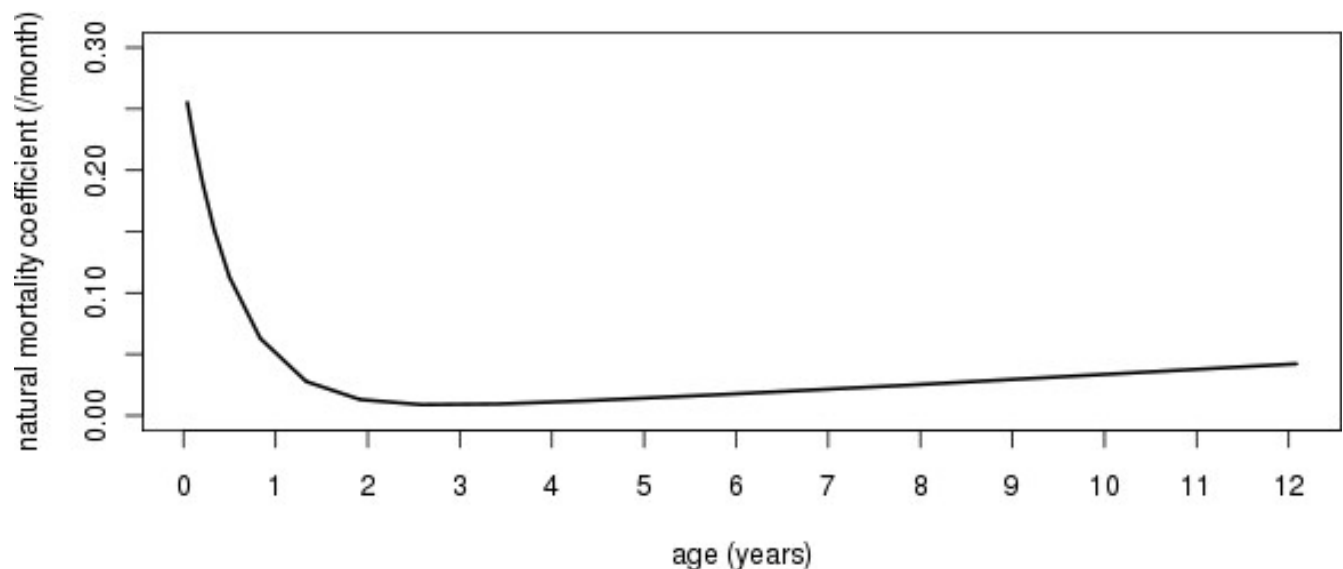


Figure 7: Natural mortality at age (month⁻¹). Age 0 actually corresponds to 1 month-old juveniles in this configuration.

Stock-recruitment

The stock-recruitment relationship in SEAPODYM is expressed at the cell level following the Beverton-Holt function and using the local spawning (adult fish) biomass. It is applied to the first cohort of the model (here the juvenile cohort of the 1st month of life). The value of this stock-recruitment relationship is weighted by the environmentally-driven spawning index (Lehodey et al 2008) to give the final density of juveniles released in each cell of the grid. This relationship, together with the mortality rates, determines the total level of the population. Stock assessment studies use a stock-recruitment steepness of 1 for swordfish, indicating that recruitment is not reduced at lower levels of spawning biomass (Kolody et al 2009, Courtney & Piner 2009, Hinton & Maunder 2011 - draft), but this relationship can not be directly compared with the one used in SEAPODYM.. Starting from an initial value of 1, the steepness of the local stock-recruitment relationship of SEAPODYM was estimated at 0.1 after optimization. Recruitment was initially fixed at the lowest possible level to sustain catches from all fisheries and then estimated by the model (Fig. 8).

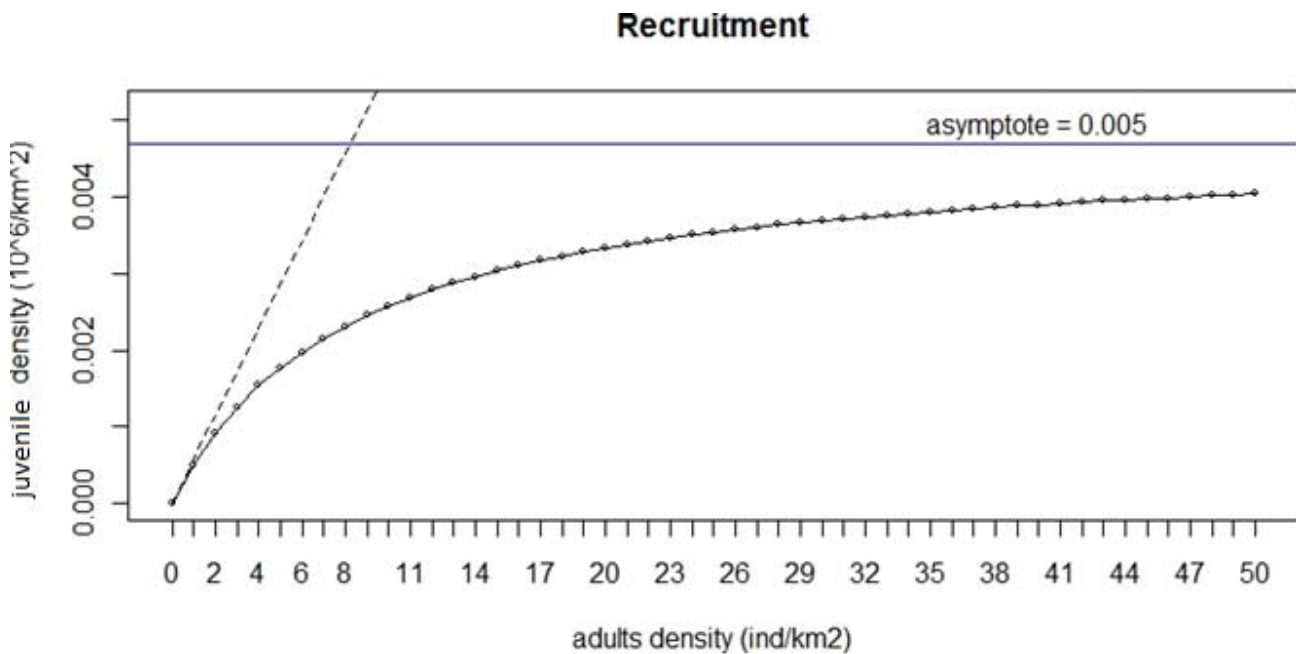


Figure 8: SEAPODYM (local) juvenile stock-recruitment relationship

Temperature / oxygen preferences / constraints

The thermal habitat by age resulting from the optimization experiment is shown on Fig. 9. The optimal spawning temperature was estimated at 26.9°C. The standard deviation could not be estimated and was fixed at 1°C, which still allowed predicting juveniles in the areas with surface temperatures between 22 and 32°C (Fig. 10). Similarly, the estimate for the optimal feeding habitat temperature of the oldest cohort reached the minimum boundary allowed (5°C, which was also the case for bigeye tuna with this forcing, Lehodey et al 2010). The standard deviation was fixed at 1.5 °C for the youngest cohort. The standard deviation for each adult cohort is then computed as $a_sst_habitat + 2.5 * W / W_{max}$ (with W the mean weight of the cohort and W_{max} the mean weight of the oldest cohort).

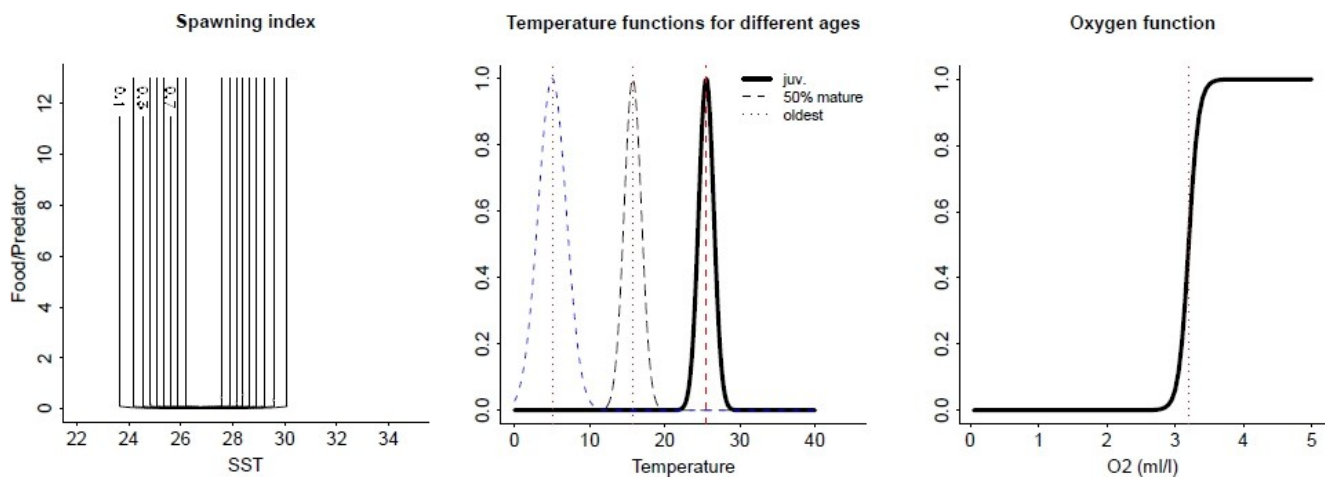


Figure 9: Estimated spawning (contour lines), temperature and oxygen indexes

The spawning season (in the Northern hemisphere) was estimated to peak at the end of September (Julian day #267) to last from July to November at high latitudes (40-50N) and from August to October at about 25N (Table 2). At latitudes lower than 22N, the seasonal switch between feeding and spawning (Lehodey et al. 2008) does not occur, resulting in year-round spawning in areas where favorable spawning index coincides with presence of mature adults. The spawning index becomes positive when SST reaches 24°C, up to about 30°C (Fig. 9 left). The optimization was not sensitive to the trade-off between food for larvae and the presence of their predators (parameter alpha spawning, Table 2). This is the usual tendency when there is a lack of information in the data concerning the size frequency, especially for the small size classes. Therefore, the recruitment of juvenile fish is driven by the temperature function (Fig. 9 left) and the stock-recruitment relationship only.

The oxygen threshold parameter (the value at which the oxygen index is 0.5) estimated by the model was 3.2 ml/l (Fig. 9).

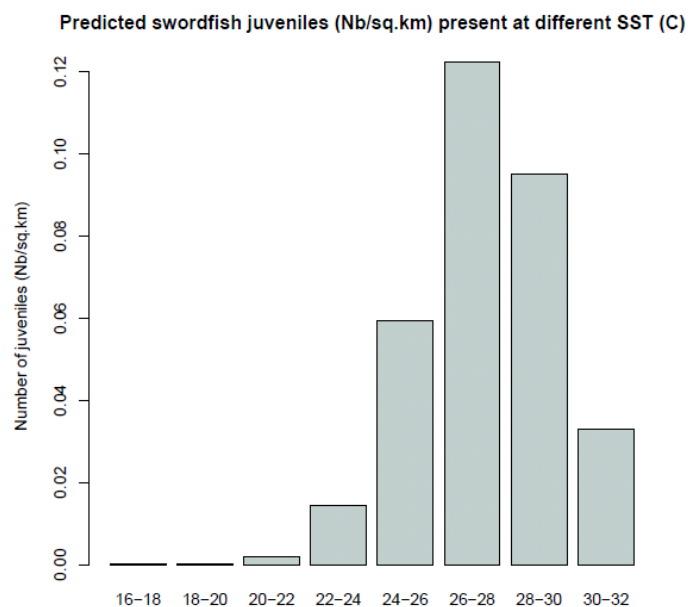


Figure 10. Average (1990-2000) predicted number of swordfish juveniles in waters corresponding to different SST values.

MODEL VALIDATION

LF data for the fishery L5 (Korean fishery) was so scarce that the model consistently overestimated the length threshold of its selectivity to achieve better fit for CPUE data, so the selectivity parameters for L5 were fixed manually to match the LF distribution. No LF data was available for L7 (Australia), so we let the model estimate the selectivity in order not to fix it arbitrarily. All other fishery parameters (catchabilities and selectivities) were estimated from the model and data (Table 1 & 2, Fig. 11). Linear trends in catchability were set manually for some of the fisheries to reflect changes in CPUE (Table 4). The fit to the LF data for each fishery is shown in Fig. 12. Asymmetric Gaussian types of selectivity were chosen for L1 and L2 as they provided a better fit to the LF data than the default sigmoid selectivity functions. The fit to L3 (Hawaii deep sets) LF data is the poorest and the reasons for that need to be explored further. The fit to L1 (Hawaii shallow sets) LF data is slightly shifted towards bigger fish and the fit to L6 (Taiwan), while capturing the peak for younger fish, misses the second peak for bigger fish. The predicted LF distributions for the other fisheries are in good agreement with the observations (Fig. 12).

Despite the lack of contrast and coverage in the fishing data that was available, the experiments showed a generally good fit to the spatially aggregated monthly CPUE time series (Fig. 13). The fits to L1 and L2, the two fisheries targeting swordfish for which high-resolution data were provided, as well as the fit to L7 (Australia), for which we excluded data prior to 1996, when the fishery can be considered homogeneous, are the best fits (correlation coefficient = 0.94). The fit to L4 (Japan) is the poorest in the amplitude of the seasonal signal, but it captures the trend fairly well. This result may not be too surprising since the Japanese longline data covers the whole time series and the entire Pacific, thus probably consisting in several types of gear and target species which makes the fitting with one single selectivity function and one catchability coefficient challenging.

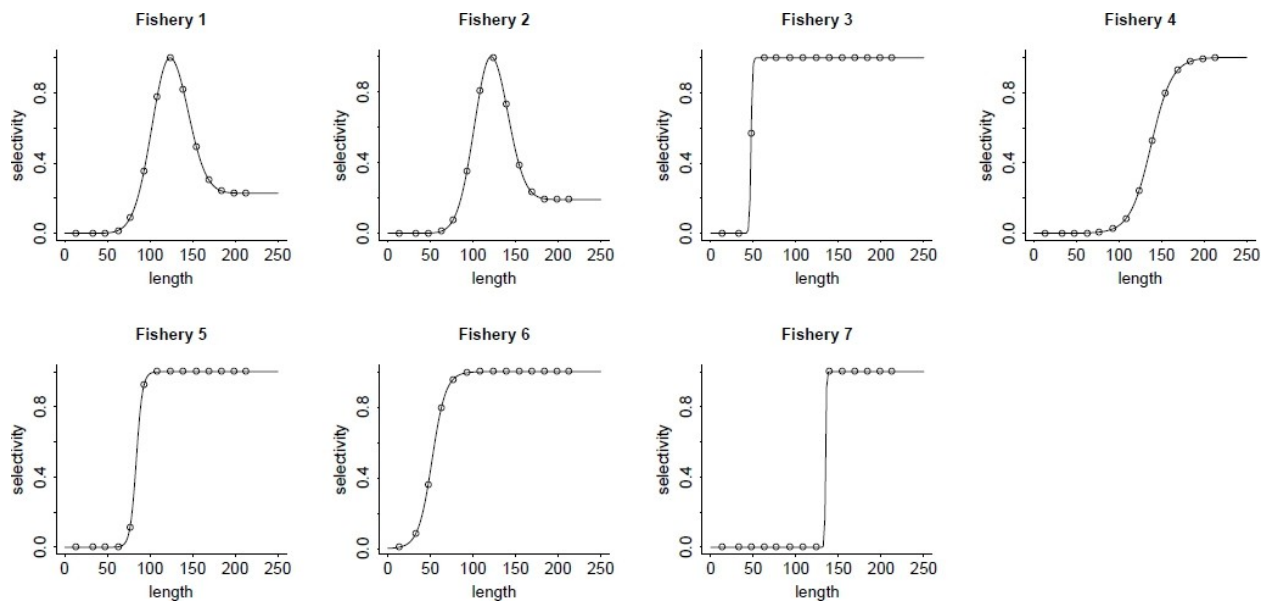


Figure 11. Selectivity functions estimated by the model for fisheries L1 to L7

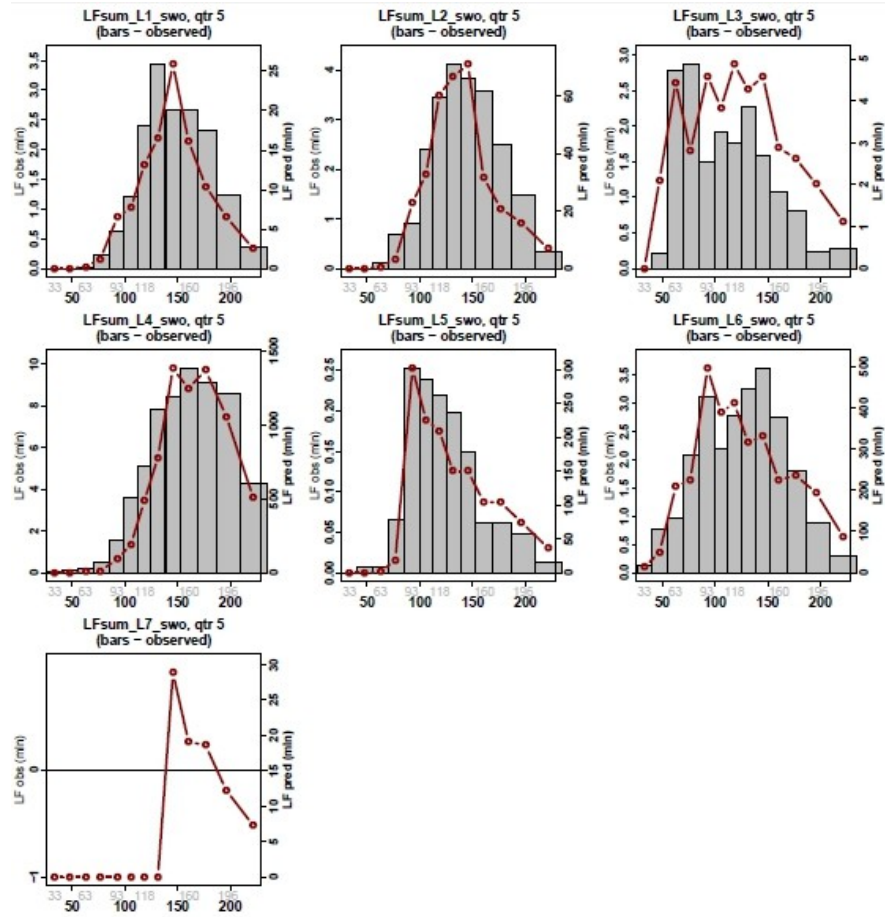


Figure 12: Fit to length frequency data. (bars: observations, red line : model predictions)

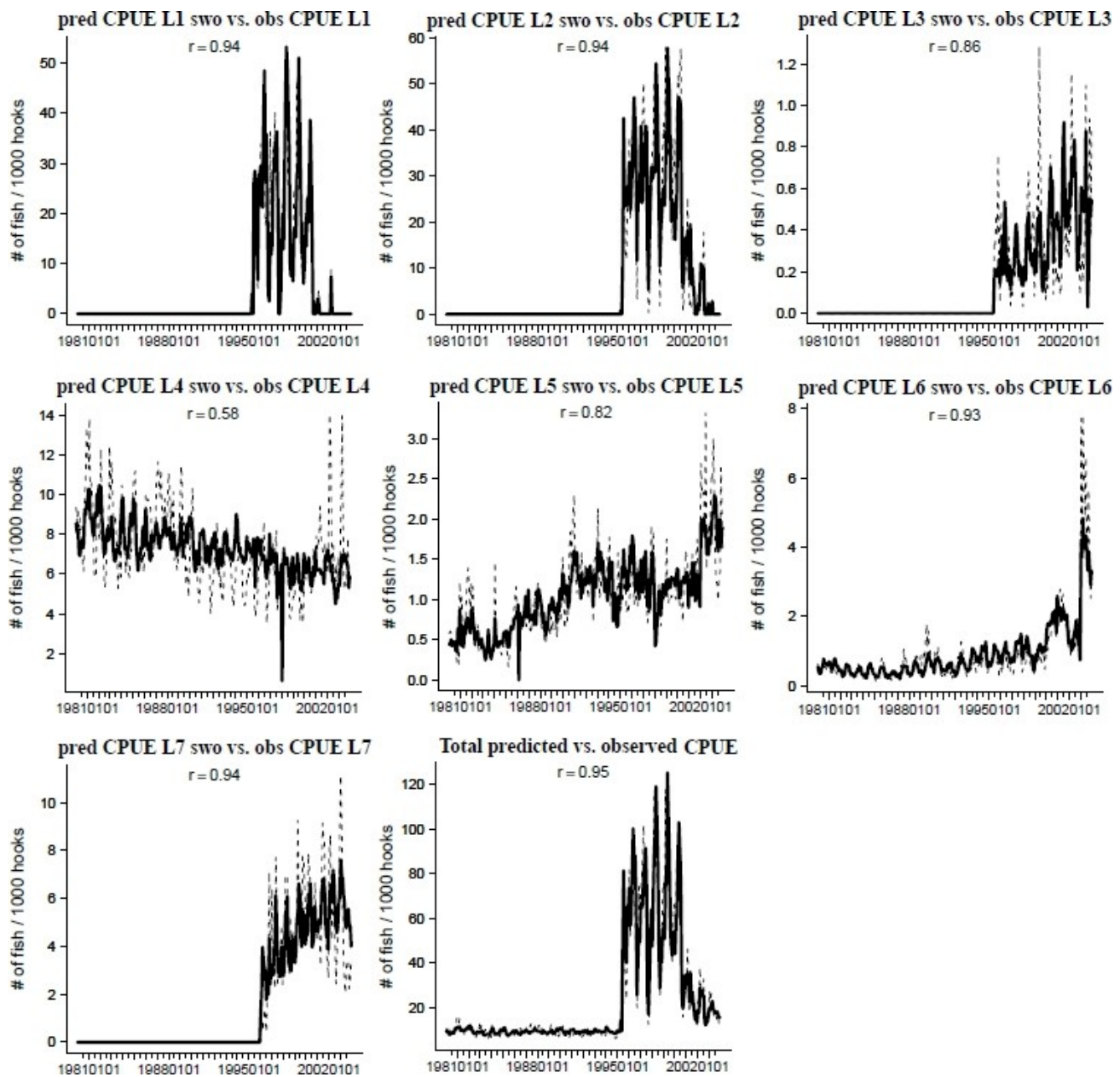


Figure 13: Fit to CPUE data (in # fish per 1000 hooks. dashed line: observations, solid line: model predictions), with correlation coefficient.

Fishery	Linear coefficient
L1	0
L2	0
L3	-0.00015
L4	-0.000925
L5	0.0039
L6	0.0045
L7	0

Table 4. Linear trends added to the catchability of fisheries.

Fig. 14 (top left) shows a map of the R-squared goodness of fit metrics representing the spatial fit over the period used for optimization, overlaid with the total catch in each cell. Except for a few exceptions, the poorly fitted areas correspond to areas of low levels of catch. Fig. 14 (top right) shows the Pearson r-squared metric, which quantifies the percentage of the CPUE variance explained by the model in each cell, overlaid with the number of observations (fishing events), and Fig. 14 (bottom) shows a map of the mean error. Some areas, especially the area covered by the Hawaii-based longline fishery are relatively well fitted by the model, but large areas of the western Pacific and a latitudinal band (between about 10 and 20°N) are poorly fitted. These areas also coincide with the regions of low effort, catch and CPUE.

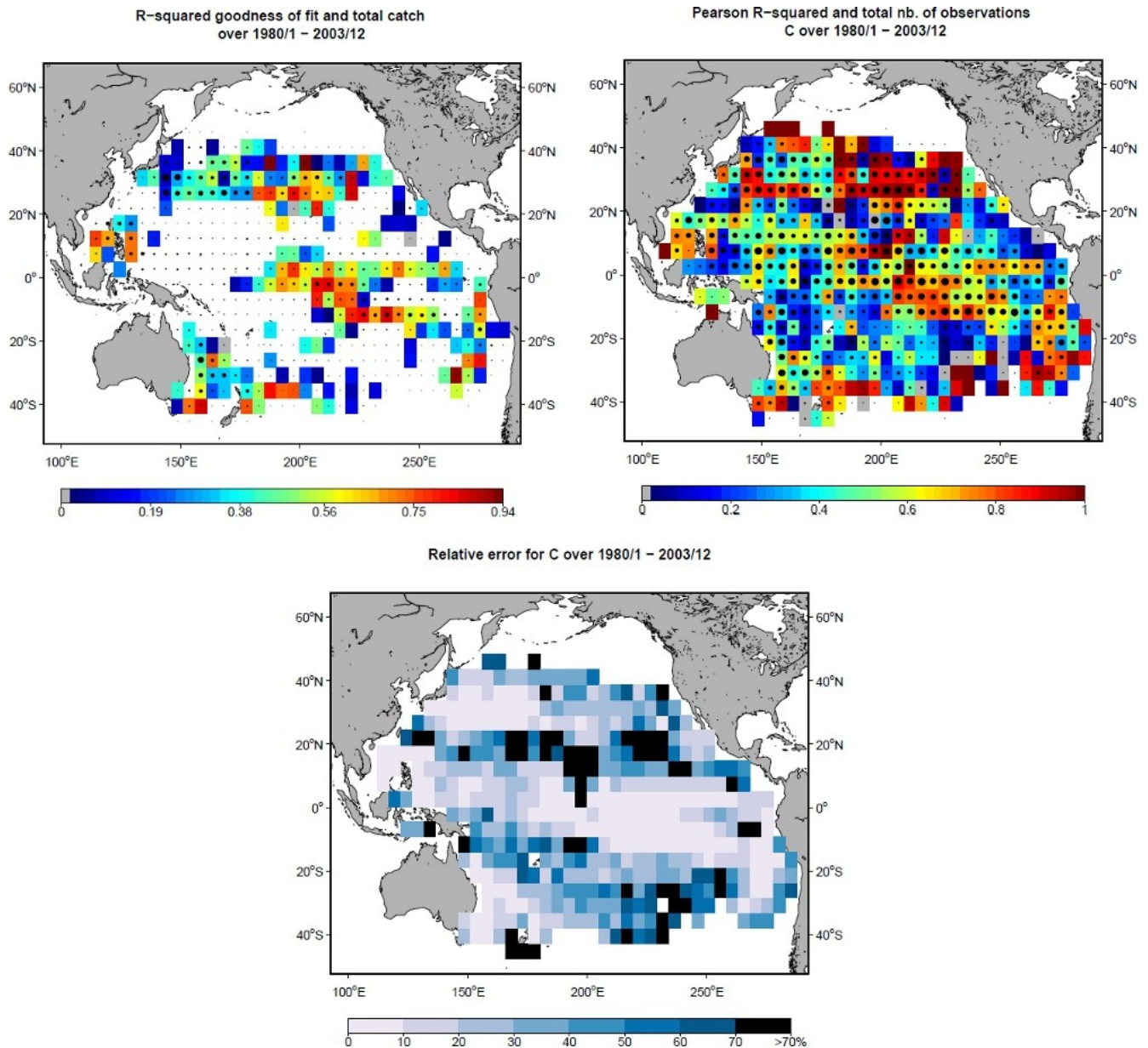


Figure 14: R-squared goodness of fit overlaid with the total catch (top left, blank areas indicate cells with negative correlation between observations and predictions), Pearson R-squared overlaid with the number of catch observations (top right), and relative error (bottom) for the fit to CPUEs over the optimization period.

As Figs. 11 & 12 suggest, the Japanese fishery catches mostly adult swordfish and the Korean fishery mostly young fish. Therefore, it is interesting to compare spatial distribution of CPUEs from these fisheries with the mean predicted density of adult and young swordfish respectively (Fig. 15). Although the two spatial distributions differ substantially, there is a fairly good agreement between CPUEs and predicted densities in both cases. This provides good confidence in the validity of the estimated parameters. Predicted young fish concentrations occur in the central equatorial region in agreement with high CPUEs of the Korean fishery. Adult fish are concentrated in the Kuroshio extension area, the subtropical convergence zone from the eastern Australian coast to the north-east of New Zealand, and the eastern Pacific in the equatorial region and off the Peru-Chile coast.

The inter-annual variability associated to the ENSO index can modify drastically the distribution of young swordfish with a large eastward shift of the equatorial fish concentration as indicated by exceptionally high catch rates in the Korean fishery (Fig. 16). Though the model doesn't predict the areas of highest catch, the general El Niño / La Niña pattern is captured, with higher densities in the Eastern Pacific during El Niño.

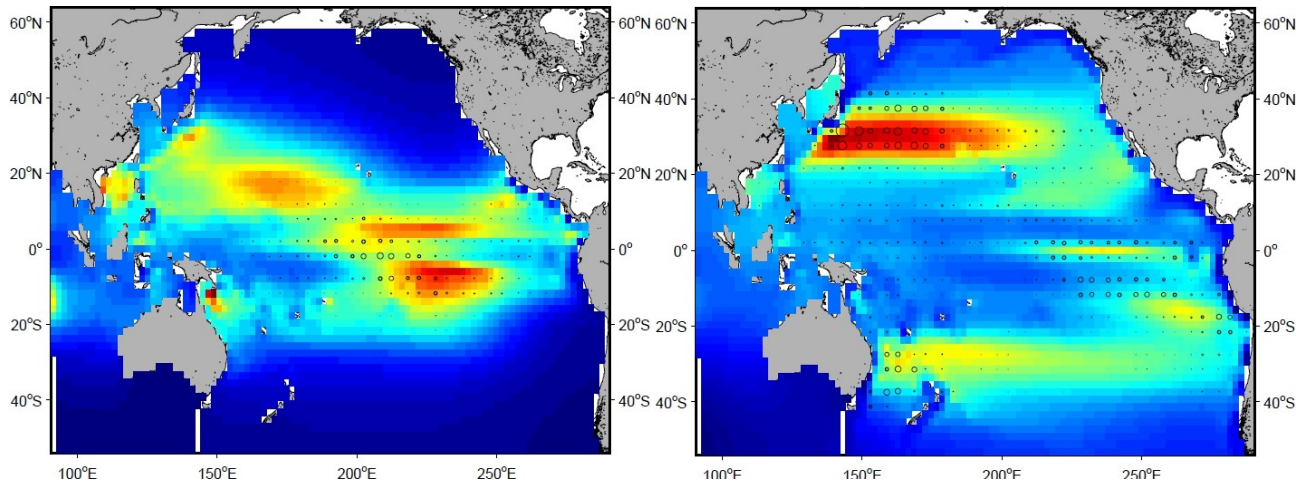


Figure 15. Mean distributions (in Nb/sq.km) of young (left) and adults (right) from 1992-2001 overlaid with Korean (L5) and Japanese (L4) CPUEs (circles), respectively.

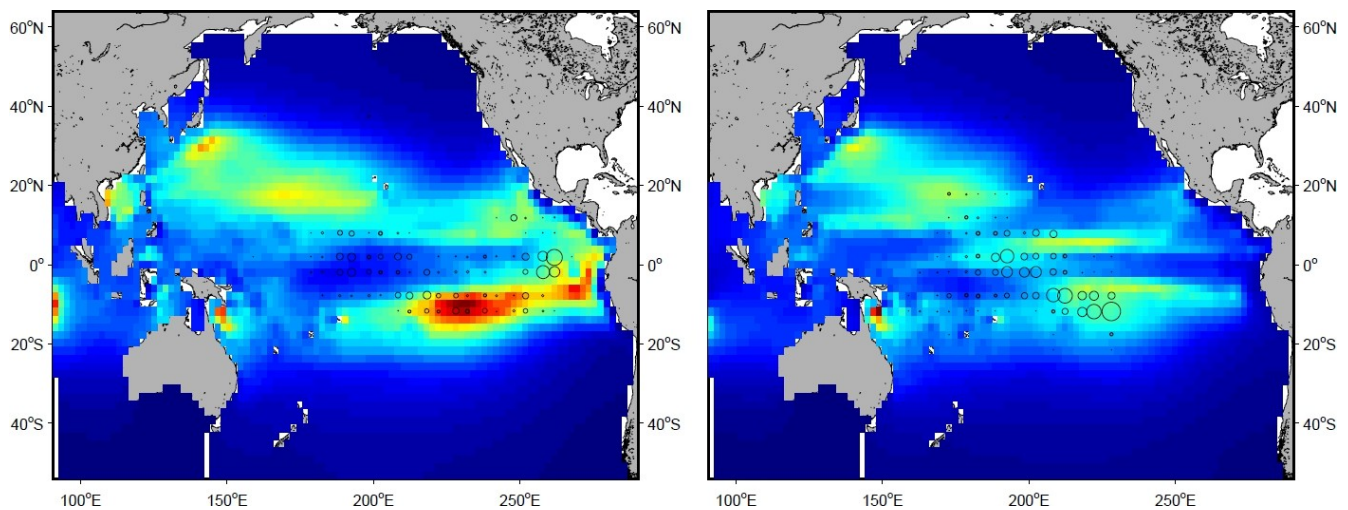


Figure 16. Mean distributions of young swordfish biomass (N/sq.km) overlaid with Korean CPUEs (L5) during the 1998 El Niño event (left, Oct. 1997 – Feb. 1998) and during La Niña (right, Jul. 1998 – Jan. 1999)

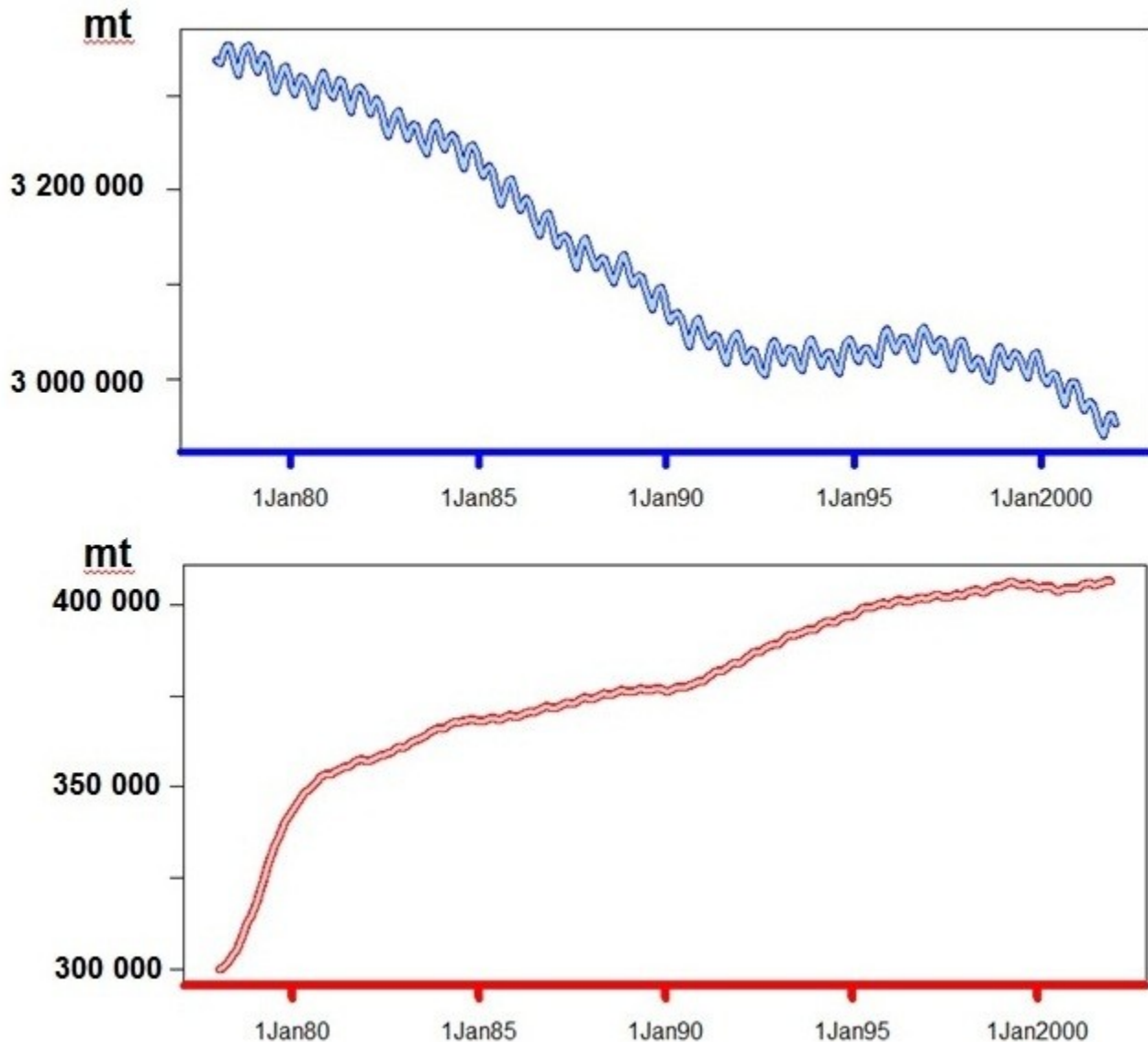


Figure 17. Estimated biomass of adults (mt). Top : with the initial condition left free. Bottom : with the model initial condition constrained to realistic levels of biomass.

Fig. 17 (top) shows the biomass of adults estimated by the model. When left free to estimate the initial condition, the model estimated very unrealistic levels of biomass, above 3 million tons. This is most likely due to the discrepancy between the coarse resolution of the forcing and the high resolution of the Hawaii fishing data with very high CPUEs. Because of the low resolution of the forcing which does not resolve the mesoscale, the model can not predict the local concentrations of fish. Additionally, because of its high resolution, the Hawaii data contains a much higher number of observations, which gives it an important weight in the likelihood function, forcing the model to fit these observed localized high CPUEs. In order to achieve that, the model estimates high biomasses in much larger regions which yields unrealistic total biomasses.

In a subsequent run (Fig. 17, bottom), the initial condition was artificially constrained to more realistic levels of biomass, around 300,000 mt. The biomass of adults estimated by the model was then

predicted to increase to 450,000 mt between 1980 and 2003. This explosive trend is unrealistic for an exploited stock and shows that the model is not at equilibrium.

Fig. 18 shows the mean seasonal spatial distributions of each age class. The distribution of juveniles matches the U-shaped pattern of gene flow encountered by Reeb et al 2000, with contiguous distributions between the northern and southern parts of the eastern Pacific (especially during quarter 2), but separate populations in the north and south of the western Pacific. Youngs are mostly distributed in the equatorial part of the basin year-round with two tropical pools in the north-west and south-east. Adults are very widespread longitudinally in the subtropics. During the spawning migration phase, part of the spawning biomass still stays in the feeding grounds and its distribution becomes more diffused due to the switch to the spawning habitat, which is unfavorable in subtropical regions.

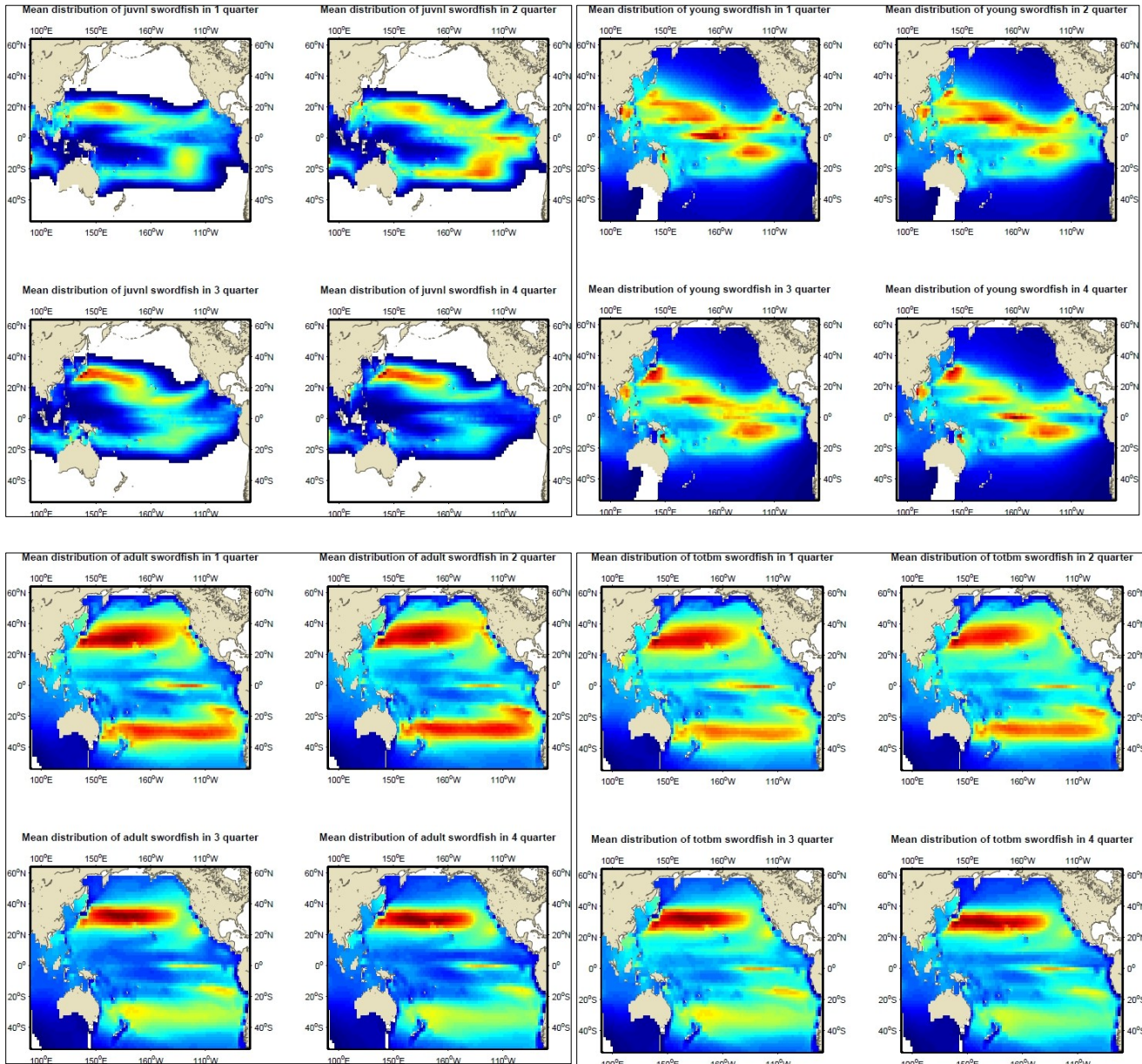


Figure 18. Mean distributions of biomass (mt/sq.km) between 1996 and 2000 of (from top left) : juveniles, young, adults, and total population.

OVERLAP BETWEEN SWORDFISH AND TURTLES

Fig. 19 shows the distribution of adult swordfish, targeted by the longline fisheries, overlaid with hotspots of loggerhead turtles habitat (Abecassis et al, in prep. See Chap. 2). During quarters 3 and 4, the turtles' hotspots are predicted to be much far to the North of the swordfish populations and almost completely separate spatially. During quarters 1 and 2 on the other hand, when the thermal preferences of loggerheads bring them southward, is when their habitat coincides with the peak of the swordfish distribution in the central western Pacific. The whole eastern part of the loggerheads' hotspots, along the west coast of the US and Baja California is predicted to be separate from the main swordfish aggregations year-round.

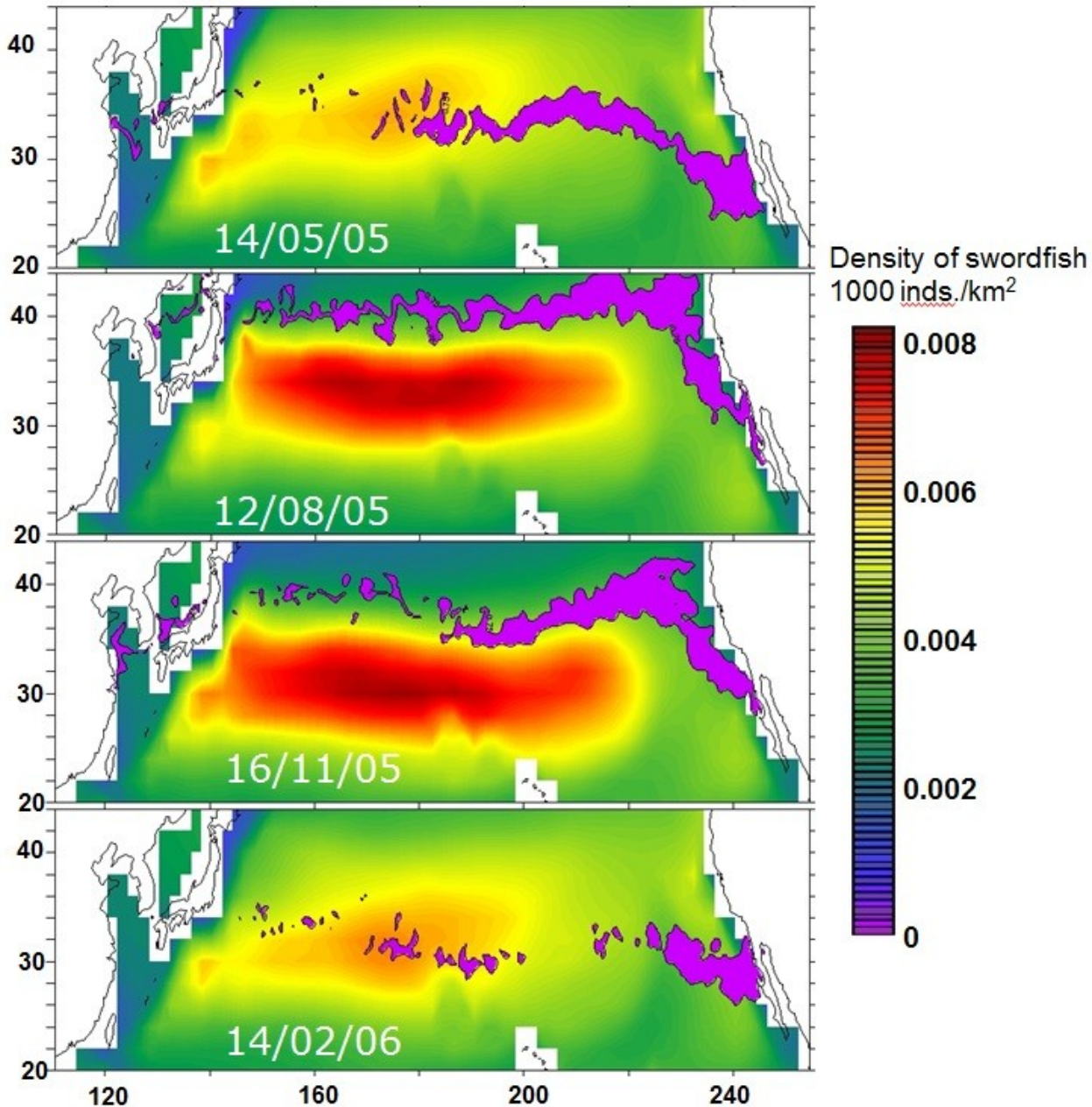


Figure 19. Comparison between swordfish distributions (mt/sq. km, color scale) and loggerhead turtles hotspots (purple area corresponding to values of the habitat index between 0.8 and 1, from Abecassis et al in prep).

However, Hawaii-based longline vessels targeting swordfish typically operate during quarters 1 and 2 when the transition front is closest to Hawaii (Polovina et al 2000). This indicated that the seasonality estimated by the model is off. This again is likely due to the much higher weight on the Hawaii fishing data which is too localized to allow the model to calibrate basin-wide migrations.

DISCUSSION AND CONCLUSIONS

MODEL LIMITATIONS

Sexual dimorphism

There are big differences between the growth rate, the size and the age at maturity of males and females (DeMartini et al 2007, Ward & Elscot 2000). Females live longer, grow faster after the third year and reach larger sizes. They also mature later. The different sexes may also have different spatial distributions (Ward & Elscot 2000). The present SEAPODYM version doesn't allow two different sets of parameters for males and females, so the biological parameters had to be averaged between males and females.

Forcing

Due to the coarse resolution of the NCEP forcing ($2^\circ \times 2^\circ$), these simulations do not reproduce mesoscale activity and underestimate the intensity of oceanic circulation in the most dynamical oceanic areas, e.g., Kuroshio and east equatorial Pacific (Lehodey & Senina (2009)). It would be interesting in a later study to compare these results with those obtained using a higher-resolution forcing.

Fishing data

We worked with incomplete fishing data (lacking data for Chile, Mexico, Spain and Peru in the Eastern Pacific), and data that pools all types of gear together for most fisheries. Swordfish CPUE can vary greatly between night-time shallow longline sets targeting swordfish and daytime deep sets targeting tuna (Fig. 20), by as much as two orders of magnitude in the Hawaii-based fisheries. Unfortunately, no information on target species or hooks per float was available for the SPC data. The absence of information on the target species makes it very difficult to fit pooled catch data in SEAPODYM, where each fishery is modeled with a unique selectivity function and a unique catchability. In addition, data provided by the SPC only accounted for parts of the swordfish catch in the Pacific Ocean. As mentioned, catch data for non-WCPFC fisheries were not available. Because our analysis did not include these catch data, the fishing mortality in our model is underestimated in the eastern Pacific. Despite this lack of comprehensive fishing data, the model optimization experiments yielded good spatial fit to catch and CPUE over the period of optimization and allowed reasonable estimated values of most parameters defining the feeding habitat of the population at the Pacific basin scale. However, key parameters still remain unestimated and had to be fixed leading to large uncertainty, especially in the total biomass and distribution of adults. The level of this uncertainty needs to be evaluated through sensitivity studies. Much progress could be quickly achieved if more comprehensive fishing data were available at the scale of the Pacific Ocean. These data, including all available size frequency data, should be stratified by space, gear and target species.

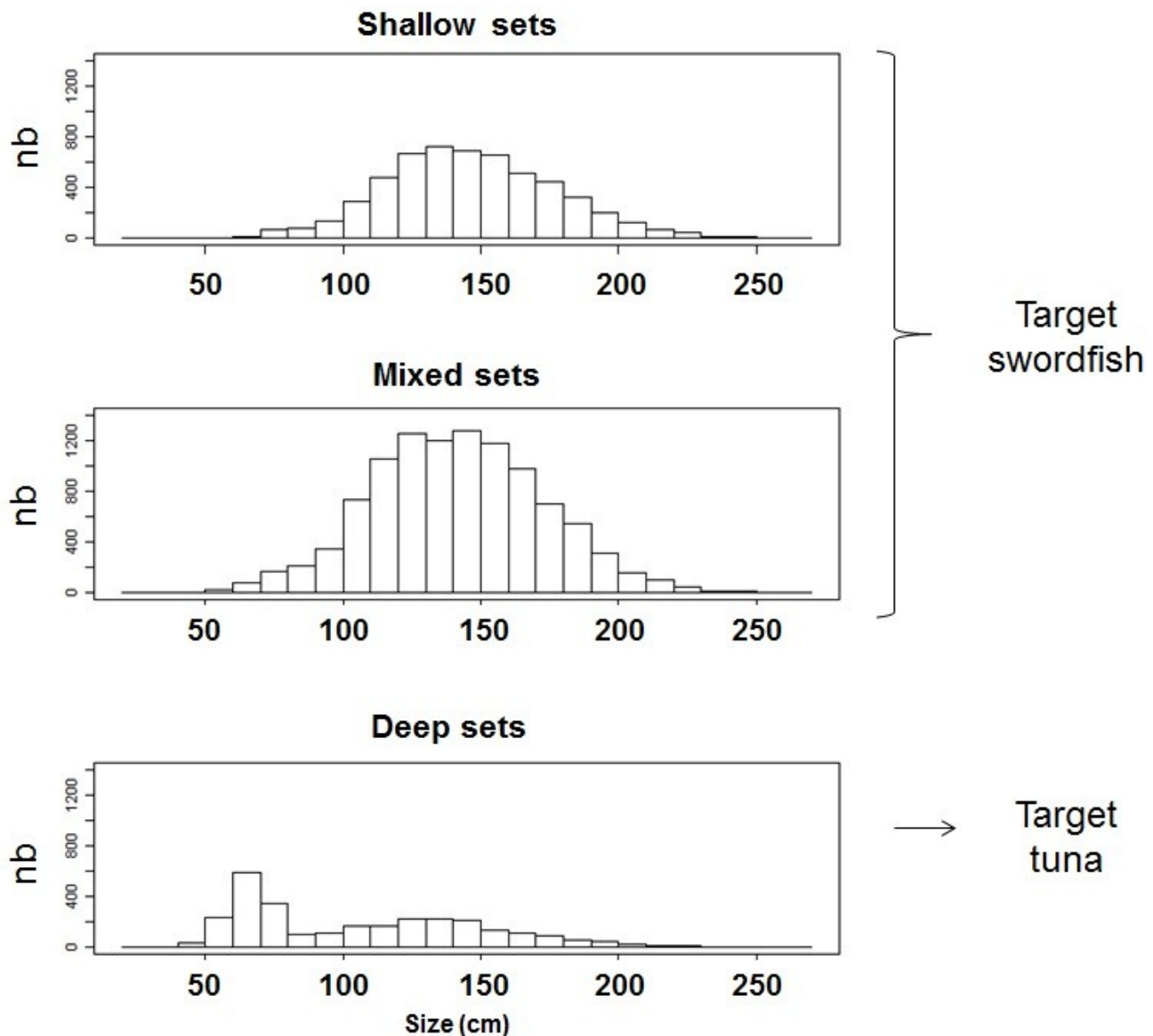


Figure 20. Distributions of length frequencies in the Hawaii-based longline fishery, separated by type of sets. From top to bottom : shallow, mixed and deep sets.

ESTIMATED PARAMETERS

Biomass

Due to the lack of comprehensive fishing data and the discrepancy in the resolution of the fishing data and the forcing, it was not possible to achieve a realistic estimation of biomass at this stage. We initially assumed that it would be best to give a higher weight in the likelihood to the high-quality fishing data from Hawaii provided by NMFS, thinking this would favor an adequate parameter estimation in the area best covered by the data. However, since no prior SEAPODYM study to date had benefitted from such high-resolution fishing data, we had not realized that such a discrepancy in resolution could produce important biases in the biomass estimation, forcing the model to estimate high

catches in grid cells whose size is much larger than the areas of high CPUEs spanned by the longline sets.

The stock synthesis model described in Courtney & Piner (2009) estimated a biomass of swordfish age 2 and over around 30,000 and 70,000 mt in areas NP1 and NP2 respectively (Figs. 3 & 21), i.e. roughly the northern and part of the eastern Pacific stocks, between 1995 and 2000. The stock synthesis model of Hinton & Maunder (2011 - draft) estimated the spawning biomass to be around 60,000 mt during the same period in the eastern Pacific (areas SE1 and SE2 in Figs. 3 & 21). And the Multifan-CL stock assessment of Kolody et al. estimated maximum spawning biomass around 25,000 mt in the southwest Pacific (areas SW and SC in Figs. 3 & 21). Ignoring the overlap between the three assessment regions, this would amount to about 185,000 mt of adult swordfish in the Pacific Ocean. Despite the uncertainties associated with each of those assessments and the differences in methodology used, this constitutes our best estimate of levels of swordfish biomass in the Pacific Ocean to date.

Our attempt to constrain the model initial condition to levels of biomass consistent with that estimate clearly showed that our model was not at equilibrium and that biomass estimation with the current forcing is not possible (Fig. 17). The Hawaiian fishery is spatially localized, limited to recent years and highly seasonal. Thus even with very detailed catch data, the information provided by this fishery is very partial with regards to the basin scale distribution of the species and its long term dynamics. Indeed, the high resolution of data for the Hawaiian fishery could be seen as a source of bias in the model optimization approach by contributing too heavily in the total likelihood and thus weakening the key information that wider and permanent fisheries like the Japanese longline can provide. This needs to be accounted for in further simulations either by increasing the resolution (weight) of other fisheries or allowing to weigh the likelihood terms of each fishery.

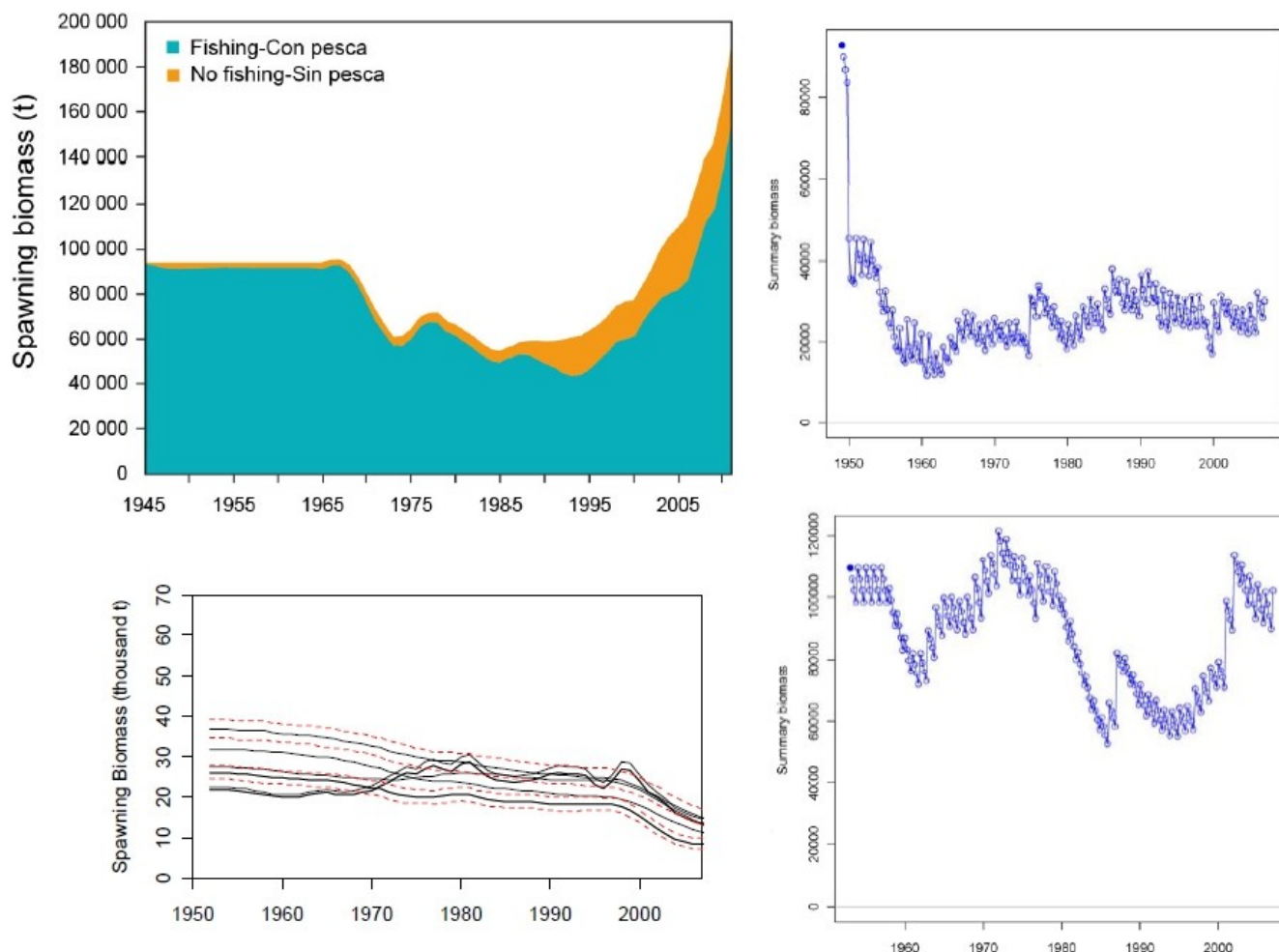


Figure 21. Biomass of mature adults estimated by Hinton & Maunder 2010 (top left), Kolody et al 2009 (bottom left) and Courtney & Piner 2009 (top and bottom right, for areas NP1 and NP2 respectively, see Fig. 3).

Habitat parameters

The estimated optimal temperature (26.9°C) for spawning is in agreement with published values since swordfish are known to spawn in waters with sea surface temperature between 24 and 29 °C (Ward & Elscot 2000). Swordfish do not seem to have a specific spawning period but rather spawn whenever SST is higher than 24°C. At higher latitudes, this limits spawning to spring and summer. The model estimated a long spawning season peaking at the end of September, which seems somewhat late. It's unclear whether this is due to a lack of data in critical regions.

The estimated threshold in dissolved oxygen (~3.2 mL/L) seems quite high since satellite tracking data suggest that swordfish are more tolerant to low ambient dissolved oxygen concentration than most tuna species (Abecassis et al in press, Dewar et al. 2011). Similar SEAPODYM studies for bigeye and skipjack tunas using the same forcing found oxygen thresholds around 0.74 and 1.5 mL/L respectively (Lehodey et al, 2010). Swordfish certainly has lower oxygen constraints than skipjack tuna (Carey & Robison 1981, Wegner et al 2010). The estimation of such a high oxygen threshold is likely due to the lack of fishing data for the eastern Pacific, where the oxygen minimum layer is quite shallow. Some

catch and effort data from that region would have allowed to calibrate the oxygen constraints of swordfish more accurately.

OVERLAP BETWEEN SWORDFISH AND TURTLES

This first model parameterization will likely evolve under the combined effects of both improved fishing data sets and more realistic environmental forcing resolving the mesoscale. In particular, the question of seasonality in the north-south migrations needs to be investigated in more details. The current prediction seems off seasonally. The Hawaii-based shallow set longline fishery, targeting swordfish, operates mostly during quarters 1 & 2, when swordfish move south towards Hawaii (Polovina et al 2000). The most southern distribution of swordfish as predicted by our model (Fig. 19) occurs during quarters 3 & 4. The shallow set fishery usually deploys very few sets during quarter 3 and a few more during quarter 4, sometimes as many as in quarter 2, but definitely not nearly as many as in quarter 1 (NOAA/NMFS longline reports: <http://www.pifsc.noaa.gov/fmb/reports.php>). This would indicate that the estimated seasonality parameters are offset despite the fact that the CPUE seasonality is well predicted around Hawaii, suggesting a potential inversion of the seasonal switch between feeding and spawning migrations. The correct seasonal signal may not be sufficiently clear to be detected because too much weight was allocated to the seasonal Hawaiian fishing data in absence of sufficient accuracy in the definition of Pacific wide fisheries (e.g. Japan) at the 5°x 5° resolution.

To conclude, these results are encouraging and, with most of the parameters now estimated at biologically plausible values and yielding good fits to the fishing data and spatial distributions, a switch to a finer-resolution forcing would be very valuable and allow to infer more detailed predictions for management purposes. Most importantly, the inclusion of better and exhaustive fishing data would quickly improve the model, especially in terms of seasonality and oxygen dependency.

APPENDIX – LIST OF SEAPODYM NOTATIONS

notation	Name	unit
NFE	Number of function evaluations	-
L	Likelihood	-
Gmax	Maximum gradient of standardized habitat	-
Mp mean max	Maximal mortality rate due to predation	month ⁻¹
Mp mean exp	Slope coefficient in predation mortality	-
Ms mean max	Maximal mortality rate due to senescence	month-1
Ms mean slope	Slope coefficient in senescence mortality	-
M mean range	Coefficient of variability of mortality with food requirement index	-
a sst spawning	Coefficient of variability of tuna mortality with food requirement index	°C
b sst spawning	Optimum of the spawning temperature function	°C
alpha spawning	Larvae food–predator trade-off coefficient	-
a sst habitat	Std. Err. of the adult temperature function for the young	°C
b sst habitat	Optimum of the adult temperature function at maximum age	°C
a oxy habitat	Curvature coefficient of the oxygen function	-
b oxy habitat	Oxygen threshold	mL.L ⁻¹
MSS species	Maximum sustainable speed	bl.s ⁻¹
sigma species	Diffusion coefficient	Nmi ² /mo
c diff fish	Curvature coefficient of the diffusion function	-
nb recruitment	Maximum number of larvae at large spawning biomasses of adults	1e6 / km ²
a adults spawning	Slope coefficient in the Beverton–Holt function	-
spawning seasonal peak	Peak of the spawning season	julian day
spawning seasonal start	Defines the duration of the spawning season	-
Q	Catchability of the fishery	-
s sp fishery	Steepness of the selectivity function	-
length threshold	Threshold of fish length in the selectivity function	-
right asymptote	Asymptote in selectivity function (for the asymmetric gaussian type)	-

REFERENCES

- Abecassis M, Dewar H, Hawn D, Polovina J (in press) Modeling swordfish daytime vertical habitat in the north pacific ocean from pop-up archival tags. *Mar Ecol Prog Ser*
- Abecassis M, Lehodey P, Polovina J, Senina I, Gaspar P, Calmettes B, Balazs G, Parker D (in prep). Analysis of loggerhead turtles tracks in the North Pacific to parameterize a feeding habitat and movement model.
- Aumont O, Maier-Reimer E, Blain S, Monfray P (2003) An ecosystem model of the global ocean including fe, si, p colimitations. *Global Biogeochemical Cycles* 17
- Aumont L O; & Bopp (2006) Globalizing results from ocean in situ iron fertilization studies. *Global Biogeochemical Cycles* 20:1–15
- Beverly S, Robinson E, Itano D (2004) Trial setting of deep longline techniques to reduce bycatch and increase targeting of deep-swimming tunas. Tech. Rep. FTWG - WP-7a, Standing Committee on Tuna and Billfish
- Boggs, C.H. (2003) Pacific research on longline sea turtle bycatch. In: K.J. Long and B.A. Schroeder (eds). *Proceedings of the International Technical Expert Workshop on Marine Turtle Bycatch in Longline Fisheries*. US Department of Commerce, NOAA Technical Memorandum NMFS-F/OPR-26, Silver Spring, MD, USA, p. 189
- Bopp L, Aumont O, Cadule P, Alvain S, Gehlen M (2005) Response of diatoms distribution to global warming and potential implications: A global model study. *Geophysical Research Letters* 32:1–4
- Carey F, Robison B (1981) Daily patterns in the activities of swordfish, *Xiphias gladius*, observed by acoustic telemetry. *Fish Bull* 79:277–292
- Cerna F (2009) Age and growth of the swordfish (*Xiphias gladius* Linnaeus, 1758) in the southeastern pacific off chile (2001). *Lat Am J Aquat Res* 37:59–69
- Courtney D, Piner K (2009) Preliminary age structured stock assessment of north pacific swordfish (*xiphias gladius*) with stock synthesis under a two stock scenario. Tech. Rep. ISC/09/BILLWG-3/07
- DeMartini EE, Uchiyama JH, Humphreys Jr RL, Sampaga JD, Williams HA (2007) Age and growth of swordfish (*Xiphias gladius*) caught by the Hawaii-based pelagic longline fishery. *Fishery Bulletin* 105:356–367
- Dewar H, Prince ED, Musyl MK, Brill RW, Sepulveda C, Luo J, Foley D, Orbesen ES, Domeier ML, Nasby-Lucas N, Snodgrass D, Laurs RM, Hoolihan JP, Block BA, Mcnaughton LM (2011) Movements and behaviors of swordfish in the atlantic and pacific oceans examined using pop-up satellite archival tags. *Fish Oceanogr* 20:219–241
- Gorgues T, Menkes C, Aumont O, Vialard J, Dandonneau Y, Bopp L (2005) Biogeochemical impact of tropical instability waves in the equatorial pacific. *Geophysical Research Letters* 32:L24615

- Hinton MG, Maunder MN (2011 - draft) Status of swordfish in the eastern pacific ocean in 2010 and outlook for the future. Tech. rep., IATTC
- Howell E, Kobayashi D, Parker D, Balazs G, Polovina J (2008) Turtlewatch: a tool to aid in the bycatch reduction of loggerhead turtles *Caretta caretta* in the Hawaii-based pelagic longline fishery. *Endangered Species Research* 5(2-3):267–278
- Kolody D, Campbell R, Davies N (2009) South-west pacific swordfish (*xiphias gladius*) stock assessment 1952-2007. Tech. Rep. WCPFC-SC5-2009/GN-IP-2, WCPFC/CSIRO
- Lehodey P., (2001). The pelagic ecosystem of the tropical Pacific Ocean: dynamic spatial modelling and biological consequences of ENSO. *Progress in Oceanography*, 49: 439-468
- Lehodey P., Chai F., Hampton J. (2003). Modelling climate-related variability of tuna populations from a coupled ocean-biogeochemical-populations dynamics model. *Fisheries Oceanography*, 12(4): 483-494.
- Lehodey P, Senina I, Murtugudde R (2008) A spatial ecosystem and populations dynamics model (SEAPODYM) - modeling of tuna and tuna-like populations. *Prog Oceanogr* 78:304–318
- Lehodey P, Senina I (2009) An update of recent developments and applications of the SEAPODYM model. Tech. Rep. WCPFC-SC5-2009/EB-WP-10, WCPFC
- Lehodey P, Senina I, Calmettes B, Abecassis M, Molina JJ, Briand K, Hampton J, Polovina J, Williams P, Nicol S (2010) Project 62: SEAPODYM applications in wcpo - progress report. Tech. Rep. -SC6-2010/EB- IP 02, WCPFC
- Lehodey P, Senina I, Calmettes B, Hampton J, Nicol S, Williams P, Jurado Molina J, Ogura M, Kiyofuji H, Okamoto S (2011) SEAPODYM working progress and applications to pacific skipjack tuna population and fisheries. Tech. Rep. SC7-2011/EB-WP 06, WCPFC
- Polovina J, Kobayashi R, Parker M, Seki P, Balazs H (2000) Turtles on the edge: movement of loggerhead turtles (*Caretta caretta*) along oceanic fronts, spanning longline fishing grounds in the central north pacific, 1997-1998. *Fisheries Oceanography* 9(1):71–82
- Reeb, C. A., L. Arcangeli, and B. A. Block. 2000. Structure and migration corridors in Pacific populations of the swordfish *Xiphias gladius*, as inferred through analyses of mitochondrial DNA. *Mar. Biol.* 136: 123–1131
- Senina I, Sibert J, Lehodey P (2008) Parameter estimation for basin-scale ecosystem-linked population models of large pelagic predators: Application to skipjack tuna. *Prog Oceanogr* 78:319–3
- Sun, C.-L., S.-P. Wang, and S.-Z. Yeh. 2002. Age and growth of the swordfish (*Xiphias gladius* L.), in the waters around Taiwan determined from anal-fin rays. *Fish. Bull.* 100:822–835
- Uchiyama JH, Demartini EE, Williams HA (1999) Length-weight interrelationships for swordfish, *Xiphias gladius* L., caught in the central North Pacific. Tech. rep., NOAA/SWFSC

Ward P, Elscot S (2000) Broadbill swordfish: status of world fisheries. Bureau of Rural Sciences, Canberra, Australia

Wegner NC, Sepulveda CA, Bull KB, Graham JB (2010) Gill morphometrics in relation to gas transfer and ram ventilation in high-energy demand teleosts: Scombrids and billfishes. *J Morphol* 271:36.49

Young J, Drake A (2004) Age and growth of broadbill swordfish (*Xiphias gladius*) from Australian waters. Tech. rep., FRDC & CSIRO

CONCLUSIONS

Ce projet de thèse a consisté à étudier les habitats de deux espèces, l'espadon et la tortue caouanne, au moyen de marques satellites et de modèles numériques afin d'évaluer de potentielles stratégies d'évitement des tortues par les palangres qui ciblent l'espadon.

RESUME DES RESULTATS

Le premier chapitre consiste en l'analyse de marques satellites déployées sur 40 espadons dans le Pacifique Nord. Les données de profondeur, température et lumière enregistrées par les marques le long des trajectoires des poissons furent analysées conjointement à des données environnementales pour caractériser les facteurs qui régissent la profondeur moyenne des espadons durant la journée. Ces facteurs sont la concentration en chlorophylle de surface, la concentration d'oxygène dissous en profondeur, et la température de l'eau en profondeur. Ces trois facteurs expliquent 77% de la variabilité de la profondeur moyenne diurne au sein d'un modèle additif généralisé (GAM). Moins l'eau est froide et productive, et plus elle est riche en oxygène, plus les espadons ont tendance à se trouver à des profondeurs importantes, ce qui se traduit par des profondeurs moyenne de 600 - 650 m au nord d'Hawaïi dans le gyre subtropical, et d'environ 300 – 350 m près des côtes californiennes. Toutefois une grande incertitude existe tant sur la précision des positions des poissons dérivées du niveau de lumière enregistré par les marques satellites, que sur la qualité des données d'oxygène utilisées dans cette étude.

Nos résultats montrent également que lorsque les espadons ne somnolent pas en surface (phénomène de « basking »), ils se maintiennent verticalement dans des eaux caractérisées par un niveau de lumière ambiante très restreint (plongeant en profondeur juste avant l'aube et remontant vers la surface après le crépuscule), ce qui suggère qu'ils suivent une partie de la couche dispersante profonde comportant des proies dont ils se nourrissent de jour comme de nuit.

Le second chapitre traite de l'analyse de 224 marques satellites déployées sur des tortues caouannes capturées par des palangriers ou élevées en captivité. L'étude des températures de surface le long de leurs trajectoires, et de leurs mouvements propres (une fois soustraite l'influence des courants océaniques), a permis de calibrer une version simplifiée du modèle SEAPODYM décrit en détail dans l'introduction. L'analyse des traces montra que les vitesses de nage moyennes ne dépassent pas 1 km/h, et que les tortues les plus petites (~ 25 cm) ont des vitesses maximales plus importantes que les tortues plus larges (~ 80 cm), proportionnellement à leur taille. L'analyse des vitesses de nage a également permis de démontrer que de très jeunes tortues (mesurant 25 cm) sont capables de mouvements propres significatifs et ne sont pas soumises entièrement aux aléas des courants océaniques. La température optimales des tortues caouannes, quelle que soit leur taille, semble se situer aux alentours de 17°C dans le Pacifique nord. Des différences saisonnières suggèrent que les tortues de taille plus importante plongent plus profond que les plus petites. En été, lorsque la thermocline est peu profonde, elles se retrouvent probablement dans des eaux plus froides que leur température optimale et ciblent ensuite des eaux de surface plus chaudes pour se réchauffer. La modélisation du champ des proies est à améliorer pour refléter le régime alimentaire des tortues de manière plus adéquate (proies neustoniques plutôt que proies épipélagiques). Cependant, les simulations conduites en utilisant les paramètres de température et de vitesse inférés de l'analyse des marques fournissent des indices d'habitat et des migrations saisonnières Nord-Sud en très bon accord avec les trajectoires des tortues observées. En revanche, le modèle ne reproduit pas les mouvements Est-Ouest

observés pour certaines des tortues les plus larges entre 1997 et 2000, ce qui suggère que les contraintes thermiques, la vitesse propre des tortues, et les concentrations locales de proies ne suffisent pas à expliquer la totalité des mouvements des tortues caouannes dans la Pacifique Nord. D'autres mécanismes de retour vers les plonges de ponte seraient notamment nécessaires, mais la périodicité de tels retours éventuels est mal connue. De plus, certains juvéniles passent probablement des décennies dans l'océan, tandis que d'autres passent peut-être la quasi-totalité de leur phase juvénile dans des habitats côtiers (notamment en Basse-Californie). Des marquages électroniques couvrant plusieurs décennies sont encore loin d'être réalisables technologiquement, mais se révéleront probablement nécessaires pour mieux comprendre la dynamique Est-Ouest des mouvements des tortues. Par ailleurs, les simulations réalisées ici ne remontent pas au-delà de 2002 et elles devront être mises à jour lorsque des réanalyses historiques plus longues seront disponibles.

Enfin, le dernier chapitre détaille l'adaptation du modèle SEAPODYM, originellement développé pour les espèces de thons tropicaux, à l'espadon. A l'aide de certains résultats du premier chapitre et de données issues de la littérature, un premier paramétrage manuel a été effectué, puis raffiné automatiquement par assimilation de données de pêche. Malheureusement, les données de pêche disponibles pour cette étude étaient incomplètes, et surtout, étaient agrégées par pays. Si une telle agrégation peut être suffisante pour les thons, pour les espadons, en revanche, un plus grand degré de détail est nécessaire. En effet, les espadons sont capturés par deux types de pêche à la palangre, les palangres qui ciblent l'espadon de nuit en surface, et celles qui ciblent le thon, de jour, en profondeur. La vulnérabilité de l'espadon à ces deux types de pêche est radicalement différente, et l'agrégation de différents types de pêche au sein du modèle dilue le signal et rend l'estimation des paramètres d'habitat très délicate. Du fait de ces limitations, et malgré un très bon accord entre les captures prédites et observées (temporellement), certains paramètres n'ont pas pu être estimés et ont dû être fixés à des valeurs plausibles biologiquement. La saisonnalité (mouvements Nord-Sud) ne paraît pas non plus être en adéquation avec les saisons de pêche. Des améliorations majeures seraient possibles avec de meilleures données de pêche et un forçage résolvant la méso-échelle. Une étude détaillée des zones de coïncidence est peu réaliste à ce stade, du fait de la basse résolution du forçage utilisé pour l'application espadon.

STRATEGIES D'EVITEMENT

Plusieurs types de stratégie d'évitement peuvent être envisagés :

- un évitement vertical, autrement dit, régler la profondeur de la palangre bien plus profonde que la couche verticale occupée par les tortues
- un évitement horizontal : fermer certaines zones à la pêche
- un évitement temporel : interdire la pêche à certaines périodes de l'année
- un évitement différencié : à l'aide d'une prédiction la plus précise possible et en temps réel des distributions des 2 espèces

Chacune de ces stratégies n'a de sens que si elle permet de réduire efficacement les prises accessoires de tortues tout en maintenant les captures d'espadon. En effet, l'espadon étant considéré comme sous-exploité dans le Pacifique, une stratégie ayant un impact négatif sur le succès de capture des espadons a peu de chances d'être adoptée.

L'étude au chapitre 2 confirme qu'une stratégie d'évitement prometteuse consiste à déployer les palangres à plus grande profondeur, notamment dans la zone du gyre tropical. Différents essais de modification des palangres ont prouvé que la suppression des hameçons de la couche de surface permet de réduire

drastiquement les interactions avec les tortues. Néanmoins, lors des tests effectués, les palangres étaient placées à une profondeur d'environ 300 - 400 m (près d'Hawaii, Boggs 2003), ce qui d'après nos résultats serait trop peu profond pour cibler efficacement l'espadon de jour, et expliquerait les faibles captures réalisées. Le modèle additif généralisé (GAM) développé dans le 2ème chapitre pourrait permettre de générer des cartes (hebdomadaires, par exemple) de profondeur moyenne pour guider les pêcheurs dans le déploiement de leurs lignes à une profondeur optimale. Des tests sur des lignes verticales (non des palangres) basés sur ces résultats sont actuellement en cours (D. Itano, pers. comm.) pour étudier le succès de capture de l'espadon de jour, en profondeur. Si ces tests s'avèrent concluants, il reste à déterminer la faisabilité de déployer des palangres à 650 m de profondeur. Plus la ligne est déployée à grande profondeur, plus cela prend du temps aux équipes de pêcheurs. Ces bateaux déploient généralement une ligne en quelques heures et la laissent ensuite pêcher pendant toute la nuit (ou la journée, selon le type de palangre). Toute modification impactant la durée de déploiement aura donc aussi un impact sur la durée de pêche disponible et pourrait affecter négativement les captures par unité d'effort. Par ailleurs, les palangres profondes capturent également du thon obèse, ce qui pourrait augmenter la pression de pêche sur cette espèce déjà à la limite de son maximum d'exploitation. Enfin, l'aide à la pêche est un outil de gestion potentiellement controversé qui pourrait avoir des conséquences indésirables. Il faudrait analyser les possibles répercussions d'une telle stratégie : est-ce que les pêcheurs passeront d'une pêche peu profonde à une pêche profonde, ou tenteront-ils de cibler l'espadon de jour comme de nuit grâce aux informations fournies ?

Le produit TurtleWatch, développé par la NOAA et suggérant aux pêcheurs d'éviter de pêcher entre les isothermes 17.5 et 18.5°C a rencontré un certain succès, mais le nombre de tortues capturées par les palangres hawaïennes, après avoir diminué drastiquement entre 2006 et 2010, a de nouveau commencé à croître en 2011 (atteignant 12 tortues dans l'année. Depuis 2004, la pêche est automatiquement fermée à partir de 17 interactions avec des tortues caouannes pour l'ensemble de la pêcherie, ce qui fut le cas en 2006). Par ailleurs, de nombreuses autres mesures d'évitement furent mises en place conjointement (modification des hameçons, des appâts, etc ...), il est donc délicat de mesurer l'impact qu'a pu avoir TurtleWatch sur la diminution des interactions entre les tortues et la pêcherie, mais l'adoption de l'outil par les pêcheurs démontre la faisabilité de la mise en place d'une telle stratégie d'évitement. La production et la diffusion en temps réel de l'indice d'habitat présenté au chapitre 3 pourrait être une information supplémentaire pour les pêcheurs. Cet indice demanderait à être validé et calibré, pour notamment trouver la valeur seuil de l'indice qui correspond le mieux à l'absence d'interaction avec l'engin de pêche.

Finalement, dans un future assez proche, on peut espérer arriver à une surveillance en temps réel des risques d'interactions entre les deux espèces, avec un monitoring beaucoup plus précis et une collaboration plus développée entre pêcheurs et agences de pêche. Dans la mesure où l'application de SEAPODYM à l'espadon, dont la 1^{ère} version est présentée au chapitre 4, deviendra de plus en plus réaliste et prédictive, les pêcheurs obtiendront des informations pour améliorer économiquement leur activité tout en respectant leurs quotas de capture et les mesures de conservations établies par les organismes de gestion des pêches à partir d'estimations de stock de plus en plus fiables et pouvant être produites en temps réel.

LIMITATIONS :

Inhérentes à toute approche de modélisation, ce projet s'est heurté à un certain nombre de limitations, certaines propres au modèle lui-même, d'autres aux données d'entrée.

- Tout modèle est limité directement par la qualité du forçage utilisé, dont les incertitudes se rajoutent à celles portant sur le modèle lui-même. Le forçage NCEP-PISCES utilisé dans ce projet est une nette amélioration par rapport à certains forçages utilisés lors d'études précédentes (Lehodey et al 2008, Lehodey & Senina 2009, Lehodey et al 2010), notamment grâce à une représentation explicite de l'oxygène dissous dans chaque couche au lieu de l'utilisation de la climatologie de Levitus. Néanmoins de grandes incertitudes existent en particulier pour cette variable et notamment dans le Pacifique Est, où la couche minimale d'oxygène est très peu profonde et constitue donc une contrainte forte sur l'habitat vertical des espadons.
- Un forçage à basse résolution spatiale et temporelle (2°x2°x1mois) a été utilisé pour effectuer cette première adaptation de SEAPODYM à l'espadon. En effet, du fait de la distribution de cette espèce à l'échelle du bassin, tenter d'optimiser tous les paramètres du modèle sur une région aussi large n'était pas réalisable avec un forçage plus fin, avec les capacités de calcul qui étaient disponibles.
- Malheureusement, comme expliqué au chapitre 4, du fait de l'absence, d'une part de données désagrégées par espèce cible pour les pêcheries couvrant l'ensemble du bassin (les pêcheries japonaises et koréennes notamment), d'autre part, pour les données haute qualité d'Hawaii, d'une couverture spatiale suffisante pour calibrer les migrations à l'échelle du bassin, ce forçage à basse résolution s'est révélé très limitant. Nous nous sommes rendu compte qu'une trop grande différence de résolution entre le forçage et les données de pêche, en particulier pour des pêcheries caractérisées par des CPUes élevées, introduit des biais majeurs, notamment dans l'estimation de la biomasse.
- De manière générale, l'élément le plus limitant de cette étude a été l'obtention de données de pêche adéquates. Premièrement, l'IATTC, en charge de récolter et distribuer les données de pêche des pays du Pacifique Est n'a pas obtenu l'accord de ses Pays membres pour fournir des données pour cette étude. Le volume de captures des pavillons latino-américains représentait, d'après le site internet de l'IATTC, environ 43% des prises d'espadon de 1959 à 2008. L'absence de ces données au sein du modèle entraîne donc une forte sous-estimation de la mortalité par pêche et rend l'estimation des paramètres d'habitat très délicate. Deuxièmement, à l'exception des données d'Hawaii fournies par la NOAA grâce à un accord de collaboration, l'ensemble des données de pêche disponibles étaient agrégées par pavillon, sans information sur l'espèce ciblée. Or, la vulnérabilité de l'espadon est radicalement différente entre les pêcheries qui ciblent cette espèce et celles qui ciblent le thon. Une telle agrégation dilue le signal disponible pour estimer les paramètres d'habitat du modèle.
- Dans un cas idéal où des données de pêche adéquates seraient fournies pour une telle étude, et un forçage résolvant la méso-échelle serait utilisé, l'élément le plus limitant du modèle devient alors le champ de proies (micronecton) dont la calibration est en cours à CLS, Toulouse. Un projet est entièrement dédié à l'acquisition et l'analyse de données acoustiques à l'échelle du bassin Pacifique afin d'obtenir une représentation plus détaillée et plus robuste des 6 composantes du micronecton au sein du modèle. A ce jour, cette partie du modèle n'a été validée qu'avec un faible nombre d'observations.
- SEAPODYM ne permet pas à ce jour de traiter les mâles et les femelles séparément, alors qu'un dimorphisme sexuel très important est observé chez l'espadon. Les paramètres de croissance ont

donc été moyennés entre les deux sexes et l'âge de reproduction des femelles a été utilisé. Les impacts potentiels d'une telle approximation sont difficiles à estimer.

- Au sein de Movemod, les mêmes équations développées pour les espèces de thons tropicaux ont été utilisées pour les tortues. Cette approche devient alors de fait limitée à l'étude des mouvements, la croissance et la dynamique de reproduction des tortues étant radicalement différentes et mal connues.
- La structure verticale de SEAPODYM en 3 couches n'est pas nécessairement adaptée à l'étude des mouvements des tortues, et le forçage a dû être tronqué aux 30 premiers mètres de profondeur occupés par les tortues la majorité du temps, afin d'éviter que l'impact des courants ne soit trop dilué en moyennant sur toute la couche épipélagique, ce qui est la procédure courante dans SEAPODYM.
- De même la définition des champs de proies dans SEAPODYM (6 groupes fonctionnels répartis dans les 3 couches verticales, épipélagique, mésopélagique et bathypélagique, selon leur comportement migrant ou non migrant) ne permet pas de représenter le régime alimentaire des tortues de manière adéquate. Les juvéniles de tortue caouanne dans le Pacifique se nourrissent essentiellement d'organismes neustoniques, flottant à la surface. L'utilisation du micronecton épipélagique dans la configuration tortues est une première approximation et doit être raffinée. Cette limitation complique l'évaluation de l'importance relative de la température par rapport à la concentration de proies dans la définition de l'habitat.
- Une autre limitation de ce projet est due au jeu de données disponible pour les tortues. Nous avons utilisé deux groupes de données de marquage, l'un concernant des tortues sauvages capturées par des bateaux de pêche entre 1997 et 2001 dans le Pacifique Nord central, l'autre concernant des tortues élevées en captivité à l'aquarium de Nagoya et relâchées entre 2003 et 2007, principalement près du Japon. Ces tortues étaient quasiment toutes plus petites que les tortues sauvages. Il existe très peu de recouvrement entre les deux groupes de tortues, que ce soit au niveau des tailles ou de l'année/région de largage, permettant de comparer le comportement des tortues sauvages et des tortues élevées en captivité.

PERSPECTIVES D'AMELIORATIONS :

La plupart des limitations rencontrées pourrait être facilement et rapidement levées si les données (existantes) de pêche complètes à l'échelle du bassin, et désagrégées par espèce cible étaient fournies. Cela permettrait un meilleur calibrage de la saisonnalité des migrations, des estimations de biomasses plus réalistes et probablement l'estimation d'un plus grand nombre de paramètres qui ont dû être fixés, notamment pour la tolérance en oxygène et l'habitat thermique des juvéniles.

Des études de sensibilité seront également nécessaires pour étudier l'influence des paramètres fixés sur la solution. Ceci n'a pas été effectué par manque de temps.

De plus, des forçages à plus haute résolution et résolvant la méso-échelle de manière réaliste sont d'ores et déjà disponibles, notamment la réanalyse Glorys de Mercator, utilisée dans le chapitre 3. Une fois les paramètres estimés à basse résolution avec un jeu de données plus complet et plus adéquat, le passage à un forçage plus fin devrait être relativement aisé et ne devrait nécessiter que des adaptations minimales.

L'utilisation d'un forçage résolvant la méso-échelle devrait également permettre d'obtenir une meilleure représentation des régions très dynamiques comme le courant du Kuroshio qui est une région très fréquentée par les tortues (Polovina et al 2006), ainsi que de la concentration en oxygène dans le Pacifique Est.

Enfin, la création d'un champ de proies neustoniques dédié pour les tortues permettrait une représentation plus fidèle de leur habitat d'alimentation.

PERSPECTIVES A LONG TERME :

Il serait intéressant de développer une version du modèle séparant les deux sexes pour obtenir une représentation plus adéquate des dynamiques spatiales et de reproduction de l'espadon.

Le succès d'un tel projet dépend en grande partie de la coopération entre agences de pêche et avec les organismes de recherche gouvernementaux. Actuellement, l'accès aux données de pêche à l'échelle du bassin est restreint par des accords de confidentialité forts, et leur obtention peut se révéler très problématique. Une plus grande coopération faciliterait grandement ce genre d'études à grande échelle.

Une fois résolus les problèmes décrits plus haut, dans un future assez proche, on peut espérer arriver à une surveillance en temps réel des risques d'interaction entre les deux espèces, avec un monitoring beaucoup plus précis et une collaboration plus développée entre pêcheurs et agences de pêche. Dans la mesure où l'application de SEAPODYM à l'espadon, dont la 1^{ère} version est présentée au chapitre 4, deviendra de plus en plus réaliste et prédictive, les pêcheurs obtiendront des informations pour améliorer économiquement leur activité tout en respectant leurs quotas de capture et les mesures de conservations établies par les organismes de gestion des pêches à partir d'estimations de stock de plus en plus fiables et pouvant être produites en temps réel.

BIBLIOGRAPHY

- Abascal FJ, Mejuto J, Quintans M, Ramos-Cartelle A (2010) Horizontal and vertical movements of swordfish in the southeast Pacific. *ICES J Mar Sci* 67:466–474
- Abecassis M, Dewar H, Hawn D, Polovina J (in press) Modeling swordfish daytime vertical habitat in the north pacific ocean from pop-up archival tags, *Mar Ecol Prog Ser*
- Abecassis M, Lehodey P, Polovina J, Senina I, Gaspar P, Calmettes B, Balazs G, Parker D (in prep). Analysis of loggerhead turtles tracks in the North Pacific to parameterize a feeding habitat and movement model.
- Alvarado-Bremer JR, Hinton MG, Greig TW (2006) Evidence of spatial genetic heterogeneity in Pacific swordfish (*Xiphias gladius*) revealed by the analysis of *ldh-A* sequences. *Bull Mar Sci* 79:493–503
- Alverson, D.L.; Freeberg, M.H.; Pope, J.G.; Murawski, S.A. A global assessment of fisheries bycatch and discards. FAO Fisheries Technical Paper. No. 339. Rome, FAO. 1994. 233p.
- Argano, R., R. Basso, M. Cocco, and G. Gerosa. 1992. New data on loggerhead (*Caretta caretta*) movements within the Mediterranean. *Bollettino del Museo dell' Istituto di Biologia dell' Universita di Genova* 56—57:137–164.
- Arocha, F. and Lee, D.W. (1996) Maturity at size, reproductive seasonality, spawning frequency, fecundity and sex ratio in swordfish from the Northwest Atlantic. SCRS/95/98 Collective volume of scientific papers. International Commission for the Conservation of Atlantic Tunas. Volume 45(2), pp. 350–57
- Aumont O, Maier-Reimer E, Blain S, Monfray P (2003) An ecosystem model of the global ocean including fe, si, p colimitations. *Global Biogeochemical Cycles* 17
- Aumont L O; & Bopp (2006) Globalizing results from ocean in situ iron fertilization studies. *Global Biogeochemical Cycles* 20:1–15
- Avens L, Braun-McNeill J, Epperly S, Lohmann K (2003) Site fidelity and homing behavior in juvenile loggerhead sea turtles (*Caretta caretta*). *Marine biology* 143(2):211–220
- Avens L, Lohmann K (2004) Navigation and seasonal migratory orientation in juvenile sea turtles. *Journal of Experimental Biology* 207(11):1771–1778
- Baez JC, Real R, Caminas JA (2007) Differential Distribution Within Longline Transects of Loggerhead Turtles and Swordfish Captured By the Spanish Mediterranean Surface Longline Fishery. *J Mar Biol Ass U K* 87:801–803
- Balazs G, Miya R, Beavers S (1996) Procedures to attach a satellite transmitter to the carapace of an adult green turtle, *Chelonia mydas*. In: *Proceedings of the Fifteenth Annual Symposium on Sea Turtle Biology and Conservation*.

Barnier B, Madec G, Penduff T, Molines JM, Treguier AM, Le Sommer J, Beckmann A, Biastoch A, Banić C, Dengg J, Derval C, Durand E, Gulev S, Remy E, Talandier C, Theetten S, Maltrud M, Mcclean J, De Cuevas B (2006) Impact of partial steps and momentum advection schemes in a global ocean circulation model at eddy permitting resolution. *Ocean dynamics* 56:543–567

Behrenfeld MJ, Falkowski PG (1997) Photosynthetic rates derived from satellite-based chlorophyll concentration. *Limnology and Oceanography* 42:1–20

Benson S, Dewar H, Dutton P, Fahy C, Heberer C, Squires D, Stohs S (2009) Swordfish and leatherback use of temperate habitat (SLUTH). Tech. Rep. LJ-09-06, Southwest Fisheries Science Center, NMFS/NOAA

Bertignac M., Lehodey P., Hampton J., (1998). A spatial population dynamics simulation model of tropical tunas using a habitat index based on environmental parameters. *Fisheries Oceanography*, 7: 326-334.

Beverly S, Robinson E, Itano D (2004) Trial setting of deep longline techniques to reduce bycatch and increase targeting of deep-swimming tunas. Tech. Rep. FTWG - WP-7a, Standing Committee on Tuna and Billfish

Beverly S, Curran D, Musyl M, Molony B (2009) Effects of eliminating shallow hooks from tuna longline sets on target and non-target species in the Hawaii-based pelagic tuna fishery. *Fish Res* 96:281–288

Bigelow K, Musyl MK, Poisson F, Kleiber P (2006) Pelagic longline gear depth and shoaling. *Fish Res* 77:173–183

Bjorndal KA, Bolten AB, Martins HR (2000) Somatic growth model of juvenile loggerhead sea turtles *Caretta caretta* : duration of pelagic stage. *Marine Ecology Progress Series* 202:265–272

Bolten AB, Witherington BE (2003) *Loggerhead sea turtles*. Smithsonian Books, Washington

Boden B, Kampa E (1967) The influence of natural light on the vertical migrations of an animal community in the sea. In: Marshall, N.B. (ed.) *Aspects of Marine Zoology*. Proc. Symp. zool. Soc. London. Vol. 19, 15–26

Boggs, C.H. (2003) Pacific research on longline sea turtle bycatch. In: K.J. Long and B.A. Schroeder (eds). *Proceedings of the International Technical Expert Workshop on Marine Turtle Bycatch in Longline Fisheries*. US Department of Commerce, NOAA Technical Memorandum NMFS-F/OPR-26, Silver Spring, MD, USA, p. 189.

Bopp L, Aumont O, Cadule P, Alvain S, Gehlen M (2005) Response of diatoms distribution to global warming and potential implications: A global model study. *Geophysical Research Letters* 32:1–4

Bolten, A. B., and G. H. Balazs. 1995. Biology of the early pelagic stage: the “lost year.” Pages 575–581 in K. A. Bjorndal, editor. *Biology and conservation of sea turtles*, revised edition. Smithsonian Institution Press, Washington, D.C., USA.

- Bolten AB (2003) Active swimmers—passive drifters: the oceanic juvenile stage of loggerheads in the Atlantic system. In: Loggerhead Sea Turtles (eds Bolten AB, Witherington BE), pp. 63–78. Smithsonian Books, Washington, D.C.
- Boyer T, Antonov J, Garcia H, Johnson D, Locarnini R, Mishonov A, Pitcher M, Baranova O, Smolyar I (2006) World Ocean Database 2005. NOAA Atlas NESDIS 60, U.S. Government Printing Office, Washington, D.C
- Bowen BW, Abreu-Grobois FA, Balazs GH, Kamezaki N, Limpus CJ, Ferl RJ. 1995. Trans-Pacific migrations of the logger-head sea turtle demonstrated with mito-chondrial DNA markers. *Proceedings of the National Academy of Sciences of the United States of America* 92: 3731- 3734.
- Brill RW (1987) On the standard metabolic rates of tropical tunas including the effect of body size and acute temperature change. *Fish Bull US* 85: 25-35
- Brill R (1994) A review of temperature and oxygen tolerance studies of tunas pertinent to fisheries oceanography, movement models and stock assessments. *Fish Oceanogr* 3:204–216
- Brill RW, Bigelow KA, Musyl MK, Fritches KA, Warrant EJ (2005) Bigeye tuna (*Thunnus obesus*) behaviour and physiology and their relevance to stock assessments and fishery biology. In: J Porter, ed., *Collective Volume of Scientific Papers. Second World Meeting on Bigeye Tuna*, ICCAT, Madrid, Spain, vol. 57, 142–161
- Brodziak J, Ishimura G (2011) Development of bayesian production models for assessing the north pacific swordfish population. *Fish Sci* 77:23–24
- Carey F, Robison B (1981) Daily patterns in the activities of swordfish, *Xiphias gladius*, observed by acoustic telemetry. *Fish Bull* 79:277–292
- Carey, F.G. (1982) A brain heater in the swordfish. *Science* 216, pp. 1327–28
- Carey, F.G. (1990) Further acoustic telemetry observations of swordfish. *Marine Recreational Fisheries* 13(2), pp. 103–22. Sportfishing Institute, Washington
- Carey, F.G. (1992) Through the thermocline and back again. Heat regulation in big fish. *Oceanus*, Fall, pp. 79–85
- Cerna F (2009) Age and growth of the swordfish (*xiphias gladius linnaeus*, 1758) in the southeastern pacific off chile (2001). *Lat Am J Aquat Res* 37:59–69
- Chancollon O, Pusineri C, Ridoux V (2006) Food and feeding ecology of Northeast Atlantic swordfish (*Xiphias gladius*) off the Bay of Biscay. *ICES J Mar Sci* 63:1075–1085
- Courtney D, Piner K (2009) Preliminary age structured stock assessment of North Pacific swordfish (*Xiphias gladius*) with stock synthesis under a two stock scenario. Tech. Rep. ISC/09/BILLWG-3/07
- Dagorn L, Bach P, Josse E (2000) Movement patterns of large bigeye tuna (*Thunnus obesus*) in the open ocean, determined using ultrasonic telemetry. *Mar Biol* 136:361–371

- DeMartini, E.E. (1999). Stock structure. pp. 185–95. In DiNardo, G.T. (ed.) Proceedings of the Second International Pacific Swordfish Symposium. Kahuku, Hawaii, 3–6 March 1997. NOAA Technical Memorandum NOAA–TM–NMFS–SWFC–264. National Marine Fisheries Service, Honolulu
- DeMartini EE, Uchiyama JH, Humphreys Jr RL, Sampaga JD, Williams HA (2007) Age and growth of swordfish (*Xiphias gladius*) caught by the Hawaii-based pelagic longline fishery. *Fishery Bulletin* 105:356–367
- Dewar H, Prince E, Musyl RMK, Brill RW, Sepulveda C, Luo J, Foley D, Orbesen ES, Domeier ML, Nasby-Lucas N, Snodgrass D, Laurs RM, Hoolihan JP, Block BA, McNaughton LM (2011) Movements and behaviors of swordfish in the Atlantic and Pacific oceans examined using pop-up satellite archival tags. *Fish Oceanogr* 20:219–241
- Dodd CK Jr (1988) Synopsis of the biological data on the loggerhead sea turtle *Caretta caretta* (Linnaeus, 1758). United States Fish and Wildlife Service Biology Report, 88, 1–110.
- Domeier ML, Dewar H and Nasby-Lucas N (2003) Mortality rate of striped marlin (*Tetrapturus audax*) caught with recreational tackle. *Mar Freshwater Res* 54:435–445
- Domeier ML, Kiefer D, Nasby-Lucas N, Wagschal A, O'Brien F (2005) Tracking Pacific bluefin tuna (*Thunnus thynnus orientalis*) in the northeastern Pacific with an automated algorithm that estimates latitude by matching sea-surface-temperature data from satellites with temperature data from tags on fish. *Fish Bull* 103:292–306
- Eckert S, Moore J, Dunn D, van Buiten R, Eckert K, Halpin P (2008) Modeling loggerhead turtle movement in the mediterranean: Importance of body size and oceanography. *Ecological Applications* 18(2):290–308
- Etnoyer P, Canny D, Mate BR, Morgan LE, Ortega-Ortiz JG, Nichols WJ (2006) Sea-surface temperature gradients across blue whale and sea turtle foraging trajectories off the Baja California Peninsula, Mexico. *Deep-Sea Research II* 53(3-4):340–358
- Fritsches KA, Brill RW, Warrant EJ (2005) Warm Eyes Provide Superior Vision in Swordfishes. *Curr Biol* 15:55–58
- Garcia-Cortes B, Mejuto J (2005) Scientific estimations of bycatch landed by the Spanish surface longline fleet targeting swordfish (*Xiphias gladius*) in the Indian ocean: 2001 - 2003 period. Tech. Rep. IOTC-2005-WPBy-14
- Gaspar P, Georges JY, Fossette S, Lenoble A, Ferraroli S, Le Maho Y (2006) Marine animal behaviour: neglecting ocean currents can lead us up the wrong track. *Proceedings - Royal Society of London Biological sciences* 273(1602):2697–2702
- Gilman, E., E. Zollett, S. Beverly, H. Nakano, K. Davis, D. Shidoe, P. Dalzell, and I. Kinan. 2006. Reducing sea turtle bycatch in pelagic longline fisheries. *Fish and Fisheries* 7:1–22.

- Gilman E, Zollett E, Beverly S, Nakano H and others (2007) Reducing sea turtle interactions in the Hawaii-based longline swordfish fishery. *Biol Conserv* 7:2–23
- Gorgues T, Menkes C, Aumont O, Vialard J, Dandonneau Y, Bopp L (2005) Biogeochemical impact of tropical instability waves in the equatorial pacific. *Geophysical Research Letters* 32:L24615
- Graham, MH (2003) Confronting multicollinearity in ecological multiple regression. *Ecology* 84:2809–2815
- Gunn J, Block B (2001) Advances in acoustic, archival, and satellite tagging of tunas. *Fish Physiol* 19:167–224
- Hastie T, Tibshirani R (1990) *Generalized Additive Models*. Chapman and Hall, London, U. K.
- Hays GC (2003) A review of the adaptive significance and ecosystem consequences of zooplankton diel vertical migrations. *Hydrobiologia* 503:163–170
- Hays GC, Bradshaw C, James M, Lovell P, Sims D (2007) Why do Argos satellite tags deployed on marine animals stop transmitting? *J Exp Mar Biol Ecol* 349:52–60
- Hinton MG, Maunder MN (2011 - draft) Status of swordfish in the eastern pacific ocean in 2010 and outlook for the future. Tech. rep., IATTC
- Hochscheid S, Bentivegna F, Hamza A, Hays GC (2010) When surfacers do not dive: multiple significance of extended surface times in marine turtles. *Journal of Experimental Biology* 213:1328–1337
- Holdsworth JC, Sippel TJ, Saul PJ (2007) An investigation into swordfish stock structure using satellite tag and release methods. Tech. Rep. WCPFC-SC3-BI SWG/WP- 3
- Holdsworth JC, Sippel TJ, Block BA (2009) Near real time satellite tracking of striped marlin (*Kajikia audax*) movements in the pacific ocean. *Mar Biol* 156:505–514
- Holland KN, Brill RW, Chang RKC, Sibert JR, Fournier DA (1992) Physiological and behavioral thermoregulation in bigeye tuna (*Thunnus obesus*). *Nature, Lond* 358: 410-412
- Holts DB, Bartoo NW, Bedford DW (1994) Swordfish tracking in the southern California Bight. Admin. Rep. NOAA-SWFSC-LJ-94-15
- Howell E, Kobayashi D, Parker D, Balazs G, Polovina J (2008) Turtlewatch: a tool to aid in the bycatch reduction of loggerhead turtles *Caretta caretta* in the Hawaii-based pelagic longline fishery. *Endangered Species Research* 5(2-3):267–278
- Howell EA, Dutton PH, Polovina JJ, Bailey H, Parker DM, Balazs GH (2010) Oceanographic influences on the dive behavior of juvenile loggerhead turtles (*Caretta caretta*) in the North Pacific ocean. *Marine Biology* 157:1011–1026
- Ichinokawa M, Brodziak J (2010) Using adaptive area stratification to standardize catch rates with application to North Pacific swordfish (*Xiphias gladius*). *Fish Res* 106:249–260

- Ito RY, Dollar RA, Kawamoto KE (1998) The Hawaii-based longline fishery for swordfish, *Xiphias gladius*. Tech. Rep. NOAA-NMFS-142
- Johnston D, McDonald M, Polovina J, Domokos R, Wiggins S, Hildebrand J (2008) Temporal patterns in the acoustic signals of beaked whales at Cross Seamount. *Biol Lett* 4:208–211
- Kalish JM, Greenlaw CF, Pearcy WG, Van Holliday D (1986) The biological and acoustical structure of sound scattering layers off Oregon. *Deep-Sea Res Part A* 33:631–653
- Kamezaki N, Matsui M (1997) A review of biological studies on sea turtles in Japan. *Jap J Herpetol* 17:16–32
- Kamezaki, N., Matsuzawa, K., Abe, O., Asakawa, H., Fukii, T., Goto, K., 2003. Loggerhead turtles nesting in Japan. In: Bolten, A., Witherington, B. (Eds.), *Loggerhead Sea Turtles*. Smithsonian Institution Press, Washington, DC, USA, pp. 210–217.
- Kelleher, K. Discards in the world's marine fisheries. An update. FAO Fisheries Technical Paper. No. 470. Rome, FAO. 2005. 131p.
- Kobayashi D, Polovina J, Parker D, Kamezaki N, Cheng I, Uchida I, Dutton P, Balazs G (2008) Pelagic habitat characterization of loggerhead sea turtles, *Caretta caretta*, in the north Pacific ocean (1997-2006): Insights from satellite tag tracking and remotely sensed data. *Journal of Experimental Marine Biology and Ecology* 356(1-2):96–114
- Kobayashi DR, Cheng IJ, Parker DM, Polovina JJ, Kamezaki N, Balazs GH (2011) Loggerhead turtle (*Caretta caretta*) movement off the coast of Taiwan: characterization of a hotspot in the east china sea and investigation of mesoscale eddies. *ICES J Mar Sci* advanced access
- Kolody D, Campbell R, Davies N (2009) South-west pacific swordfish (*Xiphias gladius*) stock assessment 1952-2007. Tech. Rep. WCPFC-SC5-2009/GN-IP-2, WCPFC/CSIRO
- Kutner MH, Nachtsheim CJ, Neter J, Li W (2005) *Applied linear statistical models*. McGraw-Hill/Irwin, 5th ed., NY
- Lam CH, Nielsen A, Sibert JR (2008) Improving light and temperature based geolocation by unscented Kalman filtering. *Fish Res* 91:15–25
- Lam CH, Nielsen A, Sibert JR (2010) Incorporating sea-surface temperature to the light-based geolocation model trackit. *Mar Ecol Prog Ser* 419:71–84
- Laurent, L., J. A. Camiñas, P. Casale, M. Deflorio, G. De, A. Kapantagakis, D. Margaritoulis, C. Y. Politou, and J. Valeiras. 2001. Assessing marine turtle bycatch in European drifting longline and trawl fisheries for identifying fishing regulations. Project-EC-DG fisheries 98–008. Joint project of BIOINSIGHT, IEO, IMBC, STPS, and University of Bari, Villeurbanne, France.

Le Couls, S, Bourjea, J (2010) Bilan de l'état des stocks et des mesures de gestion de l'espadon *Xiphias gladius* dans les océans Atlantique, Pacifique, Indien et en Mer Méditerranée. Rapport Ifremer RST. Délégation Réunion/2010-03

Lehodey P., André J-M., Bertignac M., Hampton J., Stoens A., C. Menkès, L., Memery, Grima N., (1998). Predicting skipjack tuna forage distributions in the Equatorial Pacific using a coupled dynamical bio-geochemical model. *Fisheries Oceanography*, **7**: 317-325.

Lehodey P., (2001). The pelagic ecosystem of the tropical Pacific Ocean: dynamic spatial modelling and biological consequences of ENSO. *Progress in Oceanography*, **49**: 439-468.

Lehodey P., Chai F., Hampton J. (2003). Modelling climate-related variability of tuna populations from a coupled ocean-biogeochemical-populations dynamics model. *Fisheries Oceanography*, **12**(4): 483-494.

Lehodey P., (2004a). A Spatial Ecosystem And Populations Dynamics Model (SEAPODYM) for tuna and associated oceanic top-predator species: Part I – Lower and intermediate trophic components. 17th meeting of the Standing Committee on Tuna and Billfish, Majuro, Republic of Marshall Islands, 9-18 Aug. 2004, Oceanic Fisheries Programme, Secretariat of the Pacific Community, Noumea, New Caledonia, Working Paper: **ECO-1**: 26 pp. <http://www.spc.int/OceanFish/Html/SCTB/SCTB17/ECO-1.pdf>

Lehodey P., (2004b) A Spatial Ecosystem And Populations Dynamics Model (SEAPODYM) for tuna and associated oceanic top-predator species: Part II – Tuna populations and fisheries. 17th meeting of the Standing Committee on Tuna and Billfish, Majuro, Republic of Marshall Islands, 9-18 Aug. 2004, Oceanic Fisheries Programme, Secretariat of the Pacific Community, Noumea, New Caledonia, Working Paper: **ECO-2**: 36 pp. <http://www.spc.int/OceanFish/Html/SCTB/SCTB17/ECO-2.pdf>

Lehodey P, Senina I, Murtugudde R (2008) A spatial ecosystem and populations dynamics model (SEAPODYM) - modeling of tuna and tuna-like populations. *Prog Oceanogr* **78**: 304–318

Lehodey P., Senina I., (2009). An update of recent developments and applications of the SEAPODYM model. Fifth regular session of the Scientific Committee of the Western and Central Pacific Fisheries Commission, 10–21 August 2009, Port Vila, Vanuatu, WCPFC-SC5-2009/EB-WP-10, 44 pp. <http://www.wcpfc.int/meetings/2009/5th-regular-session-scientific-committee>

Lehodey P, Murtugudde R, Senina I (2010a) Bridging the gap from ocean models to population dynamics of large marine predators: a model of mid-trophic functional groups. *Progress in Oceanography* **84**: 69–84.

Lehodey P., Senina I., Calmettes B., Abecassis M., Jurado Molina J., Briand K., Hampton J., Polovina J., Williams P., Nicol S. (2010b). Project 62: SEAPODYM applications in WCPO – Progress Report. 6th regular session of the Scientific Steering Committee, 10-19 August 2010, Nukualofa, Tonga. WCPFC-SC6-2010/EB- IP 02. <http://www.wcpfc.int/meetings/2010/6th-regular-session-scientific-committee>

Lehodey P, Senina I, Calmettes B, Royer F, Gaspar P, Abecassis M, Polovina J, Parker D, Domokos R, Hernandez O, Dessert M, Kloser R, Young J, Lutcvage M, Handegard NO, Hampton J (2010c) Towards operational management of pelagic ecosystems. Tech. Rep. ICES CM 2010/A, ICES

Lehodey P, Senina I, Sibert J, Bopp L, Calmettes B, Hampton J, Murtugudde R (2010d) Preliminary forecasts of Pacific bigeye tuna population trends under the A2 IPCC scenario. *Progress in Oceanography* 86: 302–315.

Lehodey P., Senina I., Calmettes B., Hampton J., Nicol S., Williams P., Jurado Molina J., Ogura M., Kiyofuji H., Okamoto S. (2011). SEAPODYM working progress and applications to Pacific skipjack tuna population and fisheries. 7th regular session of the Scientific Steering Committee, 8-17 August 2011, Pohnpei, Federate States of Micronesia. WCPFC-SC7-2011/EB-WP 06. <http://www.wcpfc.int/meetings/2011/7th-regular-session-scientific-committee>

Lewison RL, Freeman SA, Crowder LB (2004) Quantifying the effects of fisheries on threatened species: the impact of pelagic longlines on loggerhead and leatherback sea turtles. *Ecology Letters* 7:221–231

Lewison RL, Crowder LB (2007) Putting longline bycatch of sea turtles into perspective. *Conserv Biol* 21:79–86

Limpus, CJ, de Villiers, DL, de Villiers, MA, Limpus, DJ, Read, MA (2001) the loggerhead turtle, *Caretta caretta*, in Queensland : Feeding ecology in warm temperature waters. *Memoirs of the Queensland Museum* 46:631-645

Limpus, C., Limpus, D., 2003. The loggerhead turtle, *Caretta caretta*, in the Equatorial and Southern Pacific Ocean: a species in decline. In: Bolten, A., Witherington, B. (Eds.), *Loggerhead Sea Turtles*. Smithsonian Institution Press, Washington, DC, USA, pp. 199–209.

Lohmann K, Lohmann C, Ehrhart L, Bagley D, Swing T (2004) Animal behaviour – geomagnetic map used in sea-turtle navigation. *Nature* 428(6986):909–910

Lohmann K, Luschi P, Hays G (2008) Goal navigation and island-finding in sea turtles. *Journal of Experimental Marine Biology and Ecology* 356(1-2):83–95

Longhurst A (1975) *Ecology of the season*, W.B.Saunders Co., Philadelphia, chap. Vertical migration. 116–137

Matciak, M. (1997) Estimation of the attenuation of the visible light in waters of the Gulf of Gdansk with the use of Secchi transparency. *Oceanol Stud* 26:35–40.

Matsuzawa, Y., K. Sato, W. Sakamoto, and K. A. Bjorndal (2002) Seasonal fluctuations in sand temperature: effects on the incubation period and mortality of Loggerhead Sea Turtle (*Caretta caretta*) pre-emergent hatchlings in Minabe, Japan. *Marine Biology* 140:639–646

Musyl M, Brill R, Boggs C, Curran D, Kazama T, Seki M (2003) Vertical movements of bigeye tuna (*Thunnus obesus*) associated with islands, buoys, and seamounts near the main Hawaiian islands from archival tagging data. *Fish Oceanogr* 12:152–169

Nasby-Lucas N, Dewar H, Lam CH, Goldman KJ, Domeier ML (2009) White shark offshore habitat: A behavioral and environmental characterization of the eastern Pacific shared offshore foraging area. *PLOSone* 4:e1863

- Neilson JD, Smith S, Royer F, Paul SD, Porter JM, Lutcavage M (2009) Tagging and Tracking of Marine Animals with Electronic Devices, Springer Netherlands, chap. Investigations of Horizontal Movements of Atlantic Swordfish Using Pop-up Satellite Archival Tags. 145–159
- Nelson DR, McKibben JN, Strong WR Jr, Lowe CG, Sisneros JA, Schroeder DM, Lavenberg RJ (1997) An acoustic tracking of a megamouth shark, *Megachasma pelagios*: a crepuscular vertical migrator. *Environ Biol Fish* 49:389–399
- Nichols WJ, Resendiz A, Seminoff JA, Resendiz B (2000) Transpacific migration of a loggerhead turtle monitored by satellite telemetry. *Bulletin of marine science* 67(3):937–947
- Nielsen A, Sibert J (2007) State-space model for light-based tracking of marine animals. *Can J Fish Aquat Sci* 64:1055–1068
- Nishikawa, Y. and Ueyanagi, S. (1974). The distribution of the larvae of swordfish, *Xiphias gladius*, in the Indian and Pacific oceans. pp. 261–64. In Shomura, R.S. and Williams, F.18 Bureau of Rural Sciences (eds). Proceedings of the International Billfish Symposium. Kailua–Kona, Hawaii, 9–12 August 1972. Part 2. Review and contributed papers. NOAA Technical Report, NMFS SSRF–675
- Palko, B.J., Beardslay, G.L. and Richards, W.J. (1981) Synopsis of the biology of the swordfish, *Xiphias gladius* Linnaeus. United States Department of Commerce, NOAA Technical Report NMFS Circular 441 (FAO Fisheries Synopsis No. 127)
- Parker DM, Cooke WJ, Balazs GH (2005) Diet of oceanic loggerhead sea turtles (*Caretta caretta*) in the central north pacific. *Fishery Bulletin* 103:142–152
- Peckham SH, Maldonado Diaz D, Walli A, Ruiz G, Crowder LB, Nichols WJ (2007) Small-scale fisheries bycatch jeopardizes endangered Pacific loggerhead turtles. *PLoS ONE* 2(10):e1041
- Peckham SH, Maldonado-Diaz D, Koch V, Mancini A, Gaos A, Tinker MT, Nichols WJ (2008) High mortality of loggerhead turtles due to bycatch, human consumption and strandings at Baja California Sur, Mexico, 2003 to 2007. *Endangered Species Research* 5(2-3):171–183
- Peckham SH, Maldonado-Diaz D, Tremblay Y, Ochoa R, Polovina J, Balazs G, Dutton PH, Nichols WJ (2011) Demographic implications of alternative foraging strategies in juvenile loggerhead turtles *Caretta caretta* of the North Pacific ocean. *Mar Ecol Prog Ser* 425:269–280
- Petersen SL, Honig MB, Ryan PG, Nel R, Underhill LG (2009) Turtle bycatch in the pelagic longline fishery off southern Africa. *Afr J Mar Sci* 31:87-96.
- Pham DT, Verron J, Roubaud MC (1998) A singular evolutive extended kalman filter for data assimilation in oceanography. *Journal of Marine Systems* 16:323–340
- Piovano S, Swimmer Y, Giacoma C (2009) Are circle hooks effective in reducing incidental captures of loggerhead sea turtles in a Mediterranean longline fishery? *Aquat Conserv* 19:779–785

- Pitman, R. L. 1990. Pelagic distribution and biology of sea turtles in the eastern tropical Pacific. Pp. 143-148 In: Proceedings of the Tenth Annual Workshop on Sea Turtle Biology and Conservation, (T. H. Richardson, J. I. Richardson, and M. Donnelly, Compilers), NOM-TM-NMFS-SEFC- 278.
- Polovina J, Kobayashi R, Parker M, Seki P, Balazs H (2000) Turtles on the edge: movement of loggerhead turtles (*Caretta caretta*) along oceanic fronts, spanning longline fishing grounds in the central north pacific, 1997-1998. Fisheries Oceanography 9(1):71–82
- Polovina JJ, Howell E, Parker DM, Balazs GH (2003) Dive-depth distribution of loggerhead and olive ridley sea turtles in the central North Pacific: might deep longline sets catch fewer turtles? Fish Bull 101:189–193
- Polovina J, Balazs G, Howell E, Parker D, Seki M, Dutton P (2004) Forage and migration habitat of loggerhead (*Caretta caretta*) and olive ridley (*Lepidochelys olivacea*) sea turtles in the central north pacific ocean. Fisheries Oceanography 13(1):36–51
- Polovina J, Uchida I, Balazs G, Howell EA, Parker D, Dutton P (2006) The Kuroshio extension bifurcation region: A pelagic hotspot for juvenile loggerhead sea turtles. Deep Sea Research (Part II, Topical Studies in Oceanography) 53(3-4):326–339
- Polovina JJ, Hawn D, Abecassis M (2008) Vertical movement and habitat of opah (*Lampris guttatus*) in the central North Pacific recorded with pop-up archival tags. Mar Biol 153:257–267
- Potier M, Marsac F, Cherel Y, Lucas V, Sabatie R, Maury O, Menard F (2007) Forage fauna in the diet of three large pelagic fishes (lancetfish, swordfish and yellowfin tuna) in the western equatorial Indian Ocean. Fish Res 83:60–72
- Prince ED, Goodyear CP (2006) Hypoxia-based habitat compression of tropical pelagic fishes. Fish Oceanogr 15:451 – 464
- Prince ED, Luo J, Goodyear CP, Hoolihan JP, Snodgrass D, Orbesen ES, Serafy JE, Ortiz M, Schirripa MJ (2010) Ocean scale hypoxia-based habitat compression of Atlantic istiophorid billfishes. Fish Oceanogr 19:448–462
- Ramirez Cruz JC, Pena Ramirez I, Villanueva Flores D. 1991. Distribution y abundancia de la tortuga perica, *Caretta caretta* Linnaeus (1758), en la costa occidental de Baja California Sur, Mexico. Archelon 1(2): 1-4.
- Reeb C, Arcangeli L, Block B (2000) Structure and migration corridors in Pacific populations of the swordfish *Xiphus gladius*, as inferred through analyses of mitochondrial DNA. Mar Biol 136:1123–1131
- Resendiz A, Resendiz B, Nichols W, Seminoff J, Kamezaki N (1998) First confirmed east-west transpacific movement of a loggerhead sea turtle, *Caretta caretta*, released in Baja California, Mexico. Pacific Science 52(2):151–153.
- Revelles M, Cardona L, Aguilar A, San Felix M, Fernandez G (2007a) Habitat use by immature loggerhead sea turtles in the algerian basin (western mediterranean): swimming behaviour, seasonality and dispersal pattern. Marine Biology 151(4):1501–1515

- Revelles M, Isern-Fontanet J, Cardona L, San Felix M, Carreras C, Aguilar A (2007b) Mesoscale eddies, surface circulation and the scale of habitat selection by immature loggerhead sea turtles. *Journal of Experimental Marine Biology and Ecology* 347(1-2):41–57
- Rio M, Guinehut S, Larnicol G (2011) New cnes-cls09 global mean dynamic topography computed from the combination of grace data, altimetry, and in situ measurements. *J Geophys Res* 116:1–25
- Royer F, Lutcavage M (2008) Filtering and interpreting location errors in satellite telemetry of marine animals. *J Exp Mar Biol Ecol* 359:1–10
- Royer F, Lutcavage M (2009) Tagging and Tracking of Marine Animals with Electronic Devices, Springer Netherlands, chap. Positioning pelagic fish from sunrise and sunset times: error assessment and improvement through constrained, robust modeling. 323–341
- Royer F, Fromentin JM, Gaspar P (2005) A state-space model to derive bluefin tuna movement and habitat from archival tags. *Oikos* 109:473–484
- Sato K, Bando T, Matsuzawa Y, Tanaka H, Sakamoto W, Minamikawa S, Goto K (1997) Decline of the loggerhead turtle, *Caretta caretta*, nesting on Senri Beach in Minabe, Wakayama, Japan. *Chelonian Conserv Biol* 2:600–603
- Scott R, Marsh R, Hays GC (2011) Life in the really slow lane: loggerhead sea turtles mature late relative to other reptiles. *Functional Ecology* xx:1–9
- Seifert B, Gasser T (1998) Encyclopedia of Statistical Sciences, Update Vol.2, Wiley, chap. Local polynomial smoothing. 367–372
- Senina I, Sibert J, Lehodey P (2008) Parameter estimation for basin-scale ecosystem-linked population models of large pelagic predators: Application to skipjack tuna. *Prog Oceanogr* 78: 319–335
- Sepulveda CA, Knight A, Nasby-Lucas N, Domeier ML (2010) Fine-scale movements of the swordfish *Xiphias gladius* in the Southern California Bight. *Fish Oceanogr* 19:279–289
- Sibert J, Hampton J, Fournier D, Bills P (1999) An advection-diffusion-reaction model for the estimation of fish movement parameters from tagging data, with application to skipjack tuna (*Katsuwonus pelamis*). *Canadian Journal of Fisheries & Aquatic Sciences* 56(6): 925–938.
- Sibert J, Senina I, Lehodey P, Hampton J (2012). Shifting from marine reserves to maritime zoning for conservation of Pacific bigeye tuna (*Thunnus obesus*). *PNAS*, doi/10.1073/pnas.1209468109
- Sippel T (2010) Tracking of striped marlin (*Kajikia audax*) in the southwest Pacific Ocean: environmental influences on movement and behaviour. Ph.D. thesis, University of Auckland, New Zealand
- Smith HF, Sandwell DT (1997) Global Sea Floor Topography from Satellite Altimetry and Ship Depth Soundings, *Science* 277:1956-1962.

- Stramma L, Schmidtko S, Levin LA, Johnson GC (2010) Ocean oxygen minima expansions and their biological impacts. *Deep-Sea Res Part I* 57:587–595
- Sun, C.-L., S.-P. Wang, and S.-Z. Yeh. 2002. Age and growth of the swordfish (*Xiphias gladius* L.), in the waters around Taiwan determined from anal-fin rays. *Fish. Bull.* 100:822–835
- Swimmer Y, Brill R (2006) Sea turtle and pelagic fish sensory biology: Developing techniques to reduce sea turtle bycatch in longline fisheries. Technical Memorandum NMFS-PIFSC-7, NOAA
- Takahashi M, Okamura H, Yokawa K, Okazaki M (2003) Swimming behaviour and migration of a swordfish recorded by an archival tag. *Mar Freshw Res* 54:527–534
- Teo SLH, Boustany A, Blackwell S, Walli A, Weng KC, Block BA (2004) Validation of geolocation estimates based on light level and sea surface temperature from electronic tags. *Mar Ecol Prog Ser* 283:81–98
- Tont S (1975) Deep scattering layers: patterns in the Pacific. Tech. Rep. 18, SCRIPPS – CalCOFI
- Tranchant B, Testut CE, Renault L, Ferry N, Birol F, Brasseur P (2008) Expected impact of the future smos and aquarius ocean surface salinity missions in the mercator ocean operational systems: New perspectives to monitor ocean circulation. *Remote Sensing of Environment* 112:1476–1487
- Uchiyama JH, Demartini EE, Williams HA (1999) Length-Weight Interrelationships For Swordfish, *Xiphias Gladis* L., Caught In The Central North Pacific. Tech. Rep. NOAA-TM-NMFS-SWFSC-284
- Ward, P., and S. Elscot (2000) Broadbill swordfish: status of world fisheries, 242 p. Bureau of Rural Sciences, Canberra
- Ward R, Reeb C, Block B (2001) Population structure of Australian swordfish, *Xiphias gladius*. Final Report to the Australian Fisheries Management Authority, Canberra, CSIRO
- Watson J, Epperly S, Shah A, Foster D (2005) Fishing methods to reduce sea turtle mortality associated with pelagic longlines. *Can J Fish Aquat Sci* 62:965–981
- Wegner NC, Sepulveda CA, Bull KB, Graham JB (2010) Gill morphometrics in relation to gas transfer and ram ventilation in high-energy demand teleosts: Scombrids and billfishes. *J Morphol* 271:36.49
- Wilson, C.A. and Dean, J.M. (1983) The potential use of sagittae for estimating age of Atlantic swordfish, *Xiphias gladius*. In Prince, E.D. and Pulos, L.M. (eds) *Proceedings of the International Workshop on Age Determination of Oceanic Pelagic Fishes: Tunas, Billfishes and Sharks*. United States Department of Commerce, NOAA Technical Report NMFS 8, pp. 151–56
- Wilson SG, Lutcavage ME, Brill RW, Genovese MP, Cooper AB, Everly AW (2005) Movements of bluefin tuna (*Thunnus thynnus*) in the northwestern Atlantic Ocean recorded by pop-up satellite archival tags. *Mar Biol* 146(2):409–423
- Witherington BE (2003) Biological conservation of loggerheads: challenges and opportunities. In: Bolten AB, Witherington BE (eds) *Loggerhead sea turtles*. Smithsonian Books, Washington, DC, p 295–311

Wood S (2006) Generalized Additive Models: An Introduction with R. CRC Press, Boca Raton, FL.

Young J, Drake A (2004) Age and growth of broadbill swordfish (*Xiphias gladius*) from Australian waters. Tech. rep., FRDC & CSIRO

Young J, Lansdell M, Riddoch S, Revill A (2006) Feeding ecology of broadbill swordfish, *Xiphias gladius*, off eastern Australia in relation to physical and environmental variables. Bull Mar Sci 79:793-809

Zug GR, Balazs GH, Wetherall JA (1995) Growth in juvenile loggerhead sea turtles (*Caretta caretta*) in the north pacific pelagic habitat. Copeia 1995(2):484–487

Modeling interactions between swordfish, loggerhead turtles and the longline fisheries in the North Pacific.

In 2011, loggerheads were relisted as endangered in the Pacific Ocean. Numerous mitigation measures have been taken in the past decade to reduce the number of sea turtle interactions with the fisheries that target swordfish.

The goal of this project is to yield a better description of swordfish and loggerheads habitats in the Pacific from electronic tagging data, and then to use these results to calibrate numerical models aimed at predicting the spatial distributions of both species to evaluate potential by-catch reduction strategies.

The analysis of pop-up archival satellite tags deployed on swordfish allowed for a better understanding of the factors controlling their vertical behavior and led to the development of a generalized additive model (GAM) to predict swordfish mean daytime depth. That information could help longline fishermen to target swordfish during the daytime at depth, rather than at night in the surface layer where loggerheads reside.

Data from satellite tag deployed on loggerhead turtles allowed to study their movements in details in conjunction with environmental variables along their tracks.

Finally, the SEAPODYM model was adapted to swordfish in the Pacific to study the distributions of young and adult swordfish overlap periods between swordfish and loggerheads. A better fishing dataset would allow to study the regions of overlap in a detailed enough manner for management purposes.